This is to certify that the

dissertation entitled

Organometallic, Coordination and Redox Chemistry of Rhodium(II) Metalloradical Species Supported by an Oxygen Functionalized Triaryl Phosphine

presented by

Steven Christopher Haefner

has been accepted towards fulfillment of the requirements for

Ph.D. degree in Chemistry

Major professor

Date August 18, 1992

ORGANOMETALLIC, COORDINATION AND REDOX CHEMISTRY OF RHODIUM(II) METALLORADICAL SPECIES SUPPORTED BY AN OXYGEN FUNCTIONALIZED TRIARYL PHOSPHINE

By

Steven Christopher Haefner

A DISSERTATION

Submitted to
Michigan State University
in partial fulfillment of the requirements
for the degree of

DOCTOR OF PHILOSOPHY

Department of Chemistry
1992

ABSTRACT

ORGANOMETALLIC, COORDINATION AND REDOX CHEMISTRY OF RHODIUM(II) METALLORADICAL SPECIES SUPPORTED BY AN OXYGEN FUNCTIONALIZED TRIARYL PHOSPHINE

By

Steven Christopher Haefner

The study of mononuclear rhodium chemistry has focused primarily on its monovalent and trivalent oxidation states with relatively little emphasis on the chemistry of divalent species. The scarcity of mononuclear Rh(II) complexes is due, in part, to the proclivity of these systems to either undergo dimerization or disproportionation, consequently few paramagnetic Rh(II) complexes have been the subject of comprehensive studies. Recent reports of carbon monoxide and methane activation by Rh(II) metalloradicals have sparked renewed interest in this under developed area of chemistry.

This work focuses on Rh(II) radical chemistry of the multifunctionalized ether phosphine ligand tris(2,4,6-trimethoxyphenyl)-phosphine (TMPP). The unique combination of steric bulk and chelating abilities afforded by TMPP has allowed for the stabilization of a novel mononuclear, six coordinate Rh(II) homoleptic phosphine complex, $[Rh(\eta^3\text{-}TMPP)_2][BF_4]_2$. The steric bulk of the ligand precludes the formation of dinuclear species, yet the presence of labile ether interactions permits the complex to react with a variety of small molecules. Most notably, this

metalloradical species readily reacts with π-acceptors such as carbon monoxide and isocyanide ligands to form adducts of the type $[Rh(TMPP)_2L_2]^{2+}$. In the case of CO, the complex is highly unstable and immediately undergoes a series of redox reactions involving the formation of Rh(I) and Rh(III) intermediates that ultimately regenerate the original Rh(II) complex. In contrast, the reaction of $[Rh(\eta^3\text{-}TMPP)_2][BF_4]_2$ with the weaker π-acceptor ligands CNR (R = ^{t}Bu, ^{i}Pr) affords the stable four-coordinate Rh(II) adduct $[Rh(TMPP)_2(CNR)_2][BF_4]_2$.

In addition to the observed substitution chemistry with π-acceptors, $[Rh(\eta^3\text{-}TMPP)_2][BF_4]_2$ reacts with nucleophiles, resulting in dealkylation of a bound methoxy-group to give a new Rh(II) complex ligated by one phosphine and one phosphino-phenoxide ligand. This complex, formulated as $[Rh(TMPP)(TMPP\text{-}O)][BF_4]$, (TMPP-*O* = $[P\{C_6H_2(OMe)_3\}_2(C_6H_2(OMe)_2O)]^{1-}$), reacts with carbon monoxide to form unusual paramagnetic adducts that have been detected by IR and EPR spectroscopies.

The series of d^7 phosphine complexes isolated in these studies are among the first mononuclear Rh(II) complexes to be fully characterized by X-ray crystallography, EPR and a variety of other spectroscopic techniques. An account of the syntheses, characterization and reactivity of these rare paramagnetic species is presented together with preliminary results regarding the extension of this work to other radical systems.

To my wife Kelly, without whose love and patience, this work would not have been possible.

"*What is essential is invisible to the eyes. It is only with the heart with which one can see rightly.*"

Antoine de Saint Expurey

ACKNOWLEDGEMENTS

The research presented in this dissertation would not have been possible without the assistance and support of numerous individuals whose direct and indirect contributions are an integral part of this work. Foremost, I would like to thank my research adviser, Professor Kim R. Dunbar. She taught me through example, the importance of hard work and dedication in achieving your goals. Her enthusiasm and love of chemistry encouraged me to reach within myself and strive for excellence. Above all, she impressed upon me to always be critical of oneself and work. I will always hold her advice and insight in the highest regard, as I have the deepest respect and admiration for Professor Dunbar as both a scientist and a friend. I extend my gratitude to my contemporaries in the Dunbar Group for sharing the successes and failures that go along with being a graduate student. Together, they made being a member of the Dunbar Group a memorable and enjoyable experience. In particular, I would like to thank Laura Pence for her help and friendship, especially in the early years when I was only a young pup still wet behind the ears. She impressed upon me the importance of promoting oneself and chemistry. Special thanks go to Anne Quillevéré; the other half of "the match made in heaven". Her support and encouragement went along way in helping me to achieve my goals. Although she would never admit to it, she truly shares my enthusiasm for chemistry. I will forever value and treasure

her friendship. I also thank my long time friends Gene, Jim and Rob for providing that often needed outlet when things did not work quite they way they should. Furthermore, I thank my parents for their love, support and for never expecting anything less from me. In addition, I would like to acknowledge Michigan State University, College of Natural Science, and Dow Chemical for providing financial support in the form of scholarships. Finally, I thank the numerous collaborators whom I have worked with over the past several years for their individual contributions to this work.

TABLE OF CONTENTS

LIST OF TABLES

LIST OF FIGURES

LIST OF SYMBOLS AND ABBREVIATIONS

Å	Ångström
Ag/AgCl	silver-silver chloride reference electrode
Ar	aryl group
br	broad
Bu^t	tert-butyl
ca.	circa, about
cm	centimeter
cm^{-1}	wavenumber
cod	1,5-cyclooctadiene
CV	cyclic voltammetry
Cy	cyclohexyl
°C	degree centigrade
d	doublet (NMR), day, deuterated
δ	parts per million (ppm)
dCype	bis(dicyclohexylphosphino)ethane
dd	doublet of doublets
$E_{p,a}$	anodic peak potential
$E_{p,c}$	cathodic peak potential
EPR	electron paramagnetic resonance
emu	electromagnetic unit
esd	estimated standard deviation
Et	ethyl
EtOH	ethanol
ε	molar extinction coefficient
FAB	Fast Atom Bombardment
g	epr g-value, gram
G	Gauss
h	hour

TMPP-H	tris(2,4,6-trimethoxyphenyl)phosphonium
(M)Hz	(Mega)Hertz
IR	infrared
K	Kelvin
λ	wavelength
m	medium
M	moles per liter
Me	methyl
MeCN	acetonitrile
MeOH	methanol
mg	milligram
min.	minute
mL	milliliter
mmol	millimole
mult	multiplet
μ	bridging ligand
μB or B. M.	Bohr magneton
μL	microliter
nm	nanometer
ν	frequency
NBA	3-nitrobenzyl alcohol
NMR	nuclear magnetic resonance
ox	oxidation
PCy_3	tricyclohexylphosphine
PPh_3	triphenylphosphine
$P(mes)_3$	trimesitylphosphine
ppm	parts per million
Pr^i	isopropyl
psi	pounds per square inch
red	reduction
r.t.	room temperature
s	singlet (NMR), strong (IR)
sh	shoulder
SQUID	Superconducting Quantum Interference Device
t	triplet

$TBABF_4$	tetra-*n*-butylammonium tetrafluoroborate
THF	tetrahydrofuran
TMPP	tris(2,4,6-trimethoxyphenyl)phosphine
TMPP=O	tris(2,4,6-trimethoxyphenyl)phosphine oxide
TMPP-*O*	$P[\{C_6H_2(CH_3O)_3\}2\{C_6H_2(CH_3O)_2O\}]^-$
$TMPP\text{-}CH_3$	tris(2,4,6-trimethoxyphenyl)methyl phosphonium
$TMPP\text{-}CH_2Cl$	tris(2,4,6-trimethoxyphenyl)chloromethyl phosphonium
TMS	tetramethylsilane
UV	ultraviolet
V	Volt
vs	versus, very strong
w	weak
X	halide ligand

LIST OF COMPOUNDS

(1) ---------- TMPP

(2) ---------- TMPP=O

(3) ---------- $[Rh^{II}(\eta^3\text{-TMPP})_2][BF_4]_2$

(4) ---------- $[Rh^{III}(\eta^3\text{-TMPP})_2][BF_4]_3$

(5) ---------- *ax*-$[Rh^{III}(\eta^3\text{-TMPP})(\eta^3\text{-TMPP-}O)][BF_4]_2$

(6) ---------- $[Rh^{I}(TMPP)_2(CO)_2][BF_4]$

(7) ---------- $[Rh^{I}(TMPP)_2(CO)][BF_4]$

(8) ---------- $[Rh^{I}(TMPP)_2(CO)(CNBu^t)][BF_4]$

(9) ---------- $[Rh^{II}(TMPP)_2(CNBu^t)_2][BF_4]_2$

(10) ---------- $[Rh^{II}(TMPP)_2(CNPr^i)_2][BF_4]_2$

(11) ---------- $[Rh^{I}(TMPP)_2(CNBu^t)_2][BF_4]$

(12) ---------- *eq*-$[Rh^{II}(TMPP)(TMPP\text{-}O)][BF_4]$

(13) ---------- *eq*-$[Rh^{III}(\eta^3\text{-TMPP})(\eta^3\text{-TMPP-}O)][BF_4]_2$

(14) ---------- *ax,eq*-$[Rh^{III}(\eta^3\text{-TMPP-}O)_2][BF_4]$

(15) ---------- *ax,ax*-$[Rh^{III}(\eta^3\text{-TMPP-}O)_2][BF_4]$

(16) ---------- $[Rh^{I}(cod)(\eta^2\text{-TMPP})][BF_4]$

(17) ---------- $Rh^{I}(cod)(\eta^2\text{-TMPP-}O)$

(18) ---------- $Ir^{I}(cod)(\eta^2\text{-TMPP-}O)$

(19) ---------- $[Ir^{I}(TMPP)_2(CO)_2][BF_4]$

(20) ---------- $(\eta^3\text{-TMPP})Mo^0(CO)_3$

CHAPTER I

INTRODUCTION

A. Role of Tertiary Phosphines in Transition Metal Chemistry

The use of tertiary phosphines as ancillary ligands has played a prominent role in the development of modern coordination and organometallic chemistry. This statement is most evident from the observation that phosphine complexes are known for virtually all transition metals.[1] These versatile ligands are capable of stabilizing a variety of metals in a range of oxidation states. Furthermore, transition metal-phosphine complexes, particularly those of the later transition metals, catalyze a number of industrially important organic processes.[2] These range from olefin hydrogenation, hydroformylation, hydrosilation and hydrocyanation to polymerization and oligomerization of olefins and acetylenes. In addition to catalytic processes, transition metal phosphine complexes are also capable of performing a number of stoichiometric organic transformations.[3] An important aspect in the use of transition metal-phosphine complexes in catalysis has been the potential for controlling catalyst activity and selectivity by modifying the substituent groups of the phosphine. By varying the R groups of a phosphine, both the electronic and steric properties of the ligand may be changed. This in turn will affect the reactivity properties of the metal to which the phosphine is bound. It is important to realize, however, that steric and electronic effects are not independent of each another; often, substitution of one of the R substituents results not only in a change in the steric properties of ligands, but also the electronic properties as well. For instance as the size of a phosphine is increased, the C-P-C angle is forced to expand which affects the percentage of s-character in the phosphorus lone pair and hence the phosphine donor properties. Furthermore, sterically hindering substituents also affect the ability of the phosphine to interact strongly with the metal center and therefore influence

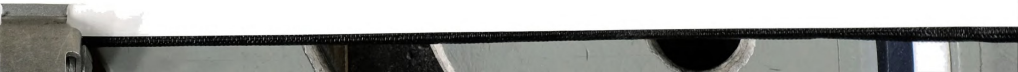

the metal phosphorus bond strength. As a consequence of this interrelationship, there is considerable interest in quantifing and separating the factors that influence transition metal-phosphorus bonding.

The electronic properties of a particular phosphine molecule are dominated by the donor capacity of the phosphorus lone pair of electrons which is quite sensitive to the nature of the phosphine substituents, or R groups. By altering the R groups, and therefore the donor ability of the phosphine, the electron density at the metal center may be tuned in order to increase or decrease the reactivity of the complex.

The electronic donating properties of phosphine ligands are typically divided into σ and π contributions.[4] Generally, the σ contribution dominates and π contributions are only evident for phosphines with electronegative substituents such as -F, -OR, -Cl and -OAr. The π-accepting behavior of phosphines has been debated for many years. Conventional wisdom has traditionally maintained that the π-acceptor capability is facilitated through back donation from filled metal d-orbitals into empty low-lying phosphorus-3d orbitals,[5] but, recent theoretical calculations suggest that the frontier orbitals responsible for π-interactions consist primarily of phosphorus 3p character having local σ^* symmetry with no involvement of phosphorus-3d orbitals.[6] Highly electronegative substituents, such as -F, Cl, and OR, result in a highly polar P-X bond, which in turn, lowers the energy of the σ^* orbitals, making them more accessible for metal π-donation.

Unfortunately, it is difficult to separate σ and π contribution due to their inherent synergistic relationship.[7] Nonetheless, the importance of understanding metal-phosphine bonding has prompted the search for methods to quantify the individual contributions. Early methods of measuring phosphine donor strength were performed by measuring the

energy of the A_1 carbonyl stretching vibration for the monosubstituted Ni carbonyl complex, $Ni(CO)_3PR_3$.[8] The energy of this band provides an indication of the total donor ability ($\sigma + \pi$) of the phosphine. The more strongly donating a phosphine, the more electron density resides at the metal center. Consequently, the degree of π-accepting of the carbonyl groups will increase, resulting in a lowering of the carbonyl stretching frequencies. Therefore, strongly donating phosphines will result in lower values of ν(CO) for $Ni(CO)_3L$.

Another commonly used measure of phosphine donor strength is pK_a.[9] Values of pK_a for the conjugate acid R_3PH^+ provide an indication of the σ donor strength of the phosphine. However, it is often argued that these values are not a good measure of ligand donor strength because pK_a is a measure of the phosphine's affinity for a hard acid and not a soft transition metal. Furthermore, variations in phosphine size may result in differing solvation energies that will effect the pK_a. In spite of these considerations, pK_a values have been found to correlate well with other experimental observations regarding phosphine basicity.[10a,b]

Others have sought more quantitative methods to measure ligand σ and π effects; these have met with mixed success.[11] In particular, Giering *et al.* have divided phosphine ligands into three classes based upon the correlation of oxidation potential for the phosphine complex η^5-$MeCpMn(CO)_2PR_3$ and phosphine pK_a values:[11a]

Class I (σ-donor / π-donor)
PR_3 (R = Et, Bu, Cy, etc.)

Class II (σ-donor only)

PR_3 (R = Me), $PPh_{3-n}(R)_n$ (n = 1, 2; R = Me, Et, Bu)

$P(p\text{-X-Ph})_3$ (X = H, Me, OMe)

Class III (σ-donor / π-acceptor)

$P(OR)_3$ R = Et, Ph, Pr^i, Me

$P(p\text{-X-Ph})_3$ (X = F, Cl)

Similar correlations were found between pK_a, $E_{ox}°$, ν_{co}, cone angle and heats of reactions for other systems.[11a-f] Although Giering classified phosphine ligands in terms of π-acidity and π-basicity, it is important to stress that these π-effects are relatively small compared to those observed for true π-acids and bases such as CO or Cl^-. Furthermore, the classification system is specific to the particular system under investigation, although in practice, these class boundries differ only slightly.

In addition to varying the electronic properties of the phosphine, substitution of the R groups often affects the size of the ligand. Altering the size can have major ramifications on the subsequent chemistry of the phosphine, as in the case of phosphines with unusually large steric requirements, such as tricyclohexylphosphine, tri-tert-butylphosphine, tri-*o*-tolylphosphine and trimesitylphosphine; these ligands are capable of kinetically stabilizing metal complexes with low coordination numbers, thereby engendering electronically unsaturated metal centers that are highly reactive.[12] For example, bulky phosphines have been used to isolate a series of two-coordinate, 14-electron complexes of Pt^0 and Pd^0.[13] Although these systems are formally electron deficient, their reactivity is governed by the degree of steric overcrowding that is present.[14]

Another example of the use of bulky phosphines to stabilize electronically unsaturated metal centers is provided by the recent work of Kubas and co-workers who used sterically hindering phosphines to create coordinatively unsaturated Mo^0 and W^0 complexes with the general formula trans-$M(CO)_3(PR_3)_2$ (R = cyclohexyl, iso-propyl).[15] These 5-coordinate complexes are stabilized by an "agostic" interaction of a C-H bond on one of the phosphines with the metal center. This interaction is readily displaced in favor of small substrates including N_2 and H_2. One consequence of steric crowding is that these complexes tend to undergo intramolecular C-H bond activation to form metallated phosphine complexes.[16,17]

Whitesides and co-workers have used steric effects to generate a highly reactive "Pt^0L_2" fragment *in situ* by reductive elimination of neopentane from cis-Pt^{II}(dCype)H($CH_2C(CH_3)_3$) (dCype = bis(dicyclohexylphosphino)ethane, $(Cy)_2P(CH_2)_2P(Cy)_2$) (eq 1)[18] 14-electron complex activates a variety of aryl

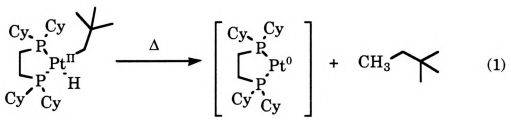

(1)

and aliphatic C-H bonds, but does not undergo intramolecular C-H activation, due, presumably, to the bent configuration of the dCype moiety, which precludes interaction of the C-H bonds of the cyclohexyl groups and affords the substrate better access to the metal center.[18]

The steric interactions of phosphines is also implicated in the activity of many homogenous catalysts by facilitating ligand dissociation that opens up coordination sites for an incoming substrate. Mechanistic studies of Wilkinson's catalyst, $Rh(PPh_3)Cl$, have shown that initial dissociation of

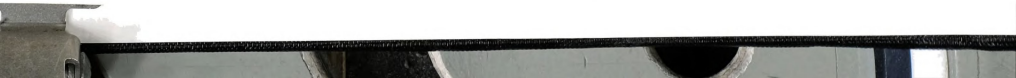

phosphine is a key step in olefin hydrogenation.[19] The size of the ancillary ligands also imparts selectivity to a number of reactions, a factor that is particularly important in the development of homogeneous catalysts for asymmetric synthesis.

Although it is certainly true that both steric and electronic properties of phosphine play a role in the reactivity and catalytic behavior of transition metal phosphine complexes, steric effects tend to dominate. In order to address the size of a phosphine ligand, the concept of cone angle, Θ, was developed by Tolman.[20] This method, which is based on rigid space filling models, defines the cone angle of a phosphine as the apex angle of a solid cone, centered 2.28 Å from the phosphorus atom, that encompasses the phosphine substituents atoms at their van der waal radii. Cone angles thus described have been found to correlate well with a number of spectroscopic and physical properties of transition metal phosphine complexes.[21] A more realistic description of ligand size was provided by the development of cone angle profiles.[22] This method, based on X-ray crystallographic data, accounted for the clefts and intermeshing of the phosphine substituents and gave a better indication of the true ligand requirements.

B. Development of Ether-Phosphines

An important aspect in any homogenous catalytic process is the availability of accessible coordination sites in which an incoming substrate molecule may bind.[23] Typical catalysts employing tertiary phosphine complexes rely on the steric bulk of the phosphine to promote ligand dissociation in order to create a coordinately unsaturated metal center. Another strategy is to incorporate weak donor atoms (e.g. solvent molecules) into the metal coordination sphere that can be easily displaced in favor of the incoming substrate. For example, recent work with zirconium

cyclopentadienyl systems has shown that replacement of a chloride ion with THF in the coordination sphere creates a highly reactive cationic metal center, capable of performing a variety of organic transformations.[24] A number of compounds that incorporate solvent into their coordination sphere have been found to be quite effective hydrogenation, hydroformylation and polymerization catalysts.[25] Furthermore, although many catalyst precursors use olefins as supporting ligands, under catalytic conditions, the olefins are hydrogenated and replaced by solvent to form the active catalyst (eq 2).[26]

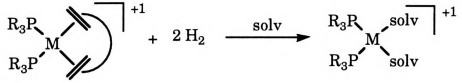

(2)

An alternative approach to the design of a new catalyst with open coordination sites is to structurally modify the ancillary phosphine ligands by incorporating weak donor groups directly into the phosphine. A variety of functional groups that are capable of acting as weak donors have been combined with phosphines to form polydentate ligands;[27] these provide additional stabilization to the complex by chelating to the metal center, but because of their weak donor nature these groups are easily displaced in favor of the incoming substrate. After the transformations are complete and the product dissociates, the tethered donor atom is able to quickly reassociate.[28] As a result of this "arm on/arm off" behavior, these functionalized ligands have been described as being hemi-labile.[29] A further advantage of a tethered donor group, particularly an oxygen donor atom, is the observed rate enhancement for oxidative addition reactions, which are well recognized as important steps in many catalytic processes.[30] These reactions are facilitated

by the presence of the oxygen atom, which provides anchimeric assistance to the oxidative addition of polar substrates.

The successful implementation of phosphine ligands bearing oxygen donor substituents to catalysis has been demostrated in a number of important reactions.[27] For example, Shells Higher Olefin Process (SHOP) uses a nickel complex ligated by the phosphino-carboxylate ligand, $Ph_2PCH_2CO_2H$, to selectively polymerize ethylene in the presence of other olefins.[31] Further work in this area was carried out by Knowles and co-workers who developed a series of chiral phosphines (shown below) that incorporate ortho substituted phenyl groups.[32] Cationic rhodium complexes supported by these chiral ligands successfully hydrogenate pro-chiral olefins, an important step in the synthesis of α-amino acids, achieving enantiomeric excesses > 95%. The asymmetric hydrogenation of

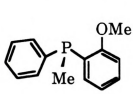

pamp

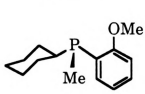

camp

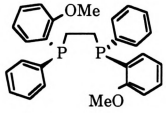

dipamp

(N-acylamino)-cinnamic acid catalyzed by the diphosphine complex $[Rh(cod)(diPAMP)]^{1+}$ (diPAMP = (R,R)-1,2-bis[2-methoxyphenyl)phenyl-phosphino]ethane), a key step in Monsanto's L-Dopa synthesis, represents the first commercialized catalytic asymmetric process.[33] The development of these catalysts ignited a revolution in the area of asymmetric hydrogenation promoted by transition metal complexes. Although the role of the ortho-methoxy group is primarily steric in nature, replacement of the methoxy substituent with sterically equivalent groups resulted in lower catalytic

activity, suggesting that the methoxy groups provide an electronic influence as well.[34]

Although a variety of donor groups, ranging from amines and thioethers to enolates and diketonates, have been used as functional groups on phosphine ligands, ether donors are the most prevalent.[27a] Being uncharged, ethers are very weak donors, which renders them highly highly labile, particularly for the soft late transition metals, with which they are relatively incompatible.

The first crystallographic evidence for the coordinating ability of a pendent ether group was reported for the Rh(III) arsine complex $RhCl_3[MeAs(o\text{-}C_6H_4(OMe)]_2$.[35] Later in the mid 1970's, research on the chemistry of ether-phosphines expanded due to the independent work of Roundhill, Rauchfuss and Shaw.[36] These groups were able to show that ortho-substituted phenylphosphines were capable of binding a variety of late transition metals through both the oxygen and phosphorus atoms. Rauchfuss found that the coordinated methoxy groups were loosely bound and could dissociate readily, thus generating vacant coordination sites. As a result, many of these complexes exhibit stereochemically non-rigid behavior and reversible substrate addition.

More recently, Lindner and co-workers have developed a comprehensive series of ether-phosphines in which the ether group is tethered by an ethylene group as opposed to a rigid phenyl ring.[37] In addition to being the first to use a more flexible linkage in a ether-phosphine ligand, Lindner has also pioneered the use of chiral and cyclic ether donors such as THF and dioxane. His work has focused on the use of these chelating phosphines for the development of catalysts that assist in the carbonylation of methanol to acetic acid. These phosphino-ether complexes, like others in

the same category, exhibit fluxional behavior, reversible substrate binding, and enhanced oxidative addition and reductive elimination chemistry promoted by the on/off nature of the ether donors. Others have found similar results with both mono- and di- phosphines containing pendent ether substituents.[38]

C. Chemical Aspects of Tris(2,4,6-trimethoxyphenyl)phosphine

Although the use and development of ether-phosphines is extensive, largely due to the recent efforts of Lindner *et al.*, none of the aforementioned systems have addressed the combined effects of high basicity and steric bulk on complex stability and reactivity. We are interested in developing the coordination chemistry of ether-phosphine ligands that combine steric bulk and strong donor capability with chelating ability to stabilize complexes in highly reactive and uncommon oxidation states. To this end, we have undertaken the comprehensive study of the coordination chemistry of the highly basic and sterically hindering ether-phosphine, tris(2,4,6-trimethoxyphenyl)phosphine (Figure 1).

The molecule tris(2,4,6-trimethoxyphenyl)phosphine, which we refer to as TMPP, was originally prepared by Soviet chemists in the late 1950's.[39] The phosphine later reappeared in literature in the mid 1980's, when Wada and co-workers described its extraordinarily high basicity (pK_a = 11.2) and steric properties (cone angle ~ 184°).[40] Wada has exploited the phosphine's unusual basic properties in a variety of organic transformations, including mild ring opening reactions of terminal epoxides and facile dealkylations.[41] More recently, the basicity and solubility properties of its phosphonium salts have been applied in the extraction of metal ions.[42] The unusual properties of this phosphine are derived from the presence of the methoxy groups in the ortho and para positions. The electron releasing nature of the methoxy

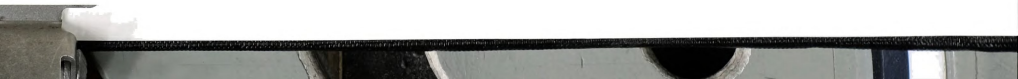

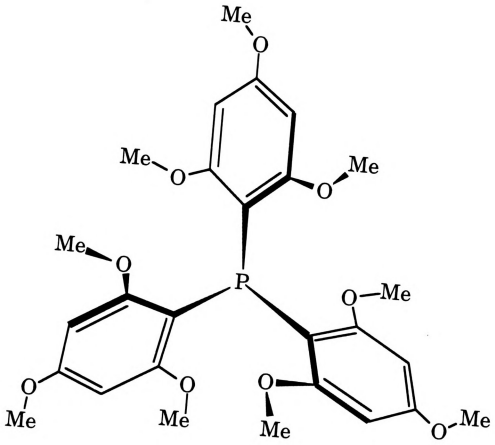

Figure 1. Schematic drawing of tris(2,4,6-trimethoxyphenyl) phosphine (TMPP).

substituents increases the nucleophilicity of the phosphorous lone pair via the mesomeric effect of the phenyl rings. The affect of sequential methoxy substitution at the ortho and para ring positions on the phosphine's basicity is shown in Table 1.[42b] As the number of methoxy substituents is increased, there is an increase in the basicity. Substitution of a -OMe group in the para position has a greater effect on the basicity than substitution in the ortho positions. In addition, the presence of two or more methoxy groups on one ring results in a dramatic increase in nucleophilicity of the phosphine. For example, the presence of one 2,6-dimethoxy substituted ring results in a higher basicity (pK_a = 5.39) than either of the tris 2-ortho- or para-substituted phosphines (pK_a = 4.47 and 4.75). In any event, there is an overall increase in phosphine basicity as the number of substituted aryl groups are increased. The electron donating effect of the methoxy groups is dramatically illustrated by the comparison of the pK_a of TMPP with that of the unsubstituted phosphine, triphenylphosphine (pK_a = 2.73).[43]

In addition to increasing the nucleophilicity, the presence of the methoxy groups in the 2 and 6 positions also serves to augment the steric bulk of the ligand. The cone angle of TMPP was reported by Wada and later confirmed by our group to be approximately 184°. Comparision with other phosphines reveals that TMPP is one of the most sterically encumbering phosphines known (Figure 2). The cone angle of TMPP is nearly 40° larger than that of triphenylphosphine, commonly considered a sterically hindering ligand (cone angle = 145°).[20] As evidenced by the results of numerous studies, sterically encumbering ligands lend kinetic stability to normally very reactive transition metal centers, thus creating electron deficient complexes. Such complexes would be expected to exhibit unusual reactivity not normally observed for complexes ligated by more conventional ligands.

Table 1. pK_a values for methoxy substituted triphenylphosphines (from reference 42b).

	2-MeO	4-MeO	2,6-MeO	2,4,6-MeO
$(x\text{-}MeOPh)_3P$	4.47	4.75	9.33	11.2
$(x\text{-}MeOPh)_2PPh$	4.01	4.06	7.28	8.22
$(x\text{-}MeOPh)PPh_2$	3.33	3.67	5.39	5.77

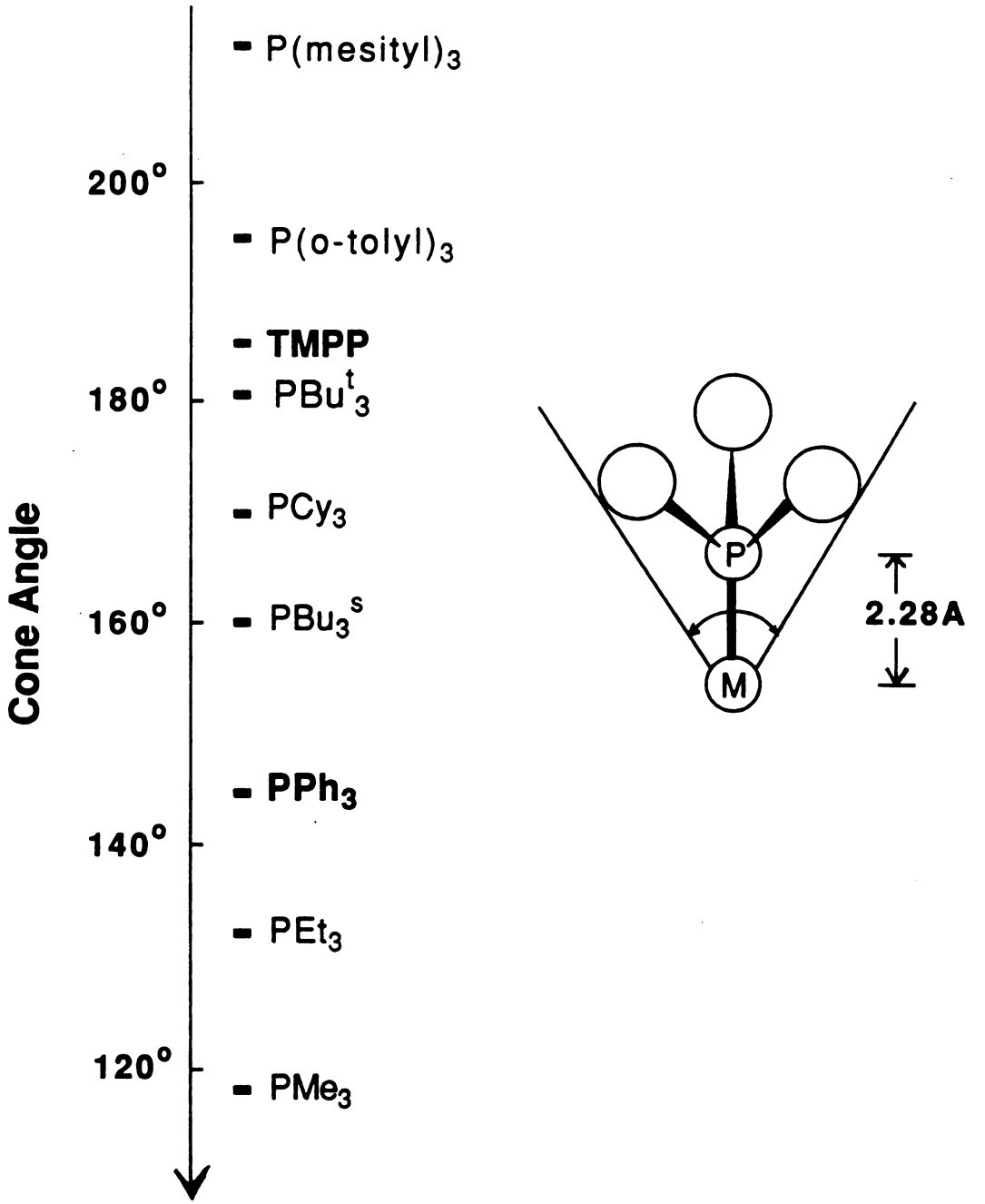

Figure 2. Tolman cone angles for various tertiary phosphines.

Perhaps most importantly for the purpose of our research goals, the presence of ether donors in the ortho positions provide the opportunity for multidentate coordination modes for the phosphine. Unlike other ether-phosphines that contain only one ether substituents, the presence of methoxy groups in the ortho positions of all three aryl rings allow for TMPP to participate in η^1 through η^3 bonding arrangements (Figure 3). Most other ether-phosphines typically have only one ether donor and therefore may only participate in η^1 or η^2 type bonding. The multiple chelating ability of TMPP will be of paramount importance in this work for the stabilization of coordinatively unsaturated, electronic deficient, metal diphosphine complexes. Moreover, the multidentate capabilities afford versatility, by facilitating adjustments to the electronic requirements dictated by the metal center. As the electronic requirements of the metal change, TMPP compensates by altering its bonding mode. As a result, the phosphine may accommodate a number of different metal oxidation states. The physical and structural properties of TMPP and its corresponding oxide are fully described in Chapter 2.

The combination of the chelate effect provided by the multidentate capability of TMPP, together with the kinetic stability afforded by the steric size of the ligand, render TMPP an excellent ligand to stabilize highly reactive metal centers in unusual oxidation states. Moreover, unlike other transition metal complexes stabilized by bulky phosphines, the presence of hemi-labile ether donors will provide these complexes with open coordination sites in which further chemistry, particularly with small substrates, may take place. Interestingly, with the exception of our work, only four reports of transition metal TMPP complexes have appeared in the literature.[44]

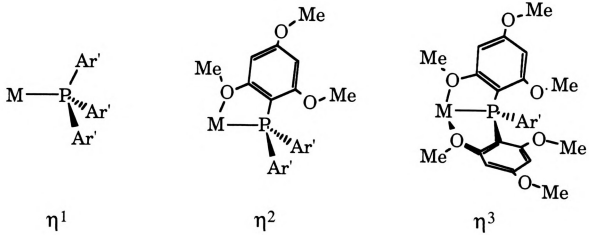

Figure 3. η^1, η^2 and η^3 bonding modes of TMPP.

D. Chemistry of Mononuclear Rh(II) Complexes

Based on these considerations, our goal is to exploit the unique properties of TMPP in order to stabilize, isolate and study the chemistry of odd electron transition-metal systems. We are particularly interested in the chemistry of mononuclear d^7 rhodium complexes. A survey of the literature reveals that the bulk of rhodium coordination and organometallic chemistry is dominated by the catalytically important +1 and +3 oxidation states.[45] These oxidation states form the basis for oxidative addition and reductive elimination reactions that are key steps in many important catalytic processes.[46] In contrast to the ubiquity of mononuclear Rh(I) and Rh(III) complexes, the chemistry of the paramagnetic, divalent oxidation state remains relatively unexplored. Generally, these species exist only as highly reactive, fleeting intermediates or as impurities in the chemistry of d^6 and d^8 rhodium.[47] The lack of stability of mononuclear Rh(II) complexes is a result of the proclivity of these systems to (a) dimerize to form a metal-metal bonded species and (b) disproportionate to the more stable Rh(I) and Rh(III) oxidation states. These factors notwithstanding, a number of the Rh(II) metallo-radicals are known.[48]

Under suitable conditions, sterically encumbering phosphines react with Rh(III) trihalides in alcohol to yield paramagnetic Rh(II) compounds formulated as *trans*-$RhCl_2(PR_3)_2$ (PR_3= PCy_3, P(*o*-tolyl)$_3$, $P(Bu^t)_2Me$).[49] With a few exceptions, these complexes are poorly characterized, prone to decomposition and invariably contaminated with diamagnetic hydrido species. As a result, there has been no comprehensive investigation of the chemistry of these paramagnetic species undertaken and only a few studies have appeared.[50] In fact, only recently, the first structural studies of such

species were finally reported.[51,52] Paramagnetic mononuclear species of rhodium that are coordinated by less sterically demanding ligands are also known; these complexes , however, are ligated by "non-innocent" ligands in which extensive delocalization of the unpaired electron is possible.[56] Typically, such species are not considered to be authentic metallo-radicals.

In addition to the aforementioned phosphine complexes, a variety of meta-stable mononuclear Rh(II) complexes have been generated by electrochemical oxidation and reduction of Rh(III) and Rh(I) species.[53] Few stable mononuclear Rh(II) organometallic complexes have been reported; many of these exist as short-lived intermediates and hence are poorly characterized.[54] A recent exception is the unprecedented Rh(II) dialkyl species $Rh(2,4,6\text{-}Pr^{i}_{3}C_{6}H_{2})_{2}(tht)_{2}$ (tht = tetrahydrothiophene) prepared by Wilkinson and co-workers from $Rh^{III}Cl_{3}(tht)_{3}$.[55] This complex is one of the rare examples of a paramagnetic Rh(II) complex to be structurally characterized by X-ray crystallography.

By far the most promising results for Rh(II) complexes have been found in the realm of Rh(II) porphyrin chemistry. Highly reactive, short-lived Rh(II) species have been implicated in a number of unusual and fundamental organometallic reactions involving mononuclear and dinuclear rhodium porphyrin complexes.[57] Wayland and co-workers have reported strategies that favor the existence of these paramagnetic intermediates that involve introducing bulky substituents onto the porphyrins that discourage metal-metal bond formation through steric interactions. By studying such key systems, they were able to isolate Rh(II) radicals that reversibly couple carbon monoxide to form dimetal-α-diketones (eq 3 - 5).[58] Through the use of even more sterically demanding porphyrins, dimerization of the carbonyl radicals is disfavored and a 17 electron Rh(II) monocarbonyl species may be

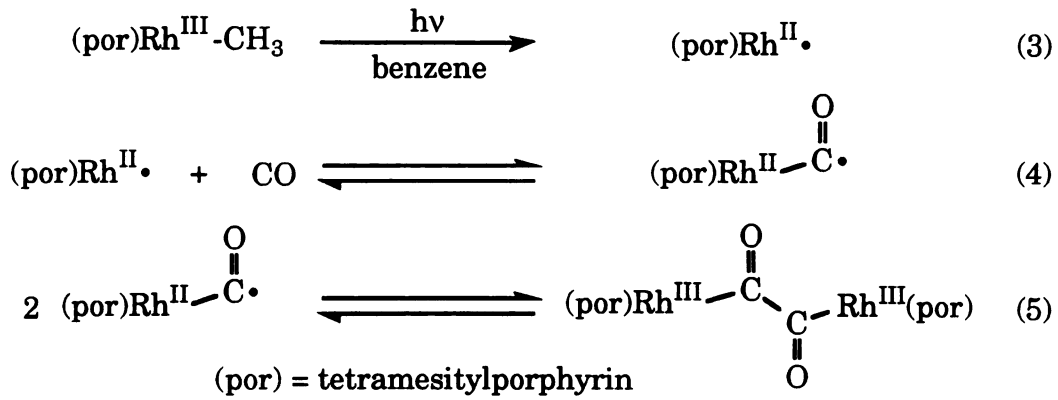

observed directly.[58c] In contrast to other 17 electron d^7 carbonyl complexes, the nonlinear RhCO• unit behaves as an acyl radical, undergoing reactions at the carbon and not at the metal center. Even more fascinating are the recent reports that these Rh(II) porphyrin systems reversibly and selectively activate methane to form Rh(III)-hydride and Rh(III)-alkyl species (eq 6).[59] Thermodynamic data point to the presence of a linear four-centered transition state that precludes the activation of aromatic C-H bonds due to steric inhibition by the porphyrin ligands. As a result, these Rh(II) porphyrin systems are highly selective towards the activation of alkyl versus aryl C-H bonds. Recent results by Wayland and co-workers indicate that these Rh(II) metalloradicals also react with acrylates to produce C-C bonded oligomers.[60]

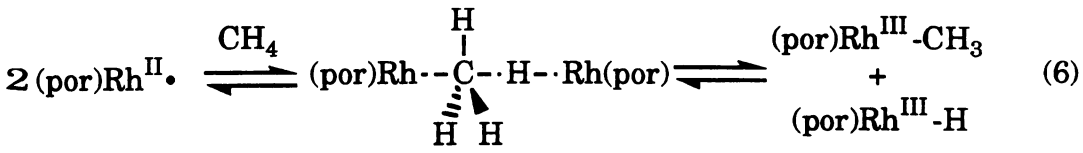

In light of these recent results, the study of rhodium based odd electron systems is becoming an important area of research. In general, these species

must be afforded kinetic stabilization by sterically encumbering ligands that preclude dimerization. In the case of Rh(II), further stabilization must be provided by electronic factors that favor the +2 oxidation state relative to the +1 and +3 oxidation states, hence avoiding undesirable disproportionation reactions. The work in this thesis supports the use of TMPP as a good candidate for providing the proper combination of kinetic and thermodynamic stability for the isolation of mononuclear Rh(II) complexes. As a backdrop for this work we note that Shaw and co-workers had earlier demonstrated that mixed phosphorus and oxygen donor chelate ligands are capable of stabilizing d^7 metal centers.[61] Reactions of $P(Bu^t)_3(o\text{-}MeOC_6H_4)$ with $MCl_3 \cdot xH_2O$ (M = Rh, Ir) in refluxing alcohol produced the paramagnetic mononuclear Rh(II) and Ir(II) complexes, $M(P(Bu^t)_2(o\text{-}OC_6H_4))_2$ (eq 7). During the reaction the metals are reduced from M(III) to M(II) and the phosphine undergoes dealkylation to form a phosphino-phenoxide chelating ligand. The Ir complex represents one of the few crystallographically characterized examples of a stable Ir(II) mononuclear species. The remarkable stability of these species illustrates the potential for other bulky mixed P,O chelates to stabilize odd

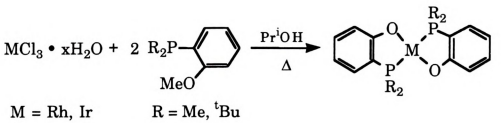

(7)

electron systems.

This thesis reports the results of investigations concerning the isolation and reactivity of paramagnetic Rh(II) centers using the triaryl phosphine ligand TMPP. Our entry into the area of mononuclear d^7 rhodium

chemistry began with the synthesis of the bis-phosphine complex [*cis*-Rh(η^3-TMPP)$_2$][BF_4]$_2$ from a reaction between TMPP and the solvated dinuclear salt [$Rh_2(MeCN)_{10}$][BF_4]$_4$. The details of the synthesis and characterization of this metalloradical is presented in chapter 3 together with its associated redox chemistry. Chapter 4 examines in detail the reversible CO chemistry that was observed for [*cis*-Rh(η^3-TMPP)$_2$][BF_4]$_2$. This rather complicated chemistry involves the disproportionation of [Rh^{II}(η^3-TMPP)$_2$]$^{2+}$ to give Rh(I) carbonyl and Rh(III) species that upon loss of CO, recombine to form the original Rh(II) species. The reversible CO behavior of the Rh(I) carbonyl species is examined more closely in chapter 5, wherein we describe the potential application of this process for the development of a CO sensing composite material by incorporation the Rh(I) carbonyl species into a porous sol-gel derived glass. As an extension of the reversible CO chemistry discussed in chapter 3, reactions of [Rh(η^3-TMPP)$_2$][BF_4]$_2$ with isocyanide ligands is presented in chapter 6. Unlike the complex electron transfer chemistry that was observed with CO, the weaker π-acidity of isocyanides allows for the isolation of paramagnetic Rh(II) diisocyanide complexes, rare examples of stable organometallic Rh(II) complexes. The redox properties and reactivity of these organometallic species are also discussed. Chapter 7 examines the effect of nucleophiles on the stability of Rh(II) and Rh(III) bis-TMPP complexes. Nucleophilic attack on [Rh(η^3-TMPP)$_2$][BF_4]$_2$ results in dealkylation of a coordinated methoxy substituent to yield a Rh(II) complex stabilized by a phosphino-phenoxide interaction. The chemistry of this species is discussed along with its relationship to analogous Rh(III) compounds formed from dealkylation reactions of [Rh(η^3-TMPP)$_2$][BF_4]$_3$. Chapter 8 discusses the formation of Rh(I) and Ir(I) olefin species with TMPP and the subsequent formation of the Ir(I) dicarbonyl cation

$[Ir(TMPP)_2(CO)_2]^{1+}$, which, unlike its rhodium counterpart, is stable with respect to CO loss. Attempts to oxidize this complex to yield an Ir(II) species are also presented. Finally, the application of the η^3-bonding mode to group VI metal tricarbonyl fragments is presented in Appendix B. Specifically, the isolation and characterization of the highly fluxional molecular species (η^3-TMPP)$Mo(CO)_3$ is discussed.

List of References

1. McAuliffe, C. A. In *Comprehensive Coordination Chemistry;* Wilkinson, G.; Gillard, R. D.; McCleverty, J. A., eds.; Pergamon: Oxford, **1987**, chapter 14, p 989.

2. (a) Pignolet, L. H. *Homogeneous Catalysts with Metal Phosphine Complexes*; Plenum: New York, **1983**. (b) Parshall, G. W. *Homogeneous Catalysis: The Applications and Chemistry of Catalysis by Soluble Transition Metal Complexes*; Wiley: New York, **1980**. (c) Cornils, B. In *New Syntheses with Carbon Monoxide*; Falbe, J., ed.; Springer-Verlag: Berlin, **1980**. (d) *Catalytic Aspects of Metal Phosphine Complexes, Advances in Chemistry Series 196*; Alyea, E. C.; Meek, D. W. Eds.; American Chemical Society: Washington, D. C. **1982**. (e) Hughes, R. P. in *Comprehensive Organometallic Chemistry*; Wilkinson, G.; Stone, F. G. A.; Abel, E. W., eds.; Pergamon: New York, **1982**; vol. 5, p 228.

3. Collman, J. P.; Hegedus, L. S.; Norton, J. R.; Finke, R. G. *Principles and Applications of Organotransition Metal Chemistry*; University Science Books: Mill Valley, Ca. **1987**.

4. Cotton, F. A.; Wilkinson, G.; *Advanced Inorganic Chemistry, 5th ed.*; Wiley: New York, **1988**, pp 64-68.

5. For instance, see Huheey, J. E. *Inorganic Chemistry*; Harper and Row: New York, **1983**; p 832.

6. (a) Marynick, D. S. *J. Am. Chem. Soc.* **1984**, *106*, 4064. (b) Xiao, S.; Trogler, W. C.; Ellis, D. E.; Berkovitch-Yellin, Z. *J. Am. Chem. Soc.* **1983**, *105*, 7033. (c) Whango, M. H.; Steward, K. R. *Inorg. Chem.* **1982**, *21*, 1720.

7. Honeychuck, R. V.; Hersh, W. H. *Inorg. Chem.* **1987**,*26*, 1826.

8. Tolman, C. A. *J. Am. Chem. Soc.* **1970**, *92*, 2953.

9. (a) Allman, T.; Goel, R. G. *Can. J. Chem.* **1982**,*60*, 716. (b) Henderson, W. A.; Streuli, C. A. *J. Am. Chem. Soc.* **1960**,*82*, 5791. (c) Streuli, C. A. *Anal. Chem.* **1960**,*32*, 985. (d) Schuster-Woldan, H. G.; Basolo, F. *J. Am. Chem. Soc.* **1966**, *88*, 1657.

10. (a) Golovin, M. N.; Rahman, Md. M.; Belmonte, J. E.; Giering, W. P. *Organometallics* **1985**,*4*, 1981. (b) Rahman, Md. M.; Liu, H.-Y.; Prock, A.; Giering, W. P. *Organometallics* **1987**, *6*, 650. (c) Dahlinger, K.; Falcone, F.; Pöe, A. J. *Inorg. Chem.* **1986**, *25*, 2654.

11. (a) Rahman, Md. M.; Liu, H.-Y.; Prock, A.; Giering, W. P. *Organometallics* **1989**,*8*, 1. (b) Eriks, K.; Giering, W. P.; Liu, H.-Y.; Prock, A. *Inorg. Chem.* **1989**,*28*, 1759. (c) Liu, H.-Y.; Eriks, K.; Prock,

A.; Giering, W. P. *Organometallics*, **1990**, *9*, 1758. (d) Pöe, A. J. *Pure Appl. Chem.* **1988**, *60*, 1209. (e) Zizelman, P. M.; Amatore, C.; Kochi, J. K. *J. Am. Chem. Soc.* **1984**, *106*, 3771. (f) Nolan, S. P.; Hoff, C. D. *J. Organomet. Chem.* **1985**, *290*, 365. (g) Bush, R. C.; Angelici, R. J. *Inorg. Chem.* **1988**, *27*, 681. (h) Bodner, G. M.; May, M. P.; McKinney, L. E. *Inorg. Chem.* **1980**, *19*, 1951. (i) Colton, R.; Tomkins, I. B., *Aust. J. Chem.* **1967**, *19*, 1143. (j) Graham, W. A. G. *Inorg. Chem.* **1968**, *7*, 315. (k) Treichel, P. M. *Inorg. Chem.* **1968**, *7*, 1942.

12. Clark, H. C.; Hampden-Smith, M. J. *Coord. Chem. Rev.* **1987**, *79*, 229.

13. (a) Immirzi, A.; Musco, A. A. *J. Chem. Soc., Chem. Commun.* **1974**, 400. (b) Immirzi, A.; Musco, A.; Zambelli, P.; Carturan, G. *Inorg. Chem. Acta* **1975**, *13*, L13. (c) Matsumoto, M.; Yoshida, H.; Nakatsu, N.; Yoshida, T.; Otsuka, S. *J. Am. Chem. Soc.* **1974**, *96*, 3322. (d) Moynihan, K. J.; Chieh, C.; Goel, R. G. *Acta Cryst.* **1979**, *B35*, 3060. (e) Otsuka, S.; Yoshida, T.; Matsumoto, M.; Nakatsu, K. *J. Am. Chem. Soc.* **1976**, *98*, 5850. (f) Yoshida, T.; Yamagata, T.; Tulip, T. H.; Ibers, J. A.; Otsuka, S. *J. Am. Chem. Soc.* **1978**, *100*, 2063.

14. (a) Clark, H. C.; Hampden-Smith, M. J. *J. Am. Chem. Soc.* **1986**, *108*, 3829. (b) Clark, H. C.; Ferguson, G.; Hampden-Smith, M. J.; Kaitner, B.; Ruegger, H. *Polyhedron*, **1988**, *7*, 1349. (c) Forries, J.; Green, M. L. H.; Spencer, J. L.; Stone, F. G. A. *J. Chem. Soc., Dalton Trans.* **1977**, 1006. (d) Yoshida, T.; Otsuka, S. *J. Am. Chem. Soc.* **1977**, *99*, 2134.

15. (a) Kubas, G. J. *J. Chem. Soc., Chem. Commun.* **1980**, 61. (b) Kubas, G. J.; Ryan, R. R.; Swanson, B. I.; Vergamini, P. J.; Wasserman, H. J. *J. Am. Chem. Soc.* **1984**, *106*, 451. (c) Kubas, G. J.; Ryan, R. R.; Wrobleski, D. A. *J. Am. Chem. Soc.* **1986**, *108*, 1339. (d) Wasserman, H. J.; Kubas, G. J.; Ryan, R. R. *J. Am. Chem. Soc.* **1986**, *108*, 2294. (e) Kubas, G. J.; Unkefer, C. J.; Swanson, B. I.; Fukushima, E. *J. Am. Chem. Soc.* **1986**, *108*, 7000. (f) Kubas, G. J. *Acc. Chem. Res.* **1988**, *21*, 120. (g) Kubas, G. J. *Comments Inorg. Chem.* **1988**, *7*, 17.

16. Examples of cyclometallation in Pt^0 and Pd^0 complexes: (a) Clark, H. C.; Goel, A. B.; Goel, R. G.; Ogini, W. *J. Organomet. Chem.* **1978**, *157*, 219. (b) Clark, H. C.; Goel, A. B.; Goel, S. *Inorg. Chem.* **1979**, *18*, 2803. For reviews of cyclometallation reactions see: (c) Omae, I. *Coord. Chem. Rev.* **1980**, *32*, 235. (d) Dehand, J.; Pfeffer, M. *Coord. Chem. Rev.* **1976**, *18*, 327. (e) Bruce, M. I. *Angew Chem., Int. Ed. Engl.* **1977**, *16*, 73. (f) Parshall, G. W. *Acc. Chem. Res.* **1970**, *3*, 139.

17. (a) Crabtree, R. H.; Holt, E. M.; Lavin, M.; Morehouse, S. M. *Inorg. Chem.* **1985**, *24*, 1986. (b) Shaw, B. L. *J. Am. Chem. Soc.* **1975**, *97*, 3856. (c) Jones, C. E.; Shaw, B. L.; Turtle, B. L. *J. Chem. Soc., Dalton Trans.* **1974**, 992. (d) Cheney, A. J.; Shaw, B. L. *J. Chem. Soc., Dalton Trans.* **1972**, 754.

18. (a) Hackett, M.; Whitesides, G. M. *J. Am. Chem. Soc.* **1988**, *110*, 1449. (b) Hackett, M.; Ibers, J. A.; Whitesides, G. M. *J. Am. Chem. Soc.* **1988**, *110*, 1436. (c) Hackett, M.; Ibers, J. A.; Jernakoff, P.; Whitesides, G. M. *J. Am. Chem. Soc.* **1986**, *108*, 8094.

19. (a) Halpern, J. *Inorg. Chem. Acta* **1981**,*50*, 11. (b) Halpern, J.; Wong, C. S. *J. Chem. Soc., Chem. Commun.* **1973**, 629. (c) Halpern, J.; Okamoto, T.; Zakhariev, A. *J. Mol. Catal.* **1977**,*2*, 65.

20. (a) Tolman, C. A. *Chem. Rev.* **1977**, *77*, 313.

21. McAuliffe, C. A. In *Comprehensive Coordination Chemistry;* Wilkinson, G.; Gillard, R. D.; McCleverty, J. A., eds.; Pergamon: Oxford, **1987**, chapter 14, p 1027.

22. (a) Ferguson, G.; Alyea, E. C.; Dias, S. A.; Restivo, R. J. *Inorg. Chem.*, **1977**, *16*, 2329. (b) Ferguson, G.; Alyea, E. C.; Khan, M. *Inorg. Chem.* **1978**, *17*, 2965. (c) Ferguson, G.; Alyea, E. C., Dias, S. A.; Pavez, M. *Inorg. Chem. Acta.* **1979**, *37*, 45. (d) Aylea, E. C.; Ferguson, G.; Somogyvari, A. *Inorg. Chem.* **1982**, *21*, 1369. (e) Aylea, E. C.; Ferguson, G.; Siew, P. Y. *Can. J. Chem.* **1983**, *61*, 257. (f) Ferguson, G.; Siew, P. Y.; Goel, A. B. *J. Chem. Res.* **1979**, 4337. (g) Richardson, J. F.; Payne, N. C. *Can. J. Chem.* **1977**, *55*, 3203. (h) Smith, J. D.; Oliver, J. D. *Inorg. Chem.* **1978,** *17*, 2585.

23. Crabtree, R. H. *Comments Inorg. Chem.* **1985**, *4*, 229.

24. (a) Guram, A. S.; Jordan, R. F.; Taylor, D. F. *J. Am. Chem. Soc.* **1991**, *113*, 1833. (b) Jordan, R. F.; Bradley, P. K.; Baenziger, N. C.; LaPointe, R. E. *J. Am. Chem. Soc.* **1990**, *112*, 1289. (c) Jordan, R. F.; LaPointe, R. E.; Baenziger, N.; Hinch, G. D. *Organometallics*, **1990**, *9*, 1539. (d) Jordan, R. F.; Taylor, D. F.; Baenziger, N. C. *Organometallics* **1990**, *9*, 1546. (e) Guram, A. S.; Jordan, R. F. *Organometallics* **1990**, *9*, 2190. (f) Jordan, R. F.; Guram, A. S. *Organometallics* **1990**, *9*, 2116. (g) Jordan, R. F.; Bradley, P. K.; LaPointe, R. E.; Taylor, D. F. *New J. Chem.* **1990**, *14*, 505. (h) Jordan, R. F.; LaPointe, R. E.; Bradley, P. K.; Baenziger, N. *Organometallics* **1989**, *8*, 2892. (i) Jordan, R. F.; Taylor, D. F. *J. Am. Chem. Soc.* **1989**, *111*, 778. (j) Jordan, R. F.; Bajgur, C. S.; Dasher, W. E.; Rheingold, A. L. *Organometallics* **1987**, *6*, 1041. (k) Jordan, R. F.; Bajgur, C. S.; Willet, R.; Scott, B. *J. Am. Chem. Soc.* **1986**, *108*, 7410. (l) Jordan, R. F.; LaPointe, R. E.; Bajgur, C. S.; Echols, S. F.; Willett, R. *J. Am. Chem. Soc.* **1987**, *109*, 4111.

25. (a) Sen, A. *Acc. Chem. Res.* **1988**, *21*, 421 and references therein. (b) Sen, A.; Lai, T.-W. *Organometallics*, **1984**, *3*, 866. (c) Sen, A.; Lai, T.-W. *Organometallics*, **1982**, *1*, 415.

26. (a) Crabtree, R. *Acc. Chem. Res.* **1979**, *12*, 331 and references therein. (b) Schrock, R. R.; Osborn, J. A. *J. Am. Chem. Soc.* **1976**, *98*, 2134. (c) Schrock, R. R.; Osborn, J. A. *J. Am. Chem. Soc.* **1976**, *98*, 2143.

27. For recent reviews on functionalized phosphines see: (a) Bader, A.; Lindner, E. *Coord. Chem. Rev.* **1991**, *108*, 27. and references therein. (b) Rauchfuss, T. B. *Homogeneous Catalysis with Metal Phosphine Complexes;* L. Pignolet, Ed.: Plenum, New York, **1983**, 239.

28. (a) Horner, L.; Simons, G. *Z. Naturforsch.* **1984**, *39b*, 504. (b) Horner, L.; Simons, G. *Z. Naturforsch.* **1984**, *39b*, 512.

29. Jeffrey, J. C.; Rauchfuss, T. B. *Inorg. Chem.* **1979**, *18*, 2658.

30. (a) Miller, E. M.; Shaw, B. L. *J. Chem. Soc., Dalton Trans.* **1974**, 480. (b) Empsall, H. D.; Hyde, E. M.; Jones, C. E.; Shaw, B. L. *J. Chem. Soc., Dalton Trans.* **1974**, 1980.

31. (a) Keim, W.; Behr, A.; Gruber, B.; Hoffmann, B.; Kowaldt, F. H.; Kürschner, U.; Limbäcker, B.; Sistig, F. P. *Organometallics* **1986**, *5*, 2356 and references therein. (b) Keim, W.; Kowaldt, F. H.; Goddard, R.; Krüger, C. *Angew. Chem., Int. Ed. Engl.* **1978**, *17*, 466. (c) Freitas, E. R.; Gum, C. R. *Chem. Engin. Progr.* **1979**, *75*, 73. (d) Peuckart, M.; Keim. W. *Organometallics* **1983**, *2*, 594.

32. (a) Knowles, W. S. *Acc. Chem. Res.* **1983**, *16*, 106 and references therein. (b) Knowles, W. S.; Sabacky, M. J.; Vineyard, B. D. *Adv. Chem Ser.* **1974**, *132*, 274. (c) Knowles, W. S.; Sabacky, M. J.; Vineyard, B. D. *J. Chem. Soc., Chem. Commun.* **1972**, 10.

33. (a) Vineyard, B. D.; Knowles, W. S., Sabacky, M. J.; Bachman, G. C.; Weinkauff, D. J. *J. Am. Chem. Soc.* **1977**, *99*, 5946. (b) Knowles, W. S.; Sabacky, M. J.; Vineyard, B. D.; Weinkauff, D. J. *J. Am. Chem. Soc.* **1975**, *97*, 2567.

34. Studies relavent to the mechanism of asymmetric hydrogenation by Rh-dipamp complexes: (a) Landis, C. R.; Halpern, J. *J. Am. Chem. Soc.* **1987**, *109*, 1746. (b) Halpern, J. *Pure & Appl. Chem.* **1983**, *55*, 99. (c) Brown, J. M.; Maddox, P. J. *J. Chem. Soc., Chem. Commun.* **1987**, 1276. (d) Alcock, N. W.; Brown, J. M.; Derome, A. E.; Lucy, A. R. *J. Chem. Soc., Chem. Commun.* **1985**, 575. (e) Brown, J. M.; Cutting, I. *J. Chem. Soc., Chem. Commun.* **1985**, 578. (f) Brown, J. M.; Chaloner, P. A.; Morris, G. A. *J. Chem. Soc., Chem. Commun.* **1983**, 664. (g) Brown, J. M.; Parker, D. *J. Chem. Soc., Chem. Commun.* **1980**, 342. (h) Brown, J. M.; Chaloner, P. A. *J. Chem. Soc., Chem. Commun.* **1980**, 344.

35. Graziani, R.; Bombieri, G.; Volponi, L.; Panattoni, C. *J. Chem. Soc. (A)* **1969**, 1236.

36. (a) Mason, R.; Thomas, K. M.; Empasall, H. D.; Fletcher, S. R.; Heys, P. N.; Hyde, E. M. Jones, C. E; Shaw, B. L. *J. Chem. Soc., Chem. Comm.* **1974**, 612. (b) Jones, C. E.; Shaw, B. L.; Turtle, B. L. *J. Chem. Soc., Dalton Trans.* **1974**, 993. (c) Rauchfuss, T. B.; Patino, F. T.; Roundhill, D. M. *Inorg. Chem.* **1975**, *14*, 652. (d) Jeffrey, J. C.; Rauchfuss, T. B. *Inorg. Chem.* **1979**, *18*, 2658.

37. (a) Lindner, E.; Rothfuß, H.; Fawzi, R.; Hiller, W. *Chem. Ber.* **1992**, *125*, 541. (b) Lindner, E.; Bader, A.; Mayer, H. A. *Z. Anorg. Allg. Chem.* **1991**, *598/599*, 235. (c) Lindner, E.; Dettinger, J.; Möckel, A. *Z. Naturforsch.* **1991**, *46b*, 1519. (d) Lindner, E.; Dettinger, J. *Z. Naturforsch.* **1991**, *46b*, 432. (e) Lindner, E.; Reber, J.-P. *Z. Naturforsch.* **1991**, *46b*, 1581. (f) Lindner, E.; Karle, B. *Chem. Ber.* **1990**, *123*, 1469. (g) Lindner, E.; Norz, H. *Chem. Ber.* **1990**, *123*, 459. (h) Lindner, E.; Bader, A.; Braunling, H.; Jira, R. *J. Mol. Catal.* **1990**, *57*, 291. (i) Lindner, E.; Fawzi, R.; Mayer, H. A.; Eichele, K.; Pohmer, K. *J. Organomet. Chem.* **1990**, *386*, 63. (j) McCann, G. M.; Carvill, A.; Lindner, E.; Karle, B.; Mayer, H. A. *J. Chem. Soc., Dalton Trans.* **1990**, 3107. (k) Lindner, E.; Karle, B. *Chem. Ber.* **1990**, *123*, 1464. (l) Lindner, E.; Karle, B. *Z. Naturforsch.* **1990**, *45b*, 1108. (m) Lindner, E.; Speidel, R. *Z. Naturforsch.* **1989**, *44b*, 437. (n) Lindner, E.; Norz, H. *Z. Naturforsch.* **1989**, *44b*, 1493. (o) Lindner, E.; Reber, J. P.; Wegner, P. *Z. Naturforsch.* **1988**, *43b*, 1268. (p) Lindner, E.; Andres, B. *Z. Naturforsch.* **1988**, *43b*, 369. (q) Lindner, E.; Schober, U. *Inorg. Chem.* **1988**, *27*, 212. (r) Lindner, E.; Andres, B. *Chem. Ber.* **1988**, *121*, 829. (s) Lindner, E.; Sickinger, A.; Wegner, P. *J. Organomet. Chem.* **1988**, *349*, 75. (t) Lindner, E.; Meyer, S. *J. Organomet. Chem.* **1988**, *339*, 193. (u) Lindner, E.; Andres, B. *Chem. Ber.* **1987**, *120*, 761. (v) Lindner, E.; Schober, U.; Fawzi, R.; Hiller, W.; Englert, U.; Wegner, P. *Chem. Ber.* **1987**, *120*, 1621. (w) Lindner, E.; Meyer, S.; Wegner, P.; Karle, B.; Sickinger, A.; Steger, B. *J. Organomet. Chem.* **1987**, 335, 59. (x) Lindner, E.; Schober, U.; Stängle, M. *J. Organomet. Chem.* **1987**, *331*, C13. (y) Lindner, E.; Schrober, U.; Glaser, E.; Norz, H.; Wegner, P. *Z. Naturforsch.* **1987**, *42b*, 1527. (z) Lindner, E.; Scheytt, C.; Wegner, P. *J. Organomet. Chem.* **1986**, *308*, 311. (aa) Lindner, E.; Scheytt, C. *Z. Naturforsch.* **1986**, *41b*, 10. (bb) Lindner, E.; Mayer, H. A.; Wegner, P. *Chem. Ber.* **1986**, *119*, 2616. (cc) Lindner, E.; Sickinger, A.; Wegner, P. *J. Organomet. Chem.* **1986**, *312*, C37. (dd) Lindner, E.; Raudeler, H.; Scheytt, C.; Mayer, H. A.; Hiller, W.; Fawzi, R.; Wegner, P. *Z. Naturforsch.* **1984**, *39b*, 632.

38. (a) Mason, M. R.; Verkade, J. G. *Organometallics* **1992**, *11*, 1514. (b) Mason, M. R.; Verkade, J. G.; *J. Am. Chem. Soc.* **1991**, *113*, 6309. (c) Mason, M. R.; Su, Y.; Jacobson, R. A.; Verkade, J. G. *Organometallics* **1991**, *10*, 2335. (d) Werner, H.; Stark, A.; Shulz, M.; Wolf, J. *Organometallics* **1992**, *11*, 1126. (e) Werner, H.; Hampp, A.; Peters, K.; Peters, E. M.; Walz, L.; von Schnering, H. G. *Z. Naturforsch.* **1990**, *45b*, 1548. (f) Anderson, G. K.; Kumar, R. *Inorg. Chem.* **1984**, *23*, 4064. (g) Anderson, G. K.; Corey, E. R.; Kumar, R. *Inorg. Chem.* **1987**, *26*, 97.

(h) Anderson, G. K.; Kumar, R. *Inorg. Chim. Acta.* **1988**, *146*, 89. (i) Alcock, N. W.; Platt, A. W. G.; Pringle, P. G. *J. Chem. Soc., Dalton Trans.* **1989**, 2069. (j) Reddy, V. V. S.; Whitten, J. E.; Redmill, K. A.; Varshney, A.; Gray, G. M. *J. Organomet. Chem.* **1989**, *372*, 207. (k) Reddy, V. V. S.; Varshney, A.; Gray, G. M. *J. Organomet. Chem.* **1990**, *391*, 259.

39. (a) Protopopov, I. S.; Kraft, M. Y. *Zhurnal Obshchei Khimii* **1963**, *33*, 3050. (b) Protopopov, I. S.; Kraft, M. Y. *Med. Prom. SSSR*, **1959**, *13*, 5; *Chem. Abstr.* **1960**, *54*, 10914c.

40. (a) Wada, M.; Higashizaki, S.; *J. Chem. Soc., Chem. Commun.* **1984**, 482. (b) Wada, M.; Higashizaki, S.; Tsuboi, A. *J. Chem. Res.* **1985**, (S), 38; (M), 0467.

41. (a) Wada, M.; Tsuboi, A. *J. Chem. Soc., Perkin Trans. I* **1987**, 151. (b) Wada, M.; Tsuboi, A.; Nishimura, K.; Erabi, T. *Nippon Kagaku Kaishi* **1987**, *7*, 1284.

42. (a) Yamashoji, Y.; Matsushita, T.; Wada, M.; Shono, T. *Chem. Lett.* **1988**, 43. (b) Yamashoji, Y.; Matsushita, T.; Tanaka, M.; Shono, T.; Wada, M. *Polyhedron* **1989**, *8*, 1053.

43. Streuli, C. A. *Anal. Chem.* **1960**, *32*, 985.

44. (a) Bowmaker, G. A.; Cotton, J. D.; Healy, P. C.; Kildea, J. D.; Silong, S. B.; Skelton, B. W.; White, A. H. *Inorg. Chem.* **1989**, *28*, 1462. (b) Li, G. Q.; McAuliffe, C. A.; Mackie, A. G.; Mac Rory, P. P.; Ndifon, P. T. *J. Chem. Soc., Dalton Trans.* **1992**, 1297. (c) Kurosawa, H.; Tsuboi, A.; Kawasaki, Y.; Wada, M. *Bull. Chem. Soc. Jpn.* **1987**, *60*, 3563. (d) Baker, L.-J.; Bowmaker, G. A.; Camp, D.; Effendy,; Healy, P. C.; Schmidbauer, H.; Steigelmann, O.; White, A. H.*Inorg. Chem.* **1992**, *31*, 3656.

45. (a) Hughes, R. P. in *Comprehensive Organometallic Chemistry*; Wilkinson, G.; Stone, F. G. A.; Abel, E. W., eds.; Pergamon: New York, 1982; vol. 5.

46. Collman, J. P.; Hegedus, L. S.; Norton, J. R.; Finke, R. G. *Principles and Applications of Organotransition Metal Chemistry*; University Science Books: Mill Valley, Ca. 1987; chapter 5 and references therein.

47. Busetto, C.; D'Alfonso, A.; Maspero, F.; Perego, G.; Zazzetta, A. *J. Chem. Soc., Dalton Trans.* **1977**, 1733.

48. For a review of Rh(II) complexes see Felthouse, T. R. *Prog. Inorg. Chem.* **1982**, *29*, 73 and references therein.

49. (a) Bennett, M. A.; Lonstaff, P. A. *J. Am. Chem. Soc.*, **1969**,*91*, 6266. (b) Moers, F. G.; DeJong, J. A. M.; Beaumont, P. M. J. *J. Inorg. Nucl. Chem.* **1973**,*35*, 1915. (c) Masters, C.; Shaw, B. L. *J. Chem. Soc. (A)* **1971**, 3679. (d) Empsall, H. D.; Heys, P. N.; Shaw, B. L. *Transition Met. Chem.* **1978**, *3*, 165. (e) Empsall, H. D.; Hyde, E. M.; Pawson, D.; Shaw, B. L.; *J. Chem. Soc., Dalton Trans.* **1977**, 1292.

50. (a) Vleck, A. *Inorg. Chim. Acta* **1980**, *43*, 35. (b) Holah, D. G.; Hughes, A. N.; Hui, B. C. *Can. J. Chem.* **1975**, *53*, 3669. (c) Valentini, G.; Braca, G.; Sbrana, G.; Colligiani, A. *Inorg. Chim. Acta* **1983**, *69*, 215. (d) Valentini, G.; Braca, G.; Sbrana, G.; Colligiani, A. *Inorg. Chim. Acta* **1983**,*69*, 221.

51. (a) Harlow, R. L.; Thorn, D. L.; Baker, R. T.; Jones, N. L. *Inorg. Chem.* **1992**,*31*, 993. (b) Rappert, T.; Wolf, J.; Schulz, M.; Werner, H. *Chem. Ber.* **1992**,*125*, 839.

52. The crystal structure of $Rh^{II}Cl_2(PPh_3)_2$ was reported recently, Ogle, C. A.; Masterman, T. C.; Hubbard, J. L. *J. Chem. Soc., Chem. Commun.* **1990**, 1733, but it was later shown to be that of the Rh(I) complex $Rh(PPh_3)_2(CO)Cl$, Dunbar, K. R.; Haefner, S. C. *Inorg. Chem.* **1992**, *31*, 0000.

53. Examples of coordination and organometallic Rh(II) complexes prepared electrochemically: (a) Cooper, S. R.; Rawle, S. C.; Yagbasan, R.; Watkin, D. J. *J. Am. Chem. Soc.* **1991**,*113*, 1600. (b) Rawle, S. C.; Yagbasan, R.; Prout, K.; Cooper, S. R. *J. Am. Chem. Soc.* **1987**, *109*, 6181. (c) Blake, A. J.; Gould, R. D.; Holder, A. J.; Hyde, T. I.; Schröder, M. *J. Chem. Soc., Dalton Trans.* **1988**, 1861. (d) Anderson, J. E.; Gregory, T. P. *Inorg. Chem.* **1989**, *28*, 3905. (e) Scwarz, H. A.; Creutz, C. *Inorg. Chem.* **1983**,*22*, 207. (e) Mulazzani, Q. G.; Emmi, S.; Hoffman, M. Z.; Venturi, M. *J. Am. Chem. Soc.* **1981**, *103*, 3362. (f) Kölle, U.; Kläui, W. *Z. Naturforsch.* **1991**, *46b*, 75. (g) Bianchini, C.; Laschi, F.; Ottaviani, M. F.; Peruzzini, M.; Zanello, P.; Zanobini, F. *Organometallics* **1989**,*8*, 893. (h) Bianchini, C.; Meli, A.; Laschi, F.; Vizza, F.; Zanello, P. *Inorg. Chem.* **1989**, *28*, 227. (i) Pilloni, G.; Schiavon, G.; Zotti, G.; Zecchin, S. *J. Organomet. Chem.* **1977**, *134*, 305. (j) Fischer, E. O.; Lindner, H. H. *J. Organomet. Chem.* **1964**, *1*, 307. (k) Fischer, E. O.; Wawersik, H. *J. Organomet. Chem.* **1966**,*5*, 559. (l) Keller, H. J.; Wawersik, H. *J. Organomet. Chem.* **1967**,*8*, 185. (m) Dessy, R. E.; King, R. B.; Waldrop, M. *J. Am. Chem. Soc.* **1966**,*88*, 5112. (n) Dessy, R. E.; Kornmann, R.; Smith, C.; Hayter, R. *J. Am. Chem. Soc.* **1968**,*90*, 2001.

54. (a) Bianchini, C.; Laschi, F.; Ottaviani, F.; Peruzzini, M.; Zanello, P. *Organometallics* **1988**, *7*, 1660. (b) Bianchini, C.; Laschi, F.; Meli, A.; Peruzzini, M.; Zanello, P.; Frediani, P. *Organometallics* **1988**, *7*, 2575.

55. Hay-Motherwell, R. S.; Koschmieder, S. U.; Wilkinson, G.; Hussain-Bates, B.; Hursthouse, M. B. *J. Chem. Soc., Dalton Trans.* **1991**, 2821.

56. (a) Billig, E.; Shupack, S.I.; Waters, J.H.; Williams, R.; Gray H.B. *J. Am. Chem. Soc.* **1964**, *86*, 926.(b) Pneumatikakis, G.; Psaroulis, P. *Inorg. Chim. Acta* **1980**, *46*, 97. (c) Pandey, K. K.; Nehete, D. T.; Sharma, R. B. *Polyhedron* **1990**, *9*, 2013. (d) Peng, S. M.; Peters, K.; Peters, E. M.; Simon, A. *Inorg. Chim. Acta* **1985**, *101*, L35.

57. (a) Wayland, B. B.; Woods, B. A.; Coffin, V. L. *Organometallics* **1986**, *5*, 1059. (b) Del Rossi, K. J.; Wayland, B. B. *J. Am. Chem. Soc.* **1985**, *107*, 7941. (c) Paonessa, R. S.; Thomas, N. C.; Halpern, J. *J. Am. Chem. Soc.* **1985**, *107*, 4333. (d) Kadish, K. M.; Yao, C.-L.; Anderson, J. E.; Cocolios, P. *Inorg. Chem.* **1985**, *24*, 4515. (e) Anderson, J. E.; Yao C.-L.; Kadish, K. M. *Organometallics* **1987**, *6*, 706. (f) Anderson, J. E.; Yao, C.-L.; Kadish, K. M. *J. Am. Chem. Soc.* **1987**, *109*, 1106. (g) Aoyama, Y.; Yoshida, T.; Sakurai, K.-I.; Ogoshi, H. *Organometallics* **1986**, *5*, 168.

58. (a) Wayland, B. B.; Sherry, A. E.; Coffin, V. L. *J. Chem. Soc., Chem. Commun.* **1989**, 662. (b) Wayland, B. B.; Sherry, A. E. *J. Am. Chem. Soc.* **1989**, *111*, 5010. (c) Wayland, B. B.; Sherry, A. E.; Poszmik, G.; Bunn, A. G. *J. Am. Chem. Soc.* **1992**, *114*, 1673.

59. (a) Wayland, B. B.; Ba, S.; Sherry, A. E. *J. Am. Chem. Soc.* **1991**, *113*, 5305. (b) Sherry, A. E.; Wayland, B. B. *J. Am. Chem. Soc.* **1990**, *112*, 1259.

60. (a) Bunn, A. G.; Wayland, B. B. *J. Am. Chem. Soc.* **1992**, *114*, 6917. (b) Poszmik, G; Wayland, B. B. presented at the 203rd National meeting of the American Chemical Society, San Francisco, CA, April 5-10, 1992; paper INOR 67.

61. (a) Empsall, H. D.; Hyde, E. M.; Jones, C. E.; Shaw, B. L. J. Chem. Soc., Dalton Trans. 1974, 1980. (b) Mason, R.; Thomas, K. M.; Empasall, H. D.; Fletcher, S. R.; Heys, P. N.; Hyde, E. M. Jones, C. E; Shaw, B. L. J. Chem. Soc., Chem. Comm. 1974, 612. (c) Empsall, H. D.; Hyde, E. M.; Shaw, R. L. J. Chem. Soc., Dalton Trans. 1975, 1690. (d) Empsall, H. D.; Heys, P. N.; McDonald, W. S.; Norton, M. C.; Shaw, B. L. J. Chem. Soc., Dalton Trans. 1978, 1119.

CHAPTER II

STRUCTURAL AND SPECTROSCOPIC PROPERTIES OF TRIS(2,4,6-TRIMETHOXYPHENYL)PHOSPHINE AND TRIS(2,4,6-TRIMETHOXYPHENYL)PHOSPHINE OXIDE

1. Introduction

Before delving directly into the coordination chemistry of tris(2,4,6-trimethoxyphenyl)phosphine (TMPP), a summary of its spectroscopic and structural properties is in order. The initial synthetic report describing TMPP and several related quaternary phosphonium salts did not report any spectroscopic information about the phosphine; in fact only melting points and elemental analyses were given.[1] Later, Wada described a more conventional route for the preparation of TMPP along with an account of its ^1H NMR and infrared spectral data.[2] In addition to providing some spectral data for TMPP and several of its quaternary phosphonium salts, Wada estimated the pK_a of the phosphine to be 11.2 by titration of the protic phosphonium salt with a series of bases and monitoring the process by ^1H NMR spectroscopy. Later the value was redetermined by non-aqueous titrimetry in nitromethane and found to be 11.02.[3] The high nucleophilicity of TMPP is readily apparent from its observed chemical reactivity. Although some of the physical and spectroscopic properties of TMPP appeared during the course of our studies, a complete structural and spectroscopic study of this ligand has not yet been published to our knowledge.[4] In this chapter, we describe the results of such studies completed in our laboratories.

In addition to the spectroscopic and structural properties of TMPP, we are also interested in those of the corresponding phosphine oxide, in particular the affect that phosphine oxidation has on the spectroscopic and structural properties. Transition metal catalyzed oxidations of phosphines are not uncommon, particularly in the chemistry of late transition metal-phosphine complexes.[5] An example of such a process was investigated in our own laboratories. In this work, TMPP was reacted with $FeCl_3$ in the presence of oxygen to form a TMPP oxide-$FeCl_3$ complex.[6] In order to identify the

possible formation of any phosphine oxide by-products, it is necessary to study their physical properties, thus the oxide derivative of TMPP was prepared and fully characterized by spectroscopic and crystallographic methods.

2. Experimental

A. Synthesis

(1) Preparation of Tris(2,4,6-trimethoxyphenyl)phosphine (TMPP)

TMPP was prepared by using a modification of the method previously described by Wada.[2b] A 1 liter 3-necked flask equipped with a condenser, a gas inlet, and a 120 mL addition funnel, was charged with 1,3,5-trimethoxybenzene (42.05 g, 0.25 mol) and diethyl ether (150 mL). The resulting solution was cooled to 0°C with an ice bath and a 2.5 M solution of butyllithium in hexanes (100 mL) was slowly added dropwise over a period of 1-2 h. The resulting suspension was stirred at 0°C for a total of 12 h. After this time, triphenylphosphite (19.65 mL, 0.075 mol) was slowly added dropwise to the suspension at 0°C. While stirring for 10-12 h, the reaction was allowed to slowly warm to r.t. The solvent was decanted off and the remaining white solid was filtered in air and washed with a minimal amount of cold EtOH (2 x 10 mL).

The product was recrystallized in air by dissolving the solid in a large volume of hot EtOH (1 L), followed by filtration of the hot solution and concentration on a rotary evaporator. The resulting white crystalline solid was filtered, washed with cold EtOH (2 x 10 mL) and diethyl ether (4 x 10 mL), and dried *in vacuo*; yield, 26-28 g (65-70% based on $P(OPh)_3$). IR (Nujol, CsI) cm^{-1}: 1596, 1581, 1398, 1321, 1293, 1223, 1202, 1182, 1154, 1120, 1086, 1036, 949, 919, 816, 805, 789, 675, 634, 474. Electronic absorption spectrum

(CH_3CN) λ_{max}, nm (ε): 276 (21.6 x 10^3), 245 sh (~29.3 x 10^3), 214 (87.2 x 10^3). ^1H NMR (CD_3CN) δ ppm: 3.45 (s, 18H, *o*-OCH_3), 3.75 (s, 9H, *p*-OCH_3), 6.07 (d, $^4J_{P-H}$ = 2.51 Hz, 6H, *m*-H). ^{31}P (CD_3CN) δ ppm: -66.3 (s). ^{13}C (CD_3CN) δ ppm: 109.19 (d, $^1J_{P-C}$ = 22.78 Hz, C1), 163.01 (d, C2,6), 92.21 (s, C3,5), 164.12 (s, C4), 56.42 (s, *o*-OCH_3), 55.80 (s, *p*-OCH_3). Cyclic Voltammetry (0.1 M $TBABF_4$ / CH_3CN, vs Ag / AgCl): $E_{p,a}$ = + 0.49 V, $E_{p,c}$(chemical) = - 0.09 V.

(2) Preparation of Tris(2,4,6-trimethoxyphenyl)phosphine Oxide (TMPP=O)

An excess of a 30% aqueous solution of H_2O_2 (1 mL) was added to a solution of TMPP (1.00 g, 1.98 mmol) in 10 mL of acetone. The colorless solution was gently refluxed for 8 h, after which time the solution was cooled and the volume was reduced to approximately 5 mL under reduced pressure. Slow addition of diethyl ether (50 mL) effected the precipitation of a large amount of white crystalline solid. The product was collected by suction filtration, washed with diethyl ether (4 x 5 mL) and dried *in vacuo* for 1 h; yield, 0.897 g (87%). IR (Nujol, CsI), cm^{-1}: 1596, 1579, 1406, 1333, 1293, 1230, 1206, 1184, 1159, 1120, 1096, 1028, 952, 921, 812, 789, 692, 665, 640, 594, 527, 520, 501, 482, 449. Electronic absorption spectrum (MeCN) λ_{max}, nm (ε): 285 sh (~10,100), 253 (36,600), 216 (114,600). ^1H NMR (CD_3CN) δ ppm: 3.46 (s, 18H, *o*-OCH_3), 3.78 (s, 9H, *p*-OCH_3), 6.08 (d, $^4J_{P-H}$ = 4.1 Hz, 6H, *m*-H). ^{31}P (CD_3CN) δ ppm: + 10.8 (s). ^{13}C (CD_3CN) δ ppm: 109.66 (d, $^1J_{P-C}$ = 121.6 Hz, C1), 164.40 (d, $^2J_{P-C}$ = 1.3, C2,6), 92.04 (d, $^3J_{P-C}$ = 6.9, C3,5), 164.00 (d, $^4J_{P-C}$ = 1.1, C4), 56.42 (s, *o*-OCH_3), 55.98 (s, *p*-OCH_3). Cyclic voltammetry (0.1 M $TBABF_4/CH_3CN$, vs Ag/AgCl): $E_{p,c}$(irrev.)^1 = - 0.65 V, $E_{p,a}$(chemical) = - 0.09 V, $E_{p,c}^2$ = -1.29 V, $E_{p,a}$ = + 1.41 V. Mass spectrum (EI), m/z: 548 (TMPP=O), 517, 367, 335, 374, 197, 181, 167, 151, 136, 121.

(3) Preparation of $Ni(CO)_3TMPP$

The compound $Ni(CO)_3TMPP$ was prepared *in situ* by a modification of the method described by Tolman for the preparation of other $Ni(CO)_3PR_3$ complexes.[7] An amount of $Ni(CO)_4$ (100 μL, 0.77 mmol) was syringed into a flask containing 15.4 mL of a 0.05 M solution of TMPP in benzene. The reaction was shaken briefly and allowed to stand for 15 min. The solution was then diluted with fresh benzene. The infrared spectrum was obtained by removing a small sample and transferring it to a 0.1 mm CaF_2 solution IR cell: ν(CO) (cm^{-1}); 2048 (A_1) and 1963 (E).

B. X-ray Crystallography

The structure of tris(2,4,6-trimethoxyphenyl)phosphine (**1**) and tris(2,4,6-trimethoxyphenyl)phosphine oxide (**2**) were determined by application of general procedures which have been fully described elsewhere.[8] Geometric and intensity data were collected on a Rigaku AFC6S diffractometer with graphite-monochromated MoKα ($\lambda_{\bar{\alpha}}$ = 0.71069 Å) radiation and were corrected for Lorentz and polarization effects. All calculations were performed with VAX computers on a cluster network within the Department of Chemistry at Michigan State University using the Texsan software package of the Molecular Structure Corporation.[9] Important crystallographic parameters for the structures of **1** and **2** are summarized in Table 2.

(1) TMPP

(i) Data Collection and Reduction. Large single crystals of TMPP (**1**) were obtained by slow evaporation of a benzene solution of TMPP in air. A suitable single crystal, with the approximate dimensions of 0.49 x 0.47 x

Table 2. Summary of Crystallographic Data for TMPP (**1**) and TMPP=O · $2H_2O$ (**2**)

Compound	**1**	**2**
Formula	$PO_9C_{27}H_{33}$	$PO_{12}C_{27}H_{37}$
Formula weight	532.53	548.53
Space group	P_n (#7)	P-1 (#2)
a, Å	8.092 (4)	12.768 (4)
b, Å	24.871 (4)	13.506 (5)
c, Å	13.455 (3)	9.927 (4)
α, deg	90	109.56 (3)
β, deg	96.83 (3)	109.96 (3)
γ, deg	90	98.99 (3)
V, $Å^3$	2689 (1)	1444 (2)
Z	4	2
d_{calc}, g/cm^3	1.315	1.262
μ (Mo Kα), cm^{-1}	1.47	1.41
Temperature, °C	23 °C	-80°C
Trans. factors, max., min.	1.00, 0.95	1.00, 0.95
R[a]	0.040	0.045
R_w[b]	0.038	0.051
Quality-of-fit indicator[c]	2.08	2.65

[a] $R = \Sigma \; | \; |F_o| - |F_c| \; | / \Sigma |F_o|$

[b] $R_w = [\Sigma w (|F_o| - |F_c|)^2 / \Sigma w |F_o|^2]^{1/2}$; $w = 1/\sigma^2(|Fo|)$

[c] Quality of fit = $[\Sigma w (|F_o| - |F_c|)^2 / (N_{obs} - N_{parameters})]^{1/2}$

0.31 mm^3, was cleaved from a larger crystal and mounted on the tip of a glass fiber with epoxy cement. Cell constants were obtained from a least-squares refinement using 24 carefully centered reflections in the range $21 < 2\theta < 32°$, and were found to correspond to a monoclinic cell with the following cell constants: a = 8.092 (4) Å, b = 24.871 (4) Å, c = 13.455 (3) Å, $\alpha = \gamma = 90°$, β = 96.83 (3)°, V = 2689 (1) $Å^3$. Data were collected at 23±2°C, by using the ω–scan method, in the range $4 \leq 2\theta \leq 47°$. Weak reflections, those with $F < 10.0\sigma(F)$, were rescanned at a maximum of 2 rescans and the counts were accumulated to ensure good counting statistics. A total of 4403 reflections were collected. Equivalent reflections were averaged (R_{merge} = 2.6%) to yield a total of 4088 unique data and 3035 data with $F_o^2 \geq 3\sigma(F_o)^2$. Periodic measurement of three representative reflections at regular intervals showed no loss of diffraction intensity had occurred during data collection. An empirical absorption correction was applied on the basis of azimuthal scans of 3 reflections with χ near 90° and resulted in transmission factors ranging from 0.95 to 1.00.

(ii) Structure Solution and Refinement. The positions of all non-hydrogen atoms were obtained by direct-methods[10] and refined by successive full-matrix least-squares cycles. All non-hydrogen were refined with anisotropic thermal parameters. Hydrogen atoms were treated as fixed contributors at idealized positions and were not refined. Final least squares refinement of 665 parameters resulted in residuals of R = 0.040 and R_w = 0.038 and a goodness-of-fit = 2.08. Refinement of both enantiomorphs established the correct one at the 97.5% confidence level by application of the Hamilton Significance test.[11] A final difference Fourier map revealed no peaks above 0.42 $e^-/Å^3$.

(2) TMPP=O · 2 H_2O

(i) Data Collection and Reduction. A large crop of colorless crystals were grown in air by slow evaporation of a benzene solution of TMPP=O. A single crystal of approximate dimensions 0.36 x 0.13 x 0.10 mm^3 was taken up with silicon grease on the end of a glass fiber and placed in a cold N_2 stream. Least squares refinement of 21 orientation reflections in the range $20 < 2\theta < 38°$ resulted in cell constants consistent with a triclinic cell. Intensity measurements were performed at -80 ± 2°C using the ω-2θ scan technique. Routine measurement of three check reflections at regular intervals throughout data collection revealed that the crystal had experienced only a slight decay (1.6%) in diffraction intensity. Nonetheless, a linear decay correction was applied to compensate for the observed loss. In addition, an empirical absorption correction was applied based on azimuthal scans of 3 reflections with Eulerian angle χ near 90°. A total of 4476 data were collected in the range of $7.36 \leq 2\theta \leq 47°$. After averaging equivalent reflections (R_{merge} = 2.1%), there remained 4254 unique data of which 3045 were in the category $F_o^2 \geq 3\sigma(F_o)^2$.

(ii) Structure Solution and Refinement. The positions of all non-hydrogen atoms were obtained by application of the direct methods programs MITHRIL and DIRDIF.[12] Hydrogen atoms of the phosphine oxide were placed at calculated positions, while the positions of the hydrogen atoms of the interstitial H_2O molecules were located from difference Fourier maps. All hydrogen atoms were treated as fixed contributors to the structure factor calculation and were not refined. Final least-squares refinement of 361 parameters gave residuals of R = 0.045 and R_w = 0.051 and a goodness-of-fit of 2.65. The highest peak remaining in the Fourier difference map was 0.22 $e^-/Å^3$.

3. Results and Discussion

A. Synthesis and Characterization

The tertiary phosphine compound tris(2,4,6-trimethoxyphenyl)-phosphine (TMPP) (**1**)can be prepared in good yield (60-70%) by lithiation of 1,3,5-trimethoxybenzene followed by coupling with triphenylphosphite at 0°C (eq 8). The phosphine was isolated as a white solid after recrystallization from hot ethanol. Alternatively, TMPP can be prepared in an unusual one-pot synthesis following a Soviet literature procedure.[1a] This method entails

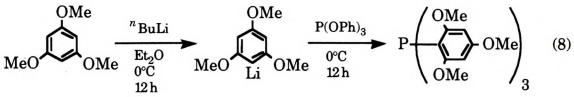

(8)

refluxing 1,3,5-trimethoxybenzene with zinc chloride in neat PCl_3 for 8 hours (eq 9). Yields are comparable to those obtained from the lithiated arene. Both procedures are currently used in our laboratories.

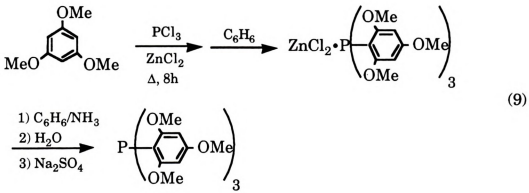

(9)

Despite the known sensitivity of many phosphine lingands towards aerial oxidation, TMPP is air-stable both in solution and in the solid state. The phosphine is highly soluble in acetone and acetonitrile and moderately

soluble in THF, MeOH and EtOH. The molecule exhibits limited solubility in both benzene and toluene, is relatively insoluble in diethyl ether, and is completely insoluble in water and hydrocarbon solvents. Although soluble in methylene chloride, TMPP readily decomposes ($t_{1/2}$ < 15 min) to form the chloromethyl phosphonium salt $[(C_6H_2(OMe)_3)_3P\text{-}CH_2Cl^+][Cl^-]$ (eq 10).[2]

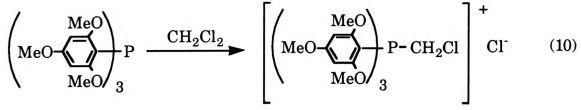

(10)

The infrared spectrum of TMPP reveals a number of vibrations between 400 and 1600 cm^{-1} that render the presence of TMPP in a sample readily apparent. The ^1H NMR spectrum of TMPP in MeCN exhibits three resonances: 3.45 (s,18H, *o*-OMe); 3.75(s, 9H, *p*-OMe); 6.07(d, $^4J_{P\text{-}H}$ = 2.51 Hz, 6H, *m*-H) corresponding to the meta-ring protons, and the ortho- and para-methoxy protons, respectively. The appearance of only 3 resonances indicates that fast rotation about the P-C_{ipso} bond is equilibrating all-exchangeable meta-ring and methoxy protons. This rotation is quite facile, in so much as the ^1H NMR spectrum remains unchanged down to -100°C in d_8-toluene.

The $^{31}P\{^1H\}$ NMR spectrum in CD_3CN exhibits a single resonance at -66.3 ppm. The extreme upfield chemical shift is attributed to an unusually large γ effect caused by the presence of the ortho-methoxy substituents on the aryl rings of TMPP.[12] The γ effect is believed to arise from the additional shielding provided by the proximity of an ortho substituent to the phosphorus lone pair. The effect is lost upon quaternarization of the phosphine and the ^{31}P chemical shifts of the corresponding phosphonium salts are similar to non-ortho substituted phosphonium salts.[13]

In addition to the spectroscopic properties of TMPP, we are also interested in its nucleophilicity. In order to ascertain the donating capabilities of TMPP to metal centers, we measured the A_1 mode of the carbonyl stretching vibration of the nickel complex $Ni(CO)_3TMPP$. The complex was prepared *in situ* by the method described by Tolman to measure the donor properties of a host of other phosphines.[7] The IR spectrum of $Ni(CO)_3TMPP$ measured in benzene registers 2 CO bands, 2047.9 cm^{-1} and 1962.7 cm^{-1} which are assigned to the A_1 and E stretching modes respectively.[14] A comparison of the A_1 stretching mode of TMPP with those of other phosphines is shown in Figure 4.[15] The stretching frequency is the lowest reported for a phosphine complex of $Ni(CO)_3$ and is indicative of the highly donating nature of TMPP. This result agrees well with the reported pK_a value for TMPP (pK_a = 11.02)[3] and further supports that TMPP is one of the most strongly donating tertiary phosphines.

The oxide derivative of TMPP was prepared by refluxing an acetone solution of TMPP with aqueous H_2O_2 and was isolated as a white crystalline solid in high yield (87%) (eq 11). The TMPP oxide molecule is air-stable and has similar solubility properties as those of the parent phosphine.Attempts to prepare TMPP=O by reaction of TMPP and Me_3NO under refluxing conditions met with failure, yielding only unreacted phosphine. Other work has shown that TMPP oxide can be prepared by catalytic oxidation of TMPP with O_2 in the presence of $FeCl_3$.[16]

$$\underset{\mathbf{1}}{\text{TMPP}} + 30\%\ H_2O_2(aq) \xrightarrow[\Delta]{\text{acetone}} \underset{\mathbf{2}}{\text{TMPP=O}} \qquad (11)$$

The infrared spectrum of TMPP=O displays a number of vibrations between 400 and 1600 cm^{-1} that are slightly shifted from those found for the

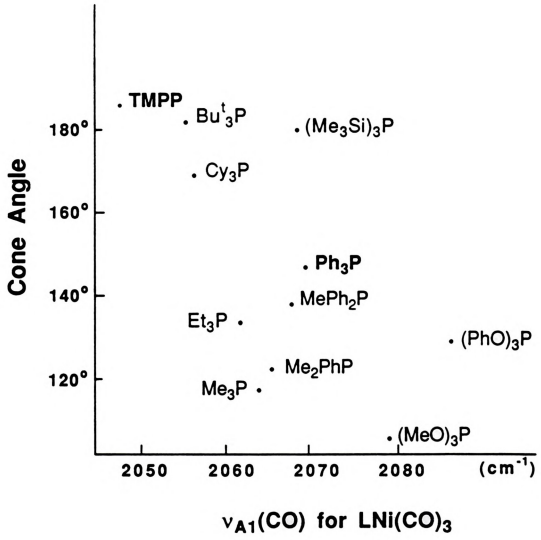

Figure 4. Plot of the cone angle versus the $\nu(CO)_{A1}$ stretch for various $Ni(CO)_3(PR_3)$ complexes.

parent phosphine. The ν(P-O) band is obscured by the other vibrations of TMPP in this region and is not discernible. The purity of the solid product was confirmed by ^{1}H and ^{31}P NMR spectroscopy. The ^{1}H NMR spectrum of TMPP=O in CD_3CN exhibits three resonances at δ ppm, 3.46 (s, 18H, *o*-Me), 3.78 (s, 9H, *p*-OMe) and 6.08 (d, $^{4}J_{P-H}$ = 4.1 Hz, 6H, *m*-H). As was observed for TMPP, the appearance of only three resonances suggests that the aryl groups are free to rotate about the P-C_{ipso} bond. In spite of the change in phosphorus oxidation state, these resonances are only slightly shifted from the free phosphine. In sharp contrast, the ^{31}P chemical shift difference between TMPP and TMPP=O is over 75 ppm, as the ^{31}P displays a single resonance at +10.8 ppm. This dramatic chemical shift difference is a result of deshielding of the phosphorus nucleus upon oxidation from +3 to +5 and illustrates the sensitivity of ^{31}P NMR spectroscopy to changes in phosphorus oxidation state.

B. Molecular Structures

(1) TMPP

Single crystals of TMPP were grown by slow evaporation from a benzene solution. The compound was found to crystallize in the acentric space group P_{2_n} (#7), resulting in the presence of two independent TMPP molecules per asymmetric unit. Refinement of the structure in the centric space group $P_{2_1/n}$ (#13) proved unsatisfactory as evidenced by abnormally high residuals. Therefore, the final refinement was performed in the acentric group. Further evidence for the acentric space group was provided by the computer program MISSYM,[17] which showed that the two independent molecules are not symmetry related. ORTEP drawings for both independent molecules are depicted in Figure 5. Pertinent bond distances and angles are summarized in Table 3.

As expected, the aryl rings of the phosphine adopt a pseudo-propeller arrangement about the phosphorus atom. However, the angles that the aryl rings adopt with respect to the plane described by the ipso-carbon atoms vary considerably from ideality, ranging in value from 36.61° to 74.12° (Table 4). The average $P\text{-}C_{ipso}$ bond length, 1.842 Å, is slightly longer than that reported for triphenylphosphine ($P\text{-}C_{ave}$ = 1.828 Å),[18] but comparable to that reported for the structure of tris(2,6-dimethoxyphenyl)phosphine ($P\text{-}C_{ave}$ = 1.844 Å)[19] and trimesitylphosphine ($P\text{-}C_{ave}$ = 1.837 Å).[20] As expected, the average C-P-C bond angle of TMPP ($C\text{-}P\text{-}C_{ave}$ = 105.2°) is larger than that of triphenylphosphine ($C\text{-}P\text{-}C_{ave}$ = 103.0°), yet smaller than trimesitylphosphine ($C\text{-}P\text{-}C_{ave}$ = 109.7°). Although the presence of the ortho-methoxy groups contributes to the deformation of the C-P-C bond angle, the steric interactions between these groups are not nearly as great as those observed for the analogous methyl substituted phosphines tris(2,6-dimethylphenyl)phosphine and trimesitylphosphine. As a result, the cone angle of TMPP is not as large as those observed for the methyl substituted analogs.

Just as was observed in the structure of the 2,6-dimethoxy substituted phosphine, the ortho-methoxy groups of TMPP are bent slightly towards the phosphorus lone pair. For example, the O-C-C angle, O(3)-C(6)-C(5) is 122.3(8) while the O-C-C angle O(3)-C(6)-C(1) is 116.0(8), indicating a bending towards the P-C bond. This effect is opposite to that observed for trimesitylphosphine, in which the methyl groups bend away from the P-C bond. The methoxy groups of phosphine are approximately in the plane of the phenyl ring with the methoxy group torsion angles relative to the phenyl rings varying from 0.32° to 21.42°.

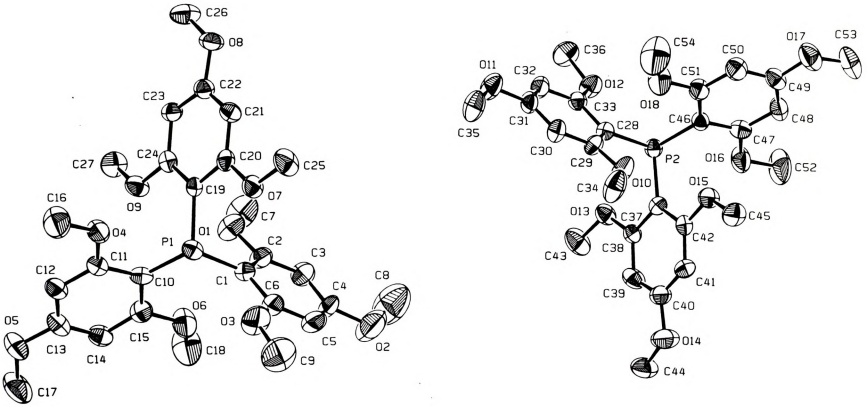

Figure 5. ORTEP representations of the two crystallographically independent molecules of TMPP.

Table 3. Selected bond distances (Å) and angles (deg) for TMPP (**1**).

Atom 1	Atom 2	Distance	Atom 1	Atom 2	Distance
P(1)	C(1)	1.823(8)	P(2)	C(28)	1.835(7)
P(1)	C(10)	1.847(8)	P(2)	C(37)	1.850(7)
P(1)	C(19)	1.842(7)	P(2)	C(46)	1.853(7)
O(1)	C(2)	1.377(9)	O(10)	C(29)	1.342(8)
O(1)	C(7)	1.43(1)	O(10)	C(34)	1.38(1)
O(2)	C(4)	1.40(1)	O(11)	C(31)	1.368(8)
O(2)	C(8)	1.35(1)	O(11)	C(35)	1.42(1)
O(3)	C(6)	1.35(1)	O(12)	C(33)	1.372(9)
O(3)	C(9)	1.34(1)	O(12)	C(36)	1.442(9)

Atom 1	Atom 2	Atom 3	Bond angle
C(1)	P(1)	C(10)	106.4(3)
C(1)	P(1)	C(19)	101.6(3)
C10)	P(1)	C(19)	108.1(3)
C(28)	P(2)	C(37)	102.5(3)
C(28)	P(2)	C(46)	106.5(3)
C(37)	P(2)	C(46)	106.2(3)

Table 4. Dihedral angles (deg) between the planes of the aryl rings and the plane described by C_{ipso} for TMPP (**1**) and TMPP=O • $2H_2O$ (**2**).

	TMPP (**1**)	TMPP=O • 2 H_2O (**2**)
C(1) - C(6)	74.12	89.66
C(10) - C(15)	56.41	28.81
C(19) - C(24)	40.05	41.71
C(28) - C(33)	72.09	-------
C(37) - C(42)	53.55	-------
C(46) - C(51)	36.61	-------

(2) TMPP=O · 2 H_2O

An ORTEP drawing of TMPP oxide is presented in Figure 6. A listing of selected bond distances and angles is given in Tables 5. In contrast to the propeller-like geometry of phenyl rings of TMPP, only two of the phenyl rings of TMPP=O are tilted at 28.81° and 41.71° with respect to the plane described by the ipso-carbon atoms. The third phenyl group is perpendicular to this plane and hence parallel to the P=O bond. (Table 4). A similar arrangement of the phenyl rings was observed in the structure of tris(2,6 dimethoxyphenyl) phosphine. The average P-C_{ipso} distance (1.817Å) is slightly contracted from that of the parent phosphine and the average C-P-C angle has opened up from 105.2° in TMPP to 107.8°. However, the flattening of the C-P-C angles is not as extensive as that observed for the metal bound phosphine oxide in the structure of $FeCl_3$(O=TMPP) (C-P-C_{ave}= 111.2[5]°).[6] Not surprisingly the P-O bond distance is much shorter in the free phosphine oxide than in the coordinated ligand (P-O_{free}= 1.497(2) Å vs P-O_{coord}= 1.550(7) Å), but nevertheless, it is slightly longer than that observed for other documented structures of phosphine oxide ligands. One explanation for this is the presence of two hydrogen bonded water molecules in the structure of TMPP=O (*vide infra*). Finally, the observed torsion angles involving the methoxy groups and the phenyl rings vary from 2.86° to 9.66°, placing the methoxy substituents in an essentially co-planar arrangement with the phenyl rings.

Interestingly, although the TMPP=O compound was crystallized from dry benzene, the structure shows that there are two H_2O molecules per molecule of TMPP=O. Obviously, these were carried along in the crude product prepared in 30% H_2O_2 solution. The location of the H_2O molecules

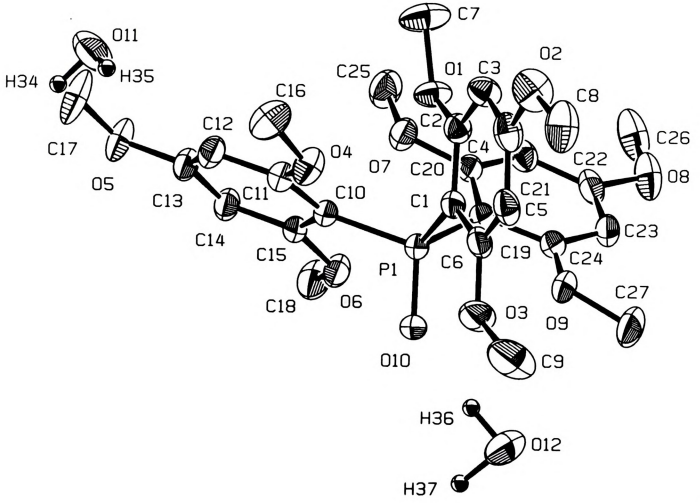

Figure 6. ORTEP diagram of TMPP=O • $2H_2O$.

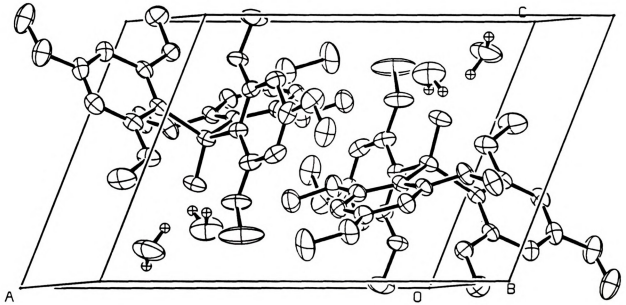

Figure 7. Packing diagram of TMPP=O • $2H_2O$.

Table 5. Selected bond distances (Å) and angles (deg) for TMPP=O • $2H_2O$ (**2**).

Atom 1	Atom 2	Distance	Atom 1	Atom 2	Distance
P(1)	O(10)	1.497(2)	O(1)	C(2)	1.367(4)
P(1)	C(1)	1.813(4)	O(1)	C(7)	1.421(4)
P(1)	C(10)	1.810(3)	O(2)	C(4)	1.375(4)
P(1)	C(19)	1.828(4)	O(2)	C(8)	1.433(5)
C(1)	C(2)	1.401(5)	O(3)	C(6)	1.369(4)
C(1)	C(6)	1.397(5)	O(3)	C(9)	1.398(5)
C(10)	C(11)	1.394(5)	O(4)	C(11)	1.365(4)
C(10)	C(15)	1.401(5)	O(4)	C(16)	1.421(4)
C(19)	C(20)	1.403(5)	O(5)	C(13)	1.373(4)
C(19)	C(24)	1.410(4)	O(5)	C(17)	1.432(5)

Atom 1	Atom 2	Atom 3	Angle
O(10)	P(1)	C(1)	114.2(2)
O(10)	P(1)	C(10)	107.9(1)
O(10)	P(1)	C(19)	111.5(2)
C(1)	P(1)	C(10)	110.0(2)
C(1)	P(1)	C(19)	101.5(2)
C(10)	P(1)	C(19)	11.8(2)

suggests that they are both hydrogen bonded to the terminal oxygen atom of the phosphine oxide. Their positions relative to the phosphine is clearly seen in the packing diagram (Figure 7). The hydrogen atoms of the water molecules were located in the Fourier difference map but were treated only as fixed contributors to the structure factor calculation and their positions were not refined. Hydrogen atoms, H(34) and H(36), lie at a distance of 1.82 Å and 1.86 Å from O(10) and are clearly interacting with the oxygen lone pairs. The resulting P-O---H bond angles are approximately 124.5° and 141.7°. Apparently, the occurrence of a phosphine oxide involved in two hydrogen bonds is rare, as only three other cases have been reported.[21] In each of the reported structures, the P-O bond is slightly longer than that of the non hydrogen bonded phosphine oxide.

List of References

1. (a) Protopopov, I. S.; Kraft, M. Y. *Zhurnal Obshchei Khimii* **1963**, *33*, 3050. (b) Protopopov, I. S.; Kraft, M. Y. *Med. Prom. SSSR*, **1959**, *13*, 5; *Chem. Abstr.* **1960**, *54*, 10914c.

2. (a) Wada, M.; Higashizaki, S.; *J. Chem. Soc., Chem. Commun.* **1984**, 482. (b) Wada, M.; Higashizaki, S.; Tsuboi, A. *J. Chem. Res.* **1985,** (S), 38; (M), 0467.

3. Yamashoji, Y.; Matsushita, T.; Wada, M.; Shono, T. *Chem. Lett.* **1988**, 43.

4. A preliminary structural report of TMPP has appeared: Wada, M. *J. Syn Org. Chem. Jpn.* **1986**, 957.

5. For examples of phosphine oxidation promoted by platinum group metals see: (a) Sen, A.; Halpern, J. *J. Am. Chem. Soc.* **1977**, *99*, 8337. (b) Van Vungt, B.; Koole, N.; Drenth, W.; Kuijpers, F. P. *Rec. Trav. Chim., Pays-Bas* **1973**, *92*, 1321. (c) Takao, K.; Fujiwara, Y.; Imanaka, T.; Teranishi, S. *Bull. Chem. Soc. Jpn.* **1970**, *43*, 1153. (d) Wilke, G.; Schott, H.; Heinbach, P. *Angew. Chem. Int. Ed.* **1967**, *6*, 92.

6. (a) Dunbar, K. R.; Haefner, S. C.;**1990**, *9*, 1695. (b) Dunbar, K. R.; Quillevéré, A. *Polyhedron* in press.

7. Tolman, C. A. *J. Am. Chem. Soc.* **1970**, *92*, 2953.

8. (a) Bino, A.; Cotton, F. A.; Fanwick, P. E. *Inorg. Chem.* **1979**, *18*, 3558. (b) Cotton, F. A.; Frenz, B. A.; Deganello, G.; Shaver, A. *J. Organomet. Chem.* **1973**, *50*, 227.

9. TEXSAN - TEXRAY Structure Analysis Package, Molecular Structure Corporation, 1985.

10. (a) MITHRIL: Integrated Direct Methods Computer Program, Gilmore, C. J. *J. Appl. Cryst.* **1984**, *17*, 42-46. (b) DIRDIF: Direct Methods for Difference Structure, An Automatic Procedure for Phase Extension; Refinement of Difference Structure Factors. Beurskens, R. T. Technical Report **1984**.

11. Hamilton, W. C. *Acta Cryst.* **1965**, *18*, 502.

12. (a) Grim, S. O.; Yankowsky, A. W. *Phosphorus and Sulfur* **1977**, *3*, 191. (b) Quin, L. D.; Breen, J. J. *Org. Mag. Resonance* **1973**, *5*, 17.

13. Grim, S. O.; Yankowsky, A. W. *J. Org. Chem.* **1977**, *42*, 1236.

14. Band assignment is based on the work of (a) Stromeier, W.; Müller, F. J. *Chem. Ber.* **1967**, *100*, 2812. (b) Bigorgne, M. *Bull. Soc. Chim. Fr.* **1960**, 1986.

15. Tolman, C. A. *Chem. Rev.* **1977**, *77*, 313.

16. Dunbar, K. R.; Quillevéré, A. submitted for publication in *Polyhedron*.

17. Le Page, Y. *J. Appl. Cryst.* **1988**, *21*, 983.

18. Daly, J. J. *J. Chem. Soc.* **1964**, 3799.

19. Livant, P.; Sun, Y. J.; Webb, T. R. *Acta Cryst.* **1991**, *C47*, 1003.

20. Blount, J. F.; Maryanoff, C. A.; Mislow, K. *Tetrahed. Lett*. **1975**, 913.

21. (a) Llamas-Saiz, A. L.; Foces-Foces, C.; Elguero, J.; Molina, P.; Alajarin, M.; Vidal, A. *J. Chem. Soc., Chem. Commun.* **1991**, 1694. (b) Jones, R.; Warrens, C. P.; Williams, D. J.; Woollins, J. D. *J. Chem. Soc., Dalton Trans.* **1987**, 907. (c) Antipin, M. Yu.; Akhmedov, A. I.; Struchkov, Yu. T.; Matrosov, E. I.; Kabachnik, M. I. *Zh. Strukt. Khim.* **1983**, *24*, 888.

CHAPTER III

ISOLATION, CHARACTERIZATION AND REDOX CHEMISTRY OF THE MONONUCLEAR Rh(II) COMPLEX $[Rh(\eta^3\text{-TMPP})_2][BF_4]_2$

1. Introduction

This chapter addresses the synthesis, solution properties, redox chemistry, and solid-state structure of a remarkable rhodium(II) phosphine complex. These findings are of considerable interest in the general context of small molecule binding to paramagnetic metal centers, which has been well investigated in the case of Co(II), but for which parallel studies are essentially non-existent for Rh(II).[1] The reason for this is undoubtedly the paucity of stable mononuclear complexes Rh(II) that have been established as authentic metal-based radicals.[2] The uncertainty as to the location of the unpaired electron is especially high in the reported Rh(II) compounds with non-innocent sulfur- and nitrogen-based ligands.[3] Only recently, through the work of Wayland and co-workers,[4] has the tremendous potential of Rh(II) metallo-radical systems become apparent.

Our entry into mononuclear Rh(II) chemistry came about by a less traditional method than previous approaches, but it is one that holds great promise for preparing many previously unknown rhodium compounds. Typically mononuclear Rh(II) species are prepared by either reduction of hydrated Rh(III) halides in alcohol[5] or by oxidation of Rh(I) complexes.[6,7] Often such routes yield impure products that are inevitably contaminated with diamagnetic species. In contrast, there have been few reports of paramagnetic Rh(II) species being prepared from dinuclear Rh(II) complexes.[8] This is, in part, due to the lack of suitable dinuclear starting materials. Currently, a major focus of our research group is the development of solvated metal systems, particularly dinuclear species, as synthetic precursors for radical mononuclear complexes.[9] To this end we are exploring the chemistry of the solvated $Rh_2^{II,II}$ complex $[Rh_2(MeCN)_{10}][BF_4]_4$.[10] The use of solvated metal systems in conjunction with TMPP have produced a

number of homoleptic phosphine complexes. For example, acetonitrile complexes of Co^{2+} and Ni^{2+} react with TMPP to give neutral bis-phosphinophenoxide compounds.[11] More significantly, the reaction of $[Rh_2(MeCN)_{10}][BF_4]_4$ with TMPP has resulted in the first structurally characterized six-coordinate Rh(II) complex without a metal-metal bond. Herein, the synthesis, spectroscopy, structural characterization, and redox chemistry of the remarkably stable Rh(II) complex $[Rh(\eta^3\text{-TMPP})_2][BF_4]_2$ (**3**) is presented.

2. Experimental

A. Synthesis

All reactions were carried out under an argon atmosphere by the use of standard Schlenk-line techniques unless otherwise stated. The solvated dirhodium complex, $[Rh_2(MeCN)_{10}][BF_4]_4$, was prepared as described in the literature.[12] Tris(2,4,6-trimethoxyphenyl)phosphine (TMPP) (**1**) was prepared by the reaction of triphenylphosphite with the lithium salt of trimethoxybenzene as described in chapter II. $[Cp_2Fe][BF_4]$ was prepared by oxidation of Cp_2Fe with hydrofluoroboric acid in the presence of p-benzoquinone.[13] The reagents $NOBF_4$, $NOPF_6$, and Cp_2Co were purchased from Strem Chemicals and used without further purification.

(1) Preparation of $[Rh(\eta^3\text{-TMPP})_2][BF_4]_2$ (3)

An amount of $[Rh_2(MeCN)_{10}][BF_4]_4$ (0.650 g, 0.675 mmol) was dissolved in 10 mL of MeCN and cooled to -15°C with a dry ice/ethylene glycol bath. The reaction was covered with aluminum foil to avoid photochemical generation of Rh(I) and Rh(III) species.[14] A solution of TMPP (1.437 g, 2.698 mmol) in 20 mL of MeCN was added dropwise over a 15 minute period. The resulting purple solution was stirred for 1 h at -15°C and then evaporated to

a residue. The crude purple solid was washed several times with copious amounts of THF. It was then redissolved in 50 mL of CH_2Cl_2, filtered, and treated with THF (approximately 10-15 mL). The volume of the solution was reduced with the use of a rotary evaporator to approximately 10 mL to yield a purple crystalline solid. The solid was filtered, washed with 4 x 10 mL of THF, followed by 4 x 10 mL of diethyl ether, and dried *in vacuo*.; yield 1.647 g (91%). *Anal.* Calcd for $C_{55}H_{66}F_8P_2O_{18}B_2Rh$: C, 48.34; H, 4.96. Found: C, 48.56; H, 4.86. IR (Nujol, CsI) cm^{-1}: 1599 vs, 1585 vs, 1412 s, 1380 m, 1230 vs, 1207 vs, 1190 m, 1161 vs, 1135 s, 1110 s, 1049 vs/br, 950 m, 920 w, 908 m, 820 m, 785 w, 720 w, 700 w, 680 w, 673 w, 637 w, 520 w, 490 m, 450 w, 435 w, 415 w. Electronic absorption spectrum (CH_2Cl_2) λ_{max}, nm (ε): 537 (2050), 420 sh, 329 (13,400), 298 (17,500), 233 (62,400). ^1H NMR (CD_2Cl_2) δ ppm: Broad. ^{31}P NMR (CD_2Cl_2) δ ppm: not observed.

(2) Preparation of [Rh(η³-TMPP)₂][BF₄]₃ (4)

(i) Oxidation of [Rh(η³-TMPP)₂][BF₄]₂ with NOBF₄. A quantity of [Rh(η³-TMPP)₂][BF₄]₂ (0.200 g, 0.14 mmol) and $NOBF_4$ (0.016 g, 0.14 mmol) was dissolved in 5 mL of MeCN which resulted in the immediate formation of a deep red solution. The reaction was stirred at -40 °C for 45 min with periodic pumping to remove the evolved NO gas, after which time 20 mL of diethyl ether was added to precipitate the product. The red solid was collected by filtration under argon, washed with 3 x 5 mL of diethyl ether and dried *in vacuo*; yield, 0.085 g (80%). Due to thermal instability, solid and solution forms of **4** must be stored anaerobically at -20°C. *Anal.* Calcd for $C_{54}H_{66}F_{12}P_2O_{18}B_3Rh$: C, 45.40; H, 4.66. Found: C, 44.39; H, 5.14. Electronic absorption spectrum (CH_2Cl_2) λ_{max}, nm (ε): 363 (22,000), 260 sh, 245 (65,000). ^1H NMR (CD_2Cl_2) δ ppm: -OCH_3, 2.93 (s, 6H), 3.57 (s, 6H,), 3.59 (s, 6H), 3.64 (s, 6H), 3.90 (s, 6H), 3.92 (s, 6H), 3.97 (s, 6H), 4.19 (s, 6H),

4.69 (s, 6H); *m*-H, 5.73 (dd, 2H), 6.05 (dd, 2H), 6.18 (dd, 2H), 6.32 (dd, 2H), 6.50 (dd, 2H), 6.68 (dd, 2H). ^{31}P NMR (CD_2Cl_2) δ ppm: 37.4 (d, $^1J_{Rh\text{-}P}$= 107 Hz).

(ii) Oxidation of [Rh(η^3-TMPP)$_2$][BF$_4$]$_2$ with [Cp$_2$Fe][BF$_4$]. A solution of [Rh(η^3-TMPP)$_2$][BF$_4$]$_2$ (0.100 g, 0.07 mmol) and [Cp2Fe][BF4] (0.014 g, 0.07 mmol) in 5 mL of CH_2Cl_2 was stirred at -40°C for 30 min. The red solution was treated with 20 mL of diethyl ether to precipitate a solid which was collected by filtration, washed with 2 x 10 mL of diethyl ether to remove unreacted ferrocene and finally dried *in vacuo*; yield, 0.091 g (85%).

(iii) Oxidation of [Rh(η^3-TMPP)$_2$][BF$_4$]$_2$ with HBF$_4$ • Et$_2$O. An amount of [Rh(η^3-TMPP)$_2$][BF$_4$]$_2$ (**3**) (0.015 g, 0.011 mmol) was dissolved in ~ 0.7 mL of CD_3CN. The purple solution was then transferred to a NMR tube and ~ 0.1 mL of HBF_4 • Et_2O. Within 12 h, the solution colored had changed from purple to red. A ^{31}P NMR spectrum of the solution at this time revealed the presence of [Rh^{III}(η^3-TMPP)$_2$][BF$_4$]$_3$ (**4**).

(3) Demethylation of [Rh(η^3-TMPP)$_2$][BF$_4$]$_3$: Formation of [Rh(η^3-TMPP)(C$_6$H$_2$(OMe)$_2$OP{C$_6$H$_2$(OMe)$_3$}$_2$)][BF$_4$]$_2$ (5)

(i) Solution A quantity of [Rh(η^3-TMPP)$_2$][BF$_4$]$_3$ (**4**) (0.150 g, 0.11 mmol) was dissolved in 10 mL of acetone to give a red solution which was stirred overnight at r.t. The pale orange solution was filtered through Celite and treated with 20 mL of diethyl ether to produce an orange solid which was collected by suction filtration, washed with 2 x 5 mL of diethyl ether, and dried under a reduced pressure; yield, 0.085 g (61%). *Anal.* Calcd for $C_{53}H_{63}F_8P_2O_{18}B_2Rh$: C, 47.98; H, 4.79. Found: C, 47.28; H, 5.21. Electronic absorption spectrum (CH_2Cl_2) λ_{max}, nm (ε): 329 (25,000) 260 sh, 242 sh. ^{1}H NMR (CD_2Cl_2) δ ppm: -OCH_3, 2.94 (s, 3H), 3.06 (s, 3H), 3.32 (s, 3H), 3.41 (s, 3H), 3.46 (s, 3H), 3.52 (s, 3H), 3.53 (s, 3H), 3.55 (s, 3H), 3.68 (s, 3H), 3.84 (s,

3H), 3.85 (s, 6H), 3.90 (s, 3H), 3.92 (s, 3H), 4.16 (s, 3H), 4.33 (s, 3H), 4.51 (s, 3H); *m*-H, 5.60 (mult, 3H), 5.84 (dd, 1H), 5.89 (dd, 1H), 5.98 (dd, 1H), 6.11 (dd, 1H), 6.19 (dd, 1H), 6.23 (dd, 1H), 6.36 (dd, 1H), 6.53 (dd, 1H), 6.96 (dd, 1H). ^{31}P NMR (CD_2Cl_2) δ ppm: + 31.5 (dd, $^1J_{Rh\text{-}P}$= 140 Hz, $^2J_{PA\text{-}PB}$= 13.7 Hz), + 37.9 (dd, $^1J_{Rh\text{-}P}$= 139 Hz, $^2J_{PA\text{-}PB}$= 13.7 Hz).

(ii) Solid State. An amount of [Rh(η^3-TMPP)$_2$][BF_4]$_3$ (**4**) (0.015 g, 0.010 mmol) was placed in a Schlenk tube and heated to 50°C for 36 hrs in an oil bath, during which time the color of the solid changed from deep red to pale orange. After cooling to room temperature, the ^{1}H NMR spectrum of the solid was recorded and compared to an authentic sample of **5** prepared as in (**i**). Conversion of **4** to **5** was quantitative based on this result.

(iii) Reaction of [Rh(η^3-TMPP)$_2$][BF_4]$_3$ (4) with TMPP. A quantity of [Rh(η^3-TMPP)$_2$][BF_4]$_3$ (**4**) (0.015 g, 0.010 mmol) and TMPP (0.006 g, 0.011 mmol) was dissolved in ~ 0.7 mL of CD_3CN. The solution color immediately went from red to orange. The solution was pippetted into a NMR tube and the conversion of **4** to **5** was confirmed by ^{1}H NMR spectroscopy.

(iv) Reaction of [Rh(η^3-TMPP)$_2$][BF_4]$_3$ (4) with [(Bu^n)$_4$N][I]. A mixture of [Rh(η^3-TMPP)$_2$][BF_4]$_3$ (**4**) (0.015 g, 0.010 mmol) and tetra-butyl ammonium iodide (0.004 g, 0.011 mmol) were dissolved in ~ 0.07 mL of d_6-acetone. The solution color changed from red to orange within 5 min. The solution was transferred to a NMR tube in order to monitor the reaction progress by ^{1}H and ^{31}P NMR spectroscopy. Conversion of **4** to *cis*-[Rh^{III}(η^3-TMPP)(η^3-TMPP-*O*)][BF_4]$_2$ (**5**) was found to be quantitative by ^{31}P NMR spectroscopy. The presence of CH_3I (δ = 2.16 ppm), presumably formed as a by-product, was detected by ^{1}H NMR.

(4) Chemical Reduction of $[Rh(\eta^3\text{-TMPP})_2][BF_4]_2$

In a typical reaction, a mixture of $[Rh(\eta^3\text{-TMPP})_2][BF_4]_2$ (0.100 g, 0.075 mmol) and Cp_2Co (0.014 g, 0.075 mmol) was dissolved in acetonitrile (5 mL). The resulting purple solution was stirred for 5 h at r.t. During this period the solution color transformed from purple to red-brown. The solvent was removed under vacuum and the resulting residue was taken up in THF (5-10 mL) leaving behind undissolved $[Cp_2Co][BF_4]$. The red-brown solution was filtered through Celite and subsequently pumped to dryness. Finally, the brown residue was washed with diethyl ether (2 x 10 mL) and dried under reduced pressure. ^1H NMR (d_6-acetone) δ ppm: -OCH_3: 3.46 (s, 3H), 3.47 (s, 6H), 3.52 (s, 18H), 3.67 (s, 3H), 3.80 (s, 12H), 3.86 (s, 6H), 3.90 (s, 3H); *m*-H: 4.83 (mult, 1H), 5.18 (mult, 1H), 5.87 (dd, 1H), 6.08 (t, $^4J_{P\text{-}H} = {}^4J_{Ha\text{-}Hb}$ = 2.1 Hz, 1H), 6.17 (d, $^4J_{P\text{-}H}$= 2.7 Hz, 4H), 6.26 (d, $^4J_{P\text{-}H}$= 3.6 Hz, 2H), 6.40 (d, $^4J_{P\text{-}H}$= 3.0 Hz, 2H). ^{31}P NMR (CD_3CN) δ ppm: -8.9 (dd, $^1J_{Rh\text{-}P}$= 131.8 Hz, $^2J_{PA\text{-}PB}$= 392.4 Hz), -13.4 (dd, $^1J_{Rh\text{-}P}$= 120.9 Hz, $^2J_{PA\text{-}PB}$= 392.4 Hz). Samples were contaminated with a small amount of TMPP-CH_3^+, ^1H NMR (d_6-acetone) δ ppm: 2.47 (d, $^2J_{P\text{-}H}$= 15 Hz, 3H, P-CH_3), (3.66 (s, 18H, *o*-OME), 3.84 (s, 9H, *p*-OMe), 6.34 (d, $^4J_{P\text{-}H}$= 4.8, 6H, *m*-H); and $[Cp_2Co]^+$: ^1H NMR (d_6-acetone) δ ppm: 5.92 (s, 10H, Cp-H). Similar results were also obtained when acetone was used as the reaction solvent.

(5) Preparation of $[Rh(TMPP)_2][PF_6]_2$

In an Erlenmeyer flask, a quantity of $[Rh(TMPP)_2][BF_4]_2$ (0.100 g, 0.975 mmol) and $NaPF_6$ (0.125 g, 0.750 mmol) was dissolved in 5 mL of acetone. The solution was stirred for 15 min, filtered and an additional amount of $NaPF_6$ was added (0.125 g, 0.750 mmol). Again, the solution was stirred for 15 minutes and filtered. The solvent was evaporated and the purple solid was redissolved in 20 mL of CH_2Cl_2. After filtration of the

solution to remove the undissolved sodium salts, the solution was treated with 10 mL of THF and concentrated on a rotary evaporator to approximately 5 mL. The resulting purple crystalline solid was collected by suction filtration, washed with cold THF (2 x 3 mL), diethyl ether (2 x 5 mL) and finally dried under reduced pressure; yield, 0.085 g (78%).

B. X-ray Crystallography

The structures of the complexes $[Rh(\eta^3\text{-}TMPP)_2][BF_4]_2$ (**3**) and $[Rh(\eta^3\text{-}TMPP)_2][BF_4]_3$ (**4**) were determined by application of general procedures which have been fully described elsewhere.[15] Geometric and intensity data were collected on a Nicolet P3/F diffractometer with graphite monochromated MoKα ($\lambda_{\bar{\alpha}}$ = 0.71073 Å) radiation and were corrected for Lorentz and polarization effects. All calculations were performed on a VAXSTATION 2000 computer. Data reduction and the initial refinement were performed using the programs from the Enraf-Nonius Structure Determination Package (SDP).[16] The modeling of the $[BF_4]^-$ ion and final refinement for **4** were carried out with the use of the Texsan crystallographic software package of Molecular Structure Corporation.[17]

(1) $[Rh(\eta^3\text{-}TMPP)_2][BF_4]_2$ (3).

(i) Data Collection and Reduction. Single crystals of **3** were grown by a careful layering of toluene on a solution of the compound in CH_2Cl_2. A red-purple parallelepiped with approximate dimensions 0.67 x 0.35 x 0.22 mm^3 was mounted on the tip of a glass fiber with epoxy cement. Geometric and intensity data were collected at 22 ± 2°C. Indexing and refinement of 16 reflections in the range $4 \leq 2\theta \leq 12°$ selected from a rotational photograph gave unit cell parameters for an orthorhombic crystal system. The cell was

Table 6. Summary of crystallographic data for $[Rh^{II}(\eta^3\text{-TMPP})_2][BF_4]_2$ (**3**) and $[Rh^{III}(\eta^3\text{-TMPP})_2][BF_4][PF_6]_2$ (**4a**).

	3	**4a**
Formula	$RhP_2F_8O_{18}C_{54}B_2H_{66}$	$RhP_4F_{16}O_{18}C_{54}B_1H_{66}$
Formula weight	1341.5	1544.68
Space group	Pbcn	Pcca
a, Å	15.938(5)	21.205(7)
b, Å	17.916(7)	11.694(6)
c, Å	21.015(8)	29.10(2)
α, deg	90	90
β, deg	90	90
γ, deg	90	90
V, $Å^3$	6001(6)	7216(6)
Z	4	4
d_{calc}, g/cm^3	1.427	1.422
μ, cm^{-1}	4.20	4.17
Temperature, °C	22 ± 2	-90 ± 3
Trans. factors, max., min.	1.00, 0.87	1.00, 0.38
R^a	0.073	0.118
$R_w{}^b$	0.089	0.139
quality-of-fit[c]	2.89	4.57

[a] $R = \Sigma \; | \; |F_o| - |F_c| \; | / \Sigma |F_o|$

[b] $R_w = [\Sigma w(|F_o| - |F_c|)^2 / \Sigma w |F_o|^2]^{1/2}$; $w = 1/\sigma^2(|F_o|)$

[c] $\text{quality-of-fit} = [\Sigma w(|F_o| - |F_c|)^2 / (N_{obs} - N_{parameter})]^{1/2}$

further refined by a least squares fit of 20 reflections in the range of $13 \leq 2\theta \leq 25°$. The Laue class was determined to be mmm by axial photography. A total of 3952 unique data were collected in the range $4 \leq 2\theta \leq 45°$ by using the θ-2θ scan technique. Three standard reflections, measured at regular intervals every 97 reflections, decayed by 2%; a decay correction was applied to the data by using the program CHORT in SDP. After data reduction, a total of 2462 reflections remained with $F_o^2 > 3\sigma(F_o^2)$.

(ii) Structure Solution and Refinement. The position of the Rh atom was located by the direct methods program in SHELXS-86.[18] The remaining non-hydrogen atoms were located through successive cycles of least-squares refinements and difference Fourier maps. After isotropic convergence had been achieved, an empirical absorption correction based upon the program DIFABS was applied to the data.[19] In the end, refinement of 369 parameters gave residuals of R = 0.080 and R_w = 0.098 and a quality-of-fit index of 2.89. The largest shift/esd was 0.58 and the highest peak in the final difference Fourier map was 1.91 $e^-/Å^3$.

(2) [Rh(η^3-TMPP)$_2$][PF$_6$]$_2$[BF$_4$]

(i) Data Collection and Reduction. Dark red crystals of [Rh(η^3-TMPP)$_2$][PF$_6$]$_2$[BF$_4$] were prepared by oxidation of [Rh(η^3-TMPP)$_2$][BF$_4$]$_2$ (**3**) with $NOPF_6$ and were grown from a mixture of CH_3CN/toluene/Et_2O at -5°C in the presence of excess PF_6^-. A crystal with the approximate dimensions 0.52 x 0.39 x 0.31mm^3 was selected, taken up on the tip of a glass fiber with viscous oil and immediately placed in a cold stream of N_2 at -90°C. Indexing and refinement of 13 reflections selected from a rotational photograph gave cell parameters consistent with an orthorhombic space group. After further refinement of 20 reflections in the range $13 < 2\theta < 25°$, the Laue symmetry was determined to be mmm by axial photography. Data were collected using

the ω-scan technique. Three check reflections were monitored at regular intervals throughout data collection and showed an average decay of 6%. The data were corrected for the observed decay by application of the program CHORT in SDP. After averaging equivalent reflections, 4722 unique data remained of which 2390 were observed with $F_o^2 \geq 3\sigma(F_o)^2$.

(ii) Structure Solution and Refinement. The position of the Rh atom was located by the direct methods program in SHELXS-86. The remaining non-hydrogen atoms were found after a series of alternating least-squares refinements and difference Fourier maps. The positional and thermal parameters of the hydrogen atoms were calculated and treated as fixed contributors to the structure factor calculation. An absorption correction was applied using the program DIFABS,[19] which resulted in relative minimum and maximum transmission factors of 0.38 and 1.00. All non-hydrogen atoms of the $[Rh(TMPP)_2]^{3+}$ cation were refined anisotropically with the exception of C(10), C(13), C(20), C(21), C(24), and C(25) which were refined isotropically. Thermal parameters for the $[PF_6]^-$ and $[BF_4]^-$ anions were also refined isotropically. Treatment of the $[BF_4]^-$ ion is described in the following section. The final refinement converged with residuals R and R_w of 0.118 and 0.139, respectively, and a quality-of-fit of 4.60. After convergence, the largest shift/esd was 0.58 and the highest peak in the difference Fourier map was 2.23 $e^-/Å^3$ which is associated with the boron atom of the $[BF_4]^-$ counterion.

The first counterion located in the difference map occupied a general position in the cell and was determined to be a $[PF_6]^-$ ion based on the initial height of the peak and the presence of six other peaks in the difference map distributed in an octahedral arrangement about the central atom. The central atom of the second counterion was found to reside on a crystallographic two-fold rotation axis and was accompanied by two other

atoms situated with a bond angle that approximated that of a tetrahedron. Refinement of the group as a $[BF_4]^-$ ion led to a satisfactory thermal parameter for boron, but unfortunately, the fluorine atoms could not be successfully refined. Therefore the entire $[BF_4]^-$ anion was treated as a rigid group at a population of 0.5 using the rigid group parameters located in the Texsan software package. The group was fixed on the two-fold axis and allowed to rotate relative to this axis. This resulted in the formation of two rigid tetrahedral $[BF_4]^-$ units, at 0.5 occupancy each, that shared a central boron atom. Isotropic refinement of the $[BF_4]^-$ moiety led to the formation of a pseudo-cage of eight fluorine atoms at a population of 0.5 each about the boron atom. Other attempts to refine this group as part of a PF_6^- ion failed, leading to an unsatisfactorily high isotropic thermal parameter (> 35) for the central atom.

3. Results

The highly unusual mononuclear rhodium(II) complex, $[Rh(\eta^3\text{-TMPP})_2][BF_4]_2$ (**3**) was isolated in high yield from the reaction of TMPP and $[Rh_2(MeCN)_{10}][BF_4]_4$, and although the complex possesses extraordinary air and thermal stability for a radical species, it nonetheless exhibits a rich and varied chemistry. Chemical or electrochemical oxidation of **3** produces the d^6 Rh(III) complex $[Rh(\eta^3\text{-TMPP})_2][BF_4]_3$ (**4**) with a ligand arrangement identical to that found in the parent complex. In striking contrast to the remarkable stability of the divalent complex $[Rh(\eta^3\text{-TMPP})_2][BF_4]_2$ (**3**), the Rh(III) species **4** is air-sensitive and thermally unstable, eventually forming the demethylated complex Rh(III) complex, $[Rh^{III}(\eta^3\text{-TMPP})(\eta^3\text{-TMPP-}O)][BF_4]_2$ (**5**), where TMPP-*O* = $[(OC_6H_2(OMe)_2P\{C_6H_2(OMe)_3\}_2]^{1-}$.

The structures of compounds **3** and **4** have been determined by single crystal X-ray diffraction methods. Crystal parameters and basic information pertaining to data collection and structure refinement are summarized in Table 6. ORTEP representations of $[Rh(\eta^3\text{-TMPP})_2][BF_4]_2$ (**3**) and $[Rh(\eta^3\text{-TMPP})_2][PF_6]_2[BF_4]$ are depicted in Figures 9 and 13. Selected bond distances and angles for each structure are listed in Tables 8 and 9. Full tables of positional and anisotropic thermal parameters for compounds **3** and **4** are located in the appendices.

A. Preparation and Spectroscopic Properties of $[Rh(\eta^3\text{-TMPP})_2][BF_4]_2$ (3)

Slow addition of TMPP to $[Rh_2(MeCN)_{10}][BF_4]_4$, both dissolved in CH_3CN, produces a dark red-purple solution of **3**, with the reaction being complete within one hour (eq 12). The reaction is performed in the dark in order to avoid formation of Rh(I) and Rh(III) species that result from room light photolysis of $[Rh_2(MeCN)_{10}]^{4+}$ in acetonitrile.[20] Free TMPP reacts with $[Rh(\eta^3\text{-TMPP})_2][BF_4]_2$ to dealkylate one of the coordinated methoxy

$$[Rh_2(MeCN)_{10}][BF_4]_4 + \underset{\mathbf{1}}{4\ TMPP} \xrightarrow[0°C]{MeCN} 2\ \underset{\mathbf{3}}{[Rh^{II}(\eta^3\text{-TMPP})_2][BF_4]_2} \quad (12)$$

groups. This results in the formation a new Rh(II) complex that is ligated by one neutral TMPP ligand and a phenoxy-phosphine derivative of TMPP. Therefore, in order to maximize yields of **3**, the presence of excess phosphine must be avoided during the reaction. As a result, dilute solutions of TMPP are added dropwise to highly concentrated of $[Rh_2(MeCN)_{10}][BF_4]_4$ to maintain an excess of $[Rh_2(MeCN)_{10}][BF_4]_4$. Moreover, the reaction is kept at 0° C to further retard nucleophilic attack by free phosphine. Unlike

$[Rh^{II}(\eta^3\text{-TMPP})_2][BF_4]_2$ (**3**), the demethylated Rh(II) complex is air-sensitive and readily decomposes to an intractable mixture of diamagnetic species. Details of the deliberate synthesis of this species by reaction of **3** with various nucleophiles is presented in chapter VII.

Initially, $[Rh(\eta^3\text{-TMPP})_2][BF_4]_2$ was synthesized by addition of a methanolic solution of TMPP to a suspension of $[Rh_2(MeCN)_{10}][BF_4]_4$ in MeOH. This method was attractive because the relatively low solubility of **3** in MeOH leads to the precipitation of the product. However, the yields were typically lower than those found for reactions carried out in MeCN; this is presumably due to the low solubility of the Rh_2^{4+} salt in MeOH which serves to keep the phosphine ligand in excess and increases the likelihood of the demethylation side-reaction. Furthermore, samples of **3** obtained from methanolic solutions were invariably contaminated by a gray solid with unusual properties. When redissolved in acetonitrile, the solid produces orange solutions that analyzed as $[Rh_2(MeCN)_{10}]^{4+}$ by ^1H NMR. This gray solid is believed to be a mixed-valence linear tetramer formed by one electron reduction of the dirhodium species.[21] Evidence for the formation of this species is found in the photochemistry of $[Rh_2(MeCN)_{10}][BF_4]_4$ and a similar species has been prepared directly by electrochemical reduction of $[Rh_2(MeCN)_{10}][BF_4]_4$ in high ionic strength media by another member of this research group.[20,21]

As a final synthetic approach to preparing Rh(II) complexes of TMPP, we reacted TMPP with $RhCl_3{\cdot}xH_2O$ in refluxing ethanol, a method that has been widely used to prepare many of the reported Rh(II) species with bulky phosphines.[5] In the present case, however, an intractable mixture of diamagnetic products was detected by ^1H NMR spectroscopy. We rationalize

that this is largely due to the demonstrated instability of $[Rh(\eta^3\text{-}TMPP)_2][BF_4]_2$ in the presence of free halides.

The compound $[Rh(\eta^3\text{-}TMPP)_2][BF_4]_2$ is soluble in methylene chloride and acetonitrile, partially soluble in methanol, chloroform and acetone, and completely insoluble in water, tetrahydrofuran, diethyl ether and hydrocarbon solvents. The complete lack of solubility of **3** in THF is important, since the reaction by-products formed in the synthesis of **3** exhibit limited solubility in THF and can therefore be separated from **3** by repeated washings with THF. Recrystallization of $[Rh(\eta^3\text{-}TMPP)_2][BF_4]_2$ also relies on its insolubility in THF; recrystallization is accomplished by concentrating 3:1 CH_2Cl_2 / THF solutions of **3** on a rotary evaporator until the solutions are sufficiently rich in THF to precipitate the paramagnetic complex as a purple crystalline solid. In contrast to the $[BF_4]^-$ salt, the $[PF_6]^-$ salt of $[Rh^{II}(\eta^3\text{-}TMPP)_2]^{2+}$ is slightly solubile in THF.

Remarkably, $[Rh(\eta^3\text{-}TMPP)_2][BF_4]_2$ is air-stable, but CH_2Cl_2 solutions decompose slowly over periods of several weeks, depositing a finely divided insoluble gray solid presumed to be rhodium metal. Solid samples, on the other hand, are stable for indefinite periods in air. These observations are somewhat surprising considering the documented, sensitive nature of Rh(II) monomers. Typically these molecules can only be synthesized by electrochemical methods and subsequently decompose within short periods of time even under anaerobic conditions.[22]

The infrared spectrum of $[Rh(\eta^3\text{-}TMPP)_2][BF_4]_2$ displays bands assignable to coordinated TMPP ligands and a broad feature at 1050 cm-1 which is indicative of the $[BF_4]^-$ counterion. The electronic spectrum recorded in CH_2Cl_2 exhibits a d-d transition at λ_{max} = 537 nm (2050 M^{-1} cm^{-1}) which is responsible for the intense purple color of the compound. Several higher

energy charge-transfer transitions are located at λ_{max} = 329 nm (1.34 x 10^4 $M^{-1}cm^{-1}$), 298 nm (1.53 x 10^4 $M^{-1}cm^{-1}$) 285 nm (1.75 x 10^4 $M^{-1}cm^{-1}$), 233 nm (6.24 x 10^4 $M^{-1}cm^{-1}$), 420 nm (sh).

Not unexpectedly for a d^7 metal complex, the ^1H and ^{31}P NMR signals are broad and reveal no information about the structure. In general, Rh(II) phosphine complexes have been characterized by their EPR activity and their broad, largely unidentifiable NMR features. We note that this data and ours are in sharp contrast to several puzzling instances in which paramagnetic Rh(II) compounds have evidently exhibited sharp and unshifted NMR signals as well as EPR signals.[3c,23]

B. Magnetic and EPR Spectroscopic Properties of [Rh(η^3-TMPP)$_2$][BF_4]$_2$ (3)

The paramagnetism of **3** was investigated by EPR spectroscopy and magnetic susceptibility, the results of which are presented in Table 7. EPR measurements of **3** were carried out in a variety of solvents at 298 K and at 77 K. At room temperature, solutions of **3** in CH_2Cl_2, acetonitrile/toluene (1:1) and CH_2Cl_2/Me-THF (1:1) produce identical spectra with a single isotropic homogeneous line at $g \approx 2.20$. The EPR spectrum of [Rh(η^3-TMPP)$_2$][BF_4]$_2$ in a CH_2Cl_2/MeTHF glass at 77 K exhibits a rhombic signal as shown in Figure 8. The g-values of the CH_2Cl_2/MeTHF system are g_{xx} = 2.26, g_{yy} = 2.30 and g_{zz} = 1.99. The proximity of g_{zz} to that of the free-electron value is consistent with a d_z^2 ground state for the unpaired electron and confirms the radical nature of **3**. The average of the three anisotropic g-values equals that of the isotropic line at room temperature, therefore the change in line shape is due to the rapid tumbling of the complex in solution,

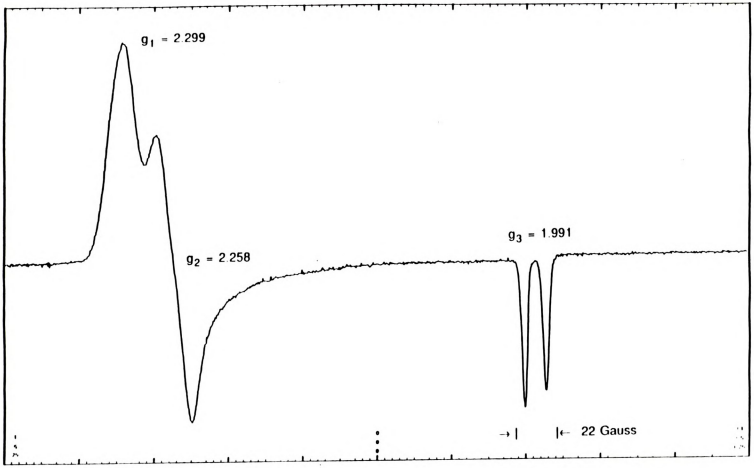

Figure 8. EPR spectrum of $[Rh(\eta^3\text{-TMPP})_2][BF_4]_2$ (**3**) in a CH_2Cl_2/Me-THF glass at 77 K.

as opposed to being frozen in random orientations with respect to the applied field at 77 K. In the anisotropic spectrum (77 K), g_{zz} is split into a doublet (A_{zz}= 2.0 x 10^{-3} cm^{-1}) due to the hyperfine interaction with the I=1/2 nucleus of ^{103}Rh. Since the linewidths along g_{xx} and g_{yy} are broader than the hyperfine tensor components along these axes, hyperfine coupling is not observed. Similar behavior has been reported for Rh(II) species trapped in zeolites.[24] In the zeolite study, a doublet splitting of g_{zz} of ~32 G was reported and a dynamic Jahn-Teller effect was observed at high temperatures (400°C). Even so, examples of ^{103}Rh hyperfine coupling along all three principal directions are not unknown; Wilkinson and co-workers observed hyperfine coupling along all three axes (A_x = 4.7 x 10^{-3} cm^{-1}, $A_y = A_z$ = 5.6 x 10^{-3} cm^{-1}) in the organometallic species Rh(2,4,6-$Pr^i_3C_6H_2)_2$(tht)$_2$.[25]

The magnetic moment of [Rh(η^3-TMPP)$_2$][BF_4]$_2$ (**3**) was measured both in solution and the solid state. The results of these studies are listed in Table 7. Solid state susceptibility measurements were performed over a temperature range of 5-286 K at a variety of field strengths. Compound **3** exhibited Curie-Weiss behavior over the entire range of temperatures. A plot of χ_m vs 1/T yielded a temperature independent paramagnetism (T.I.P.) contribution of 424 x 10^{-6} cgsu, which was applied, along with a correction for diamagnetism, to the average magnetic moment giving a value of 1.80(3) μ_B. Solution studies were carried out using the Evans NMR method[26] and resulted in a μ_{eff} of 2.10 μ_B. Both measurements are consistent with a S=1/2 ground state, as is expected for a low spin d^7 ion. Similar values have been reported for several other mononuclear Rh(II) complexes.[2]

Table 7. EPR Spectroscopic and Magnetic Susceptibility Data for $[Rh(\eta^3\text{-}TMPP)_2][BF_4]_2$ (**3**)

	$[Rh(\eta^3\text{-}TMPP)_2][BF_4]_2$ (**3**)
EPR (CH_2Cl_2/Me-THF glass)[a]	
g_{xx}	2.26
g_{yy}	2.30
g_{zz}	1.99
A_{zz}, G (cm^{-1})	22 (2.0 x 10^{-3})
magnetic moment, μ_{eff}, μ_B[b]	
solution[c]	2.10
solid[d]	1.80

[a] Measured at 77 K. [b] A diamagnetic correction of -724 x 10^{-6} was applied based on -20 x 10^{-6} for Rh^{2+}, -39 x 10^{-6} for BF_4^- and -313 x 10^{-6} for TMPP. [c] Measured in CH_2Cl_2 at 294 K using Evans method[18]. [d] Average magnetic moment measured over a temperature range of 5-286 K at several field strengths.

C. Crystal Structure of $[Rh(\eta^3\text{-TMPP})_2][BF_4]_2$ (3)

The molecular cation shown in Figure 9, consists of two phosphine ligands bonded to the Rh atom in a face capping tridentate mode through the oxygen atoms of two pendant methoxy-groups and the phosphorus atom. This bonding arrangement of TMPP is identical to that observed in the molybdenum tricarbonyl complex $(\eta^3\text{-TMPP})Mo(CO)_3$.[27] The geometry about the Rh center is a distorted octahedron, with the Rh atom residing on a two-fold axis that bisects the P-Rh-P' angle (Figure 10). Perhaps the most striking feature of the structure is the fact that the phosphines lie *cis* to each other rather than *trans*, as expected on the basis of steric arguments. The consequences of steric repulsion resulting from the *cis* geometry are evident in the P(1)-Rh-P(1)' bond angle of 105.2(1)°. Indeed Rh(II) complexes with the formula RhX_2L_2 where L is a bulky tertiary phosphine have been shown to exist in a *trans*conformation.[6] While it is conceivable that the cis complex is a kinetic product, we have been unsuccessful in isomerizing the compound to a *trans*geometry at higher temperatures. It is interesting in the context of this discussion to note that Rauchfuss *et al.* also observed a *cis* arrangement of $PPh_2(o\text{-}MeOC_6H_4)$ groups for $RuCl_2(PR_3)_2$, in which the ether-phosphine also participated in a chelating interaction with the metal.[28] Furthermore, Shaw noted similar *cis* isomers in the reaction of $PPh_2(C_6H_4OH)$ with Pd and Pt chlorides.[29] Apparently, electronic factors play a prominent role in stabilizing the *cis* conformation relative to the sterically favored *trans* geometry for these mixed ether-phosphine donors.

In the case of **3**, the chelation results in the formation of a five-membered metallacyclic ring, the geometric requirements of which distort the molecule as evidenced by the strained P(1)-Rh(1)-O(6) bond angles of 77.7(2)° and 80.5(1)° (Table 8). This distortion is of the same magnitude as that

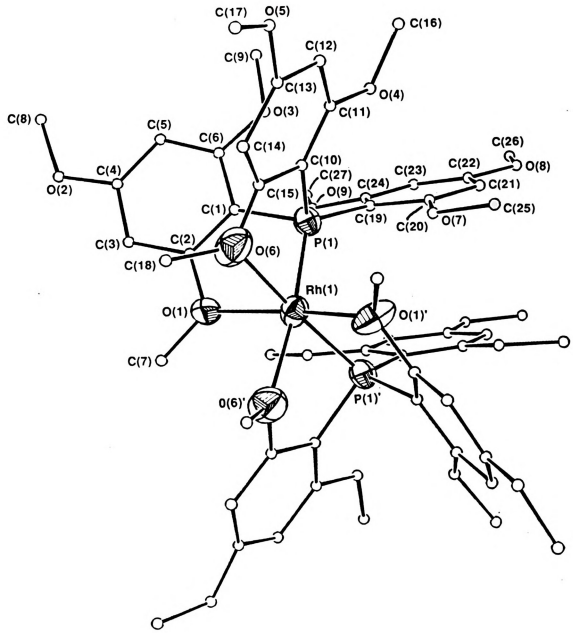

Figure 9. ORTEP representation of the $[Rh(\eta^3\text{-}TMPP)_2]^{2+}$ (**3**) molecular cation with 40% probability ellipsoids. Phenyl ring atoms are shown as small spheres of arbitrary size for clarity.

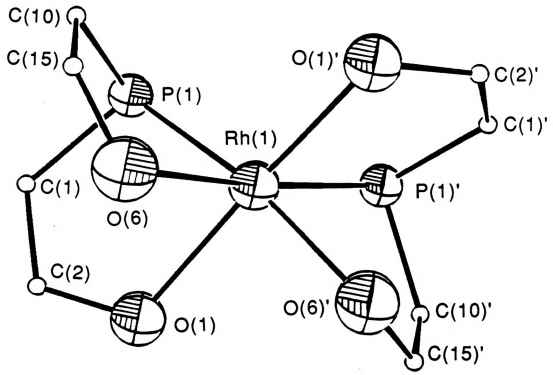

Figure 10. ORTEP drawing emphasizing the coordination sphere of $[Rh(\eta^3\text{-TMPP})_2]^{2+}$.

observed for other complexes containing similar chelate rings, such as $AsCl_3(PR_3)_2$[30] $RuCl_2(PR_3)_2$[28] and (η^3-TMPP)$Mo(CO)_3$[27]

The distances within the immediate coordination sphere of Rh are worth commenting upon as they show some unusual features. The Rh(1)-P bond distance of 2.216(2)Å is significantly shorter than the corresponding distances found in most Rh(I) and Rh(III) phosphine complexes, which are generally in the range of 2.28 Å to 2.37 Å.[31] As for the Rh-P bond distances in other mononuclear Rh(II) compounds, the only other example which we are aware, trans-$RhCl_2(PPr^i_3)_2$, exhibits Rh-P bonds that are slightly longer, 2.366(1) Å.[6, 32] This is not unexpected, since in $RhCl_2(PPr^i_3)_2$ the phosphines exert a significant trans effect on each other. In contrast, complex **3** contains ether donors in positions opposite to the phosphorus donors; these would be expected to exhibit little if any trans effect.[33] Indeed the Rh-O bond distances in **3** are quite long as compared to those of metal alkoxides or other anionic oxygen donor ligands and are indicative of the weak nature of the Rh-ether bond.[34] Rauchfuss arrived at a similar conclusion upon observing that $RuCl_2(PR_3)_2$, with phosphorus atoms *trans* to methoxy-groups, exhibits Ru-P bond distances that are much shorter than in other Ru(II) phosphine complexes.[28]

Of further importance in the solid state structure of $[Rh^{II}(\eta^3\text{-TMPP})_2]^{2+}$ is the presence of two chemically distinct metal-ether interactions. The oxygen atoms that are *trans* to phosphorus are bonded at a distance of 2.201(6) Å, whereas the mutually *trans* oxygen atoms exhibit Rh-O distances of 2.398(1) Å. The axial elongation is undoubtedly the result of the unpaired electron residing in the d_z^2 orbital and constitutes the first structural evidence for such an effect in d^7 Rh(II) chemistry. Removal of the odd electron via chemical oxidation results in shortening of the Rh-OMe

Table 8. Selected bond distances (Å) and angles (deg) for $[Rh^{II}(\eta^3\text{-TMPP})_2][BF_4]_2$ (**3**).

Bond Distances

atom 1	atom 2	distance	atom 1	atom 2	distance
Rh(1)	P(1)	2.216(2)	O(3)	C(9)	1.449(8)
Rh(1)	O(1)	2.398(5)	O(4)	C(11)	1.37(1)
Rh(1)	O(6)	2.201(6)	O(4)	C(16)	1.48(1)
P(1)	C(1)	1.829(7)	O(6)	C(15)	1.39(1)
P(1)	C(10)	1.826(7)	O(6)	C(18)	1.45(1)
P(1)	C(19)	1.770(7)	O(7)	C(20)	1.351(9)
O(1)	C(2)	1.393(9)	O(7)	C(25)	1.49(1)
O(1)	C(7)	1.470(9)	O(9)	C(24)	1.367(8)
O(2)	C(4)	1.380(9)	O(9)	C(27)	1.445(9)
O(2)	C(8)	1.44(1)	C(1)	C(2)	1.39(1)
O(3)	C(6)	1.370(8)	C(1)	C(6)	1.41(1)

Bond Angles

atom 1	atom 2	atom 3	angle	atom 1	atom 2	atom 3	angle
P(1)	Rh(1)	P(1)'	105.2(1)	C(4)	O(2)	C(8)	118.8(7)
P(1)	Rh(1)	O(1)	80.5(1)	C(6)	O(3)	C(9)	119.6(6)
P(1)	Rh(1)	O(1)'	107.1(1)	C(11)	O(4)	C(16)	120.5(8)
P(1)	Rh(1)	O(6)	77.9(2)	Rh(1)	O(6)	C(15)	113.9(5)
P(1)	Rh(1)	O(6)'	171.5(2)	C(15)	O(6)	C(18)	118.5(7)
O(1)	Rh(1)	O(1)'	167.8(3)	C(20)	O(7)	C(25)	118.3(6)
O(1)	Rh(1)	O(6)	91.1(2)	C(24)	O(9)	C(27)	117.3(6)
O(1)	Rh(1)	O(6)'	81.1(2)	P(1)	C(1)	C(2)	122.1(6)
O(6)	Rh(1)	O(6)'	100.2(3)	P(1)	C(1)	C(6)	120.7(6)
Rh(1)	P(1)	C(1)	102.9(3)	C(2)	C(1)	C(6)	116.7(7)
Rh(1)	P(1)	C(10)	99.6(3)	O(1)	C(2)	C(1)	115.6(6)
Rh(1)	P(1)	C(19)	124.5(3)	O(1)	C(2)	C(3)	120.8(7)
C(1)	P(1)	C(10)	100.8(3)	C(1)	C(2)	C(3)	123.4(7)
C(1)	P(1)	C(19)	113.5(4)	C(2)	C(3)	C(4)	116.3(7)
C(10)	P(1)	C(19)	112.3(4)	O(2)	C(4)	C(3)	112.7(7)

distances, so that both sets of methoxy bonds to the metal, axial and equatorial, are essentially equivalent in length (vide infra). Interestingly, although the axial ether groups are located at long distances, they afford protection from attack by donor solvents such as MeCN or oxidizing solvents such as CH_2Cl_2. Similar protective properties of ortho methoxy substituents were also noted by Rauchfuss.[28]

D. Redox properties of $[Rh(\eta^3\text{-TMPP})_2][BF_4]_2$ (3)

A cyclic voltammogram of $[Rh(\eta^3\text{-TMPP})_2][BF_4]_2$ (**3**) (shown in Figure 11) exhibits two accessible redox couples, one reversible oxidation at $E_{1/2}$ = + 0.46 V and a quasi-reversible reduction at $E_{1/2}$ = -0.65 V (vs Ag/AgCl). Accordingly, we expected that **3** would undergo chemical redox reactions to form Rh(I) and Rh(III) compounds with minimal structural rearrangement.

(1) Oxidation of $[Rh(\eta^3\text{-TMPP})_2][BF_4]_2$ (3)

(i) Synthesis and spectroscopic characterization of $[Rh(\eta^3\text{-TMPP})_2][BF_4]_3$

Oxidation of **3** with either $[NO][BF_4]$ or $[Cp_2Fe][BF_4]$ in MeCN or CH_2Cl_2 solutions results in the formation of a deep red solution of $[Rh(\eta^3\text{-TMPP})_2][BF_4]_3$ (**4**). The product was isolated as an oily solid by addition of Et_2O or evaporation of the solvent. Complex **4** is both air sensitive and thermally unstable. The latter point is illustrated by the fact that solutions of **4** readily decompose at ambient temperatures (vide infra). To circumvent this problem, the synthesis of **4** was carried out at -40°C. The cyclic voltammogram of **4** is identical to that of **3** except that the two redox couples correspond to one-electron reductions to form Rh(II) and Rh(I) species (Figure 12). Shröeder and Cooper reported analogous electrochemical behavior for the homoleptic Rh(III) thioether complexes $[Rh(9S3)_2]^{3+}$, $[Rh(10S3)_2]^{3+}$ and $[Rh(12S3)_2]^{3+}$, for which both the Rh(II) and Rh(I)

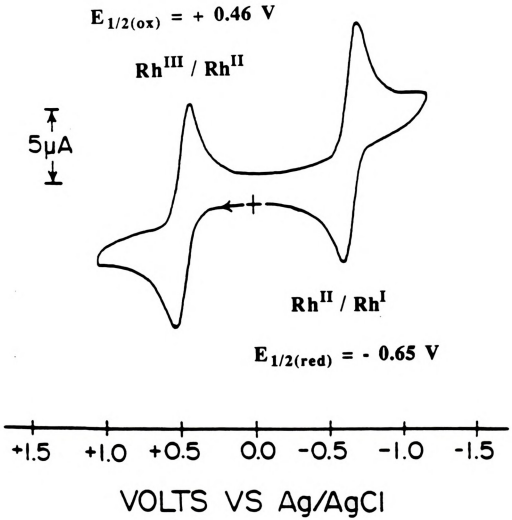

Figure 11. Cyclic voltammogram of $[Rh^{II}(\eta^3\text{-TMPP})_2][BF_4]_2$ (**3**) in 0.1 M $TBABF_4$ in CH_2Cl_2.

oxidation states are accessible.[22a-c] Interestingly, acetonitrile solutions of **3** may also be oxidized to **4** by the addition of an excess of $HBF_4 \cdot Et_2O$. The reaction, which occurrs slowly over a period of 12 hours, was monitored by both ^1H and ^{31}P NMR spectroscopy. Presumably, H^+ is reduced to H_2 during the course of the reaction, although the formation of H_2 was not readily apparent from the ^1H NMR spectrum.

Infrared spectral measurements of **4** show a typical pattern for coordinated TMPP in addition to a strong broad band at 1050 cm^{-1} which corresponds to the $[BF_4]^-$ counterion. The ^1H NMR spectrum of **4** in CD_2Cl_2 exhibits nine resonances between $\delta = 2.93$ and $\delta = 4.69$ corresponding to the 12 methoxy substituents for two magnetically equivalent TMPP ligands. Further downfield there are a set of six poorly resolved doublets of doublets of equal intensity found in the region of the meta-protons of the phenyl rings. The ABX pattern of the resonance corresponds to coupling of one ring proton to the other ring proton as well as to the phosphorus. The ^{31}P NMR spectrum in CD_2Cl_2 shows a doublet centered at $\delta = +37.4$ ppm ($J_{Rh\text{-}P} = 107$ Hz), further indicating that the two TMPP ligands are equivalent. Therefore, it appears that the ABX pattern of the meta-protons arises from coupling of proximal and distal protons on the individual chelating rings, which then further couple to a phosphorus nucleus to produce the observed ABX splitting pattern. Although only two rings participate in the chelation to the metal, it is apparent that the meta-protons on the third non-interacting ring are magnetically inequivalent as these protons also exhibit an ABX splitting pattern. These results suggest that the non-interacting ring is sterically locked into an asymmetric environment and is unable to rotate freely about the P-C bond, thereby rendering the ring protons inequivalent.

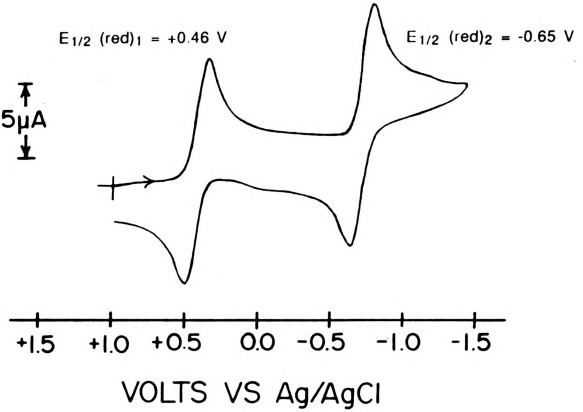

Figure 12. Cyclic voltammogram of $[Rh^{III}(\eta^3\text{-TMPP})_2][BF_4]_3$ (**4**) in 0.1 M $TBABF_4$ in CH_2Cl_2.

(ii) Crystal Structure of $[Rh(\eta^3\text{-TMPP})_2][PF_6]_2[BF_4]$

Difficulties encountered while modeling a disorder of the $[BF_4]^-$ anions have precluded a satisfactory refinement of the structure in these regions. Attempts to model the highly disordered counterions are described in the experimental section. These problems notwithstanding, the Rh(III) molecular cation itself is well behaved, and therefore, a brief description of this species is presented here. The preliminary X-ray results show that the Rh atom lies on a two-fold axis that bisects the cis phosphine ligands as in the structure of the parent complex $[Rh(\eta^3\text{-TMPP})_2]^{2+}$ (**3**) (Figure 13). As a result of this symmetry, the two phosphines are crystallographically equivalent just as was observed in solution by ^1H and ^{31}P NMR studies. Both TMPP ligands bind to the metal in the familiar capping tridentate fashion observed in the structure of **3** and in the molecule $(\eta^3\text{-TMPP})Mo(CO)_3$.[27] The most striking feature of the structure **4** compared to **3** is the dramatic contraction of the axial Rh-OMe bonds while the equatorial distances remain essentially unchanged (Table 9). The Rh(1)-O(1) bond distance has shortened from 2.398(5) Å in $[Rh(\eta^3\text{-TMPP})_2][BF_4]_2$ to 2.18(2) Å in the structure of **4**, and is now is roughly equivalent to the equatorial Rh-O(6) distance (2.22(1) Å). Thus, removal of the odd electron from the d_z^2 orbital of **3** alleviates the observed axial distortion. The above result is important because it illustrates the TMPP ligand's ability to adjust to and accommodate electronic changes at the metal center.

(iii) Decomposition of $[Rh(\eta^3\text{-TMPP})_2][BF_4]_3$ (4)

As mentioned earlier, solutions of $[Rh(TMPP)_2][BF_4]_3$ are thermally unstable with respect to loss of a methyl group to form $[Rh(\eta^3\text{-TMPP})(\eta^3\text{-TMPP-}O)][BF_4]_2$ (**5**) (η^3-TMPP-*O* = $P\{C_6H_2(OMe)_3\}_2\{C_6H_2(OMe)_2O\}$) as shown in equation 13. At room temperature, solutions of **4** in CD_3CN show

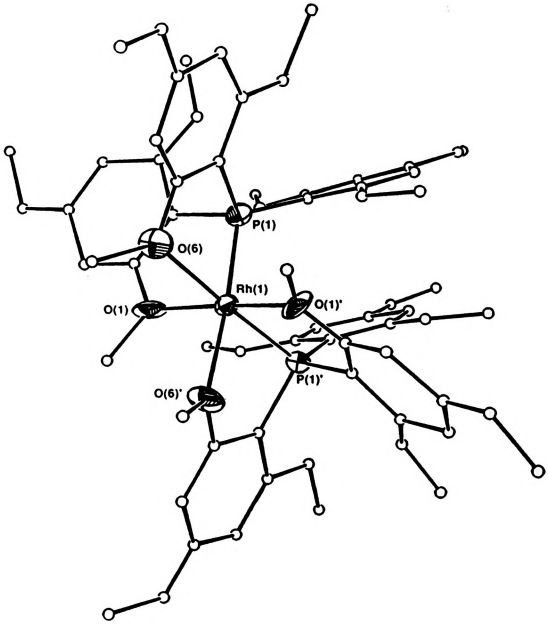

Figure 13. ORTEP drawing of the $[Rh^{III}(\eta^3\text{-TMPP})_2]^{3+}$ (**4**) molecular cation. Phenyl ring atoms are shown as small spheres of arbitrary size for clarity.

Table 9. Selected bond distances (Å) and angles (deg) for $[Rh^{III}(\eta^3\text{-TMPP})_2][PF_6]_2[BF_4]$ (**4a**).

Bond Distances

atom 1	atom 2	distance	atom 1	atom 2	distance
Rh(1)	P(1)	2.231(6)	O(3)	C(9)	1.41(4)
Rh(1)	O(1)	2.18(2)	O(4)	C(11)	1.35(3)
Rh(1)	O(6)	2.22(1)	O(4)	C(16)	1.49(4)
P(1)	C(1)	1.81(3)	O(5)	C(13)	1.37(3)
P(1)	C(10)	1.84(2)	O(5)	C(17)	1.38(3)
P(1)	C(19)	1.79(2)	O(6)	C(15)	1.38(3)
O(1)	C(2)	1.36(3)	O(7)	C(20)	1.33(3)
O(1)	C(7)	1.42(3)	O(7)	C(25)	1.39(3)
O(2)	C(4)	1.31(4)	O(8)	C(22)	1.41(3)
O(2)	C(8)	1.36(6)	O(8)	C(26)	1.31(4)
O(3)	C(6)	1.34(3)	O(9)	C(24)	1.39(3)

Bond Angles

atom 1	atom 2	atom 3	angle	atom 1	atom 2	atom 3	angle
P(1)	Rh(1)	P(1)'	103.6(3)	C(4)	O(2)	C(8)	118(3)
P(1)	Rh(1)	O(1)	81.9(5)	C(6)	O(3)	C(9)	124(2)
P(1)	Rh(1)	O(1)'	103.9(5)	C(11)	O(4)	C(16)	115(2)
P(1)	Rh(1)	O(6)	77.5(4)	Rh(1)	O(6)	C(15)	115(1)
P(1)	Rh(1)	O(6)'	173.9(6)	C(15)	O(6)	C(18)	119(2)
O(1)	Rh(1)	O(1)'	170.7(8)	C(20)	O(7)	C(25)	119(2)
O(1)	Rh(1)	O(6)	82.1(7)	C(24)	O(9)	C(27)	120(2)
O(1)	Rh(1)	O(6)'	92.0(7)	P(1)	C(1)	C(2)	121(2)
O(6)	Rh(1)	O(6)'	102.0(7)	P(1)	C(1)	C(6)	118(2)
Rh(1)	P(1)	C(1)	100.1(9)	C(2)	C(1)	C(6)	121(3)
Rh(1)	P(1)	C(10)	100.0(7)	O(1)	C(2)	C(1)	118(2)
Rh(1)	P(1)	C(19)	121.2(8)	O(1)	C(2)	C(3)	119(2)
C(1)	P(1)	C(10)	104(1)	C(1)	C(2)	C(3)	123(3)
C(1)	P(1)	C(19)	117(1)	C(2)	C(3)	C(4)	119(3)
C(10)	P(1)	C(19)	112(1)	O(2)	C(4)	C(3)	119(3)

evidence of demethylation within minutes by NMR spectroscopy, but upon cooling to -20 °C the process is slowed considerably Dealkylation eventually occurs regardless of solvent choice, but the reaction is much faster in acetone and acetonitrile than in methylene chloride. The process is quite facile, as evidenced by the fact that even solid samples of **4** slowly convert to **5** over a period of weeks at room temperature. If one heats solid samples of **4** to 50 °C under vacuum, nearly quantitative conversion to **5** occurs within 36 hours.

$$\underset{\mathbf{4}}{[Rh^{III}(\eta^3\text{-TMPP})_2][BF_4]_3} \xrightarrow[CH_2Cl_2,\ r.\ t.]{-CH_3^+} \underset{\mathbf{5}}{[Rh^{III}(\eta^3\text{-TMPP})(\eta^3\text{-TMPP-}O)][BF_4]_2} \quad (13)$$

Compound **5** was prepared in bulk by stirring acetone solutions of $Rh(\eta^3\text{-TMPP})_2[BF_4]_3$ at room temperature for 12 hours; during this time the solution color changed from deep red to orange. The product was isolated as a pale orange solid by addition of diethyl ether, and while its infrared spectrum is nearly indistinguishable from that of $[Rh(\eta^3\text{-TMPP})_2][BF_4]_3$ (**4**), the ^1H NMR spectrum reveals the magnetic inequivalence of the two phosphine ligands (Figure 14). The spectrum, shown in Figure 14, displays nine distinct resonances between δ = 5.84 and 6.96 with an ABX coupling pattern and a set of three overlapping signals centered about δ = 5.60 ppm. Upfield resonances between δ = 4.51 and δ = 2.94 ppm correspond to the ortho and para methoxy substituents on the phenyl rings and number 17 by integration, as compared to 18 in the parent complex $[Rh(\eta^3\text{-TMPP})_2]^{3+}$, thereby confirming the loss of a methyl group from one of the methoxy substituents. The appearance of the ^1H NMR spectrum is highly solvent dependent.

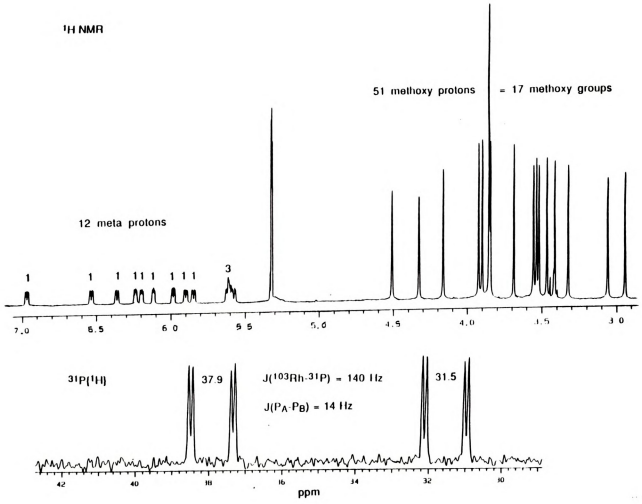

Figure 14. ^{1}H and ^{31}P NMR spectra of *ax*-[Rh^{III}(TMPP)(TMPP-*O*)][BF_4]$_2$ in CD_2Cl_2.

The conversion of $[Rh(\eta^3\text{-TMPP})_2][BF_4]_3$ (**4**) to $[Rh(TMPP)(TMPP\text{-}O)][BF_4]_2$ (**5**) has been monitored by ^1H NMR in d^6-acetone, d_3-acetonitrile and d_2-methylene chloride; each of these studies revealed the onset of new resonances for **5**, but none that could be assigned to the protons of a methylated by-product were observed. This observation coupled with the solid state transformation of **4** to **5** is consistent with the formation of a volatile species that we believe to be CH_3F resulting from attack by $[BF_4]^-$ on the complex (eq 14).[35] Although uncommon, such transformations are not unprecedented; In fact, several examples of activation of $[BF_4]^-$ by transition

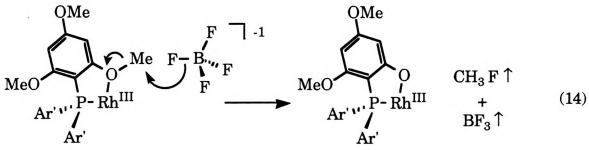

(14)

metal complexes have been reported.[36] Generally these transformations involve highly charged electrophilic metal centers. Such complexes are so susceptible to activation that researchers are resorting to highly deactivated fluoro-substituted anions such as $[(C_6F_5)_4B]^-$ and $[(3,5\text{-}CF_3\text{-}C_6H_3)_4B]^-$ in order to stabilize these highly electrophilic metal centers.[37] It is apparent that in order to further expand the chemistry of $[Rh(\eta^3\text{-TMPP})_2][BF_4]_3$, similar strategies must be adopted in our laboratories.

The ^{31}P NMR spectral data provide information regarding the coordination geometry about the metal center.[38] ^{31}P NMR spectral measurements of **5** (Figure 14) reveal two resonances with an ABX splitting pattern at δ = + 37.9 ppm for P_A ($^1J_{Rh\text{-}P}$=138.9 Hz, $^2J_{P\text{-}P}$=13.73 Hz) and δ = +

31.5 ppm for P_B ($^1J_{Rh\text{-}P}$=140.4 Hz, $^2J_{P\text{-}P}$=13.73 Hz). The small magnitude of the P-P coupling is indicative of a *cis* disposition of phosphines.[39] Furthermore, the similarity in the two Rh-P coupling constants suggests that the phenoxide interaction is *cis* to both phosphorus atoms, in an axial (*ax*) position relative to the plane containing the phosphorus atoms. Presence of a Rh-phenoxide bond in a *trans* disposition to one of the phosphorus nuclei would be expected to result in a larger difference in the Rh-P coupling constants. The structure of **5,** shown below, is rationalized by considering that a methoxy interaction with a metal center weakens the O-CH_3 bond thus rendering the carbon susceptible to nucleophilic attack. It follows that the stronger the metal-oxygen interaction, the more electrophilic the methyl group becomes. Methoxy groups exert a weaker *trans* influence than the

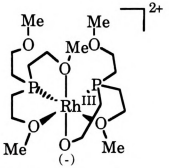

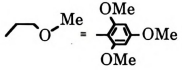

ax-[Rh^{III}(η^3-TMPP)(η^3-TMPP-*O*)]$^{2+}$

phosphorus atoms, resulting in stronger M-O interactions for the mutually *trans* methoxy groups than for those *trans* to the phosphines. It is worth noting that dealkylation of ether groups in methoxy-phosphines has been previously observed, including for a dirhodium carboxylate complex prepared in our laboratories, but in contrast to the present study, these were found to occur under more forcing conditions and in the presence of much stronger nucleophiles.[40,41] The instability of [Rh(η^3-TMPP)$_2$][BF_4]$_3$ (**4**) may, in part, be

explained by the relatively hard nature of the Rh^{3+} cation compared to that of other platinum group metals in the +1 and +2 oxidation states. Furthermore, from their work with ether-phosphines, Shaw and co-workers observed that the ease of dealkylation increased with increased steric bulk of the ancillary substituents on the phosphine.[41b] It is reasonable to assume that the considerable bulk of the methoxy substituted phenyl rings of TMPP contributes to facile demethylation of $[Rh(\eta^3\text{-TMPP})_2][BF_4]_3$ (**4**).

We found that dealkylation of a coordinated methoxy-group significantly alters the electrochemistry of the complex. Electrochemical measurements performed on CH_2Cl_2 solutions of **5** show that the molecule undergoes an irreversible oxidation at $E_{p,a}$ = +1.55 V vs Ag/AgCl that most likely corresponds to a ligand-based process based on the fact that a number of other TMPP species undergo similar processes near this potential. More importantly, **5** exhibits an irreversible reduction at $E_{p,c}$ = -0.80 V vs. Ag/AgCl with a coupled chemical oxidation wave at -0.02 V vs Ag/AgCl. Chemical reduction with cobaltocene yields a deep red solution that exhibits a broad ^1H NMR signal characteristic of a paramagnetic compound. The latter species resembles the product obtained by the direct reaction of the Rh(II) complex $[Rh^{II}(\eta^3\text{-TMPP})_2][BF_4]_2$ (**3**) with additional TMPP. In fact, comparison of the EPR spectroscopic properties of this newly formed Rh(II) complex with that of the product obtained from nucleophilic attack on $[Rh^{II}(\eta^3\text{-TMPP})_2][BF_4]_2$ (**3**) reveal that the two compounds are identical. We propose that the two products obtained by both routes are the Rh(II) analog of **5**, i.e. the Rh(II) phosphino-phenoxide complex [Rh(TMPP)(TMPP-*O*)][BF_4]. Details of the chemical and structural relationship between **5** and its Rh(II) analog are presented in chapter VII.

(2) Reduction of $[Rh(\eta^3\text{-TMPP})_2][BF_4]_2$ (3)

In light of the synthesis of $[Rh(\eta^3\text{-TMPP})_2][BF_4]_2$ and $[Rh(\eta^3\text{-TMPP})_2][BF_4]_3$, isolation of a analogous Rh(I) complex ligated solely by TMPP has proven elusive. Chemical reduction of $[Rh(\eta^3\text{-TMPP})_2][BF_4]_2$ (**3**) by cobaltocene in either acetone or acetonitrile produces a red-brown solution within several hours at room temperature. No reaction occurs at temperatures less than -15°C. The product was isolated from THF as a brown diamagnetic solid. Samples were invariable contaminated with minor amounts of salts containing $[TMPP\text{-}CH_3]^+$ and $[Cp_2Co]^+$. The complex series of multiplets and doublets observed for the meta proton resonances in the ^1H NMR spectrum of the solid, clearly indicates that the two phosphines are magnetically inequivalent. Moreover, integration of the spectrum reveals that only 17 methoxy resonances are observed, clearly supporting that a dealkylation reaction occurs following reduction of the metal. This is not surprising, in light of the demonstrated presence of $[TMPP\text{-}CH_3]^+$ in isolated samples. While the complexity of the ^1H NMR spectrum precludes further analysis of the coordination geometry, important information may be gleaned from the ^{31}P NMR spectrum. The ^{31}P NMR spectrum of the product in CD_3CN exhibits two resonances with an ABX spin system at δ = -8.9 ppm (dd, $^1J_{Rh\text{-}P}$= 131.8 Hz, $^2J_{PA\text{-}PB}$= 392.4Hz) and -13.4 ppm (dd, $^1J_{Rh\text{-}P}$= 120.9 Hz, $^2J_{PA\text{-}PB}$= 392.4 Hz) (Figure 15). The magnitude of the P_A-P_B coupling constant is in agreement with the presence of two magnetically inequivalent TMPP ligands that have a *trans* relationship to each other. Based on the the NMR spectral data presented, it appears that the reduction of **3** ultimately results in the formation of *trans*- $Rh^I(\eta^2\text{-TMPP})(\eta^2\text{-TMPP-}O)$ (eq. 15). Apparently, the Rh(I) cation, $[Rh(TMPP)_2]^{1+}$, formed upon initial reduction of

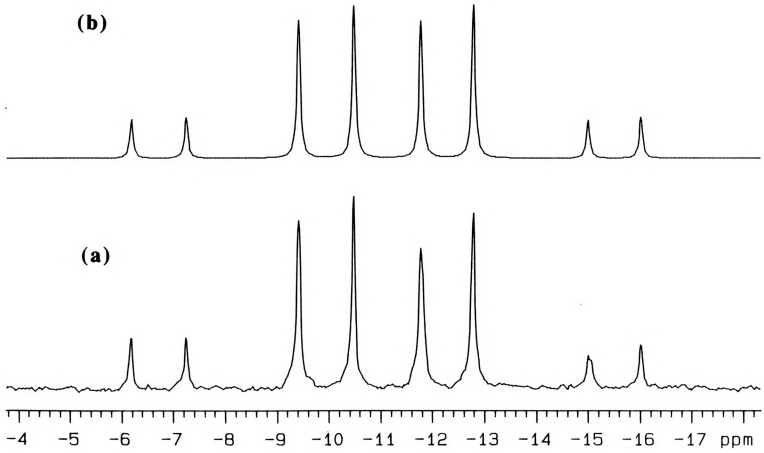

Figure 15. ^{31}P NMR spectrum of the product from the reduction of $[Rh^{II}(\eta^3\text{-TMPP})_2][BF_4]_2$ (**3**) with cobaltocene: (a) observed (b) simulated.

3, is unstable with respect to phosphine dissociation. Upon dissociation, the

$$[Rh^{II}(\eta^3\text{-TMPP})_2]^{2+} \xrightarrow{Cp_2Co} \text{"}[Rh^{I}(TMPP)_2]^{1+}\text{"} \qquad (15a)$$

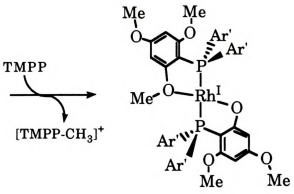

(15b)

free TMPP then acts as a nucleophile resulting in the demethylation of a coordinated phosphine. Further evidence for phosphine dissociation was provided by the appearance of $[TMPP\text{-}CH_2Cl]^+$ impurities in samples prepared in CH_2Cl_2.

4. Discussion

As far as we are aware, $[Rh(\eta^3\text{-TMPP})_2]^{2+}$ represents the only case of a structurally characterized six-coordinate mononuclear Rh(II) complex. The utility of $[Rh_2(MeCN)_{10}][BF_4]_4$ as a synthon for unusual mononuclear and polynuclear rhodium species is illustrated by the observation that chemistry of TMPP with other dinuclear starting materials, such as $Rh_2(OAc)_4(MeOH)_2$, yield only partially substituted dinuclear TMPP complexes.[40, 42] The stability of the (formally) 19 e⁻ species is attributed to the presence of four interacting ether groups which serve to stabilize the complex both electronically and sterically. The presence of these pendent groups serve two purposes: (1) to kinetically stabilize the metal center from

dimerization and (2) to provide thermodynamic stability for the +2 oxidation state relative to either Rh(I) or Rh(III) oxidation states. Without the "built-in" coordinative saturation afforded by the tethered "solvent" molecules, one would expect the molecule to undergo the usual disproportionation or dimerization reactions which are commonly observed in divalent Rh chemistry. However, unlike many complexes kinetically stabilized by sterically encumbering ligand sets, the lability of the ether groups opens up coordination sites so that further reactivity may occur. Moreover, the ready availability of the dangling ether groups allows for reversible substitution reactions with a variety of substrates, a situation which is generally not possible with complexes that undergo dissociative loss of a ligand. We have exploited these aspects of the ligand in order to further develop the potentially rich area of mononuclear Rh(II) chemistry, results of which are presented in subsequent chapters.

List of References

1. (a) Kemmit, R. D. W.; Russel, D. R.; in *Comprehensive Organometallic Chemistry*; Wilkinson, G.; Stone, F. G. A.; Abel, E. W., eds.; Pergamon: New York, 1982; vol. 5. (b) Smith, T. D.; Pilbrow, J. R. *Coord. Chem. Rev.* **1981**, *39*, 295. (c) Stoppioni, P; Dapporto, D.; Sacconi, L. *Inorg. Chem.* **1978**, *17*, 718. (d) Klein, H.-F.; Karsch, H. H. *Chem. Ber.* **1976**, *109*, 1453. (e) Mu, X. H.; Kadish, K. M. *Inorg. Chem.* **1989**, *28*, 3743.

2. Felthouse, T. R. *Prog. Inorg. Chem.* **1982**, *29*, 73 and references therein.

3. (a) Billig, E.; Shupack, S.I.; Waters, J.H.; Williams, R.; Gray H.B. *J. Am. Chem. Soc.* **1964**, *86*, 926.(b) Pneumatikakis, G.; Psaroulis, P. *Inorg. Chim. Acta* **1980**, *46*, 97. (c) Pandey, K. K.; Nehete, D. T.; Sharma, R. B. *Polyhedron* **1990**, *9*, 2013. (d) Peng, S. M.; Peters, K.; Peters, E. M.; Simon, A. *Inorg. Chim. Acta* **1985**, *101*, L35.

4. (a) Wayland, B. B.; Sherry, A. E.; Coffin, V. L. *J. Chem. Soc., Chem. Commun.* **1989**, 662. (b) Wayland, B. B.; Sherry, A. E. *J. Am. Chem. Soc.* **1989**, *111*, 5010. (c) Wayland, B. B.; Sherry, A. E.; Poszmik, G.; Bunn, A. G. *J. Am. Chem. Soc.* **1992**, *114*, 1673. (d) Wayland, B. B.; Ba, S.; Sherry, A. E. *J. Am. Chem. Soc.* **1991**, *113*, 5305. (e) Sherry, A. E.; Wayland, B. B. *J. Am. Chem. Soc.* **1990**, *112*, 1259. (f) Bunn, A. G.; Wayland, B. B. *J. Am. Chem. Soc.* **1992**, *114*, 6917.

5. (a) Bennett, M. A.; Lonstaff, P. A. *J. Am. Chem. Soc.*, **1969**, *91*, 6266. (b) Moers, F. G.; DeJong, J. A. M.; Beaumont, P. M. J. *J. Inorg. Nucl. Chem.* **1973**, *35*, 1915. (c) Masters, C.; Shaw, B. L. *J. Chem. Soc. (A)* **1971**, 3679. (d) Empsall, H. D.; Heys, P. N.; Shaw, B. L. *Transition Met. Chem.* **1978**, *3*, 165. (e) Empsall, H. D.; Hyde, E. M.; Pawson, D.; Shaw, B. L.; *J. Chem. Soc., Dalton Trans.* **1977**, 1292.

6. (a) Harlow, R. L.; Thorn, D. L.; Baker, R. T.; Jones, N. L. *Inorg. Chem.* **1992**, *31*, 993. (b) Rappert, T.; Wolf, J.; Schulz, M.; Werner, H. *Chem. Ber.* **1992**, *125*, 839.

7. Van Gaal, H. L. M.; Verlaak, J. M. J.; Posno, T. *Inorg. Chim. Acta.* **1977**, *23*, 43.

8. (a) Zhilyaev, A. N.; Rotov, A. V.; Kuz'menko, I. V.; Baronovskii, I. B. *Doklady Akad. Nauk* **1988**, *302*, 275. (b) Pneumatikakis, G.; Psaroulis, P. *Inorg. Chim. Acta.* **1980**, *46*, 97.

9. Dunbar, K. R. *Comments Inorg. Chem.* **1992**, *13*, 0000.

10. (a) Dunbar, K. R. *J. Am. Chem. Soc.* **1988**, *110*, 8247. (b) Dunbar, K. R.; Pence, L. E. manuscript in preparation.

11. (a) Dunbar, K. R.; Quillevéré, A. *Inorg. Chem.* submitted for publication. (b) Quillevéré, A. Ph. D. Dissertation, Michigan State University, **1992**.

12. Dunbar, K. R.; Pence, L. E. *Inorg. Synth.* **1992**,*29*, in press.

13. Gray, H. B.; Hendrickson, D. N.; Sohn, Y. S. *Inorg. Chem.* **1971**, *10*, 1559.

14. Morris, D. E.; Dunbar, K. R.; Arrington, C. A.; Doorn, S. K.; Pence, L. E.; Woodruff, W. H. submitted to *J. Am. Chem. Soc.*

15. (a) Bino, A.; Cotton, F. A.; Fanwick, P. E. *Inorg. Chem.* **1979**, *18*, 3558. (b) Cotton, F. A.; Frenz, B. A.; Deganello, G.; Shaver, A. *J. Organomet. Chem.* **1973**, *50*, 227.

16. Structure Determination Package: Enraf-Nonius, Delft, The Netherlands (1979).

17. TEXSAN-TEXRAY: Structure analysis package, Molecular Structure Corporation (1985).

18. SHELXS-86: Sheldrick, G. M. in *Crystallographic Computing 3*; Sheldrick, G. M.; Goddard, R. Eds; Oxford University Press, 1984; p. 175.

19. Walker, N.; Stuart, D. *Acta. Cryst.* **1983**,*A39*, 158.

20. Morris, D. E.; Dunbar, K. R.; Arrington, C. A.; Doorn, S. K.; Pence, L. E.; Woodruff, W. H. submitted to *J. Am. Chem. Soc.*

21. For other tetranuclear Rh_4^{6+} species see (a) Miskowski, V. M.; Gray, H. B. *Inorg. Chem.* **1987**, *26*, 1108. (b) Mann, K. R.; DiPierro, M. J.; Gill, T. P. *J. Am. Chem. Soc.* **1980**, *102*, 3965. (c) Miskowski, V. M.; Sigal, I. S.; Mann, K. R.; Gray, H. B.; Milder, S. J.; Hammond, G. S.; Ryason, P. R. *J. Am. Chem. Soc.* **1979**, *101*, 4384-5. (d) Mann, K. R.; Gray, H. B. *Adv. Chem. Ser.* **1979**, *173*, 225. (e) Mann, K. R.; Lewis, N. S.; Miskowski, V. M.; Erwin, D. K.; Hammond, G. S.; Gray, H. B. *J. Am. Chem. Soc.* **1977**, *99*, 5525.

21. Pence, L. E. Ph. D. Thesis, Michigan State University, **1992**.

22. Examples of coordination and organometallic Rh(II) complexes prepared electrochemically: (a) Cooper, S. R.; Rawle, S. C.; Yagbasan, R.; Watkin, D. J. *J. Am. Chem. Soc.* **1991**,*113*, 1600. (b) Rawle, S. C.; Yagbasan, R.; Prout, K.; Cooper, S. R. *J. Am. Chem. Soc.* **1987**, *109*, 6181. (c) Blake, A. J.; Gould, R. D.; Holder, A. J.; Hyde, T. I.; Schröder, M. *J. Chem. Soc., Dalton Trans.* **1988**, 1861. (d) Anderson, J. E.; Gregory, T. P. *Inorg. Chem.* **1989**, *28*, 3905. (e) Scwarz, H. A.; Creutz,

C. *Inorg. Chem.* **1983**, *22*, 207. (e) Mulazzani, Q. G.; Emmi, S.; Hoffman, M. Z.; Venturi, M. *J. Am. Chem. Soc.* **1981**, *103*, 3362. (f) Kölle, U.; Kläui, W. *Z. Naturforsch.* **1991**, *46b*, 75. (g) Bianchini, C.; Laschi, F.; Ottaviani, M. F.; Peruzzini, M.; Zanello, P.; Zanobini, F. *Organometallics* **1989**, *8*, 893. (h) Bianchini, C.; Meli, A.; Laschi, F.; Vizza, F.; Zanello, P. *Inorg. Chem.* **1989**, *28*, 227. (i) Pilloni, G.; Schiavon, G.; Zotti, G.; Zecchin, S. *J. Organomet. Chem.* **1977**, *134*, 305. (j) Fischer, E. O.; Lindner, H. H. *J. Organomet. Chem.* **1964**, *1*, 307. (k) Fischer, E. O.; Wawersik, H. *J. Organomet. Chem.* **1966**, *5*, 559. (l) Keller, H. J.; Wawersik, H. *J. Organomet. Chem.* **1967**, *8*, 185. (m) Dessy, R. E.; King, R. B.; Waldrop, M. *J. Am. Chem. Soc.* **1966**, *88*, 5112. (n) Dessy, R. E.; Kornmann, R.; Smith, C.; Hayter, R. *J. Am. Chem. Soc.* **1968**, *90*, 2001.

23. Ogle, C. A.; Masterman, T. C.; Hubbard, J. L. *J. Chem. Soc., Chem. Commun.* **1990**, 1733.

24. Goldfarb, D.; Kevan, L. *J. Phys. Chem.* **1986**, *90*, 264; 2137; 5787.

25. Hay-Motherwell, R. S.; Koschmieder, S. U.; Wilkinson, G.; Hussain-Bates, B.; Hursthouse, M. B. *J. Chem. Soc., Dalton Trans.* **1991**, 2821.

26. (a) Evans, D. F. *J. Chem. Soc.* **1959**, 2003. (b) Deutsch, J. L.; Poling, S. M. *J. Chem. Ed.* **1969**, *46*, 167.

27. Dunbar, K. R.; Haefner, S. C.; Burzynski, D. J. *Organometallics* **1990**, *9*, 1347.

28. Jeffrey, J. C.; Rauchfuss, T. B. *Inorg. Chem.* **1979**, *18*, 2658.

29. Empsall, H. D.; Shaw, B. L.; Turtle, B. L. *J. Chem. Soc., Dalton Trans.* **1976**, 1500.

30. Granziani, R.; Bombiere, G.; Volponi, L.; Panattoni, C.; Clark, R. J. H. *J. Chem. Soc. (A)* **1969**, 1236.

31. Corbridge, D. E. C. *The Structural Chemistry of Phosphorus*; Elsevier: Amsterdam, 1974, chapter 11.

32. The structure $Rh(PPh_3)_2Cl$(s-bqdi) (s-bqdi = semi-o-benzoquinone diimine) of has appeared. However, no magnetic evidence was presented to support the assignment of the rhodium oxidation state: Peng, S. M.; Peters, K.; Peters, E. M.; Simon, A. *Inorg. Chim. Acta* **1985**, *101*, L35.

33. Cetinkaya, B.; Lapport, M. F.; McLaughlin, G. M.; Turner, K. *J. Chem. Soc., Dalton Trans.* **1974**, 1591.

34. For example see: (a) Chebi, D. E.; Fanwick, P. E.; Rothwell, I. P. *Polyhedron* **1990**, *9*, 969. (b) Mehrotra, R. C.; Agarwal, S.K.; Singh, Y. P. *Coord. Chem. Rev.* **1985**, *68*, 101. (c) Boyar, E. B.; Robinson, S.D. *Coord. Chem. Rev.* **1983**, *50*, 109. (d) Graham, D.E.; Lamprecht, G. J.; Potgieter, I. M.; Roudt, A.; Leipoldt, J. G. *Trans. Met. Chem.* **1991**, 193. (e) Bryndza, H. E.; Tam, W. *Chem. Rev.* **1988**, *88*, 1163.

35. Igau, A.; Gladysz, J. A. *Polyhedron* **1991**, *10*, 1903. (b) Ferandez, J. M.; Gladysz, J. A. *Organometallics* **1989**, *8*, 207.

36. (a) Gorrel, I. B.; Parkin, G. *Inorg. Chem.* **1990**, *29*, 2452. (b) Thomas, R. R.; Chebolu, V.; Sen. A. *J. Am. Chem. Soc.* **1986**, *108*, 4096. (c) Crabtree, R. H.; Hlatky, G. G.; Holt, E. M. *J. Am. Chem. Soc.* **1983**, *105*, 7302. (d) Hitchcock, P. B.; Lappert, M. F.; Taylor, R. G. *J. Chem. Soc., Chem. Commun.* **1984**, 1082. (e) Reedijk, J. *Comments Inorg. Chem.* **1982**, *6*, 379 and references therein.

37. For instance see (a) Brookhart, M.; Rix, F. C.; DeSimone, J. M.; Barborak, J. C. *J. Am. Chem. Soc.* **1992**, *114*, 5894. (b) Yang, X.; Stern, C. L.; Marks, T. J. *Organometallics* **1991**, *10*, 840. (c) Yang, X.; Stern, C. L.; Marks, T. J. *J. Am. Chem. Soc.* **1991**, *113*, 3623. (d) Horton, A. D.; Orpen, A. G. *Organometallics* **1991**, *10*, 3910. (e) Brookhart, M.; Volpe, A. F. Jr.; DeSimmone, J. M.; Lamanna, W. M. *Polym. Prepr.* **1991**, *32(1)*, 461.

38. Meek, D. W.; Mazanec, T.J. *Acc. Chem. Res.* **1981**, *14*, 226.

39. (a) Pregosin, P. S. *Phosphorus-31 NMR Spectroscopy in Stereochemical Analysis*; Verkade, J. G.; Quin, L. D. ed., VCH, 1987. (b) Pregosin, P. S.; Venanzi, L.M. *Chem. Br.* **1978**, *14*, 276.

40. (a) Chen, S. J.; Dunbar, K. R. *Inorg. Chem.* **1991**, *30*, 2018. (b) Chen, S. J.; Dunbar, K. R. *Inorg. Chem.* **1990**, *29*, 588.

41 (a) Kurosawa, H.; Tsuboi, A.; Kawasaki, Y.; Wada, M. *Bull. Chem. Soc. Jpn.* **1987**, *60*, 3563. (b) Empsall, H. D.; Heys, P. N.; McDonald, W. S.; Norton, M. C.; Shaw, B. L. *J. Chem. Soc., Dalton Trans.* **1978**, 1119. (c) Empsall, H. D.; Heys, P. N.; Shaw, B. L. *J. Chem. Soc., Dalton Trans.* **1978**, 257. (d) Empsall, H. D.; Hyde, E. M.; Shaw, B. L. *J. Chem. Soc., Dalton Trans.* **1975**, 1690. (e) Jones, C. E.; Shaw, B. L.; Turtle, B. L. *J. Chem. Soc., Dalton Trans.* **1974**, 992. (f) Empsall, H. D.; Hyde, E. M.; Jones, C. E.; Shaw, B. L. *J. Chem. Soc., Dalton Trans.* **1974**, 1980.

42. Dunbar, K. R.; Saharan, V.; Matonic, J. M. manuscript in preparation.

CHAPTER IV

REVERSIBLE CARBON MONOXIDE CHEMISTRY OF $[Rh(\eta^3\text{-}TMPP)_2][BF_4]_2$

1. Introduction

The synthesis and isolation of $[Rh(\eta^3\text{-TMPP})_2][BF_4]_2$ provided us with a unique opportunity to explore the chemistry of authentic Rh(II) d^7 metallo-radicals. Typically, radical species are highly reactive and only observed as transients resulting from homolysis of M-M and M-L bonds.[1] Such species have been implicated in a number of important stoichiometric and catalytic transformations.[2] In contrast to the well-documented chemistry of early transition metal radicals, radical species of the platinum group are less understood. Recent work with Rh(II) porphyrin complexes by Wayland and co-workers, which revealed the ability of such species to activate C-H bonds and couple CO groups, underscores the fact that platinum group radical complexes are as important an area of investigation as their early transition metal counterparts.[3]

Early studies of Rh(II) phosphine complexes revealed the proclivity of these systems to undergo rapid disproportionation reactions.[4] For example, reaction of $RhCl_2(PCy_3)_2$ with CO initially yields a paramagnetic species believed to be the Rh(II) carbonyl complex, $RhCl_2(PCy_3)_2(CO)$, which, in solution, rapidly disproportionates to the more stable Rh(I) and Rh(III) counterparts.[4e] The initial Rh(II)CO adduct is so unstable with respect to disproportionation that it can only be detected in solid state reactions. One method of preventing such a reaction is by introducing a more rigid ligand environment that disfavors ligand redistribution. This concept is elegantly illustrated by the chemistry of Rh(II) porphyrins. The porphyrin macrocyclic framework prevents ligand redistribution from occurring and therefore kinetically stabilizes the Rh(II) oxidation state with respect to disproportionation. As a consequence, reactivity is dominated by ligand association reactions and not electron transfer processes. When bulky

substituents were added to the porphyrin macrocycle, dimerization of the d^7 metal fragments was disfavored resulting in the isolation of metal centered radicals.[3]

Similar results may be obtained for Rh(II) phosphine complexes by incorporating chelating groups into the phosphine that deter ligand dissociation. Some work in the past has supported this concept, for example that of Shaw *et al.* who used this approach to isolate moderately stable Rh(II) and Ir(II) species with the general formula $M^{II}(OC_6H_4P(Bu^t)_2)_2$.[5,6] In fact, they found that the Ir(II) complexes formed stable adducts with O_2 and CO.[7] The corresponding small molecule chemistry of the Rh(II) species was not reported.

With these fascinating but limited results as a backdrop, we set out to explore the reactivity of $[Rh(\eta^3\text{-TMPP})_2][BF_4]_2$ by exploiting the weak nature of its Rh-ether bonds to study its potentially rich small molecule substitution chemistry, particularly with CO, in a quest for forming paramagnetic adducts that may exhibit novel reactivity. This chapter investigates the redox and substitution chemistry of $[Rh(\eta^3\text{-TMPP})_2][BF_4]_2$ with CO.

2. Experimental

A. Synthesis

All reactions were carried out under an argon atmosphere by the use of standard Schlenk-line techniques unless otherwise stated. Reactions at pressures greater than 1 atm were performed in a 450 mL stainless steel Parr mini reactor (model 4560) equipped with a magnetic drive stirrer and an automatic temperature control. The starting materials tris(2,4,6-trimethoxyphenyl)phosphine (**1**) (TMPP) and $[Rh(\eta^3\text{-TMPP})_2][BF_4]_2$ (**3**) were prepared as described in Chapters II and III, respectively. The starting

material $[Rh(cod)Cl]_2$ was purchased from Strem Chemicals. $[Rh(CO)_2Cl]_2$ was synthesized from $[Rh(cod)Cl]_2$ by displacement of cod with CO in THF. The salt $[Cp_2Fe][BF_4]$ was prepared by oxidation of Cp_2Fe with hydrofluoroboric acid in the presence of p-benzoquinone.[8] The reagents $CNBu^t$, $NOBF_4$, and Cp_2Co were purchased from Strem Chemicals and used without further purification. Carbon monoxide was obtained from Matheson Gas Products and was used as received. Labeled ^{13}CO (99%) was purchased from Aldrich.

(1) Reaction of $[Rh(\eta^3\text{-TMPP})_2][BF_4]_2$ (3) with CO. In a typical reaction, $[Rh(\eta^3\text{-TMPP})_2][BF_4]_2$ (**3**) (0.100 g, 0.07 mmol) in 10 mL of CH_2Cl_2 was purged with CO gas for 20 min. While maintaining a CO atmosphere, 20 mL of CO-purged diethyl ether was added to the solution which effected the separation of an oily red solid from a yellow solution. The solution was decanted from the solid, the volume of the solution was reduced to 5 mL and diethyl ether (20 mL) was slowly added to precipitate a yellow microcrystalline solid. The yellow product was filtered in air and washed with 2 x 10 mL of diethyl ether and dried *in vacuo*; yield, 0.038 g (40%). The red oil was dissolved in 5 mL of CH_2Cl_2 and layered with 20 mL of diethyl ether. A red-orange precipitate formed which was filtered off, washed with 3 x 5 mL diethyl ether, and dried *in vacuo*; yield 0.043 g (41%).

(2) Reaction of $[Rh(\eta^3\text{-TMPP})_2][BF_4]_2$ (3) with $^{12}CO/^{13}CO$ (1:1). A quantity of $[Rh(\eta^3\text{-TMPP})_2][BF_4]_2$ (**3**) (0.050 g, 0.035 mmol) was dissolved in 10 mL of CH_2Cl_2 and the solution was degassed by several freeze/pump/thaw cycles on a high vacuum line. An equimolar volume of ^{12}CO and ^{13}CO was delivered to the reaction flask with the use of a Toepler pump. The pressure above the solution was calculated to be in the range of 1-2 atm at room temperature. The reaction vessel was allowed to slowly warm to room

temperature, during which time the solution color changed from purple to murky red. After 30 min, a small amount of solution was syringed out and its infrared spectrum was measured; ν(CO) (cm^{-1}): 2011, 1985, 1968 in an approximate 1:2:1 intensity ratio.

(3) Preparation of [Rh(η^2-TMPP)(TMPP)CO][BF_4] (7)

(i) Reduction of [Rh(η^3-TMPP)$_2$][BF_4]$_2$ in the Presence of CO. A solution of [Rh(η^3-TMPP)$_2$][BF_4]$_2$ (0.100 g, 0.07 mmol) and a 3-fold excess of Cp_2Co (0.042 g, 0.22 mmol) in 5 mL of CH_2Cl_2 was stirred under a moderate purge of carbon monoxide. After 20 min, 30 mL of diethyl ether was added and the solution was cooled to -5 °C for 24 h. The yellow product was collected by suction filtration, washed with diethyl ether and recrystallized from CH_2Cl_2 (10 mL) by reduction of the volume and slow addition of diethyl ether (0.5 mL). A crop of yellow-orange crystals was collected by filtration in air, washed with diethyl ether, and dried *in vacuo*; yield: 0.057 g (60%). Anal. Calc'd for $C_{55}H_{66}F_4P_2O_{19}BRh$: C, 51.50; H, 5.19. Found: C, 50.57; H, 5.02. IR (Nujol, CsI): ν(CO) 1958 cm^{-1}; (CH_2Cl_2): ν(CO) 1970 cm^{-1}. ^1H NMR (CD_2Cl_2) δ ppm: 3.48 (s, 36H, *o*-OCH_3), 3.80 (s, 18H, *p*-OCH_3), 6.04 (t, $^4J_{P\text{-}H}$ = 2.1 Hz, 12H, *m*-H). ^{31}P NMR (CD_2Cl_2) δ ppm: -11.1 (d, $^1J_{Rh\text{-}P}$ = 128 Hz). Electronic absorption spectrum (CH_2Cl_2) λ_{max}, nm (ε): 415 sh, 345 (7770), 305 sh, 285 sh, 254 (64,400). Cyclic voltammogram (0.1 M $TBABF_4$ / CH_2Cl_2, vs Ag/AgCl): $E_{1/2(ox)}$ = + 0.50 V.

(ii) Reaction of [Rh(cod)Cl]$_2$ with TMPP in the Presence of CO. A mixture of [Rh(cod)Cl]$_2$ (0.500 g, 1.01 mmol) and $AgBF_4$ (0.395 g, 2.03 mmol) was dissolved in 5 mL THF for 15 min to give a yellow solution. The yellow solution was then filtered through a Celite plug into a 3-neck flask equipped with a gas inlet and an addition funnel containing a solution of TMPP (2.160 g, 4.056 mmol in 30 mL of THF). The entire apparatus was then cooled to 0°C

with an ice bath. The TMPP solution was added dropwise over a period of 10 min during which time the solution was gently purged with CO. After addition of the phosphine, the CO purge was discontinued and the reaction was stirred at 0°C under a CO atmosphere for 1 h. The volume was reduced to 15-20 mL and the reaction solution was stirred for another hour at 0°C to give a yellow precipitate. The yellow solid was filtered in air and washed with diethyl ether (4 x 10 mL). The product was recrystallized by redissolving the solid in 50 mL of CH_2Cl_2 followed by filtration and addition of 20 mL of THF. The volume of the solution was reduced to 10-15 mL and the solution was refrigerated at -5°C. A large crop of yellow crystalline solid was collected by filtration in air, washed with 4 x 10 mL of diethyl ether and dried under reduced pressure; yield: 2.250 g (86%).

(iii) Reaction of $[Rh(CO)_2Cl]_2$ with TMPP A solution flask was charged with $[Rh(CO)_2Cl]_2$ (0.100 g, 0.257 mmol), TMPP (0.548 g, 1.03 mmol) and $NaBF_4$ (0.056 g, 0.514 mmol) and 10 mL of MeCN. The cloudy yellow solution was stirred under reduced pressure for 30 min, after which time, the solvent was removed under vacuum. The yellow product was redissolved in 10 mL of CH_2Cl_2 and filtered through a Celite plug. THF (10 mL) was added to the solution, and the volume of the solution was reduced to approximately 3-5 mL, yielding a yellow crystalline solid. Et_2O (10 mL) was added to precipitate additional product. The solid was filtered in air, washed with 3 x 5 mL of Et_2O and dried *in vacuo*; yield: 0.530 g (80%).

(4) Preparation of $[Rh(TMPP)_2(CO)_2][BF_4]$ (6)

A quantity of $[Rh(\eta^2\text{-TMPP})(TMPP)CO][BF_4]$ (**7**) (0.100 g, 0.08 mmol) in 5 mL of CH_2Cl_2 was treated with CO gas for 5 min, after which time 30 mL of CO-saturated diethyl ether was slowly added to induce precipitation of the product. The yellow crystalline solid was collected by suction filtration in air,

washed with 2 x 5 mL of diethyl ether and dried. Prolonged drying under vacuum must be especially avoided to prevent potential loss of CO. $[Rh(TMPP)_2(CO)_2][BF_4]$ was isolated as its CH_2Cl_2 solvate; yield: 0.10 g (90%). Anal. Calc'd for $RhCl_2P_2C_{57}O_{20}BF_4H_{68}$: C, 49.05; H, 4.91. Found: C, 48.22; H, 4.96. IR (Nujol, CsI): ν(CO) 2006 cm^{-1}; (CH_2Cl_2): ν(CO) 2011 cm^{-1}. ^1H NMR (CD_2Cl_2) δ ppm: 3.41 (s, 36H, *o*-OCH_3), 3.79 (s, 18H, *p*-OCH_3), 6.02 (t, $^4J_{P-H}$ = 2.1 Hz, 12H, *m*-H). ^{31}P NMR (CD_2Cl_2) δ ppm: -23.8 (d, $^1J_{Rh-P}$ = 116 Hz). Electronic absorption spectrum (CH_2Cl_2) λ_{max}, nm (ε): 438 (3400), sh, 350 (6400), 288 sh, 256 (61,500). Cyclic voltammogram (0.1 M $TBABF_4$ / CH_2Cl_2, vs Ag/AgCl): $E_{p,a}$ = + 0.80 v.

(5) Solid State Reactions of (3) - (7) with CO.

In a typical experiment, a small amount of finely divided starting compound (5-10 mg) was loaded in a polyethylene vial and placed in a Parr reactor. After several fillings and subsequent purgings with CO, the reactor was pressurized to approximately 50 psi. Reaction times were varied from 15 min to 5 days. After the vessel was depressurized, a small drop of Nujol oil was added and the sample was quickly transferred to CsI plates for infrared spectral measurements. Alternatively, the reactions were performed by purging a finely divided sample suspended in Nujol with CO at atmospheric pressure for an extended period of time.

(6) Redox Reaction of $[Rh(\eta^2\text{-TMPP})(TMPP)CO][BF_4]$ (7) with $[Rh(\eta^3\text{-TMPP})_2][BF_4]_3$ (4).

A equimolar mixture of $[Rh(TMPP)_2CO][BF_4]$ **7** (0.012 g, 0.009 mmol) and $[Rh(\eta^3\text{-TMPP})_2][BF_4]_3$ **4** (0.013 g, 0.009 mmol) was dissolved in 10 mL of CH_2Cl_2 and the reaction was stirred for 90 min under an argon purge to liberate CO. During this time, the solution color changed from red to red-purple. After stirring overnight under an Ar atmosphere, the solvent was

evaporated and a crop of purple crystals was collected, washed with a mixture of CH_2Cl_2/Et_2O (1:1 v/v) and dried in air. The product was identified as $[Rh(\eta^3\text{-TMPP})_2][BF_4]_2$ by a comparison of its electrochemical and infrared spectral properties to those of an authentic sample; yield: 0.011 g (90% based on $[Rh(\eta^2\text{-TMPP})(TMPP)CO][BF_4]$).

(7) Preparation of $[Rh(TMPP)_2][BF_4]$ (3) from $[Rh(TMPP)_2CO][BF_4]$ (7)

A solution of $[Rh(TMPP)_2(CO)][BF_4]$ (0.500 g, 0.390 mmol) and $[Cp_2Fe][BF_4]$ (0.107 g, 0.390 mmol) in 50 mL of CH_2Cl_2 was purged with N_2 overnight at -15°C. CH_2Cl_2 was added periodically to maintain the reaction volume at approximately 50 mL. During this time, the solution color slowly changed from red to purple. After the reaction was complete, the solvent was evaporated and the crude purple solid was recrystallized as previously described in Chapter III; yield: 0.460 g (88%).

(8) Reaction of $[Rh(TMPP)_2CO][BF_4]$ (7) with small molecules

(i) N_2, O_2, CO_2, H_2. In a typical experiment, a solution of $[Rh(TMPP)_2(CO)][BF_4]$ (**7**) (0.025 g, 0.020 mmol) in 5-10 mL of CH_2Cl_2 was gently purged with the appropriate gas at r.t. for 15-30 min. An aliquot was removed by either syringe or cannula and transferred to a solution IR cell. For each of the above gases, only one carbonyl stretch ($\nu(CO)$ = 1970 cm^{-1}) was observed indicating the presence of unreacted $[Rh(\eta^3\text{-TMPP})_2][BF_4]_2$ (**7**).

(ii) CNR: preparation of $[Rh(TMPP)_2(CO)(CNBu^t)][BF_4]$ (8). To a 5 mL solution of $[Rh(TMPP)_2(CO)][BF_4]$ (0.250 g, 0.20 mmol) in CH_2Cl_2, was added 22 μL of $CNBu^t$. The yellow solution was stirred for 15 min. at r.t. A yellow crystalline solid was precipitated by slow addition of 40 mL of diethyl ether. The solid was filtered in air, washed with 3 x 5 mL Et_2O and dried *in vacuo*; yield: 0.251 mg (94%). IR (CH_2Cl_2): $\nu(CO)$ 1998 cm^{-1}, $\nu(CN)$ 2188 cm^{-1}. ^1H

NMR (CD_2Cl_2) δ ppm: 0.96 (s, -Bu^t), 3.36 broad (s, -OCH_3), 3.78 broad (s, -OCH_3), 5.99 broad (s, *m*-H). ^{31}P NMR (CD_2Cl_2) δ ppm: -23.8 (d, $^1J_{Rh-P}$ = 116 Hz). Cyclic voltammogram (0.1 M $TBABF_4$ / CH_2Cl_2, vs Ag/AgCl): $E_{1/2(ox)}$ = + 0.47 V, $E_{p,c}$ = -0.01 V.

(iii) pyridine. An amount of [$Rh(TMPP)_2(CO)$][BF_4] (50 mg, 0.04 mmol) was dissolved in 5 mL of CH_2Cl_2. One equivalent of pyridine (3.2 μL, 0.04 mmol) was syringed into the solution. The yellow solution was stirred for 15 min at r.t., after which time an infrared spectrum of the solution revealed a single CO band at 1970 cm^{-1} corresponding to unreacted [$Rh(TMPP)_2(CO)$][BF_4] (**7**).

B. X-ray Crystallography

The structures of [$Rh(TMPP)_2(CO)_2$][BF_4] (**6**) and [$Rh(TMPP)_2(CO)$][BF_4] (**7**) were determined by application of general procedures that have been fully described elsewhere.[19] Geometric and intensity data for **6** was collected on a Nicolet P3/F diffractometer with graphite monochromated MoKα ($\lambda_{\bar{\alpha}}$ = 0.71073 Å) radiation and were corrected for Lorentz and polarization effects. Calculations for **6** were performed on a VAXSTATION 2000 computer by using programs from the Enraf-Nonius Structure Determination Package (SDP) programs.[9]

Crystallographic data for the compound [$Rh(\eta^2$-TMPP)(TMPP)CO][BF_4] (**7**) were collected by Molecular Structure Corporation on a Rigaku AFC5R diffractometer with monochromated CuKα radiation and a 12KW rotating anode generator. Calculations were performed by using the Texsan crystallographic software package of Molecular Structure Corporation.[10] Important crystallographic parameters pertaining to data collection and structure refinement for compounds **6** and **7** are summarized in Table 10.

(1) $[Rh(TMPP)_2(CO)_2][BF_4]\cdot CH_2Cl_2$ (6).

(i) Data Collection and Reduction. Single crystals of **6** that were suitable for X-ray diffraction studies were grown by slow diffusion of Et_2O into a CH_2Cl_2 solution of **6** under a carbon monoxide atmosphere to prevent loss of CO and formation of **7**. A yellow platelet of approximate dimensions 0.89 x 1.0 x 0.37 mm^3 was taken up in viscous oil at the end of a glass fiber and placed in a cold stream of N_2(g) at -96±3°C. The cell parameters were refined from a fit of 15 reflections in the range $20 \leq 2\theta \leq 30°$ and indicated a triclinic crystal system; axial photography confirmed the low symmetry of the lattice. A total of 8801 unique data were collected in the range $4 \leq 2\theta \leq 45°$ by using the ω-scan method. No significant decay in the data was noted, as evidenced by three check reflections that were monitored periodically throughout data collection.

(ii) Structure Solution and Refinement. The position of the Rh atom was determined from a Patterson Fourier synthesis. The remaining non-hydrogen atoms were located and refined by a series of alternating least-squares cycles and difference Fourier maps. Of the 8801 unique data, 5934 with $F_o^2 > 3\sigma(F_o)^2$ were used in the refinement of 799 parameters to give residuals of R = 0.059 and R_w = 0.084.

(2) $[Rh(\eta^2\text{-}TMPP)(TMPP)CO][BF_4]\cdot 2C_6H_6$ (7).

(i) Data Collection and Reduction. Yellow platelets of **7** were grown by slow evaporation of a mixture of CH_2Cl_2 and C_6H_6. A small crystal of approximate dimensions 0.25 x 0.10 x 0.10 mm^3 was selected and mounted on the end of a glass fiber with epoxy cement. Least-squares refinement of 25 well-centered reflections in the range $58.5 \leq 2\theta \leq 77.2°$ gave cell parameters that belong to a triclinic cell. Based on an analysis of intensities,

Table 10. Summary of crystallographic data for $[Rh(TMPP)_2(CO)_2][BF_4] \cdot CH_2Cl_2$ (**6**) and $[Rh(TMPP)_2(CO)][BF_4] \cdot 2C_6H_6$ (**7**).

	6	**7**
Formula	$RhCl_2P_2F_4O_{20}C_{57}BH_{68}$	$RhP_2F_4O_{19}C_{67}BH_{78}$
Formula weight	1395.73	1432.02
Space group	P-1	P-1
a, Å	13.318(4)	14.898(5)
b, Å	13.404(2)	18.060(8)
c, Å	18.164(4)	14.343(4)
α, deg	95.908(3)	96.56(4)
β, deg	97.037(3)	113.84(2)
γ, deg	90.711(3)	104.80(4)
V, $Å^3$	3200(2)	3308(2)
Z	2	2
d_{calc}, g/cm^3	1.448	1.438
μ, cm^{-1}	4.74	32.60
Temperature, °C	-96 ± 3	23 ± 1
Trans. factors, max., min.	1.00, 0.82	1.00, 0.95
R^a	0.059	0.067
$R_w{}^b$	0.084	0.069
quality-of-fit[c]	2.59	2.32

[a] $R = \Sigma \, | \, |F_o| - |F_c| \, | / \Sigma |F_o|$

[b] $R_w = [\Sigma w(|F_o| - |F_c|)^2 / \Sigma w |F_o|^2]^{1/2}$; $w = 1/\sigma^2(|F_o|)$

[c] quality-of-fit = $[\Sigma w(|F_o| - |F_c|)^2 / (N_{obs} - N_{parameter})]^{1/2}$

the space group was determined to be P-1. Data were collected at 23±1°C by using the ω-2θ scan technique to a maximum 2θ value of 120.3°. Weak reflections, those with $F_o^2 < 10\sigma(F_o^2)$, were rescanned at a maximum of two rescans and the counts were accumulated to assure good counting statistics. A total of 10304 reflections were collected, of which 9855 were unique. Intensity measurements of three standard reflections every 150 data points indicated that the crystal had not decayed. An empirical absorption correction based upon azimuthal scans of several reflections was applied to the data; transmission factors ranged from 1.00 to 0.95. Data were also corrected for Lorentz and polarization effects.

(ii) Structure Solution and Refinement. The structure was solved by MITHRIL and DIRDIF structure solution programs[11] and refined by full-matrix least squares refinement. With the exception of the carbon atoms of the benzene molecule in the lattice, all non-hydrogen atoms were refined with anisotropic thermal parameters. A total of 6393 observations with $F_o^2 > 3\sigma(F_o^2)$ were used to fit 757 parameters to give R = 0.067 and R_w = 0.069. The quality-of-fit index is 2.59 and the peak of highest electron density in the final difference map is 1.09 e⁻/Å^3.

3. Results

A. Reactivity of [Rh(η^3-TMPP)$_2$][BF_4]$_2$ (3) with Carbon Monoxide.

Solutions of **3** in CH_2Cl_2 react smoothly with CO at ambient temperatures and pressures. Within 15-20 minutes, the initial deep purple color of **3** converts to a red-orange hue with concomitant growth of a band at ν(CO) = 2011 cm^{-1}. Reactions of **3** with 1:1 mixtures of ^{12}CO and ^{13}CO gave a three band intensity pattern in the ν(CO) region, leading to the assignment of the 2011 cm^{-1} band to a dicarbonyl species. Subsequent purging with Ar or

N_2 produces a new species that exhibits a lower energy CO stretch at 1970 cm^{-1}. IR monitoring studies carried out during the period of inert gas purging revealed a direct correlation between the disappearance of the species at 2011 cm^{-1} and the appearance of 1970 cm^{-1}, without the observation of other CO-containing intermediates. With long purging times, both bands gradually decrease in intensity and finally disappear; at the same time the solution color converts from red-orange to purple. The purple product, obtained as a residue, was identified as the parent Rh(II) complex by cyclic voltammetry, electronic spectroscopy and epr spectroscopy. Intrigued by the indication that we were observing reversible binding of CO to the radical d^7 metal complex, we undertook a variety of experiments to elucidate the reaction pathway.

B. NMR Spectroscopic Studies.

NMR spectroscopy of CO-saturated CD_2Cl_2 solutions of **3** revealed that the paramagnetic starting material reacts rapidly to form two diamagnetic species at the same rate. Upon work-up with Et_2O, bulk reactions in CH_2Cl_2 produce a red solid and a yellow filtrate. The red solid was identified as $[Rh(\eta^3\text{-TMPP})_2][BF_4]_3$ **4** by ^1H and ^{31}P NMR spectroscopies (*vide supra*). Concentration of the yellow solution produced a crop of air-stable yellow microcrystals displaying an infrared band at $\nu(CO)$ = 1970 cm^{-1}. The ^1H NMR spectrum of **7** in CD_2Cl_2 shows 3 resonances; a virtual triplet at $\delta = 6.04$ ($^4J_{P\text{-}H}$ = 2.1 Hz) and singlets at δ = 3.80 and δ = 3.48 that correspond to the meta protons of the phenyl rings, the p-methoxy protons and the o-methoxy protons respectively. A companion ^{31}P NMR study confirmed that the phosphorus nuclei are equivalent, with a doublet appearing at $\delta = -11.1$ ppm ($J_{Rh\text{-}P}$ = 128 Hz). In light of the solid state structure (*vide infra*), the ^1H NMR can be interpreted to mean that a low energy fluxional process occurs in solution to exchange all ortho-methoxy groups. The exchange mechanism is

envisioned to occur through association of a free methoxy group, leading to formation of a 5-coordinate trigonal bipyramidal structure, which is followed by labilization of a methoxy interaction as shown in the schematic diagram below.[12] Upon methoxy group dissociation, the phenyl ring is free to rotate about the P-C bond thereby bringing a second *o*-methoxy group into a proximal position to the metal. Rotation about the Rh-P bond eventually allows all *o*-methoxy groups on the phosphine ligands to interact with the metal center, thus rendering the PR_3 ligands equivalent on the NMR time scale. Variable temperature ^{1}H and ^{31}P NMR experiments reveal that this process continues below -90°C, which attests to the unusually high lability of the ether interactions in Rh-TMPP complexes. Similar behavior has been reported for other ether-phosphine complexes of both early and late transition metals, but unlike the present case, low temperature limiting spectra were observed for these fluxional complexes.[13]

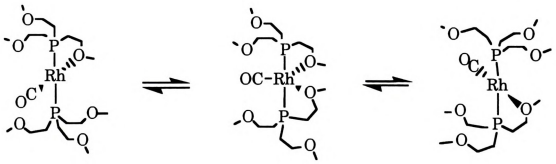

The ease of Rh-O bond dissociation in these complexes is further evidenced by the reaction of $[Rh(\eta^2\text{-TMPP})(TMPP)CO]^{1+}$ with a second equivalent of CO. Upon exposure to an atmosphere of CO, a pale yellow solution of $[Rh(\eta^2\text{-TMPP})(TMPP)CO]^{1+}$ converts to an intense yellow color, signifying the formation of the *trans* dicarbonyl species $[Rh(TMPP)_2(CO)_2]^{1+}$. This reaction is entirely reversible with loss of carbonyl ligand occurring after

a brief period of purging with Ar or N_2. The reversible addition of CO was followed by ^1H, ^{31}P NMR, cyclic voltammetry and electronic spectroscopy. $^{31}P\{^1H\}$ NMR measurements reveal that the ^{31}P resonance undergoes a shift from δ = -11.1 (J_{Rh-P} = 128 Hz) ppm for **7** to δ = -23.8 (d, J_{Rh-P} = 116 Hz) for **6** upon addition of the second carbonyl ligand. The ^1H NMR spectrum of $[Rh(TMPP)_2(CO)_2][BF_4]$ (**7**) in CD_2Cl_2 shows magnetically equivalent TMPP ligands with a triplet appearing at δ = 6.02 (J_{P-H} = 2.1 Hz) due to the meta protons and two singlets at δ = 3.41 and 3.79 which integrate in the correct ratio for ortho and para methoxy groups. The symmetrical nature of the resonances indicates that rotation about the Rh-P bond is not sterically hindered by the presence of the two carbonyl ligands.

C. Electrochemistry of $[Rh(\eta^2\text{-TMPP})(TMPP)CO][BF_4]$ (7) and $[Rh(TMPP)_2(CO)_2][BF_4]$ (6).

The cyclic voltammogram of $[Rh(\eta^2\text{-TMPP})(TMPP)(CO)]^+$ shows a quasi-reversible oxidation at $E_{1/2(ox)}$ = +0.50 V (Figure 16c). Not surprisingly, this oxidation process is less accessible than the Rh(II)/Rh(I) couple of the parent complex, $[Rh(\eta^3\text{-TMPP})_2][BF_4]_2$ (**3**).[14] The addition of a second CO ligand to give the dicarbonyl $[Rh(TMPP)_2(CO)_2]^+$ results in a large positive shift in the Rh(I)/Rh(II) couple to +0.80 V (Figure 16b) indicative of further destabilization of the Rh(II) oxidation state. The ramifications of this shift on the overall reaction pathway will be detailed in the discussion section.

D. Crystal Structures of $[Rh(TMPP)_2(CO)_n][BF_4]$ (n=1,2)

Crystallographic parameters and information regarding data collection and refinement for the structures of $[Rh(TMPP)_2(CO)_2][BF_4]$ (**6**) and $[Rh(TMPP)_2(CO)][BF_4]$ (**7**) are summarized in Table 10. Tables 11 and 12 contain a listing of pertinent bond distances and angles for **6** and **7**.

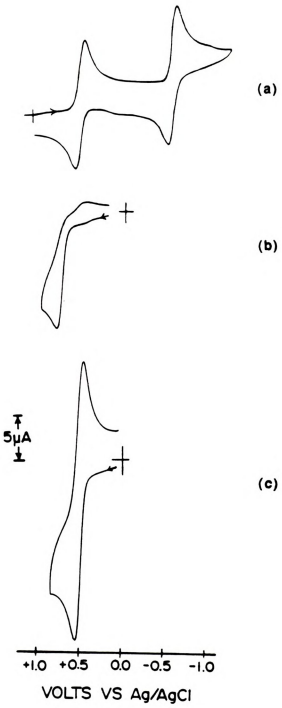

Figure 16. Cyclic voltammograms in 0.1 M $TBABF_4/CH_2Cl_2$ for (a) $[Rh^{III}(\eta^3\text{-}TMPP)_2][BF_4]_3$ (**4**), (b) $[Rh(TMPP)_2(CO)_2][BF_4]$ (**6**), (c) $[Rh(TMPP)_2(CO)][BF_4]$ (**7**).

(1) [Rh(η^2-TMPP) (TMPP)CO][BF_4] (7).

The solid state structure of **7**, shown in Figure 17, consists of a [Rh(η^2-TMPP)(TMPP)CO]$^+$ cation and a [BF_4]$^-$ anion in the asymmetric unit. The geometry about the Rh center is that of a highly distorted square planar arrangement of ligands with *trans* phosphine ligands and a CO ligand that is approximately *trans* to an oxygen atom from an interacting *o*-methoxy group (O(1)-Rh(1)-C(1)=150.2(4)°). To effect this bonding, a highly strained five-membered chelate ring is formed: M-P-C-C-O (P(1)-Rh(1)-O(1)=78.1(2)°). The presence of this rather acute angle results in a gross distortion of the structure from an ideal square planar arrangement. Related molecules with this ligand and other ether-phosphines show similar structural features.[15]

The distance for Rh(1)-O(1) in the present case of 2.319(7) Å is intermediate between the values for the axial and equatorial Rh-O distances found in [Rh(η^3-TMPP)$_2$][BF_4]$_2$ (**3**). The observed high lability of the ether group in solution reflects the weakness of the bond. Of further interest in the crystal structure of **7** is the presence of a second methoxy group from the monodentate phosphine ligand at a distance of 2.611(7) Å, which is outside the sum of the covalent bonding radii for Rh and O. As the PLUTO drawing in Figure 18 emphasizes, this oxygen atom is poised to occupy an equatorial site of a trigonal bipyramidal structure. We rationalize that, in solution, the methoxy group readily coordinates to the metal to form such a five coordinate intermediate in order to exchange all six ortho-methoxy groups in a fluxional process (*vide supra*).

(2) [Rh(TMPP)$_2$(CO)$_2$][BF_4] (6).

Compound **6** crystallizes as a symmetrical molecule ligated by two phosphine ligands and two carbonyl groups in a square planar geometry. As

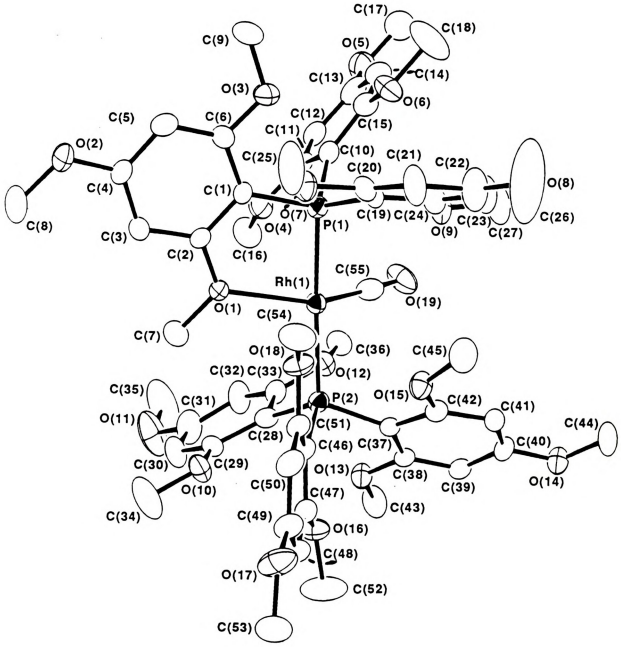

Figure 17. ORTEP representation of [Rh(TMPP)(η^2-TMPP)(CO)]$^{1+}$ (**7**).

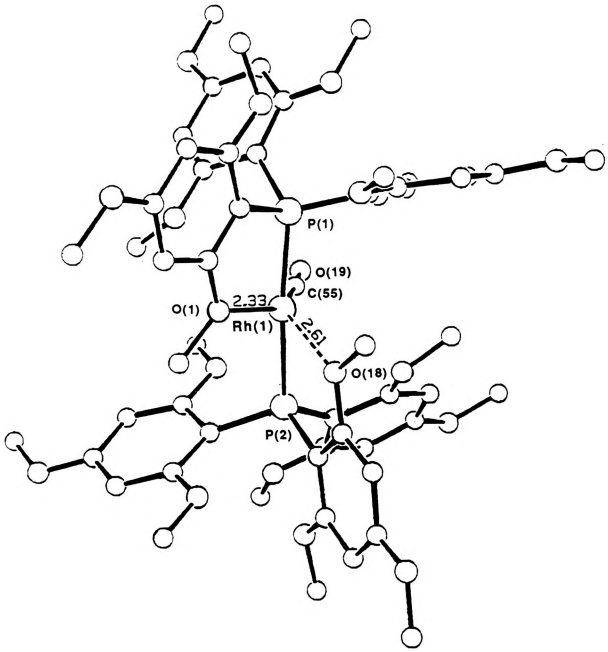

Figure 18. PLUTO drawing of [Rh(TMPP)(η^2-TMPP)(CO)]$^{1+}$ (**7**) emphasizing the coordination geometry about the Rh atom.

Table 11. Selected bond distances (Å) and angles (deg) for $[Rh(TMPP)_2(CO)][BF_4] \cdot 2C_6H_6$ (**7**).

Bond Distances

atom 1	atom 2	distance	atom 1	atom 2	distance
Rh(1)	P(1)	2.316(3)	O(1)	C(7)	1.43(1)
Rh(1)	P(2)	2.354(3)	O(2)	C(4)	1.36(2)
Rh(1)	C(55)	1.78(1)	O(2)	C(8)	1.44(1)
Rh(1)	O(1)	2.319(7)	O(3)	C(6)	1.34(1)
Rh(1)	O(18)	2.611(7)	O(3)	C(9)	1.41(2)
P(1)	C(1)	1.81(1)	O(19)	C(55)	1.14(1)
P(1)	C(10)	1.81(1)	C(1)	C(2)	1.39(1)
P(1)	C(19)	1.829(9)	C(1)	C(6)	1.40(1)
P(2)	C(28)	1.826(9)	C(2)	C(3)	1.40(2)
P(2)	C(37)	1.83(1)	C(3)	C(4)	1.37(1)

Bond Angles

atom 1	atom 2	atom 3	angle	atom 1	atom 2	atom 3	angle
P(1)	Rh(1)	P(2)	175.0(1)	Rh(1)	O(1)	C(5)	123.3(9)
P(1)	Rh(1)	O(1)	78.1(2)	Rh(1)	O(1)	C(5)	121.5(9)
P(1)	Rh(1)	C(55)	91.3(3)	C(2)	O(1)	C(11)	116.9(7)
P(2)	Rh(1)	O(1)	103.2(2)	C(4)	O(2)	C(15)	127.8(7)
P(2)	Rh(1)	C(55)	89.3(3)	C(6)	O(3)	C(15)	115.0(9)
O(1)	Rh(1)	C(55)	150.2(4)	C(15)	O(6)	C(20)	126.7(8)
Rh(1)	P(1)	C(1)	104.3(3)	P(1)	C(1)	C(24)	115.6(6)
Rh(1)	P(1)	C(10)	117.5(3)	P(1)	C(1)	C(24)	117.5(8)
Rh(1)	P(1)	C(19)	110.1(4)	C(2)	C(1)	C(29)	126.7(7)
C(1)	P(1)	C(10)	104.8(5)	O(1)	C(2)	C(33)	117.0(7)
C(1)	P(1)	C(19)	111.1(4)	O(1)	C(2)	C(33)	115.5(8)
C(1)	P(1)	C(19)	108.8(4)	C(1)	C(2)	C(38)	130.0(7)
Rh(1)	P(2)	C(28)	112.5(4)	C(2)	C(3)	C(42)	114.1(7)
Rh(1).	P(2)	C(37)	113.9(3)	O(2)	C(4)	C(42)	116(1)
Rh(1)	P(2)	C(46)	110.0(3)	O(2)	C(4)	C(47)	120.9(6)

was observed in the structure of **7**, the two TMPP ligands are *trans* to each other, but in this case each TMPP is bound through only the phosphorus atom (Figure 19). Unlike for the mono-carbonyl compound, the closest approach of ortho-methoxy groups is well outside the coordination sphere of rhodium, and there are no major structural distortions as evidenced by the nearly ideal angles P(1)-Rh(1)-P(2) = 178.46(6) Å and C(55)-Rh(1)-C(56) = 179.0(3) Å. The second CO ties up the fourth coordination site thus eliminating the need for additional donation from an ether oxygen atom. Both the Rh-P and Rh-C bond distances fall well within the range of values expected for Rh(I) complexes and are in themselves quite unremarkable.

E. Solid State Reactions of (3) - (7) with Carbon Monoxide.

Finely divided samples of $[Rh(TMPP)_2(CO)][BF_4]$ suspended in mineral oil react with CO after purging for several minutes as evidenced by the appearance of a second CO band corresponding to $[Rh(TMPP)_2(CO)_2][BF_4]$. The process, however, is slow and not quantitative as a result of poor CO diffusion into the sample. The transformation can also be effected by pressurizing powder samples with CO at 50 psi. The percent conversion of **7** to **6** was improved by exposing the sample for longer periods of time. Presumably, this is due to increased amounts of CO diffused into the solid. Just as was observed in solution, replacement of the CO atmosphere by an inert gas results in loss of coordinated CO and reformation of **7**.

Solid samples of $[Rh(\eta^3\text{-}TMPP)_2][BF_4]_2$ (**3**) also react with CO in much the same manner as was observed for solutions of **3**. Samples of **3** pressurized to 50 psi for extended time periods partially convert to $[Rh(\eta^2\text{-}TMPP)(TMPP)(CO)][BF_4]$ and $[Rh(TMPP)_2(CO)_2][BF_4]$ as evidenced by the appearance of weak CO bands at 1958 and 2006 cm^{-1} in the IR spectrum.

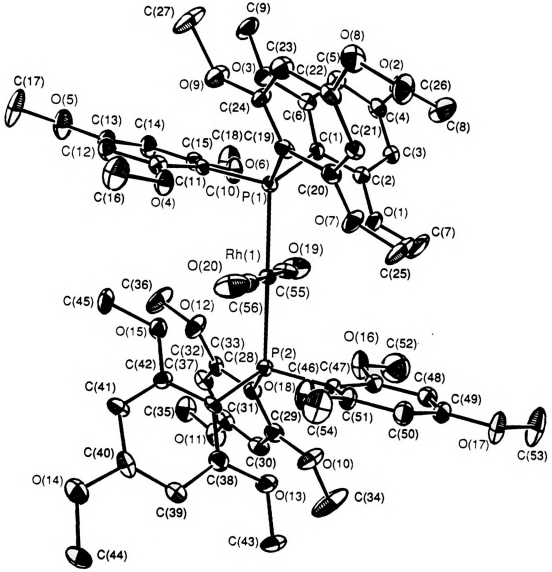

Figure 19. ORTEP drawing of $[Rh(TMPP)_2(CO)_2]^{1+}$ (**6**) with 30% probability ellipsoids.

Table 12. Selected bond distances (Å) and angles (deg) for $[Rh(TMPP)_2(CO)_2][BF_4] \cdot CH_2Cl_2$ (**6**).

Bond Distances

atom 1	atom 2	distance	atom 1	atom 2	distance
Rh(1)	P(1)	2.327(1)	O(1)	C(7)	1.391(7)
Rh(1)	P(2)	2.332(1)	O(2)	C(4)	1.374(6)
Rh(1)	C(55)	1.906(6)	O(2)	C(8)	1.451(8)
Rh(1)	C(56)	1.898(6)	O(3)	C(6)	1.356(6)
P(1)	C(1)	1.828(5)	O(3)	C(9)	1.433(6)
P(1)	C(10)	1.839(5)	O(19)	C(55)	1.125(6)
P(1)	C(19)	1.843(5)	O(20)	C(56)	1.145(6)
P(2)	C(28)	1.823(5)	C(1)	C(2)	1.409(7)
P(2)	C(37)	1.829(5)	C(1)	C(6)	1.395(7)
P(2)	C(46)	1.825(5)	C(2)	C(3)	1.406(7)
O(1)	C(2)	1.355(6)	C(3)	C(4)	1.389(7)

Bond Angles

atom 1	atom 2	atom 3	angle	atom 1	atom 2	atom 3	angle
P(1)	Rh(1)	P(2)	178.46(6)	C(37)	P(2)	C(46)	110.0(2)
P(1)	Rh(1)	C(55)	91.7(2)	P(1)	C(1)	C(2)	122.2(4)
P(1)	Rh(1)	C(56)	88.5(2)	P(1)	C(1)	C(6)	121.4(4)
P(2)	Rh(1)	C(55)	89.9(2)	C(2)	C(1)	C(6)	116.3 (5)
P(2)	Rh(1)	C(56)	89.9(2)	C(2)	C(3)	C(4)	116.3(5)
C(55)	Rh(1)	C(56)	179.0(3)	O(2)	C(4)	C(3)	122.9(5)
Rh(1)	P(1)	C(1)	116.9(2)	O(2)	C(4)	C(5)	113.6(5)
Rh(1)	P(1)	C(10)	101.8(2)	C(3)	C(4)	C(5)	123.6(5)
Rh(1)	P(1)	C(19)	119.5(2)	C(4)	C(5)	C(6)	116.6(5)
C(1)	P(1)	C(10)	108.2(2)	Rh(1)	P(2)	C(46)	101.0(2)
C(1)	P(1)	C(19)	100.6(2)	C(28)	P(2)	C(37)	101.5(2)
C(10)	P(1)	C(19)	109.6(2)	C(28)	P(2)	C(46)	109.9(2)
Rh(1)	P(2)	C(28)	119.2(2)	Rh(1)	C(55)	O(19)	179.2(5)
Rh(1)	P(2)	C(37)	115.2(2)	Rh(1)	C(56)	O(20)	178.4(5)

Interestingly, upon exposure of **3** to CO for longer than 16 hours, a very weak high energy CO stretch was observed at 2088 cm^{-1}. This species is directly related to reaction of CO with $[Rh(\eta^3\text{-TMPP})_2][BF_4]_2$, as neither samples of $[Rh(TMPP)_2(CO)][BF_4]$ nor $[Rh(\eta^3\text{-TMPP})_2][BF_4]_3$ produced this band under identical conditions.

4. Discussion

The reversible CO chemistry of $[Rh(\eta^3\text{-TMPP})_2][BF4]_2$ at ambient temperatures and pressure proceeds through a series of reactions that involve the formation of Rh(III) and Rh(I) complexes. The interrelationships of the five compounds involved in the cyclic reaction are depicted in Figure 20. These conclusions were arrived at by establishing independent synthetic routes to intermediates **4** - **7** and subsequently investigating their spontaneous redox behavior and reactivity with CO. Figure 21 outlines rational pathways to the key compounds **4** - **7** as well as their interconversions and reactions with CO.

Curiously, although $[Rh(\eta^3\text{-TMPP})_2]^{2+}$ undergoes ether-group dissociation and subsequent *cis* to *trans* isomerization in favor of π-acceptors such as CO and CNR (R = Me, Pr-i, Bu-t),[44] it is unreactive towards donors such as O_2. This is evidently a consequence of the electronic environment of the metal rather than a steric effect, since identical behavior has been noted for ether-phosphine complexes in which the ligand is not particularly bulky.[15b]

There are several key features of the chemistry in Figure 20 that must be emphasized in any discussion of this work. The initial attack of CO on the Rh(II) monomer **3** is slow, therefore unreacted starting material is in large excess during the early stages of the reaction. While we never actually

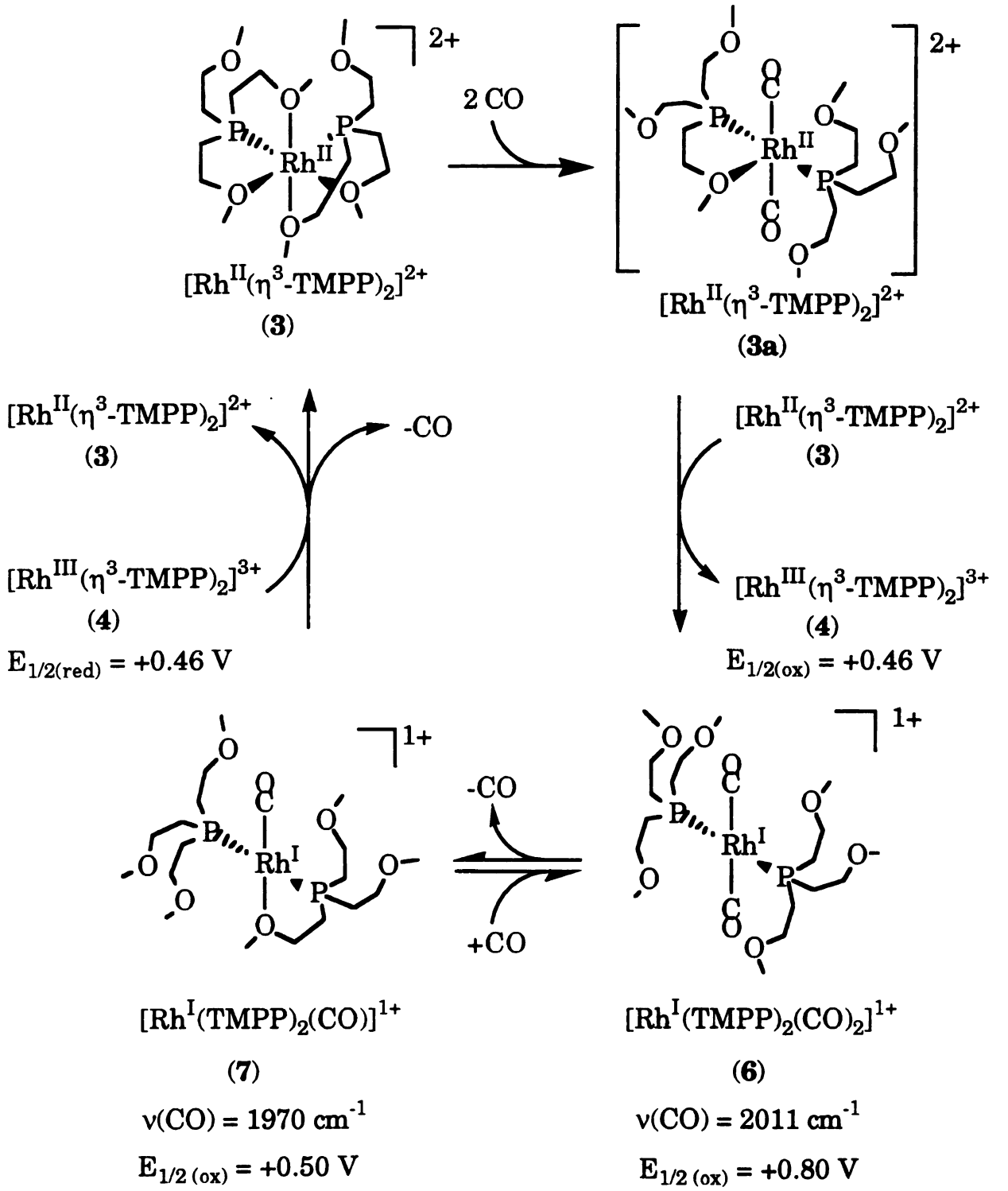

Figure 20. Proposed pathway for the reversible reaction between $[Rh^{II}(\eta^3\text{-TMPP})_2]^{2+}$ (**3**) and CO.

Figure 21. High yield synthetic routes to compounds **3-7**.[a]

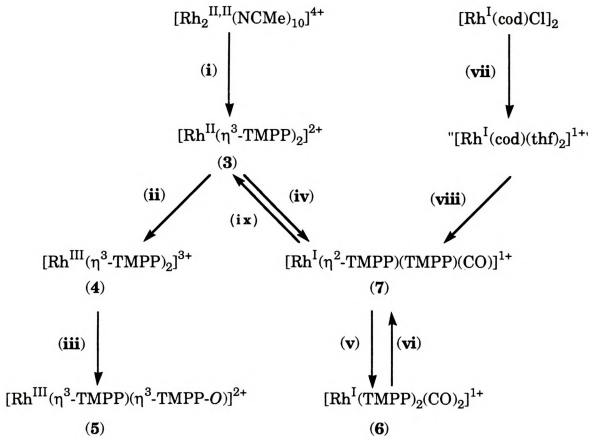

[a](i) TMPP (4 equiv), MeCN, 0°C. (ii) $NOBF_4$, MeCN, -40°C or $[Cp_2Fe][BF_4]$, CH_2Cl_2, -40°C. (iii) acetone, r. t., 24h. (iv) Cp_2Co (excess), CO, CH_2Cl_2. (v) CO, r. t. (vi) Ar, r. t. (vii) $AgBF_4$ (2 equiv), THF. (viii) CO, TMPP (2 equiv), 0°C. (ix) $[Cp_2Fe][BF_4]$ (1 equiv), N_2, CH_2Cl_2, -15°C.

observed the adducts Rh(II)(CO)x (x= 1,2) (although we attempted to do so by *in situ* infrared or epr studies), their existence is predicated on the basis of the available redox properties of the other intermediates along the reaction pathway. The fact that (**3a**) is too short-lived to be observed by ordinary spectroscopic methods is explained by the very fast electron transfer reaction that takes place between **3** and the strong oxidant (**3a**) to produce a 50:50 mixture of $[Rh(\eta^3\text{–TMPP})_2][BF_4]_3$ (**4**) and $[Rh(TMPP)_2(CO)_2][BF_4]$ (**6**). Indeed, experiments carried out in NMR tubes under a ^{12}CO atmosphere showed that two diamagnetic products were being produced at the same rate and that they were stable with respect to further reaction - provided the CO atmosphere was maintained. A parallel study using a 50:50 mixture of $^{12}CO/^{13}CO$ provided solution evidence for the assignment of **6** as a dicarbonyl species. A subsequent X-ray structural study verified this formulation. Apparently electron transfer is faster than initial CO addition to $[Rh(\eta^3\text{-TMPP})_2]^{2+}$, thus, there is never a detectable build-up of a Rh(II)CO$^{+\bullet}$ species and only the diamagnetic products are observed. Under conditions of pumping or purging with an inert gas, $[Rh(TMPP)_2(CO)_2][BF_4]$ (**6**) readily loses a CO ligand to form $[Rh(TMPP)_2(CO)_2][BF_4]$ (**7**). However, **7** is unstable with respect to oxidation by the Rh(III) complex, $[Rh(\eta^3\text{-TMPP})_2][BF_4]_3$ (**4**), and a second redox reaction occurs producing $[Rh(\eta^3\text{-TMPP})_2][BF_4]_2$ (**3**) and presumably, a Rh(II) monocarbonyl species that readily gives up CO to regenerate **3**. The proposed spontaneous redox reaction between **4** and **7** was confirmed by a deliberate 1:1 reaction of the pure compounds as shown in equation 16. Note that no reaction occurs between $[Rh(\eta^3\text{–TMPP})_2][BF_4]_3$ and $[Rh(TMPP)_2(CO)_2][BF_4]$. The intermediate Rh(II) carbonyl species **3a** is postulated to be a dicarbonyl and not a monocarbonyl complex based on the recognized redox properties of **3** - **7**;

the monocarbonyl species **7** is known to spontaneously react with $[Rh(\eta^3\text{-}TMPP)_2][BF_4]_3$ (**4**), therefore the reverse electron transfer process must be unfavorable.

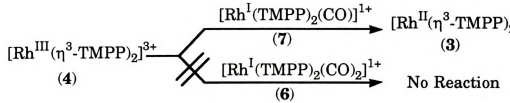

(16)

The reversible CO chemistry of $[Rh(\eta^3\text{-}TMPP)_2][BF_4]_2$ that has been observed is primarily driven by electronic considerations. That is to say, the relative stabilities of the +1, +2, and +3 oxidation states are controlled by the modulation of electron density at the metal center. The redox reactions of the cycle are driven by the π acceptor strength of CO. The strong π-accepting nature of CO greatly favors the lower oxidation states for which π-backbonding is maximized, therefore the effect of CO coordination to **3** is to destabilize the Rh(II) oxidation state relative to Rh(I). Electrochemically, this effect is manifested in a positive shift of the Rh(I)/Rh(II) redox couple, hence the resulting Rh(II) carbonyl complex is more susceptible to reduction. In the case of **3a**, the redox couple has moved to well past the Rh(II)/Rh(III) couple for **3**. As a result, electron transfer takes place between **3** and **3a** to produce $[Rh(TMPP)_2(CO)_2]^{1+}$ (**6**) and $[Rh(\eta^3\text{-}TMPP)_2]^{3+}$ (**4**). At that point the reaction is essentially complete, provided a CO atmosphere is maintained. However, upon removal of the CO atmosphere, a coordinated CO ligand is displaced by a TMPP ether group to give $[Rh(\eta^2\text{-}TMPP)(TMPP)(CO)]^{1+}$. The loss of CO makes the Rh(II) oxidation state more accessible, as evidenced by the less positive oxidation potential for **7** (+ 0.50 V) relative to that of **6** (+ 0.80) (Figure 16). The change in redox properties upon CO dissociation

triggers an electron-transfer reaction between $[Rh(\eta^2\text{-TMPP})(TMPP)(CO)]^{1+}$ and $[Rh(\eta^3\text{-TMPP})_2]^{3+}$ that ultimately results in the regeneration of $[Rh(\eta^3\text{-TMPP})_2][BF_4]_2$ (**3**). From this, we conclude that while kinetic stabilization is probably an important factor in dictating the course of the reactions with π-acceptors ligands, the modulation of the electron density at the metal center (which controls the accessibility of the Rh(I)/Rh(II) and Rh(II)/Rh(III) couple) is also a primary determinant.

The preceding analysis provides some insight into ways in which stable paramagnetic adducts of $[Rh(\eta^3\text{-TMPP})_2][BF_4]_2$ might be prepared. In the current example, the initial disproportionation reaction between **3** and **3a** is facilitated by the π-acidity of the incoming ligand. It follows then, that by reducing the π-accepting strength of the incoming ligand, such that the Rh(II)/Rh(I) redox couple occurs at less positive potentials than the Rh(II)/Rh(III) couple of (**3**), other stable Rh(II) complexes may be isolated. With this in mind, we extended our studies of $[Rh(\eta^3\text{-TMPP})_2][BF_4]_2$ to include reactions with isocyanides. The weak π-acidity of isocyanide ligands is well documented,[16] and as such, they are excellent candidates for preparing stable adducts of $[Rh(\eta^3\text{-TMPP})_2][BF_4]_2$. The results of these studies are presented in Chapter VI.

At this point, we now turn to a discussion of the major influence on the observed chemistry of $[Rh(\eta^3\text{-TMPP})_2]^{2+}$, *viz.* the flexibility of the ligand. Unlike most other sterically hindered ligands, TMPP allows the metal complex to undergo labilization of weakly held groups and isomerization to more stable geometries. The structures of the *trans*-Rh(I) complexes **6** and **7** nicely demonstrate this point. It is precisely the lack of structural rigidity that permits complexes of ether-phosphines such as TMPP to undergo reversible small molecule addition reactions. Moreover, the flexibility of the

ligand aids in the stabilization of different electronic and structural conformations. As a consequence, complexes of TMPP are expected to exhibit rich redox behavior; a fact that is nicely illustrated by the chemistry of $[Rh(\eta^3\text{-TMPP})_2][BF_4]_2$.

In order to make $[Rh^{II}(\eta^3\text{-TMPP})_2][BF_4]_2$ (**3**) a viable system for promoting C-C bond formation and other small molecule transformations, disproportionation pathways must be shut down. A strategy for achieving this goal is to tailor the ligand so that it is less accommodating to changes in metal oxidation state and structural conformation but not too rigid to prevent chemistry from occurring at the metal center. A possible solution to this dilemma would be to anchor the TMPP ligand at two points rather than just at the M-P bond, a situation that would prevent free rotation of the phosphine. One such reaction to effect this result is nucleophilic attack on a coordinated methoxy group to produce a stronger metal-phenoxide interaction. An anionic oxygen is not as susceptible to dissociation as an ether substituent, and as a result, the accessibility of the metal center to an incoming substrate is limited. Thus, it is unlikely that substitution chemistry with CO would follow the same pathway as that found in this study. Furthermore, demethylation of a methoxy group to form a phenoxide donor substantially increases the electron density at the metal center. Consequently, this should better stabilize a Rh(II) carbonyl radical with respect to reduction and CO dissociation.

Finally, while the overall pathway described in Figure 20 does not represent a simple procedure for reversible CO binding, the reaction between $[Rh(TMPP)_2(CO)_2][BF_4]$ (**6**) and $[Rh(TMPP)_2(CO)][BF_4]$ (**7**) is such a process. The high lability of the *o*-methoxy interaction for $[Rh(TMPP)_2(CO)][BF_4]$ (**7**), as evidenced by its solution fluxionality and the facile addition of CO to form

6, motivated us to further explore the lability of these weak donor groups. Previously, we observed that solid samples of $[Rh(TMPP)_2(CO)_2][BF_4]$ slowly convert to **7** when exposed to a vacuum for extended periods. This behavior prompted us to examine the reverse process, namely the addition of CO to solid state samples of **7** to form **6**. Indeed, powder or Nujol mull samples of $[Rh(\eta^3\text{-}TMPP)_2][BF_4]_2$ (**7**) were observed to reversibly uptake CO at atmospheric pressure by IR spectroscopy. The only impediment to uptake appeared to be the ability of CO to diffuse into the medium. This behavior is intriguing in the context of CO sensors.[17] Studies of $[Rh(\eta^2\text{-}TMPP)(TMPP)CO][BF_4]$ (**7**) indicate that the complex is unreactive to all other atmospheric gases besides CO. In light of these properties, we set out to investigate the incorporation of $[Rh(TMPP)_2(CO)][BF_4]$ into porous polymer matrices with the goal of developing a CO sensing material. The results of this endeavor are presented in Chapter V.

List of References

1. (a) Trogler, W. C. ed. "Organometallic Radical Processes"; Elsevier: Amsterdam, **1990**. (b) Baird, M. C. *Chem. Rev.* **1988**, *88*, 1217.

2. (a) Lappert, M. F.; Lendor, P. W. *Adv. Organomet. Chem.* **1976**, *14*, 345. (b) Kochi, J. K. "Organometallic Mechanism and Catalysis"; Academic: New York, **1978**. (c) Connelly, N. G.; Gieger, W. E. *Adv. Organomet. Chem.* **1984**, *23*, 1. (d) Connelly, N. G.; Gieger, W. E. *Adv. Organomet. Chem.* **1985**, *24*, 87. (e) Connelly, N. G. *Chem. Soc. Rev.* **1989**, *18*, 153.

3. (a) Wayland, B. B.; Sherry, A. E.; Coffin, V. L. *J. Chem. Soc., Chem. Commun.* **1989**, 662. (b) Wayland, B. B.; Sherry, A. E. *J. Am. Chem. Soc.* **1989**, *111*, 5010. (c) Wayland, B. B.; Sherry, A. E.; Poszmik, G.; Bunn, A. G. *J. Am. Chem. Soc.* **1992**, *114*, 1673. (d) Wayland, B. B.; Ba, S.; Sherry, A. E. *J. Am. Chem. Soc.* **1991**, *113*, 5305. (e) Sherry, A. E.; Wayland, B. B. *J. Am. Chem. Soc.* **1990**, *112*, 1259. (f) Poszmik, G; Wayland, B. B. presented at the 203rd National Meeting of the American Chemical Society, San Francisco, CA, April 5-10, 1992; paper INOR 67.

4. (a) Bennett, M. A.; Lonstaff, P. A. *J. Am. Chem. Soc.*, **1969**, *91*, 6266. (b) Vleck, A. *Inorg. Chim. Acta* **1980**, *43*, 35. (c) Holah, D. G.; Hughes, A. N.; Hui, B. C. *Can. J. Chem.* **1975**, *53*, 3669. (d) Valentini, G.; Braca, G.; Sbrana, G.; Colligiani, A. *Inorg. Chim. Acta* **1983**, *69*, 215. (e) Valentini, G.; Braca, G.; Sbrana, G.; Colligiani, A. *Inorg. Chim. Acta* **1983**, *69*, 221.

5. Empsall, H. D.; Hyde, E. M.; Jones, C. E.; Shaw, B. L. *J. Chem. Soc., Dalton Trans.* **1974**, 1980.

6. (a) Mason, R.; Thomas, K. M.; Empsall, H. D.; Fletcher, S. R.; Heys, P. N.; Hyde, E. M. Jones, C. E; Shaw, B. L. *J. Chem. Soc., Chem. Comm.* **1974**, 612.

7. (a) Empsall, H. D.; Hyde, E. M.; Shaw, R. L. *J. Chem. Soc., Dalton Trans.* **1975**, 1690. (b) Empsall, H. D.; Heys, P. N.; McDonald, W. S.; Norton, M. C.; Shaw, B. L. *J. Chem. Soc., Dalton Trans.* **1978**, 1119.

8. Gray, H. B.; Hendrickson, D. N.; Sohn, Y. S. *Inorg. Chem.* **1971**, *10*, 1559.

9. SDP: Structure Determination Package, Enraf-Nonius, Delft, The Netherlands, **1979**.

10. TEXSAN - TEXRAY Structure Analysis Package, Molecular Structure Corporation, **1985**.

11. (a) MITHRIL: Integrated Direct Methods Computer Program, Gilmore, C. J. *J. Appl. Cryst.* **1984**, *17*, 42. (b) DIRDIF: Direct Methods for Difference Structure, An Automatic Procedure for Phase Extension; Refinement of Difference Structure Factors. Beurskens, R. T. Technical Report **1984**.

12. For evidence supporting similar exchange processes see (a) El-Amouri, H.; Baltsoun, A. A.; Osborn, J. A. *Polyhedron* **1988**, *7*, 2035. (b) English, A. D.; Meakin, P.; Jesson, J. P. *J. Am. Chem. Soc.* **1976**, *98*, 7590 (c) Volger, H. C.; Vrieze, K.; Praat, A. P. *J. Organomet. Chem.* **1968**, *14*, 429.

13. Bader, A.; Lindner, E. *Coord. Chem. Rev.* **1991**, *108*, 27. and references therein.

14. Treichel, P. M.; Mueh, H. J.; Bursten, B. E. *Isr. J. Chem.* **1976/77**, *15*, 253.

15. For instance see (a) Dunbar, K. R.; Haefner, S. C.; Burzynski, D. J. *Organometallics* **1990**, *9*, 1347. (b) Jeffrey, J. C.; Rauchfuss, T. B. *Inorg. Chem.* **1979**, *18*, 2658. (c) Granziani, R.; Bombiere, G.; Volponi, L.; Panattoni, C.; Clark, R. J. H. *J. Chem. Soc. (A)* **1969**, 1236. (d) De V. Steyn, M. M.; English, R. B.; Ashworth, T. V.; Singleton, E. *J. Chem. Res.* (S) **1981**, 267.

16. Treichel, P. M. *Adv Organomet. Chem.* **1973**, *11*, 21.

17. *Biosensors and Chemical Sensors: Optimizing Performance Through Polymeric Materials,* ACS Symposium Series 487; Edelman, P. G.; Wang, J. Eds., American Chemical Society: Washington, D. C., **1992**.

CHAPTER V

REVERSIBLE CARBON MONOXIDE ADDITION TO SOL-GEL DERIVED COMPOSITE FILMS CONTAINING THE MOLECULE $[Rh(TMPP)_2(CO)]^{1+}$

1. Introduction

The reversible solution chemistry of the novel mononuclear Rh(II) complex $[Rh(\eta^3\text{-TMPP})_2][BF_4]_2$ (TMPP = tris(2,4,6-trimethoxyphenyl)-phosphine) with carbon monoxide was presented in Chapter 4. The reaction was found to proceed by a redox pathway that involves the formation of the Rh(I) carbonyl intermediates $[Rh(TMPP)_2(CO)][BF_4]$ (**7**) and $[Rh(TMPP)_2(CO)_2][BF_4]$ (**6**); these complexes were fully characterized by X-ray crystallography, cyclic voltammetry, as well as by infrared and NMR spectroscopies. In solution, complex **7** rapidly and reversibly binds carbon monoxide under ambient conditions to form the dicarbonyl species **6** (eq 1). In the absence of a CO atmosphere, **6** loses CO to reform **7**. The facile nature of the carbon monoxide addition to $[Rh(TMPP)_2(CO)][BF_4]$ (**7**) is exemplified by the observation that finely divided powder and Nujol mull samples of **7** are also capable of reversibly uptaking CO. Not surprisingly, these reaction

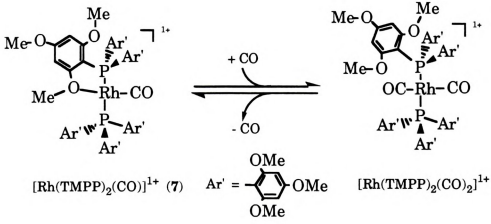

(17)

rates are sluggish due to poor diffusion of CO into the solid; this situation prompted us to investigate the incorporation of **7** into a porous material that would trap the molecular cationic species yet facilitate diffusion of CO into the matrix. Low temperature sol-gel techniques can be used to create porous

oxide glasses (pore size < 100 Å) that encapsulate large complex molecules yet allow diffusion of small substrates into the matrix.[1] Such oxide galsses fromed by the hydrolysis and polycondensation of metal alkoxides are optically transparent and can be readily probed by a number of spectroscopic techniques. Previous work has demonstrated the general usefulness of sol-gel derived glasses for the immobilization of guest molecules such as inorganic clusters, porphyrins, and lanthanide cryptate complexes.[2,3] Recently, the process has been adapted for the incorporation of biochemically active molecules that may lead to the development of novel biosensing materials.[4]

The use of sol-gel techniques provides for the immobilization of a sensing molecule, in this case $[Rh(TMPP)_2(CO)][BF_4]$ (**7**), in an environment that can be probed both by spectroscopic and electrochemical techniques, while the porous nature of the films permits facile diffusion of an exogenous substrate, such as CO, that can then bind to the sensing molecule. Herein we report the synthesis and CO binding properties of zirconia and titania glasses impregnated with a rhodium ether-phosphine compound, the results of which are promising for future adaptations of such molecular species as chemical sensors. The work described in this chapter was performed in collaboration with Professor Kris A. Berglund and Dr. Joel I. Dulebohn in the Departments of Chemical and Agricultural Engineering, Michigan State University.

2. Experimental

A. Preparation of Composite Films Containing $[Rh(TMPP)_2(CO)][BF_4]$ (7)

(1) Zirconia Films

An amount of lauric acid (0.161 g, 0.80 mmol) was added to 1 mL of 70% $Zr(OPr^n)_4$ in propanol (2.23 mmol) in a glass vial. The mixture was placed in a sonicator (Bransonic 220) until the lauric acid had completely dissolved. To this solution, was added an amount of valeric acid (1.7 mL, 15.6 mmol) and 0.2 mL of water. A solution of $[Rh(TMPP)_2(CO)][BF_4]$ **(7)** (5.9 mg, 4.6×10^{-3} mmol) in 50 μL of CH_2Cl_2 was added to 1 mL of the zirconia film solution. The resulting yellow solution was filtered through a 0.22 mm Millex-GS millipore filter.

(2) Titania Films

A quantity of of lauric acid (0.25 g, 1.25 mmol) was dissolved in neat $Ti(OPr^i)_4$ (1 mL, 3.36 mmol). The solution was sonicated to ensure that the lauric acid was completely dissolved. A mixture of valeric acid (2.5 mL, 23 mmol) and water (0.3 mL) were then added to the solution. A solution of $[Rh(TMPP)_2(CO)][BF_4]$ (**7**) (0.0059 g, 4.6×10^{-3} mmol) in 50 μL of CH_2Cl_2 was pipetted into 1 mL of the titania film solution. The resulting yellow solution was filtered through a 0.22-mm Millex-GS millipore filter to remove unreacted **7**.

B. Flow Rate Determination

A schematic diagram for the apparatus used to estimate CO concentrations in the films is shown in Figure 22. Flow rates of CO and the argon carrier gas were controlled by adjustment of screw clamps connected to each line and were estimated by measuring the time required for a soap bubble to travel a predetermined distance through a glass pipette. The CO

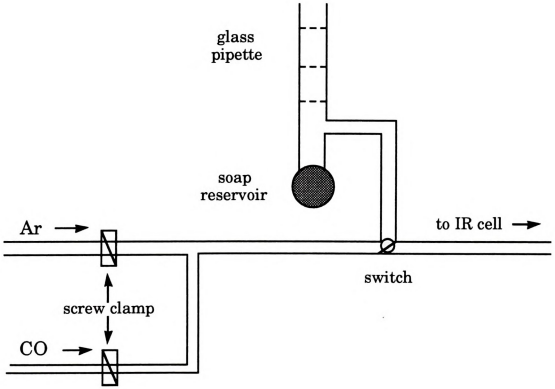

Figure 22. Schematic diagram of the apparatus used to estimate CO concentrations.

flow rate was adjusted and measured, first in the absence of argon, then the argon flow rate was adjusted and the combined flow rate for the two gases was measured. The flow rates for CO and the combined gases were measured five times and the average was determined. The % CO concentration was taken as the inverse of the flow rate ratios.

C. Electrochemical Measurements

Films used for electrochemical studies were prepared as described in section A. However, in order to make the films electrochemically active, 2.0 mg of $[Li][CF_3SO_3]$ (0.013 mmol) was added to 0.1 mL of the film solution as a supporting electrolyte. The films were cast onto a Pt disk electrode using a cotton swab and dried in a stream of cool air. Cyclic voltammetry measurements were performed in 0.1 M $[Li][CF_3SO_3]$ / H_2O at a scan rate of 200 mV/s using a platinum disk working electrode and a Ag/AgCl reference electrode.

3. Results

Sol-gel derived titania and zirconia composite films containing $[Rh(TMPP)_2(CO)][BF_4]$ (**7**) were prepared by addition of a dichloromethane solution of **7** to titania and zirconia film solutions. Thin films were fabricated by either spin casting for 5 minutes or by application to the substrate with a cotton swab followed by drying in a stream of cool air. Infrared spectroscopic studies on the films were performed by casting the composite zirconia or titania films onto a germanium ATR crystal and placing the crystal in an liquid ATR cell holder. Initially, a single carbonyl stretch was seen at 1975 cm^{-1}, which corresponds to the cation species $[Rh(TMPP)_2(CO)]^+$ (**7**) ($\nu(CO)_{CH_2Cl_2}$ = 1970 cm^{-1}) immobilized in the film. Upon exposure of the film to a CO atmosphere, the band at 1975 cm^{-1} disappeared and a second, more

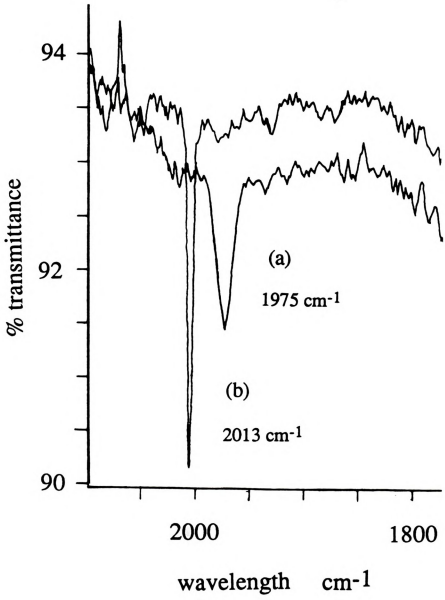

Figure 23. Infrared spectra of a zirconia composite film of $[Rh(TMPP)_2(CO)][BF_4]$ (**7**): (a) in the absence of CO. (b) exposed to CO.

intense, band appeared at 2013 cm^{-1}, signaling the binding of CO to **7** to yield the dicarbonyl species $[Rh(TMPP)_2(CO)_2][BF_4]$ (**6**) ($\nu(CO)_{CH_2Cl_2}$ = 2011 cm^{-1}) (Figure 23). The absence of the 1975 cm^{-1} band indicates that the conversion of **7** to **6** within the film is quantitative. With regards to sensitivity, the presence of CO was observable in gas mixtures of CO and Ar containing less than 0.2% CO, which was the lowest measurable concentration based on our present method for determining flow rates. In the lower concentration range, the conversion of **7** to **6** is less than quantitative as evidenced by the continued presence of the CO band for **7** at 1975 cm^{-1}. Removal of CO from the system was effected by purging the IR cell with argon for one minute, whereupon the band at 2013 cm^{-1} diminished with concomitant reappearance of the 1975 cm^{-1} band; this observation is consistent with complete conversion of $[Rh(TMPP)_2(CO)_2][BF_4]$ (**6**) back to the parent molecular species $[Rh(TMPP)_2(CO)][BF_4]$ (**7**). Alternatively, the loss of CO from the material may be achieved by simply exposing the film to the atmosphere, although the process is significantly slower under these conditions. As judged by the invariance of the IR spectra, zirconia and titania composite films of $[Rh(TMPP)_2(CO)][BF_4]$ (**7**) are selective for CO in the presence of other gases such as O_2, CO_2, N_2, and H_2.

In addition to infrared spectroscopy, the reversible addition of CO to $[Rh(TMPP)_2(CO)][BF_4]$ (**7**) within the composite films was monitored by electronic spectroscopy. A zirconia composite film containing **7** was spin cast onto a quartz slide and placed in a 1 cm quartz cuvette capped with a rubber septum. The cell was purged for 15 min with CO giving rise to an electronic spectral feature at 435 nm which is comparable to that seen in solution for $[Rh(TMPP)_2(CO)_2][BF_4]$ (**6**) (λ_{max,CH_2Cl_2} = 438 nm) (Figure 24). Subsequent removal of CO from the cell by purging with Ar resulted in the disappearance

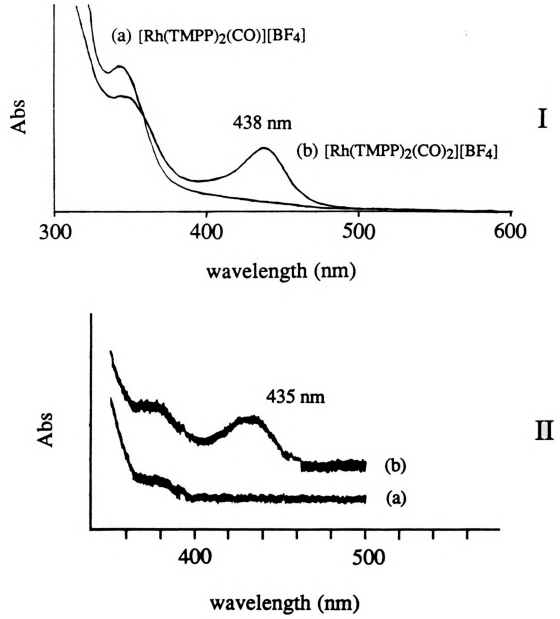

Figure 24. Electronic absorption spectra of (a) $[Rh(TMPP)_2(CO)][BF_4]$ and (b) $[Rh(TMPP)_2(CO)_2][BF_4]$ in: (I) CH_2Cl_2. (II) a zirconia composite film.

of the transition at 435 nm, leading to the conclusion that **6** had been reconverted to the monocarbonyl derivative **7**.

Initial electrochemical studies of the sol-gel derived composite films containing $[Rh(TMPP)_2(CO)][BF_4]$ (**7**) were carried out by casting a zirconia film onto a platinum disk electrode. Unfortunately, these films were found to be electrochemically inactive as no current response was observed. To circumvent this problem $[Li][CF_3SO_3]$ was added to the film solution as a supporting electrolyte prior to casting onto the electrode surface. A cyclic voltammogram of the composite film in 0.1 M $[Li][CF_3SO_3]$ / H_2O exhibited an essentially featureless voltammogram (Figure 25). Upon purging the electrochemical cell with CO for a brief period of time (< 30 sec), an irreversible oxidation wave appears at $E_{p,a}$= + 0.74 V with a chemical return wave located at $E_{p,c}$= + 0.31 V vs. Ag/AgCl. After purging with N_2 for several minutes, the oxidation wave gradually disappears and the original cyclic voltammogram is obtained. Purging the solution with N_2 removes CO from the system and results in re-formation of **7,** in agreement with the reversible addition of CO that was observed spectroscopically. Films containing only $[Li][CF_3SO_3]$, when exposed to CO under identical conditions, exhibited no significant change in current response, indicating to us that the observed signal is due to the encapsulated complex bound to CO. Although the electrochemical behavior of the carbonyl complexes **7** and **6** incorporated in these composite films differs from the solution behavior, it is apparent that CO is binding to the rhodium center; more importantly, the process is reversible. Such behavior is in contrast to the irreversible CO chemistry reported for conducting polymer films containing ferrocenylferraazetine.[5] In order to make electrochemical detection a more viable means of sensing CO in the present case, the use of a more conducting matrix is in order. One

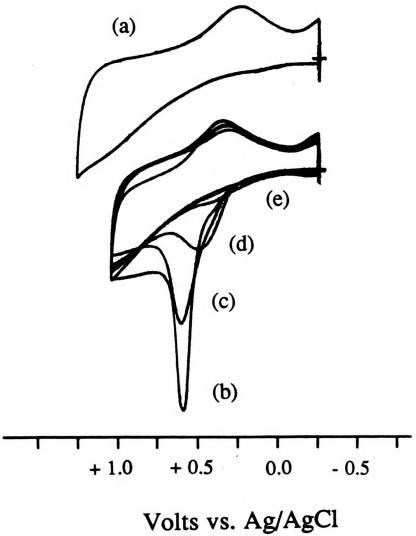

Figure 25. Cyclic voltammograms of a zirconia composite film containing $[Rh(TMPP)_2(CO)][BF_4]$ (**7**) and $LiCF_3SO_3$ cast onto a platinum disk electrode: (a) under a N_2 atmosphere. (b) after purging the cell for 30 seconds with CO. (c)-(e) after flushing the CO saturated cell with N_2 for 2, 5 and 10 min.

potential solution is the incorporation of $[Rh(TMPP)_2(CO)][BF_4]$ (**7**) into solid ionic conducting polymer films such as MEEP (poly[bis(2-(2-methoxy)ethoxy)phosphazene]).[6]

4. Discussion

These studies demonstrate that the molecular cationic complex $[Rh(TMPP)_2(CO)]^{1+}$ (**7**) reversibly binds CO within a glassy polymer matrix to form the dicarbonyl species $[Rh(TMPP)_2(CO)_2]^{1+}$ (**6**). The facile nature of the chemistry is a direct consequence of an exceedingly labile metal-ether bond, which facilitates substitution reactions even in the solid state. Furthermore, the metal-ether interaction appears to be selective towards CO as other atmospheric gases do not react. Another advantage of this system is that the substrate binds directly to the metal center. As a result, the addition of CO conveniently gives rise to dramatic changes in the spectroscopic and redox properties of the rhodium cation, commensurate with coordination of a strong π-acceptor to the metal center. Because of the transparent characteristcs of the sol-gel derived films, these spectral and electrochemical changes are readily detected.

In spite of these attributes, a number of concerns must be addressed before the application of these materials as sensing devices can be realized; these include long term stability of material, conditions under which the films will operate, detection limits and response times. Nevertheless, on the basis of these preliminary results with titania and zirconia films incorporating $[Rh(TMPP)_2(CO)][BF_4]$ (**7**), the development of other CO sensing films using molecular composites of ether-phosphine complexes appears attractive.

List of References

1. (a) Brinker, C. J.; Scherer, G. *Sol-Gel Science: The Physics and Chemistry of Sol-Gel Processing*; Academic Press: San Diego, **1989**. (b) Sanchez, C.; Livage, J. *New J. Chem.* **1990**, *14*, 513.

2. (a) Dulebohn, J. I.; Van Vlierberge, B.; Berglund. K. A.; Lessard, R. B.; Yu, J.; Nocera, D. G. *Mat. Res. Soc. Symp. Proc.* **1990**, *180*, 733. (b) Lessard, R. B.; Wallace, M. M.; Oertling, W. A.; Chang, C. K.; Berglund. K. A.; Nocera, D. G. *Mat. Res. Soc. Symp. Proc.* **1989**, *155*, 109. (c) Lessard, R. B.; Berglund. K. A.; Nocera, D. G. *Mat. Res. Soc. Symp. Proc.* **1989**, *155*, 119. (d) Newsham, M. D.; Cerreta, M. K.; Berglund. K. A.; Nocera, D. G. *Mat. Res. Soc. Symp. Proc.* **1988**, *121*, 627.

3. For other recent examples see: (a) Kuselman, I.; Kuyavskaya, B. I.; Lev, O. *Analytica Chimica Acta* **1992**, *256*, 65. (b) Dunn, B.; Zink, J. I. *J. Mater. Chem.* **1991**, *1*, 903. (c) McKiernan, J. M.; Yamanaka, S. A.; Knobbe, E.; Pouxviel, J. C.; Parveneh, S.; Dunn, B.; Zink, J. I. *J. Inorg. Organomet. Polym.* **1991**,*1*, 87. (d) Schwok, A.; Avnir, D.; Ottolenghi, M. *J. Am. Chem. Soc.* **1991**, *113*, 3984 and references therein. (e) Haruvy, Y.; Webber, S. E. *Chem. Mater.* **1991**, *3*, 501 and references therein. (f) Zusman, R.; Rottman, C.; Ottolenghi, M.; Avnir, D. *J. Non-cryst. Solids* **1990**, *122*, 107. (h) McKiernan, J. M.; Yamanaka, S. A.; Dunn, B.; Zink, J. I. *J. Phys. Chem.* **1990**, *94*, 5652. (i) McKiernan, J. M.; Pouxviel, J. C.; Dunn, B.; Zink, J. I. *J. Phys. Chem.* **1989**, *93*, 2129. (j) Pouxviel, J. C.; Dunn, B.; Zink, J. I. *J. Phys. Chem.* **1989**, *93*, 2134. (k) Dunn, B.; Knobbe, E.; McKiernan, J. M.; Pouxviel, J. C.; Zink, J. I. *Mat. Res. Soc. Symp. Proc.* **1988**, *121*, 331.

4. (a) Ellerby, L. M.; Nishida, C. R.; Nishida, F.; Yamanaka, S. A.; Dunn, B.; Selverstone-Valentine, J.; Zink, J. I. *Science* **1992**, *255*, 1113. (b) Yamanaka, S. A.; Nishida, F.; Ellerby, L. M.; Nishida, C. R.; Dunn, B.; Selverstone-Valentine, J.; Zink, J. I. *Chem. Mater.* **1992**, *4*, 495. (c) Slama-Schwok, A.; Ottolenghi, M.; Avnir, D. *Nature* **1992**, *355*, 240.

5. (a) Mirkin, C. A.; Wrighton, M. S. *J. Am. Chem. Soc.* **1990**, *112*, 8596. (b) Mirkin, C. A.; Valentine, J. R.; Ofer, D.; Hickman, J. J.; Wrighton, M. S. In *Biosensors and Chemical Sensors: Optimizing Performance Through Polymeric Materials,* ACS Symposium Series 487; Edelman, P. G.; Wang, J. Eds., American Chemical Society: Washington, D. C., **1992**, chapter 17, p. 218.

6. (a) Allcock, H. R.; Austin, P. E.; Neenan, T. X.; Sisko, J. T.; Blonsky, P. M.; Shriver, D. F. *Macromolecules* **1986**, *19*, 1508. (b) Blonsky, P. M.; Shriver, D. F.; Austin, P. E.; Allcock, H. R. *Solid State Ionics* **1986**, *18*, 258. (c) Blonsky, P. M.; Shriver, D. F.; Austin, P. E.; Allcock, H. R. *J. Am. Chem. Soc.* **1984**, *106*, 6854. (d) Austin, P. E.; Riding, G. J.; Allcock, H. R. *Macromolecules* **1983**, *16*, 719.

CHAPTER VI

CHEMISTRY OF $[Rh^{II}(\eta^3\text{-TMPP})_2][BF_4]_2$ WITH ISOCYANIDE LIGANDS

1. Introduction

A survey of the literature reveals that most of the documented research involving mononuclear rhodium complexes has focused on the +1 and +3 oxidation states, due, in large part, to their demonstrated involvement in homogeneous catalytic processes.[1] Only a limited number of reports have addressed the coordination chemistry of paramagnetic Rh(II),[2] and even fewer have focused on mononuclear organometallic complexes of Rh(II).[3] The unusual stability of **3** has presented us with a rare opportunity to investigate these elusive classes of compounds.[4] In light of the recent reports by Wayland and co-workers of carbon monoxide and methane activation by Rh(II) metalloradicals,[5] this is a particularly attractive area of research. In Chapter IV, we demonstrated that $[Rh(\eta^3\text{-TMPP})_2][BF_4]_2$ (**3**) reacts reversibly with CO through a pathway that involves the formation of Rh(I) carbonyl and Rh(III) intermediates. From the chemistry of **3** with CO it was apparent to us that the primary factor promoting the redox chemistry was the π-accepting ability of the incoming ligand. Intrigued by this unusual chemistry, we set out to explore the reactivity of $[Rh(\eta^3\text{-TMPP})_2]^{2+}$ (**3**) with other π-acceptors with the goal of understanding the factors that influence the stability of Rh(II) complexes. Herein, we describe the synthesis and full characterization of a series of novel square planar Rh(II) complexes stabilized by isocyanides and phosphines.

2. Experimental

A. Synthesis

All reactions were carried out under an argon atmosphere by the use of standard Schlenk-line techniques unless otherwise stated. The starting materials tris(2,4,6-trimethoxyphenyl)phosphine (**1**) and $[Rh(\eta^3\text{-TMPP})_2][BF_4]_2$ (**3**) were prepared as described in chapters II and III

respectively. The reagents *tert*-butyl isocyanide, *iso*-propyl isocyanide, *n*-butyl isocyanide, cyclohexyl isocyanide and cobaltocene were purchased from Strem Chemicals and used without further purification. Methyl isocyanide was prepared according to a literature procedure.[6]

(1) Preparation of $[Rh(TMPP)_2(CNBu^t)_2][BF_4]_2$ (9)

An amount of Bu^tNC (34 μL, 0.300 mmol) was carefully syringed into a rapidly stirring solution of $[Rh(\eta^3\text{-}TMPP)_2][BF_4]_2$ (**3**) (0.200 g, 0.150 mmol) in CH_2Cl_2 (3 mL). The solution color immediately changed from purple to black/purple. After stirring for 10 min, the solution was layered with 20 mL of THF. After diffusion had occurred, dark purple crystals separated from the solution; these were collected by suction filtration in air, washed with THF (3 x 5 mL) and Et_2O (2 x 5 mL), and subsequently dried under vacuum; yield, 0.213 g (90%). In an alternative work-up procedure, the solution was filtered in air after 10 min of reaction and diluted with CH_2Cl_2 (20 mL) followed by THF (8 mL). Reduction of the solution volume to 3 - 5 mL on a rotary evaporator produces a purple crystalline product upon standing overnight. Anal. Calcd for $C_{64}H_{74}F_8P_2O_{18}N_2B_2Rh$: C, 50.98; H, 4.95. Found: C, 50.45; H, 5.88. IR (CH_2Cl_2, cm^{-1}): ν(C≡N), 2200 vs; (Nujol mull, CsI, cm^{-1}): ν(C≡N), 2198 vs; other, 1595 vs, 1578 vs, 1411 s, 1332 s, 1294 w, 1228 s, 1207 s, 1185 w, 1160 s, 1122 s, 1087 s, 1054 s, 1026 s, 950 m, 917 m, 815 m, 675 w, 640 w, 536 w, 522 w, 479 m, 442 w. Electronic absorption spectrum (CH_2Cl_2) λ_{max}, nm (ε): 819 nm (1770), 546 (630), 319 (22,400), 257 (56,500). ^1H NMR and ^{31}P NMR (CD_2Cl_2) δ ppm: not observed. Cyclic voltammogram (0.1 M $TBABF_4/CH_2Cl_2$, vs Ag/AgCl): $E_{1/2(red)}$ = - 0.04 V.

(2) Preparation of $[Rh(TMPP)_2(CNPr^i)_2][BF_4]_2$ (10)

Dropwise addition of a solution of Pr^iNC (13.6 μL, 0.150 mmol) in 7 mL of CH_2Cl_2 to a solution of $[Rh(\eta^3\text{-}TMPP)_2][BF_4]_2$ (**3**) (0.100 g,, 0.075 mmol) in

3 mL of CH_2Cl_2 produced a black/purple solution over a period of 10 min. The reaction was stirred for an additional 10 min, after which time 5 mL of CH_2Cl_2 and 10 mL of THF were added. The solution was concentrated to a volume between 5 - 8 mL on a rotary evaporator and filtered through Celite. Upon standing overnight, a crop of purple crystals formed; these were isolated and washed with copious amounts of THF and Et_2O; yield 0.053 g (48%). Anal. Calcd for $C_{62}H_{80}F_8P_2O_{18}N_2B_2Rh$: C, 50.32; H, 5.45. Found: C, 49.54; H, 5.50. IR (CH_2Cl_2, cm^{-1}): ν(C≡N), 2211 vs; (Nujol mull, CsI, cm^{-1}): ν(C≡N), 2209 vs; other, 1595 vs, 1577 vs, 1411 s, 1331 s, 1297 w, 1231 s, 1206 s, 1184 w, 1161 s, 1125 s, 1088 s, 1054 s, 1025 s, 949 m, 917 m, 812 m, 478 m. Electronic absorption spectrum (CH_2Cl_2) λ_{max}, nm (ε): 843 nm (1847), 558 (645), 318 (20,685), 258 (57,933). Cyclic voltammogram (0.1 M $TBABF_4/CH_2Cl_2$, vs Ag/AgCl): $E_{1/2(red)}$ = + 0.01 V.

(3) Reaction of $[Rh(\eta^3\text{-TMPP})_2][BF_4]_2$ (3) with other isocyanides

(i) Methyl isocyanide: (a) one equivalent. In a typical reaction, MeNC (2 μL) was added to a solution of $[Rh(\eta^3\text{-TMPP})_2][BF_4]_2$ (**3**) (0.050 g, 0.037 mmol) in 5 mL of CH_2Cl_2. The solution immediately turned from purple to red with the concominant precipitation of a small quantity of red solid (see below). An IR monitoring study of the solution reveals the immediate formation of several C≡N stretching vibrations; ν(C≡N) cm^{-1}: 2239 s, 2248 s, 2267m, 2176. After 10 min, an additional band appeared at 2150 cm^{-1}.

(b) five equivalents. To a solution of $[Rh(\eta^3\text{-TMPP})_2][BF_4]_2$ (**3**) (0.100 g, 0.75 mmol) in 5 mL of CH_2Cl_2 was added 5 equivalents of MeNC (20 μL, 3.75 mmol). A red flocculent solid precipitated from the red/orange solution. The resulting suspension was stirred for 5 min, after which time the solid was collected by filtration, washed with a minimal amount of CH_2Cl_2 (< 5 mL) and THF (2 x 5 mL) and dried under vacuum; yield: 0.43 g. IR (Nujol, CsI)

cm^{-1}: ν(C≡N) 2238 s; $[BF_4]^-$ 1050 br. ^1H NMR (CD_3CN) δ ppm: 3.41 (s, 12H), 3.57(s, 18H, *o*-OCH_3), 3.83 (s, 9H, *p*-OCH_3), 6.21 (t, $^1J_{P-H}$ = 2.1 Hz, 6H, *m*-H). ^{31}P NMR (CD_3CN) δ ppm: - 39.5 (t, J = 42.7 Hz). Cyclic voltammogram (0.1 M $TBABF_4/CH_2Cl_2$, vs Ag/AgCl): $E_{p,c}$ = - 0.46 V, $E_{p,c}$ = - 1.71 V.

(ii) Cyclohexyl isocyanide. To a solution of $[Rh(\eta^3\text{-TMPP})_2][BF_4]_2$ (**3**) (0.050 g, 0.037 mmol) in 5 mL of CH_2Cl_2 was added 2 equivalents of CNCy (9.3 μL, 0.075 mmol). The purple solution immediately turned dark purple and then finally black. The IR spectrum measured within the first minute exhibited three bands; ν(C≡N): 2245 vw, 2210 m, 2173 m. Over a period of several hours, the low energy band continued to grow in as the solution color became pale.

(iii) *n*-Butyl isocyanide. In a typical reaction, two equivalents of $CNBu^n$ (7.8 μL, 0.075 mmol) were added to a purple solution of $[Rh(\eta^3\text{-TMPP})_2][BF_4]_2$ (**3**) in 5 mL of CH_2Cl_2. The solution immediately became dark brown. After 30 min, the solution IR spectrum showed several C≡N stretching vibrations; ν(C≡N): 2292 w, 2255 vs, 2220 w, 2160. The solvent was removed under reduced pressure and the resulting residue was redissolved in THF (5 mL), filtered in air to remove unreacted **3** and finally pumped to a residue.

(4) Reactions of $[Rh(TMPP)_2(CNBu^t)_2][BF_4]_2$ (9)

(i) Cobaltocene: Preparation of $[Rh(TMPP)_2(CNBu^t)_2][BF_4]$ (11). A solution containing $[Rh(TMPP)_2(CNBu^t)_2][BF_4]_2$ (**9**) (0.100 g, 0.066 mmol) and 1 equivalent of Cp_2Co (0.013 g, 0.066 mmol) in 5 mL of CH_2Cl_2 was stirred at r. t. for 30 min. The yellow solution was evaporated to dryness, and the resulting residue was redissolved in THF (10 mL). The solution was filtered through a Celite plug to remove undissolved $[Cp_2Co][BF_4]$ and reduced in volume to 5 mL. Diethyl ether (15 mL) was added and the

solution was again filtered. The solvent was then removed under vacuum and the yellow residue was taken up in 5 mL of CH_2Cl_2. To this solution, 35 mL of diethyl ether was added creating a supersaturated solution from which a yellow crystalline solid separated. The crystals were collected by filtration and washed with diethyl ether (2 x 5 mL); yield, 0.060 g (64 %). IR (CH_2Cl_2, cm^{-1}): ν(C≡N), 2118 vs; (Nujol mull, CsI, cm^{-1}): ν(C≡N), 2198 vs; other, 1595 vs, 1578 vs, 1411 s, 1332 s, 1294 w, 1228 s, 1207 s, 1185 w, 1160 s, 1122 s, 1087 s, 1054 s, 1026 s, 950 m, 917 m, 815 m, 675 w, 640 w, 536 w, 522 w, 479 m, 442 w. Electronic absorption spectrum (CH_2Cl_2) λ_{max}, nm: 395. ^1H NMR (CD_2Cl_2, 25°C) δ ppm: -$C(CH_3)_3$ 0.86 (s, 9H), 0.88 (s, 9H); -OCH_3 3.07 (s, 6H), 3.16 (s, 6H), 3.30 (s, 6H), 3.37 (s, 6H), 3.53 (s, 6H), 3.70 (s, 6H), 3.73 (s, 6H), 3.77 (s, 6H), 3.83 (s, 3H), 3.85 (s, 3H); *meta*-H 5.88 (br, 8H), 6.02 (br, 2H), 6.12 (br, 2H). ^{31}P NMR (CD_2Cl_2, 25°C) δ ppm: P_A, -19.1 (d, $^1J_{Rh\text{-}P}$ = 129.7 Hz); P_B, -20.2 (d, $^1J_{Rh\text{-}P}$ = 129.7 Hz). Cyclic voltammogram (0.1 M $TBABF_4/CH_2Cl_2$, vs Ag/AgCl): $E_{1/2(ox)}$ = - 0.04 V.

(ii) TMPP. A mixture of $[Rh(TMPP)_2(CNBu^t)_2][BF_4]_2$ (**9**) (0.020 g, 0.013 mmol) and TMPP (0.007 g, 0.013 mmol) was dissolved in approx. 0.7 mL of CD_3CN. The resulting purple solution was transferred to a NMR tube. No reaction had occurred after 12 h at r.t. as evidenced by ^1H NMR spectroscopy.

(iii) *tert*-Butyl isocyanide. A solution of $[Rh(TMPP)_2(CNBu^t)_2][BF_4]_2$ (**9**) (0.050 g, 0.033 mmol) in 5 mL of CH_2Cl_2 was treated with 3.8 μL of $CNBu^t$ (0.033 mmol) and stirred at r.t. After 10 min, the solution color had gradually changed from purple to black/green and eventually to green. After 12 h an infrared spectrum of the solution was obtained; IR (CH_2Cl_2) cm^{-1}: 2167 s, 2118 m, 2230 w. An analogous ^{31}P NMR study in CD_3CN revealed the presence of unligated TMPP and $[TMPP\text{-}CH_3]^+$ in addition to a new species; ^{31}P NMR (CD_3CN) δ ppm: - 27.5 (d, $^1J_{Rh\text{-}P}$ = 77.8 Hz)

(iv) Carbon monoxide. An amount of $[Rh(TMPP)_2(CNBu^t)_2][BF_4]_2$ (**9**) (0.025, 0.017 mmol) was dissolved in 5 mL of CH_2Cl_2. The solution was purged with CO for 30 min. An infrared spectrum of the solution showed that no reaction had occurred under these conditions.

B. X-ray Crystallography

The structures of $[Rh(TMPP)_2(CNBu^t)_2][BPh_4]_2$ and $[Rh(TMPP)_2(CNBu^t)_2][BF_4]$ were determined by application of general procedures which have been fully described elsewhere.[7] Geometric and intensity data were collected on a Rigaku AFC6S diffractometer with graphite monochromated MoKα ($\lambda_{\bar{\alpha}}$ = 0.71069 Å) radiation and were corrected for Lorentz and polarization effects. Important crystallographic data are summarized in Table 13. All calculations were performed with the use of VAX computers on a cluster network within the Department of Chemistry at Michigan State University by using the Texsan software package of the Molecular Structure Corporation.[8]

(1) $[Rh(TMPP)_2(CNBu^t)_2][BPh_4]_2$ (9)

(i) Data Collection and Reduction. We were unable to obtain suitable single crystals of $[Rh(TMPP)_2(CNBu^t)_2]^{2+}$ as a $[BF_4]^-$ salt for X-ray diffraction studies. However, metathesis of $[BF_4]^-$ with $K[BPh_4]$ in acetone followed by slow diffusion of Et_2O yielded large dark purple crystals of $[Rh(TMPP)_2(CNBu^t)_2][BPh_4]_2$. A block-shaped crystal of approximate dimensions 0.26 x 0.26 x 0.29 mm^3 was selected and secured to the tip of a glass fiber with epoxy cement. Cell constants were obtained from a least-squares fit of 25 centered reflections in the range $15 < 2\theta < 20°$ and were consistent with a monoclinic cell. Intensity data were gathered at 23 ± 1°C in the range $4 \leq 2\theta \leq 47°$ using the ω-scan technique. Reflections with $I < 10\sigma(I)$

Table 13. Summary of crystallographic data for $[Rh^{II}(TMPP)_2(CNBu^t)_2][BPh_4]_2$ (**9a**).

Formula	$RhP_2O_{18}C_{112}H_{124}B_2$
Formula weight	1972.69
Space group	$P2_1/c$
a, Å	26.810(7)
b, Å	14.076(2)
c, Å	27.809(6)
α, deg	90
β, deg	101.35(2)
γ, deg	90
V, Å^3	10,289(4)
Z	4
d_{calc}, g/cm^3	1.273
μ (Mo Kα), cm^{-1}	2.57
Temperature, °C	23±2 °C
R[a]	0.056
R_w[b]	0.071
Quality-of-fit indicator[c]	3.80

[a] $R = \Sigma \; | \; |F_o| - |F_c| \; | / \Sigma |F_o|$

[b] $R_w = [\Sigma w(|F_o| - |F_c|)^2 / \Sigma w |F_o|^2]^{1/2}$; $w = 1/\sigma^2(|F_o|)$

[c] Quality-of-fit = $[\Sigma w(|F_o| - |F_c|)^2 / (N_{obs} - N parameters)]^{1/2}$

were rescanned a maximum of three times and the counts were accumulated to ensure good counting statistics. Three representative reflections were monitored at regular intervals and exhibited a 1.5% loss in intensity. A linear correction factor was applied to the data to account for the observed decay in intensity. After equivalent data were averaged, there remained 9109 data with $F_o^2 \geq 3\sigma(F_o)^2$ which were used in the structure solution and refinement.

(ii) Structure Solution and Refinement. The position of the rhodium atom was found by direct methods.[9] The remaining non-hydrogen atoms were located and refined through successive least-squares cycles and difference Fourier maps. After isotropic convergence, an empirical absorption correction was applied using the program DIFABS.[10] Thermal parameters for all non-hydrogen atoms were then refined anisotropically with the exception of the three methyl carbons C(62), C(63) and C(64) on one of the isocyanide ligands; these were treated isotropically. Hydrogen atoms were calculated at fixed positions and were not refined. Anisotropic refinement of 1219 parameters converged to give R = 0.056 and R_w = 0.071. The quality-of-fit index was 3.80 and the largest shift/esd = 0.32.

3. Results

A. Synthesis and Spectroscopic Characterization of $[Rh(TMPP)_2(CNR)_2][BF_4]_2$ (R = Bu^t, Pr^i).

Dichloromethane solutions of $[Rh(\eta^3\text{-}TMPP)_2][BF_4]_2$ (**3**) react smoothly with two equivalents of CNR (R = Bu^t, Pr^i) to yield dark purple solutions that exhibit a characteristic $\nu(C\equiv N)$ band at 2200 cm^{-1} for $CNBu^t$ and 2211 cm^{-1} for $CNPr^i$. Both values appear at a higher energy than that of the free isocyanide which is indicative of a higher valent metal complex in which the

isocyanides act primarily as σ-donors.[11] Reaction with only one equivalent of isocyanide results in a 1:1 mixture of product and starting material, consistent with the formulation of the stable product as a bis adduct of (**3**). In both cases, concentration of the reaction solution followed by addition of THF produces a dark purple microcrystalline solid. The products, $[Rh(TMPP)_2(CNBu^t)_2][BF_4]_2$ (**9**) and $[Rh(TMPP)_2(CNPr^i)_2][BF_4]_2$ (**10**), were isolated in 90% and 48% yield, respectively. In spite of the highly reactive nature of many radical d^7 rhodium species, these Rh(II) di-isocyanide complexes are remarkably air-stable both in the solid state and in solution. The electronic spectra of $[Rh(TMPP)_2(CNBu^t)_2][BF_4]_2$ (**9**) and $[Rh(TMPP)_2(CNPr^i)_2][BF_4]_2$ (**10**) both exhibit two prominent low energy bands in the visible region at 819 nm (ε = 1770 $M^{-1}cm^{-1}$) and 546 nm (ε = 630 $M^{-1}cm^{-1}$) for **9** and at 843 nm (ε = 1847 $M^{-1}cm^{-1}$) and 558 nm (ε = 645 $M^{-1}cm^{-1}$) for **10**; these transitions give rise to the characteristic dark purple color exhibited by these paramagnetic complexes.

Although **9** and **10** are stable with respect to oxygen and moisture, both complexes readily react with additional isocyanide to give a mixture of diamagnetic products. NMR spectral measurements of CD_3CN solutions of $[Rh(TMPP)_2(CNBu^t)_2][BF_4]_2$ (**9**) in the presence of excess tert-butyl isocyanide showed that TMPP dissociates during the reaction to form a new Rh(TMPP) species. Based on the symmetrical appearance of the proton resonances, this compound is likely a Rh(I) monophosphine complex with the general formula $[Rh(TMPP)(CNBu^t)_x]^{1+}$ (x = 2 or 3). Interestingly, even though **9** and **10** react readily with excess isocyanide, methylene chloride solutions of **9** and **10** are inert towards reaction with CO at 1 atm and r.t. Furthermore, unlike many TMPP complexes, $[Rh(TMPP)_2(CNBu^t)_2][BF_4]_2$ (**9**) does not undergo nucleophilic attack by free TMPP to yield dealkylated

complexes. Such behavior suggests that the pendent methoxy groups of TMPP are not tightly bonded to the metal center and that the coordination geometry about rhodium is four coordinate. Indeed, this is the case as evidenced by X-ray crystallography .

Thus far, only *tert*-butyl and *iso*-propyl isocyanide ligands have been to produce stable Rh(II) isocyanide adducts of $[Rh(\eta^3\text{-TMPP})_2][BF_4]_2$. Reactions of **3** with other isocyanides, such as cyclohexyl or *n*-butyl isocyanide, result in the initial formation of dark colored solutions that eventually decompose to form a mixture of isocyanide products as evidenced by infrared spectroscopy. The exact nature of these products has not yet been elucidated. However, by analogy with the chemistry of **9** and **10** with excess isocyanide, it is likely that a Rh(II) complex is formed initially, but is subject to facile isocyanide dissociation. The liberated isocyanide in turn reacts with the other Rh(II) isocyanide complexes. Clearly, more evidence is required to support this hypothesis and to formulate the products.

More intriguing than the reactions with cyclohexyl and n-butyl isocyanide, however, is the chemistry of $[Rh(\eta^3\text{-TMPP})_2][BF_4]_2$ (**3**) with methyl isocyanide. Unlike the reactions of **3** with longer chain isocyanides in which the products remain in solution, addition of methyl isocyanide to methylene chloride solutions of **3** results in the immediate formation of a red precipitate. This solid is insoluble in most common organic solvents except for acetonitrile, in which the compound exhibits only limited solubility. Infrared spectroscopy reveals a single C≡N stretching vibration at 2238 cm^1 and a broad band at 1060 cm^{-1} indicating that complex is cationic. The solid is diamagnetic as evidenced by ^1H and ^{31}P spectroscopy. The ^1H spectrum of the solid exhibits one triplet resonance representing all meta-protons of the phosphine; the observed coupling pattern for the meta-protons indicates a

trans-arrangement of two phosphines about the metal. The ^{31}P NMR spectrum of the solid in CD_3CN exhibits two idependent resonances that nearly overlap each other. Each resonance is split into a doublet, presumably due to Rh-P coupling, but there no evidence for the presence of P-P coupling. Such a situation might arise if the complex existed in solution as a 1:1 ratio of two independent geometric conformers in which the *trans* phosphorus nuclei of each conformer are magnetically equivalent.[12] Further work is needed to determine the identity of this product.

B. Magnetic and EPR Spectroscopic Properties of $[Rh(TMPP)_2(CNR)_2][BF_4]_2$ (R = Bu^t, Pr^i).

The paramagnetism of $[Rh(TMPP)_2(CNBu^t)_2][BF_4]_2$ (**9**) was probed by several spectroscopic and magnetic techniques. The ^1H and ^{31}P NMR spectra of $[Rh(TMPP)_2(CNR)_2][BF_4]_2$ are broad and essentially featureless, consistent with the formulation of **9** and **10** as paramagnetic species. Solid state and solution magnetic susceptibility studies confirmed the presence of an S = 1/2 ground state for the isocyanide complexes. A solid state magnetic susceptibility measurement of **9** at 299 K led to a μ_{eff} value of 2.04 B.M. A diamagnetic correction of -880 x 10^{-6} cgs was applied based on -24 x 10^{-6} cgs for Rh^{2+}, -39 x 10^{-6} cgs for $[BF_4]^-$, -330.8 x 10^{-6} cgs for TMPP and -58.5 x 10^{-6} cgs for $CNBu^t$.[13] Variable temperature magnetic susceptibility measurements for **9** were made over the temperature range of 5 - 380 K at a field strength of 500 G; Consistent with a simple paramagnet, the sample displayed Curie-Weiss behavior over this temperature range with Θ = -3.35 K. Solution susceptibility studies by the Evans method yielded a μ_{eff} of 2.20 B.M. at 293 K, also consistent with the presence of an S = 1/2 ground state.[14]

The paramagnetism of the samples was further examined by EPR spectroscopy. The solid-state EPR spectrum of a polycrystalline sample of **9**

at 100 K (Figure 26) shows an axial signal with g = 2.45 and $g_{||}$ = 1.96 with hyperfine coupling to ^{103}Rh (I=1/2) in the $g_{||}$ region ($A_{||}$ = 62 G). The EPR spectrum in a 1:1 Me-THF/CH_2Cl_2 glass at 100 K exhibits a signal similar to that observed in the solid state except the signal has become rhombic and the g_x and g_y regions show hyperfine coupling to ^{103}Rh as well (Figure 27). Although Rh hyperfine coupling in this region is rarely observed, it has been reported by Wilkinson *et al.* for the organometallic species Rh(2,4,6-$Pr^i_3C_6H_2)_2(tht)_2$.[15] $[Rh(TMPP)_2(CNPr^i)_2][BF_4]_2$ (**10**) exhibits an EPR spectrum similar to that observed for **9** except that the g_x and g_y tensors are nearly coincidental as shown in Figure 28. The rhombic signal with $g_x \sim g_y > g_z$, observed for both **9** and **10**, is characteristic of a d_z^2 ground state.

C. Redox Chemistry of $[Rh(TMPP)_2(CNR)_2][BF_4]_2$ (R = Bu^t, Pr^i)

A cyclic voltammogram of $[Rh(TMPP)_2(CNBu^t)_2][BF_4]_2$ in 0.1 M $TBABF_4$-CH_2Cl_2 shows a reversible couple at $E_{1/2}$= -0.04 V vs Ag/AgCl, corresponding to a one-electron reduction to Rh(I). Not surprisingly, this process is shifted to more positive potentials relative to that of $[Rh(\eta^3$-$TMPP)_2][BF_4]_2$ (**3**), due to the electron-withdrawing effect of the π-acceptor ligands.[16] Compound **9** can be chemically reduced in the presence of cobaltocene to give the yellow Rh(I) complex $[Rh(TMPP)_2(CNBu^t)_2][BF_4]$ (**11**). Examination of the cyclic voltammogram for **11** shows that it is identical to that of **9**, except that the redox process at $E_{1/2}$ = -0.04 V corresponds to an oxidation of the compound. The infrared spectrum of **11** shows a strong band $\nu(C\equiv N)$ = 2118 cm^{-1}, shifted to lower energy than the corresponding stretch in **9** due to increased π-back-bonding upon reduction from Rh(II) to Rh(I). Although the complex is expected to exhibit a simple *trans*-η^1-phosphine

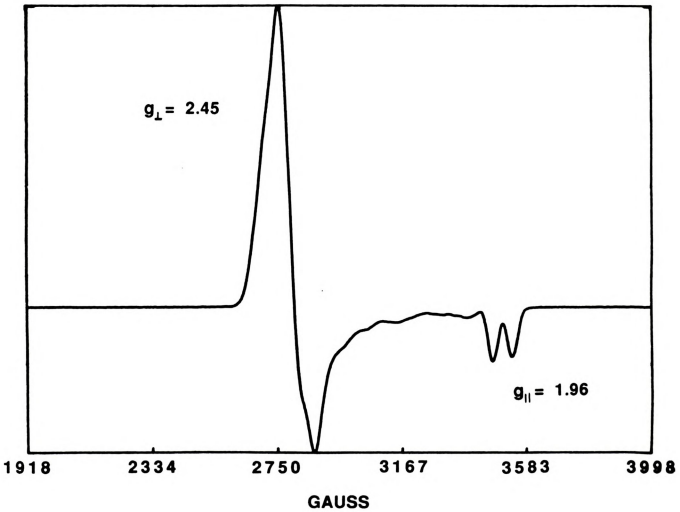

Figure 26. EPR spectrum of $[Rh^{II}(TMPP)_2(CNBu^t)_2][BF_4]_2$ (**9**) in the solid-state at 100 K.

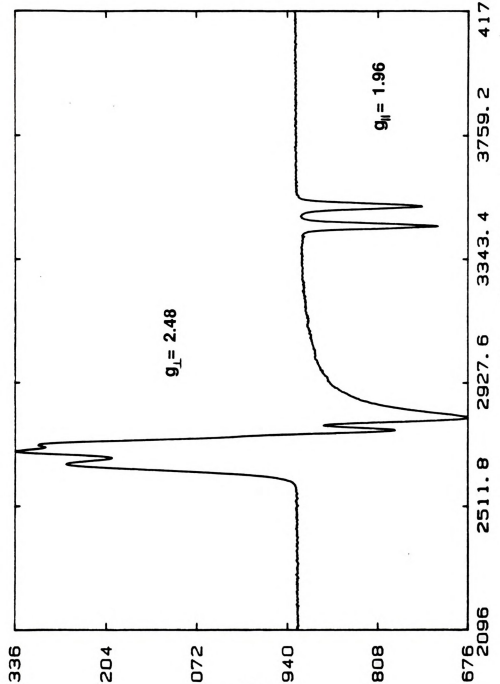

Figure 27. EPR spectrum of $[Rh^{II}(TMPP)_2(CNBu^t)_2][BF_4]_2$ (**9**) in a CH_2Cl_2/Me-THF glass at 100 K.

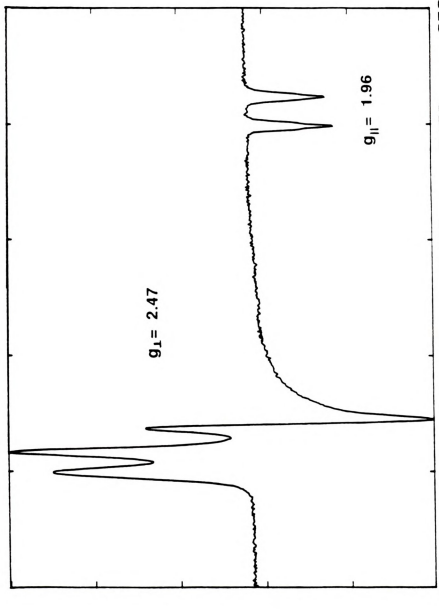

Figure 28. EPR spectrum of $[Rh^{II}(TMPP)_2(CNPr^i)_2][BF_4]_2$ (**10**) in a CH_2Cl_2/Me-THF glass at 100 K.

geometry on the basis of steric considerations, the ^1H NMR spectrum of **11** shows an unsymmetrical pattern. A likely explanation for this observation is that steric hindrance caused by the $CNBu^t$ groups restricts rotation of the phosphines about the M-P bond thereby creating *syn* and *anti* conformations for the two TMPP ligands. The different orientations of the phosphines for the two conformers are illustrated below; in both the *syn* and *anti* conformations the phosphorus nuclei are equivalent, but the spatial arrangement of the three arene rings causes two of the rings to be different from the third. The ^{31}P NMR spectrum of **11** in CD_2Cl_2 provides further

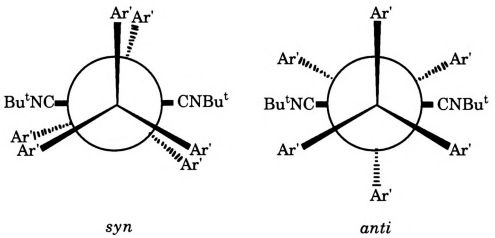

syn *anti*

evidence for the presence of two conformers in solution. The compound exhibits two independent A_2X spin systems, δ = - 19.1 ppm (d, $^1J_{Rh\text{-}P}$ = 129.7 Hz) and δ = - 20.2 ppm (d, $^1J_{Rh\text{-}P}$ = 129.7 Hz) in a 1:1 ratio resonating at nearly the same frequency. NMR experiments performed in CD_3CN reveal that the ratio of conformers was unchanged. Warming the sample to 75°C in CD_3CN caused both the proton and phosphorus resonances to broaden but neither completely coalesced. At this temperature, however, decomposition of **11** was also observed. The appearance of different conformers in solution as a result of restricted rotation about the metal-phosphorus bond has been

reported for other square planar Rh(I) and Ir(I) complexes ligated by sterically encumbering phosphines.[12] However, in contrast to the solution behavior of **11**, these complexes were found to undergo interconversions at much lower temperatures; typically, the barrier to rotation about the metal-phosphine bond was found to be low in energy and different conformers were observed only at temperatures less than -30° C. Apparently the combined size of both TMPP and the *t*-butylisocyanide ligand limits rotation about the metal-phosphorus bond well above room temperature.

D. X-ray Crystal Structure of $[Rh(TMPP)_2(CNBu^t)_2][BPh_4]$

The identity of (**9**) as $[Rh(TMPP)_2(CNBu^t)_2][BF_4]_2$ was confirmed by an X-ray crystallographic study. Large single crystals of $[Rh(TMPP)_2(CNBu^t)_2][BPh_4]_2$ were obtained by metathesis of $[Rh(TMPP)_2(CNBu^t)_2][BF_4]_2$ (**9**) with $K[BPh_4]$ in acetone followed by slow diffusion of Et_2O. An ORTEP drawing of the molecular cation $[Rh(TMPP)_2(CNBu^t)_2]^{2+}$ is shown in Figure 29. Selected bond distances and angles are listed in Table 14. The cation contains mutually *trans* phosphine and isocyanide ligands arranged in a slightly distorted square plane, as evidenced by the angles C(55)-Rh(1)-C(60) = 179.0 (3)° and P(1)-Rh(1)-P(2) = 168.78 (8)°. Coordination of the tert-butyl isocyanide ligands has effected a *cis*-to-*trans* isomerization from **3** to **9** similar to that observed in the formation of $[Rh(TMPP)_2(CO)_2][BF_4]$, with one major exception; namely the oxidation state has remained +2 in this case rather than reducing to +1 as in the CO compound. Unlike $[Rh(\eta^3\text{-}TMPP)_2][BF_4]_2$ (**3**), in which the rhodium atom is pseudo-octahedral with two metal-phosphorus and four metal-ether interactions, **9** is bound to TMPP only through the phosphorus lone pair, leading to a four-coordinate geometry. The shortest Rh-O distances

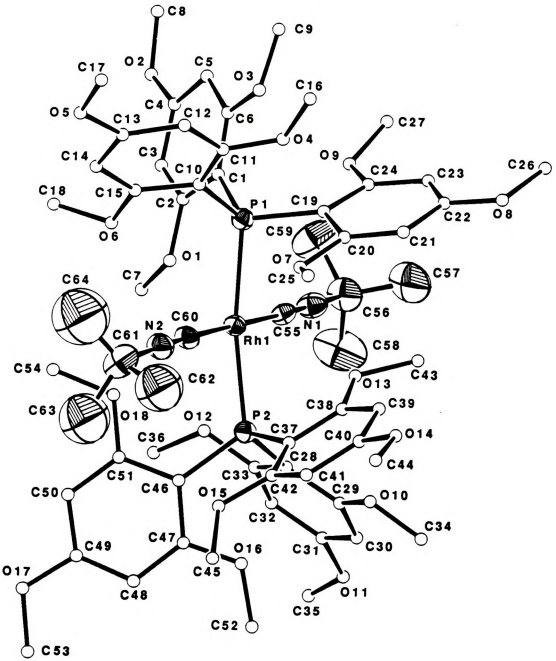

Figure 29. ORTEP representation of the molecular cation $[Rh(TMPP)_2(CNBu^t)_2]^{2+}$ in structure (**9**). Thermal ellipsoids are shown at the 40% probability level. Carbon and oxygen atoms of the phosphine ligand are shown as small spheres of arbitrary size for clarity.

Table 14. Selected bond distances (Å) and angles (deg) for $[Rh^{II}(TMPP)_2(CNBu^t)_2][BPh_4]_2$ (**9a**).

Atom 1	Atom 2	bond distance
Rh(1)	P(1)	2.364(2)
Rh(1)	P(2)	2.380(2)
Rh(1)	C(55)	1.990(9)
Rh(1)	C(60)	1.986(8)

Atom 1	Atom 2	Atom 3	bond angles
P(1)	Rh(1)	P(2)	168.78(8)
P(1)	Rh(1)	C(55)	87.9(2)
P(1)	Rh(1)	C(60)	92.6(2)
P(2)	Rh(1)	C(55)	92.2(2)
P(2)	Rh(1)	C(60)	87.1(2)
C(55)	Rh(1)	C(60)	179.0(3)
Rh(1)	P(1)	C(1)	114.1(3)
Rh(1)	P(1)	C(10)	119.8(3)
Rh(1)	P(1)	C(19)	101.0(3)

along the axial direction in **9** are Rh(1)-O(1) = 2.851 (5)Å and Rh(1)-O(13) = 2.909 (6)Å ; these are well outside the expected range for covalent bonding. The *trans* Rh-P bond distances of 2.364 (2)Å and 2.380 (2)Å are longer than those found in the parent Rh(II) complex, and are indicative of the stronger *trans* effect exerted by the phosphine as compared to that of an ether donor.

4. Discussion

At the time of this work, $[Rh(TMPP)_2(CNBu^t)_2][BF_4]_2$ represented the first mononuclear organometallic Rh(II) complex sufficiently stable to be allow for full spectroscopic and crystallographic characterization. Unlike the reactions of $[Rh(\eta^3\text{-}TMPP)_2][BF_4]_2$ with CO, alkyl isocyanide reactions of **3** forms the stable adducts with the general formula $[Rh(TMPP)_2(CNR)_2]^{2+}$ (R = Bu^t, Pr^i). The stability of these paramagnetic species is manifested in their relative redox properties. As was demonstrated by cyclic voltammetry, the Rh(II)/Rh(I) couple for **9** and **10** falls at a potential less positive than the Rh(II)/Rh(III) couple for the parent complex, $[Rh(\eta^3\text{-}TMPP)_2]^{2+}$ (**3**), however, and as a result, $[Rh(TMPP)_2(CNR)_2]^{2+}$ (R = Bu^t, Pr^i) is stable with respect to spontaneous reduction to Rh(I) in the presence of $[Rh(\eta^3\text{-}TMPP)_2]^{2+}$. This is in sharp contrast to the situation in the analogous $[Rh(\eta^3\text{-}TMPP)_2]^{2+}$ / carbon monoxide chemistry.

We have seen that subtle electronic changes in the π-acceptor ligand dramatically influence the stability of the Rh(II) complex. A case in point is the chemistry of **3** with methyl isocyanide, which is sterically and electronically very similar to CO. No stable Rh(II) adducts were isolated; instead, the reaction mixture contained several diamagnetic species, most likely Rh(I) and Rh(III) by analogy to the CO chemistry. By contrast, the ^{t}BuNC and ^{i}PrNC reactions proceed to yield only Rh(II) products.

Surprisingly, reactions of **3** with other isocyanide ligands that are sterically and electronically similar to *tert*-butyl and *iso*-propyl isocyanide appear to initially form Rh(II) complexes, but these adducts are not stable over time, probably because of pathways involving isocyanide dissociation followed by subsequent reaction with the already formed Rh(II) isocyanide complexes. Clearly, there is a subtle interplay between the steric and electronic properties of the isocyanide ligands that affects the overall stability of these paramagnetic Rh(II) isocyanide species. While it is not possible to draw any firm conclusions about the influence of the different R groups on the isocyanide chemistry of **3**, the results suggest that steric factors as well as electronic factors play a role in the stabilization of these mononuclear Rh(II) complexes.

The isolation of $[Rh(TMPP)_2(CNR)_2]^{2+}$ (R = Bu^t, Pr^i) allows for a rare opportunity to examine the chemistry of a stable organometallic radical system. One particular application is the generation of stable Rh(II) carbenes. The dinuclear Rh(II) complex $Rh_2(OAc)_4$ is known to promote the cyclopropanation of olefins by organic diazo compounds (eq 18), a highly useful organic process.[17] Although they have not been observed directly, Doyle and co-workers have implicated the intermediacy of Rh(II)-carbene species in these transformations.[18] Rh(I) and Rh(III) carbenes are readily

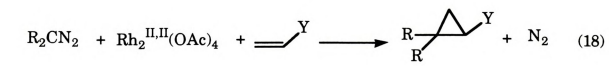

(18)

prepared by the addition of primary amines across the C≡N of coordinated isocyanides (eq 19).[19] By analogy, reaction of $[Rh(TMPP)_2(CNR)_2]^{2+}$ (R = Bu^t, Pr^i) should yield a Rh(II) carbene complex. The reaction is ligand based so no

formal redox chemistry takes place at the metal center; both isocyanides and Fisher carbenes are considered to be neutral two electron donors, therefore the formal oxidation state of rhodium will remain +2. Additional stabilization may be provided by the variable electron donating capabilities of TMPP and its demonstrated ability to adjust to the electronic

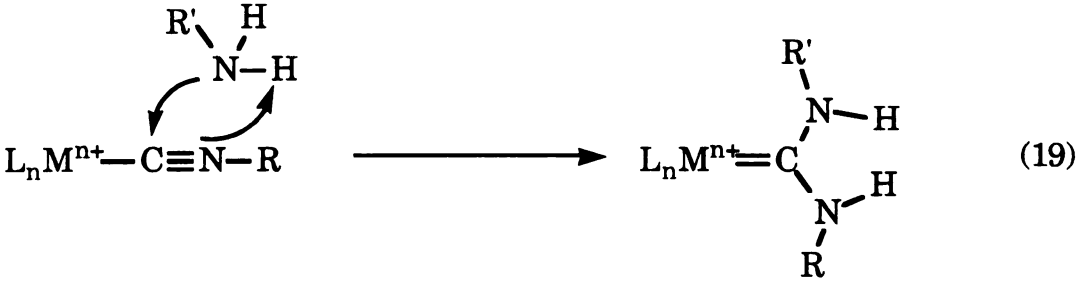

(19)

requirements of the metal center. One possible drawback to the formation of carbene complexes of **3**, however, is the additional steric congestion that would result from addition of an amine to the system. To help alleviate this problem, smaller amines will be required to minimize steric interactions. Alternatively, the steric strain may be relieved through isocyanide dissociation. The formation of stable Rh(II) carbene complexes is just one of the many potential applications for these systems.

List of References

1. (a) Hughes, R. P. in *Comprehensive Organometallic Chemistry*; Wilkinson, G.; Stone, F. G. A.; Abel, E. W., eds.; Pergamon: New York, **1982**; vol. 5, p 228. (b) *Homogenous Catalysis with Metal Phosphine Complexes*; Pignolet, L. H., ed.; Plenum: New York, **1983**. (c) Parshall, G. W. *Homogenous Catalysis*; Wiley-Interscience: New York, **1980**; p 89. (d) Collman, J. P.; Hegedus, L. S.; Norton, J. R.; Finke, R. G. *Principles and Applications of Organotransition Metal Chemistry*; University Science Books: Mill Valley, Ca. **1987**; p 523.

2. For example see (a) Felthouse, T. R. *Prog. Inorg. Chem.* **1982**, *29*, 73 and references therein. (b) Rawle, S. C.; Yagbasan, R.; Prout, K.; Cooper, S. R. *J. Am. Chem. Soc.* **1987**, *109*, 6181. (c) Blake, A. J.; Gould, R. D.; Holder, A. J.; Hyde, T. I.; Schröder, M. *J. Chem. Soc., Dalton Trans.* **1988**, 1861. (d) Cooper, S. R.; Rawle, S. C.; Yagbasan, R.; Watkin, D. J. *J. Am. Chem. Soc.* **1991**, *113*, 1600. (e) Pneumatikakis, G.; Psaroulis, P. *Inorg. Chim. Acta* **1980**, *46*, 97. (f) Pandey, K. K.; Nehete, D. T.; Sharma, R. B. *Polyhedron* **1990**, *9*, 2013. (g) Anderson, J. E.; Gregor, T. P. *Inorg. Chem.* **1989**, *28*, 3905. (h) Bianchini, C.; Meli, A.; Laschi, F.; Vizza, F.; Zanello, P. *Inorg. Chem.* **1989**, *28*, 227.

3. (a) Fischer, E. O.; Lindner, H. H. *J. Organomet. Chem.* **1964**, *1*, 307. (b) Fischer, E. O.; Wawersik, H. *J. Organomet. Chem.* **1966**, *5*, 559. (c) Keller, H. J.; Wawersik, H. *J. Organomet. Chem.* **1967**, *8*, 185. (d) Dessy, R. E.; King, R. B.; Waldrop, M. *J. Am. Chem. Soc.* **1966**, *88*, 5112. (e) Dessy, R. E.; Kornmann, R.; Smith, C.; Hayter, R. *J. Am. Chem. Soc.* **1968**, *90*, 2001. (f) Bianchini, C.; Laschi, F.; Ottaviani, F.; Peruzzini, M.; Zanello, P. *Organometallics* **1988**, *7*, 1660. (g) Bianchini, C.; Laschi, F.; Meli, A.; Peruzzini, M.; Zanello, P.; Frediani, P. *Organometallics* **1988**, *7*, 2575. (h) Bianchini, C.; Laschi, F.; Ottaviani, F.; Peruzzini, M.; Zanello, P.; Zanobini, F. *Organometallics* **1989**, *8*, 893. (i) Pilloni, G.; Schiavon, G.; Zotti, L.; Zeechin, S. *J. Organomet. Chem.* **1977**, *134*, 305.

4. Other references concerning the reactivity of mononuclear Rh(II) compounds (a) Vleck, A. *Inorg. Chim. Acta* **1980**, *43*, 35. (b) Holah, D. G.; Hughes, A. N.; Hui, B. C. *Can. J. Chem.* **1975**, *53*, 3669. (c) Valentini, G.; Braca, G.; Sbrana, G.; Colligiani, A. *Inorg. Chim. Acta* **1983**, *69*, 215. (d) Valentini, G.; Braca, G.; Sbrana, G.; Colligiani, A. *Inorg. Chim. Acta* **1983**, *69*, 221.

5. (a) Wayland, B. B.; Sherry, A. E.; Coffin, V. L. *J. Chem. Soc., Chem. Commun.* **1989**, 662. (b) Wayland, B. B.; Sherry, A. E. *J. Am. Chem. Soc.* **1989**, *111*, 5010. (c) Wayland, B. B.; Sherry, A. E.; Poszmik, G.; Bunn, A. G. *J. Am. Chem. Soc.* **1992**, *114*, 1673. (d) Wayland, B. B.; Ba, S.; Sherry, A. E. *J. Am. Chem. Soc.* **1991**, *113*, 5305. (e) Sherry, A. E.; Wayland, B. B. *J. Am. Chem. Soc.* **1990**, *112*, 1259. (f) Poszmik, G;

Wayland, B. B. presented at the 203rd National meeting of the American Chemical Society, San Francisco, CA, April 5-10, **1992**; paper INOR 67.

6. (a) Schuster, R. E.; Scott, J. E.; Casanova, J. *Org. Synth.* **1966**, *46*, 75. (b) Casanova, J.; Schuster, R. E.; Werner, N. D. *J. Chem. Soc.* **1963**, 4280.

7. (a) Bino, A.; Cotton, F. A.; Fanwick, P. E. *Inorg. Chem.* **1979**, *18*, 3558. (b) Cotton, F. A.; Frenz, B. A.; Deganello, G.; Shaver, A. *J. Organomet. Chem.* **1973**, *50*, 227.

8. TEXSAN - TEXRAY Structure Analysis Package, Molecular Structure Corporation, **1985**.

9. (a) SHELXS-86: Sheldrick, G. M. in *Crystallographic Computing 3*; Sheldrick, G. M.; Goddard, R. Eds; Oxford University Press, **1984**; p. 175. (b) DIRDIF: Direct Methods for Difference Structure, An Automatic Procedure for Phase Extension; Refinement of Difference Structure Factors. Beurskens, R. T. Technical Report **1984**.

10. Walker, N.; Stuart, D. *Acta. Cryst.* **1983**, *A39*, 158.

11. Nakamoto, K. *Infrared and Raman Spectra of Inorganic and Coordination Compounds,3rd ed*; Wiley: New York, 1978, p. 269.

12. For instance see (a) Bushweller, C. H.; Hoogasian, S.; English, A. D.; Miller, S. J.; Lourandos. M. Z. *Inorg. Chem.* **1981**, *2 0*, 3448. (b) Empsall, H. D.; Hyde, E. M.; Mentzer, E.; Shaw, B. L. *J. Chem. Soc., Dalton Trans.* **1977**, 2285. (c) Mann, B. E.; Masters, C.; Shaw, B. L.; Stainbank, R. E. *J. Chem. Soc., Chem. Commun.* **1971**, 1103.

13. O'Connor, C. J. *Prog. Inorg. Chem.* **1982**, *29*, 205.

14. (a) Evans, D. F. *J. Chem. Soc.* **1959**, 2003. (b) Deutsch, J. L.; Poling S. M. *J. Chem. Educ.* **1969**, *46*, 167.

15. Hay-Motherwell, R. S.; Koschmieder, S. U.; Wilkinson, G.; Hussain-Bates, B.; Hursthouse, M. B. *J. Chem. Soc., Dalton Trans.* **1991**, 2821.

16. For the affect of π-acceptor ligands on metal redox potentials see (a) Treichel, P. M.; Mueh, H. J.; Bursten, B. E. *Isr. J. Chem.* **1976/77**, *15*, (b) Dunbar, K. R.; Walton, R. A. *Inorg. Chim. Acta* **1984**, *87*, 185.

17. (a) Doyle, M. P. *Chem. Rev.* **1986**, *86*, 919. (b) Maas, G. *Top. Curr. Chem.* **1987**, *137*, 75. (c) Doyle, M. P. In *Catalysis of Organic Reactions*; Augustine, R. L. Ed.; Marcel Dekker: New York, **1985**. (d) Doyle, M. P.; Bagheri, V.; Wandless, T. J.; Harn, N. K.; Brinker, D. A.; Eagle, C. T.; Loh, K.-L. *J. Am. Chem. Soc.* **1990**, *112*, 1906. (e)

Collman, J. P.; Hegedus, L. S.; Norton, J. R.; Finke, R. G. *Principles and Applications of Organotransition Metal Chemistry*; University Science Books: Mill Valley, Ca. **1987**; p 800.

18. (a) Doyle, M. P. *Acc. Chem. Res.* **1986**, *19*, 348. (b) Doyle, M. P.; Dorow, R. L.; Buhro, W. E.; Griffin, J. H.; Tamblyn, W. H.; Trudell, M. L. *Organometallics* **1984**, *3*, 44. (c) Doyle, M. P.; Griffin, J. H.; Bagheri, V.; Dorow, R. L. *Organometallics* **1984**, *3*, 53. (d) Doyle, M. P.; Dorow, R. L.; Tamblyn, W. H. *J. Org. Chem.* **1982**, *47*, 4059.

19. Branson, P. R.; Green, M. *J. Chem. Soc., Dalton Trans.* **1972**, 1303.

CHAPTER VII

CHEMISTRY OF Rh(II) AND Rh(III) COMPLEXES LIGATED BY PHOSPHINO-PHENOXIDE LIGANDS

1. Introduction

Conventional wisdom holds that the hard oxygen donor atom of alkoxides are incompatible with the softer late transition metals; as a result the potentially rich area of late transition metal alkoxide chemistry went relatively unexplored for many years.[1] Only recently, have researchers demonstrated that late transition metal-oxygen bonds are not as weak as once believed, and in fact, are fairly robust when compared to the metal-carbon bonds of the analogous alkyl complexes.[2] These findings have stimulated a resurgence in the study of platinum group alkoxides, much of which has focused on the reactivity of the M-OR bond.[3] In light of this, we were intrigued by the relative ease with which dealkylation reactions of $[Rh(TMPP)_2]^{n+}$ (n = 2, 3) occur to form a rhodium phenoxide bond. We are primarily interested in the ramifications that such a ligand has on the reactivity of these phosphino-phenoxide complexes.

Previous work by Shaw and co-workers has shown the ability of mixed phosphine and phenoxide donors to impart unusual thermodynamic stability to paramagnetic Rh(II) and Ir(II) complexes.[4] Work in our own laboratories has shown that the phenoxide derivative of TMPP, TMPP-*O*, has been useful for stabilizing a variety of first-row phosphino-phenoxide complexes.[5] Furthermore, the hard anionic phenoxide donor has been found to act as a nucleating agent resulting in the formation of homo- and hetero-bimetallic and polynuclear complexes.[5, 6] Herein is described the formation and reactivity of a number of unusual mononuclear Rh(II) and Rh(III) complexes stabilized by the phosphino-phenoxide ligand, TMPP-*O*.

2. Experimental

All reactions were carried out under an argon atmosphere by the use of standard Schlenk-line techniques unless otherwise stated. The starting

materials TMPP (**1**), [Rh(η^3-TMPP)$_2$][BF_4]$_2$ (**3**), and *ax*-[Rh^{III}(η^3-TMPP)(η^3-TMPP-*O*)][BF_4]$_2$ (**5**) were prepared as described in Chapters II and III. The salt [Cp_2Fe][BF_4] was prepared by oxidation of Cp_2Fe with hydrofluoroboric acid in the presence of *p*-benzoquinone.[7] The reagents Cp_2Co (Strem), tricyclohexyl phosphine (Strem), tetra-n-butyl ammonium iodide (Aldrich), tetra-n-butyl ammonium cyanide (Aldrich), and HBF_4•Et_2O (Aldrich) were purchased from commercial sources and used without further purification.

A. Preparation of *eq*-[Rh^{II}(TMPP)(TMPP-*O*)][BF_4] (12)

(1) Reactions of [Rh(η^3-TMPP)$_2$][BF_4]$_2$ (3) with nucleophiles

(i) TMPP. Quantities of [Rh(TMPP)$_2$][BF_4]$_2$ (0.300 g, 0.224 mmol) and TMPP (0.119 g, 0.224 mmol) were dissolved in 5 mL of CH_3CN. The solution was stirred for 1 h at r.t. during which time the solution color changed from purple to red. After 1 h the solvent was removed under vacuum and the resulting dark red residue was dissolved in 20 mL of THF. An additional amount of hexanes (~4 mL) was added to precipitate any remaining [TMPP-CH_3^+][BF_4^-] from the solution. The red solution was separated from the phosphonium salt by filtration through a Celite plug and then reduced in volume to produce a red solid that was washed with 10 mL of Et_2O and dried *in vacuo*; yield: 0.137 g (49%). Cyclic voltammogram (0.1 M $TBABF_4/CH_2Cl_2$, vs Ag/AgCl): $E_{1/2(ox)}$ = - 0.02 V.

(ii) Tetra-n-butyl ammonium cyanide. A solution of [Rh(TMPP)$_2$][BF_4]$_2$ (**3**) (0.050 g, 0.037 mmol) and tetra-n-butyl ammonium cyanide (0.010 g, 0.037 mmol) in 3 mL of CH_2Cl_2 was stirred at -15°C for one hour. After observing no change in the solution color, the reaction bath was removed and the reaction was stirred at r.t. for 1 h, which resulted in a gradual color change of the solution from purple to red. The solvent was evaporated and the resulting solid was washed with 10 mL of diethyl ether

and dried under vacuum. A ^1H NMR spectrum (CD_3CN) revealed resonances attributable to: tetra-n-butyl ammonium cation, 0.96 (triplet), 1.34 (sextet), 1.56 (mult), 3.06 (mult); $[TMPP\text{-}CH_3]^+$, 3.54 (s), 3.84 (s), 6.21 (d), 2.47 (d); $[TMPP\text{-}CH_2Cl]^+$, 3.58 (s), 3.85 (s), 6.23 (d), 4.89 (d) and a paramagnetic species that was identified as *eq*-$[Rh^{II}(TMPP)(TMPP\text{-}O)][BF_4]$ (**12**) by EPR.

(iii) Tricyclohexyl phosphine. A purple solution of $[Rh(\eta^3\text{-}TMPP)_2][BF_4]_2$ (**3**) (0.050 g, 0.037 mmol) and tricyclohexyl phosphine (0.011 g, 0.037 mmol) in 5 mL of CH_2Cl_2 was stirred overnight to give a red solution. The solvent was removed under vacuum to yield a red solid which was subsequently washed with diethyl ether (2 x 5 mL) and dried under reduced pressure. ^{31}P NMR (CD_3CN) δ ppm: - 2.2 (s), + 8.6 (s), + 35.1 (s), + 35.5 (s), + 36.3 (s), + 49.7 (s). ^1H NMR spectroscopy also revealed that a complex mixture of diamagnetic and paramagnetic species were present.

(2) Reduction of *ax*-$[Rh^{III}(\eta^3\text{-}TMPP)(\eta^3\text{-}TMPP\text{-}O)][BF_4]_2$ (5)

A mixture of *ax*-$[Rh^{III}(\eta^3\text{-}TMPP)(\eta^3\text{-}TMPP\text{-}O)][BF_4]_2$ (**5**) (0.050 g, 0.038 mmol) and Cp_2Co (0.007 g, 0.038 mmol) was dissolved in 5 mL of acetone, which caused an immediate reaction as signified by the color change from orange to dark red. After 30 min, the solvent was evaporated and the residue was redissolved in 5 mL of THF and filtered through a Celite plug to remove $[Cp_2Co][BF_4]$. Toluene was added and the solution was cooled to give a red solid. The solvent was decanted from the product which was then washed with Et_2O and dried *in vacuo*; yield: 0.038 g (81%).

B. Reaction of $[Rh(\eta^3\text{-}TMPP)_2][BF_4]_2$ (3) with excess TMPP

A mixture of $[Rh(\eta^3\text{-}TMPP)_2][BF_4]_2$ (**3**) (0.025 g, 0.019 mmol) and TMPP (0.020 g, 0.038 mmol) was dissolved in ~0.7 mL of CD_3CN and transferred to a NMR tube. Within 10 min, the solution had changed from purple to dark red. A ^1H NMR spectrum recorded after 30 min indicates that

a 1:1 mixture of $[TMPP\text{-}CH_3]^+$ and TMPP was present in solution. A ^{31}P NMR spectrum of the solution after 24 h revealed resonances for a previously unidentified species; ^{31}P NMR (CD_3CN) δ ppm: + 43.7 (dd, $^1J_{Rh\text{-}P}$ = 149.7 Hz, $^2J_{P\text{-}P}$ = 19.8 Hz), + 22.9 (dd, $^1J_{Rh\text{-}P}$ = 132.8 Hz, $^2J_{P\text{-}P}$ = 19.8 Hz). In addition a phosphorus-containing compound that did not exhibit Rh-P coupling was observed at δ = +8.8 ppm (s). Integration showed that over 94 % of the TMPP had been converted to $[TMPP\text{-}CH_3]^+$. After standing for an additional 48 h, the solution color eventually became yellow. The ^{31}P NMR spectrum of the yellow solution was unchanged from above except for the appearance of *eq*-[Rh(η^3-TMPP-*O*)$_2$][BF_4] (**15**) in a 1:4 ratio with the unsymmetrical TMPP complex.

C. Oxidation of *eq*-[Rh^{II}(TMPP)(TMPP-*O*)][BF_4] (12): Synthesis of *eq*-[Rh^{III}(η^3-TMPP)(η^3-TMPP-*O*)][BF_4]$_2$ (13)

A solution of *eq*-[Rh^{III}(η^3-TMPP)(η^3-TMPP-*O*)][BF_4]$_2$ (**5**) (0.050 g, 0.040 mmol) and [Cp_2Fe][BF_4] (0.011 g, 0.040 mmol) in 5 mL of CH_3CN was stirred at -15°C for 10 min The solvent was evaporated, washed several times with Et_2O (4 x 10 mL) to remove the ferrocene by-product, and dried *in vacuo*; yield 0.035 g (65%) ^1H NMR (CD_3CN) δ ppm: -OCH_3, 2.74 (s, 3H), 2.78 (s, 3H), 3.45 (s, 3H), 3.51 (s, 3H), 3.547 (s, 6H), 3.55 (s, 3H), 3.56 (s, 3H), 3.78 (s, 3H), 3.80 (s, 3H), 3.81 (s, 6H), 3.83 (s, 3H), 3.90 (s, 3H), 3.91 (s, 3H), 4.15 (s, 3H), 4.69 (s, 3H); *m*-H, 5.76 (dd, 1H), 5.81 (m, 2H), 5.99 (m, 2H), 6.18 (dd, 2H), 6.21 (dd, 1H), 6.36 (m, 3H), 6.68 (dd, 1H). ^{31}P NMR (CD_3CN) δ ppm: + 47.3 (dd, $^1J_{Rh\text{-}P}$ = 108.8 Hz, $^2J_{P\text{-}P}$ = 13.8 Hz), + 22.5 (dd, $^1J_{Rh\text{-}P}$ = 98.8 Hz, $^2J_{P\text{-}P}$ = 13.8 Hz).

D. Reaction of *eq*-[Rh^{II}(TMPP)(TMPP-*O*)][BF_4] (12) with CO

(1) Infrared study. A solution of *eq*-[Rh^{II}(TMPP)(TMPP-*O*)][BF_4] (**12**) (0.025 g, 0.020 mmol) in 5 mL of CH_2Cl_2 was gently purged with CO to

give a green solution. An infrared spectrum taken on an aliquot showed bands at 2186 (w), 2136 (w/br), 2085 (w), 2068 (m), 1990 (m) cm^{-1}. After 15 min of additional purging, the solution color became yellow/orange and the IR spectrum showed prominent features at 2085 (m), 2068 (s) and 1990 (s) cm^{-1}. The solution was then purged with argon for 10 min, resulting in a color change of the solution to bright orange. A final aliquot was removed at this stage and its spectrum showed the three bands seen earlier, but at ~ 50% of their previous intensity.

(2) NMR study. A solution of *eq*-[Rh^{II}(TMPP)(TMPP-*O*)][BF_4] (**12**) in ~ 0.7 mL of CD_3CN was exposed briefly to an atmosphere of CO, which caused an immediate color change from red to yellow. A ^{31}P NMR spectrum of the solution obtained within 15 min revealed a mixture of identifiable diamagnetic products including [TMPP-CH_3]$^+$, *ax,eq*-[Rh(η^3-TMPP-*O*)$_2$][BF_4] (**14**), *ax,ax*-[Rh(η^3-TMPP-*O*)$_2$][BF_4] (**15**) in addition to two unidentified species. ^{31}P NMR (CD_3CN) δ ppm: product **A**, + 0.5 (d, $^1J_{Rh\text{-}P}$ = 132.8 Hz); product **B**, + 40.9 (dd, $^1J_{Rh\text{-}P}$ = 137.3 Hz, $^2J_{P\text{-}P}$ = 16.7 Hz), + 24.5 (dd, $^1J_{Rh\text{-}P}$ = 122.7 Hz, $^2J_{P\text{-}P}$ = 16.7 Hz).

E. Dealkylation of *ax*-[Rh^{III}(η^3-TMPP)(η^3-TMPP-*O*)][BF_4]$_2$ (5): Formation of *ax,eq*- and *ax,ax*-[Rh(η^3-TMPP-*O*)$_2$][BF_4] (14) and (15)

(1) TMPP

(i) Bulk reaction. A solution of *ax*-[Rh^{III}(η^3-TMPP)(η^3-TMPP-*O*)][BF_4]$_2$ (**5**) (0.050 g, 0.038 mmol) and TMPP (1) (0.020 g, 0.038 mmol) in 5 mL of CH_3CN was refluxed for 36 h and then evaporated to a yellow solid. In addition to containing [TMPP-CH_3]$^+$, the product contains a mixture of *ax,ax* and *ax,eq* isomers of [Rh(η^3-TMPP-*O*)$_2$][BF_4] in a *ax,eq* / *ax,ax* ratio of approximately 41 : 59 as evidenced by ^1H and ^{31}P NMR spectroscopy. ^{31}P NMR spectral data for *ax,eq* -[Rh(η^3-TMPP-*O*)$_2$][BF_4] (**14**) (CD_3CN, δ ppm): +

47.1 (dd, $^1J_{Rh\text{-}P}$ = 137.3 Hz, $^2J_{P\text{-}P}$ = 16.7 Hz), + 19.9 (dd, $^1J_{Rh\text{-}P}$ = 122.9 Hz, $^2J_{P\text{-}P}$ = 16.7 Hz). ^{31}P NMR spectral data for *ax,ax*-[Rh(η^3-TMPP-*O*)$_2$][BF_4] (**15**) (CD_3CN, δ ppm): + 35.7 (d, $^1J_{Rh\text{-}P}$ = 152.5 Hz). ^{1}H NMR for *ax,ax*-[Rh(η^3-TMPP-*O*)$_2$][BF_4] (**15**) (CD_3CN, δ ppm): -OCH_3, 3.01 (s, 6H), 3.27 (s, 6H), 3.39 (s, 6H), 3.43 (s, 6H), 3.64 (s, 6H), 3.78 (s, 6H), 3.85 (s, 6H), 4.14 (s, 6H); *m*-H, 5.48 (dd, 2H), 5.53 (dd, 2H), 5.77 (dd, 2H), 5.82 (dd, 2H), 6.20 (dd, 2H), 6.58 (dd, 2H).

(ii) NMR reaction. A mixture of *ax*-[Rh^{III}(η^3-TMPP)(η^3-TMPP-*O*)][BF_4]$_2$ (**5**) (0.015 g, 0.011 mmol) and TMPP (0.006 g, 0.011 mmol) was dissolved in ~ 0.7 mL of CD_3CN and transferred to a NMR tube. Within 5 min, the solution color had changed from orange to yellow. A ^{31}P NMR spectrum recorded after 20 min showed resonances corresponding to a 60 : 40 mixture of *ax,eq*-[Rh(η^3-TMPP-*O*)$_2$][BF_4] (**1 4**) and *ax,ax*-[Rh(η^3-TMPP-*O*)$_2$][BF_4] (**15**) respectively. After 12 h, the *ax,eq* to *ax,ax* isomer ratio was 55 : 45.

(2) Tetra-n-butyl ammonium iodide

Quantities of *ax*-[Rh^{III}(η^3-TMPP)(η^3-TMPP-*O*)][BF_4]$_2$ (**5**) (0.015 g, 0.011 mmol) and tetra-n-butylammonium iodide (0.004 g, 0.011 mmol) were dissolved in ~ 0.07 mL of d_6-acetone. The solution was transferred to a NMR tube in order to monitor the reaction progress by ^{1}H and ^{31}P NMR spectroscopy. Conversion of **5** to *ax,ax*-[Rh(η^3-TMPP-*O*)$_2$][BF_4] (**15**) was found to be quantitative as no *ax,eq* isomer was observed by ^{31}P NMR spectroscopy. The presence of CH_3I (δ = 2.16 ppm) was detected by ^{1}H NMR.

F. Reactions of *ax*-[Rh^{III}(η^3-TMPP)(η^3-TMPP-*O*)][BF_4]$_2$ (5)

(1) HBF_4•Et_2O

To a solution of *ax*-[Rh^{III}(η^3-TMPP)(η^3-TMPP-*O*)][BF_4]$_2$ (**5**) (0.015 g, 0.011 mmol) in ~ 0.07 mL of CD_3CN in a NMR tube was added 2 drops of

$HBF_4 \cdot Et_2O$. The tube was shaken for several minutes after which time a ^{31}P NMR spectrum was measured. ^{31}P NMR (CD_3CN) δ ppm: product **A** (major), + 36.2 (d, $^1J_{Rh\text{-}P}$ = 129.7 Hz); product **B** (minor), + 36.3 (dd, $^1J_{Rh\text{-}P}$ = 111.4 Hz, $^2J_{P\text{-}P}$ = 13.7 Hz), + 33.5 (dd, $^1J_{Rh\text{-}P}$ = 133.6 Hz, $^2J_{P\text{-}P}$ = 13.7 Hz). The relative amounts of both species remained unchanged after 48 h.

(2) CO

A solution of *ax*-[Rh^{III}(η^3-TMPP)(η^3-TMPP-*O*)][BF_4]$_2$ (**5**) (0.025 g, 0.019 mmol) in 10 mL of CH_2Cl_2 was exposed to CO at r.t. for 30 min. The solution color remained unchanged and an infrared spectrum of the solution showed no CO stretching vibrations.

(3) H_2

A solution of *ax*-[Rh^{III}(η^3-TMPP)(η^3-TMPP-*O*)][BF_4]$_2$ (**5**) (0.050 g, 0.038 mmol) in 10 mL of CH_3CN was purged at r.t. with H_2. For the first hour, additional CH_3CN was added periodically to maintain a constant solution volume. After 1 h the solution was allowed to evaporate under a constant stream of H_2 and the resulting solid was washed with diethyl ether (5 mL) and dried under reduced pressure. A ^1H NMR spectrum of the solid in CD_3CN revealed resonances corresponding only to unreacted **5**.

(4) MeOH

To a solution of *ax*-[Rh^{III}(η^3-TMPP)(η^3-TMPP-*O*)][BF_4]$_2$ (**5**) (0.015 g, 0.011 mmol) in ~ 0.07 mL of CD_3CN in a NMR tube was added ~0.1 mL of MeOH. A ^1H NMR spectrum measured after 36 h revealed that no reaction had occurred.

3. Results

A. Synthesis and Characterization of *eq*-[Rh^{II}(TMPP)(TMPP-*O*)][BF_4] (12)

One equivalent of TMPP readily reacts with [Rh(η^3-TMPP)$_2$][BF_4]$_2$ (**3**) to produce red solutions of an air sensitive paramagnetic species. Monitoring the progress of the reaction by ^{1}H NMR spectroscopy reveals that the cation [TMPP-CH_3]$^+$ is the only diamagnetic species present in solution. Based on this observation, we propose that **3** undergoes demethylation in the presence of TMPP to yield the paramagnetic Rh(II) complex *eq*-[Rh^{II}(TMPP)(TMPP-*O*)][BF_4] (**12**). Isolated yields of **12** have been generally low (~ 50%) due to difficulties encountered in separating the methylphosphonium by-product. As a result, samples of **12** prepared by this route are invariably contaminated with minor amounts of [TMPP-CH_3][BF_4] as verified by ^{1}H NMR spectroscopy. The compound [Rh(η^3-TMPP)$_2$][BF_4]$_2$ (**3**) has also been observed to react with other potential nucleophiles to produce **12**, but the reactions are typically less selective, and result in the formation of other diamagnetic species.

Not unexpectedly, the ^{1}H NMR spectrum of **12** is essentially featureless, exhibiting only broad resonances between 3 and 5 ppm. A ^{31}P NMR signal was not observed for **12**, further supporting its assignment as a paramagnetic species. Unfortunately, an accurate variable temperature magnetic susceptibility measurement could not be obtained due to the presence of [TMPP-CH_3][BF_4] in solid samples of **12**. However the paramagnetism of *eq*-[Rh^{II}(TMPP)(TMPP-*O*)][BF_4] (**12**) was verified by EPR spectroscopy. An EPR spectrum of **12** at 100 K in a 1:1 CH_2Cl_2/Me-THF glass displays a rhombic signal similar to that observed for [Rh(η^3-TMPP)$_2$][BF_4]$_2$ (**3**) with g_x = 2.26, g_y = 2.32, and g_z = 1.99 (Figure 30). The g_z region of the

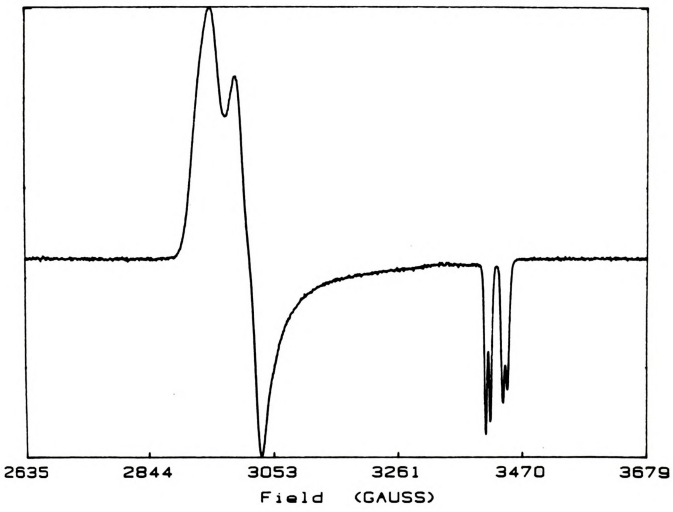

Figure 30. EPR spectrum of *eq*-[Rh^{II}(TMPP)(TMPP-*O*)][BF_4] (**12**) at 100 K in a 1:1 CH_2Cl_2/Me-THF glass.

spectrum, however, exhibits hyperfine coupling to two different types of nuclei (A_{Rh} = 29 G, A_P = 8 G), thus creating a doublet of doublets splitting pattern in the g_z tensor region. The larger of the hyperfine coupling constants results from ^{103}Rh coupling in agreement with the values reported for other Rh(II) systems. Therefore, the weaker coupling constant is likely due to interaction of the unpaired spin with one of the phosphorus nuclei. The magnitude of the phosphorus hyperfine coupling suggests that this phosphorus nucleus is not located directly along the d_z^2 axis, but nonetheless, can sufficiently interact with the unpaired electron to produce the observed coupling pattern.

B. Redox behavior of *eq*-[Rh^{II}(TMPP)(TMPP-*O*)][BF$_4$] (12)

The cyclic voltammogram of **12** exhibits a reversible oxidation at $E_{1/2}$ = - 0.02 V vs Ag/AgCl. Not surprisingly, the Rh(II)/Rh(III) couple for **12** appears at a much less positive potential than that observed for [Rh(η^3-TMPP)$_2$][BF$_4$]$_2$ (**3**) ($E_{1/2(ox)}$ = + 0.46 V). The increased ease of oxidation for **12** reflects the superior basicity of the newly formed phenoxide ligand Rh-O(R) compared to that of the neutral ether donor in the original compound Rh-OMe(R). Although the two cations, **5** and **12**, contain the same ligand set, their electrochemical behavior is quite different. A comparison of the cyclic voltammograms for the Rh(II) complex *eq*-[Rh^{II}(TMPP)(TMPP-*O*)][BF$_4$] (**12**) and the Rh(III) complex *ax*-[Rh^{III}(η^3-TMPP)(η^3-TMPP-*O*)]$^{2+}$ (**5**) is presented in Figure 31. An examination of the two cyclic voltammograms reveals that the reversible oxidation couple of [Rh^{II}(TMPP)(TMPP-*O*)]$^{1+}$ (**12**) coincides with the chemical return wave of *ax*-[Rh^{III}(η^3-TMPP)(η^3-TMPP-*O*)]$^{2+}$ (**5**). This result may be interpreted as follows; reduction of *ax*-[Rh^{III}(η^3-TMPP)(η^3-TMPP-*O*)]$^{2+}$ (**5**) produces a transient d^7 Rh(II) species, presumably *ax*-[Rh^{II}(TMPP)(TMPP-*O*)][BF$_4$] (**12a**), that immediately undergoes a rapid

$[Rh^{III}(\eta^3\text{-TMPP})(\eta^3\text{-TMPP-O})]^{2+}$

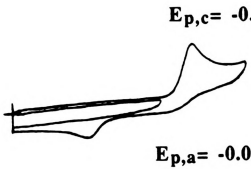

$[Rh^{II}(TMPP)(TMPP\text{-}O)]^{1+}$

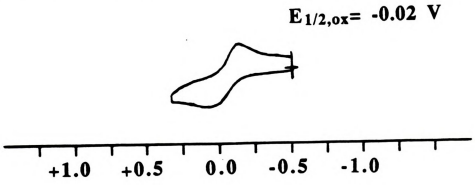

Figure 31. Cyclic voltammograms of *ax*-$[Rh^{III}(\eta^3\text{-TMPP})(\eta^3\text{-TMPP-}O)][BF_4]_2$ (**5**) and *eq*-$[Rh^{II}(TMPP)(TMPP\text{-}O)][BF_4]$ (**12**) in 0.1 M $TBABF_4/CH_2Cl_2$.

structural rearrangement to a more electronically favorable conformation. In support of this hypothesis is the chemical reduction of *ax*-[Rh^{III}(η^3-TMPP)(η^3-TMPP-*O*)][BF_4]$_2$ which yields a dark red product in good yield that is spectroscopically identical to **5**. Logic dictates that two different structural isomers are possible for compound **12** (shown as **a** and **b** below). Isomer (**a**) is formed by rearrangement of the phosphorus donors from a *cis* to a *trans* orientation. A second possibility concerns the isomerization of the phenoxide ligand from being *cis* to both phosphorus nuclei, as in the structure of **5**, to becoming *trans* to one of the phosphorus nuclei, while the phosphorus nuclei remain *cis* to each other. Unfortunately the paramagnetism of **12** precludes us from gleaning any structural information about this species by NMR spectroscopy. However, the fact that the newly formed compound **12** exhibits a chemically reversible oxidation ($i_{Pa}/i_{Pc} \sim 1$) is quite interesting. The reversibility of this couple suggests that it should be possible oxidize **12** to a diamagnetic Rh(III) species (**13**) without effecting a major structural rearrangement. Consequently, it is possible to infer the structure of [Rh^{II}(TMPP)(TMPP-*O*)][BF_4] (**12**) by investigating the NMR spectrum of the diamagnetic Rh(III) complex **13**, since, the two complexes are expected on the basis of cyclic voltammetry be structurally similar. Indeed, [Rh^{II}(TMPP)(TMPP-*O*)][BF_4] (**12**) is rapidly oxidized in the presence of [Cp_2Fe][BF_4] to yield a red/brown product **13**. As anticipated, the NMR spectral features of **13** vary significantly from those observed for the related compound, *ax*-[Rh^{III}(η^3-TMPP)(η^3-TMPP-*O*)][BF_4]$_2$. The ^{31}P NMR spectrum of **13** shows the presence of two magnetically inequivalent phosphorus nuclei that couple to both Rh centers and to each other resulting in an ABX spin system; δ ppm: + 47.3 (dd, $^1J_{Rh\text{-}P_A}$ = 108.8 Hz, $^2J_{P_A\text{-}P_B}$ = 13.8 Hz), + 22.5 (dd, $^1J_{Rh\text{-}P_B}$ = 98.8 Hz, $^2J_{P_B\text{-}P_A}$ = 13.8 Hz). Just as was observed for **5**, the small

magnitude of $^2J_{P_B\text{-}P_A}$ indicates a *cis* orientation of the two phosphorus nuclei. However, unlike the ^{31}P NMR spectrum for **5**, the chemical shifts and Rh-P coupling constants for the two nuclei are quite disparate. This is consistent with the phenoxide group bonded *trans* to the phosphorus atom of TMPP and resides in the equatorial plane defined by the two phosphorus atoms. Such a bonding arrangement would produce two distinct electronic environments for the phosphorus nuclei stemming from the different *trans* influences caused by an anionic phenoxide donor versus a neutral ether donor. Therefore on the basis of the ^{31}P NMR spectral data for **13** and the observed electrochemical relationship between complexes **5** **12** and **13**, the structure of $[Rh^{II}(TMPP)(TMPP\text{-}O)]^{1+}$ (**12**) is predicted to be a *cis* arrangement of phosphines with the phenoxide group of the dealkylated phosphine in an equatorial position.

Interestingly, when *eq*-$[Rh^{III}(\eta^3\text{-}TMPP)(\eta^3\text{-}TMPP\text{-}O)]^{2+}$ (**13**) is allowed to stand in solution, the complex rearranges slowly, over a period of weeks, to form $[Rh^{III}(\eta^3\text{-}TMPP)(\eta^3\text{-}TMPP\text{-}O)]^{2+}$ (**5**). The process, however, is complicated as evidenced by the formation of the *bis*-demethylated phosphine complex *ax,ax*-$[Rh(\eta^3\text{-}TMPP\text{-}O)_2][BF_4]$ (**1 5**). The pathway for the isomerization is not understood and merits further investigation.

C. Reactivity of *ax*-$[Rh^{III}(\eta^3\text{-TMPP})(\eta^3\text{-TMPP-}O)][BF_4]_2$ (5)

The complex $[Rh^{III}(\eta^3\text{-}TMPP)(\eta^3\text{-}TMPP\text{-}O)][BF_4]_2$ like $[Rh(\eta^3\text{-}TMPP)_2][BF_4]_2$ (**3**) and $[Rh(\eta^3\text{-}TMPP)_2][BF_4]_3$ (**4**) is also susceptible to nucleophilic attack. Compound **5** reacts swiftly with TMPP in acetonitrile to produce yellow solutions of $[Rh(\eta^3\text{-}TMPP\text{-}O)_2][BF_4]$. ^{31}P NMR data reveal that two geometric isomers are present in solution; an unsymmetrical complex, in which the two phosphorus nuclei are inequivalent, located at δ = 47.1 ppm (dd, $^1J_{Rh\text{-}P}$ = 137.3 Hz, $^2J_{P\text{-}P}$ = 16.7 Hz) and δ = + 19.9 ppm (dd,

$^1J_{Rh\text{-}P}$ = 122.9 Hz, $^2J_{P\text{-}P}$ = 16.7 Hz), and a species, with a resonance at δ = + 35.7 ppm (d, $^1J_{Rh\text{-}P}$ = 152.5 Hz), in which both phosphine ligands are magnetically equivalent. The formation of both isomers of [Rh(η^3-TMPP-*O*)$_2$][BF_4] results from non-specific nucleophilic attack taking place at different metal-ether positions in the structure of **5**. Logically there are two possible sites for this second dealkylation reaction to occur, either in the equatorial plane, *trans* to the neutral TMPP ligand or in the axial position, *trans* to the phenoxide group (Figure 32). Assuming that phosphine rearrangement does not occur, demethylation of the methoxy group that is trans to phosphorus is predicted to result in the formation of two magnetically distinct phosphine ligands that should exhibit two ABX spin systems at chemical shifts similar to those observed for the unsymmetrical product. On the other hand, dealkylation of the methoxy group *trans* to the phenoxide ligand should create two chemically equivalent phosphine ligands. Based on these arguments, the unsymmetrical product is assigned the formula *ax,eq*-[Rh^{III}(η^3-TMPP-*O*)$_2$][BF_4] (**14**) and the product with equivalent phosphino-phenoxide ligands is designated *ax,ax*-[Rh(η^3-TMPP-*O*)$_2$][BF_4] (**15**). Although both species are present in solution, the relative amounts of isomers **14** and **15** appear to be sensitive to the reaction conditions; dealkylation reactions performed at higher temperature give a greater proportion of the *ax,ax* isomer **15**. Moreover, there is apparently slow conversion of **14** to **15**in solution over extended periods of time as evidenced by NMR spectroscopy.

The susceptibility of **5** to nucleophilic attack is further demonstrated by its reaction with free iodide. *ax*-[Rh^{III}(η^3-TMPP)(η^3-TMPP-*O*)][BF_4]$_2$ readily reacts with one equivalent of [(Bu-n)$_4$N][I] to yield exclusively the *ax,ax* isomer **15**. The resulting by-product of the reaction, CH_3I, is easily

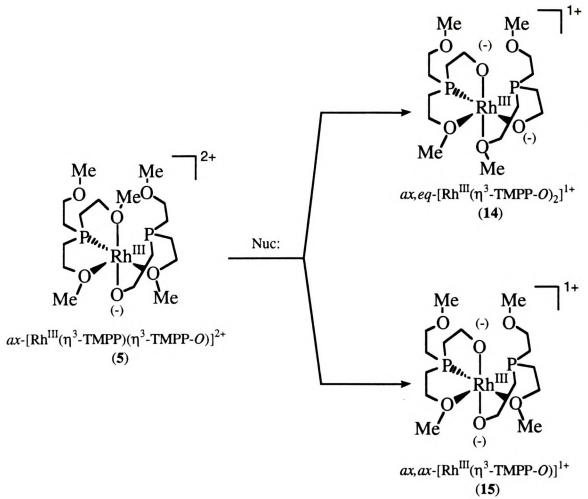

Figure 32. Possible dealkylation products resulting from nucleophilic attack on *ax*-[Rh^{III}(η^3-TMPP)(η^3-TMPP-*O*)][BF_4]$_2$ (**5**).

detected by ^1H NMR spectroscopy. Nucleophilic attack on a coordinated methoxy group is expected to be influenced by a variety of factors including steric hindrance of the ancillary ligands, electrophilicity of the -OCH_3 moiety and basicity of the attacking nucleophile. In light of this, it is not surprising that minor variations in reaction conditions lead to different relative amounts of the isomers **14** and **15**. This concept is illustrated by the fact that demethylation of **5** with a weaker nucleophile, such as iodide, produces **15** exclusively.

The phenoxide group of *ax*-[Rh^{III}(η^3-TMPP)(η^3-TMPP-*O*)][BF_4]$_2$ is easily protonated in the presence of excess HBF_4. However, the expected product [Rh^{III}(η^3-TMPP)(η^3-TMPP-*OH*)][BF_4]$_3$ appears to be present in only minor amounts as evidenced by ^{31}P NMR spectroscopy. The ^{31}P NMR spectrum of the major product exhibits a doublet at δ = + 36.2 ppm ($^1J_{Rh\text{-}P}$ = 129.7 Hz); this is indicative of two chemically equivalent phosphines. One possible explanation is that upon protonation of **5** to form [Rh^{III}(η^3-TMPP)(η^3-TMPP-*OH*)][BF_4]$_3$, a dealkylation reaction occurs similar to the one that transforms [Rh(η^3-TMPP)$_2$][BF_4]$_3$ (**4**) to **5**. By analogy with the dealkylation of **4**, such a process is not unreasonable, if one considers the high positive charge concentrated on the Rh atom. The absence of anionic ligands, which would tend to offset this charge, creates a highly electrophilic metal center that may activate another coordinated methoxy group. Following demethylation, the newly formed phenoxide ligand is quickly protonated to form [Rh(η^3-TMPP-*OH*)$_2$][BF_4]$_3$. A axial orientation of the phenol groups would result in an arrangement where both phosphino-phenol groups are chemically equivalent. Clearly, the preceding arguments represent just one of several possible scenarios and further work is needed to either prove or disprove the hypothesis.

D. Chemistry of *eq*-[Rh^{II}(TMPP)(TMPP-*O*)][BF_4] (12) with CO

One of our primary goals in preparing a demethylated analog of [Rh(η^3-TMPP)$_2$][BF_4]$_2$ (**3**) was to modify the reactivity of the system by reducing the flexibility of the ligand set. We argued that dealkylation of the pendent methoxy group would result in the formation of a less labile phenoxide interaction, thereby constraining the coordination environment about the metal. Based on the recent fascinating work of Wayland *et al.* on Rh(II) porphyrins, we anticipated that by introducing a more rigid ligand framework, we may inhibit disproportionation and therefore isolate a Rh(II) carbonyl species. The presence of an anionic phenoxide ligand is also expected to help stabilize the Rh(II) oxidation state with respect to Rh(I) and further deter disproportionation.

Moderate purging of a methylene chloride solution of *eq*-[Rh^{II}(TMPP)(TMPP-*O*)][BF_4] (**12**) with CO results in an immediate change in the solution color from red to dark green. An infrared spectrum measured within the first 10 minutes exhibits a set of moderate intensity bands at 2084, 2068, and 1990 cm^{-1}. Moreover, two weak, higher energy bands appear at 2186 and 2136 cm^{-1}. Upon continued purging of CO, the green color quickly converts to yellow/orange. An infrared spectrum of the solution at this stage reveals an absence of the two higher energy bands and an increase in the intensity of the three lower energy absorptions. Removal of the CO atmosphere by purging with argon causes a reduction in the bands at 2084, 2068, and 1990 cm^{-1}, but the original red solution color never reappears indicating that the overall addition of CO to *eq*-[Rh^{II}(TMPP)(TMPP-*O*)][BF_4] (**12**) is not a reversible process.

Intrigued by the possibility that the higher energy intermediate bands could be Rh(II) carbonyl adducts, the reaction was monitored by EPR

spectroscopy in order to detect the formation of paramagnetic intermediates. A frozen solution of **12** dissolved in a 1:1 mixture of CH_2Cl_2/Me-THF in an EPR tube was exposed to CO; the sample was gently warmed, and upon reaction was quickly refrozen. The EPR spectrum of the frozen solution at 100 K (Figure 33) revealed the presence of a new paramagnetic species (g_1 ~ 2.31, g_2 ~ 2.27, g_3 ~ 1.98, A_3 ~ 14.6 G) in addition to unreacted **12**. A similar experiment performed with labeled ^{13}CO, resulted in an EPR spectrum that showed complete conversion to a new Rh(II) species (g_1 ~ 2.31, g_2 ~ 2.27, g_3 ~ 1.99, A_3 ~ 48 G). The lack of significant ^{13}CO coupling to any of the g tensors indicates there is little electron density residing on the CO ligand and that the radical is primarily metal-based. This behavior is in contrast to the significant delocalization of electron density between the Rh and CO moiety observed for the Rh(II)-porphyrin-carbonyl complexes.[8] In fact it is exactly the delocalization that induces the carbon coupling reactions in these systems. Unfortunately, the ability of Rh(II)-TMPP complexes to effect similar coupling reactions as those observed for the porphyrin systems appears to be limited.

Although EPR spectroscopy provided evidence for the formation of transient Rh(II) CO adducts, it was evident that this was followed by a disproportionation pathway. In order to identify the key participants in this pathway, the progress of the reaction was also monitored by ^{31}P NMR spectroscopy. The ^{31}P NMR spectrum of a solution of *eq*-[Rh^{II}(TMPP)(TMPP-*O*)][BF_4] (**12**) in CD_3CN exposed to CO for one minute reveals that a complex mixture of diamagnetic species is formed. Careful inspection reveals that two of the products are a mixture of *ax,eq* and *ax,ax* isomers of [Rh^{III}(η^3-TMPP-*O*)$_2$][BF_4], characterized in the previously mentioned dealkylation chemistry. In addition, two unidentified species are also present in solution, a doublet at

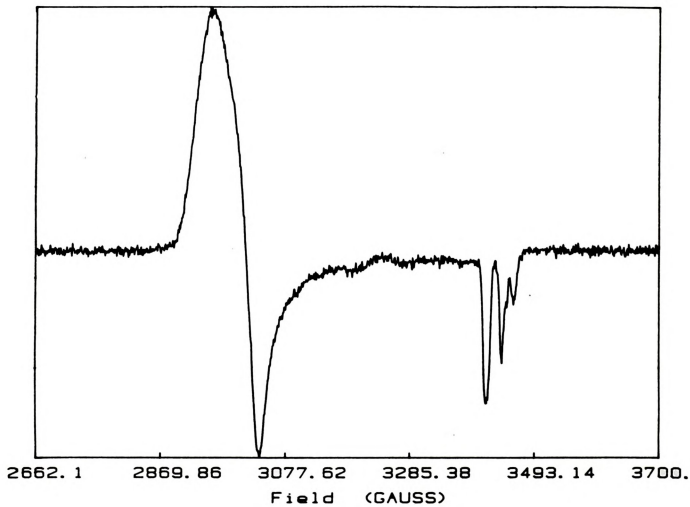

Figure 33. EPR spectrum of a frozen 1:1 CH_2Cl_2/Me-THF solution of *eq*-[Rh^{II}(TMPP)(TMPP-*O*)][BF_4] (**12**) exposed to CO.

δ = + 0.5 ppm ($^1J_{Rh\text{-}P}$ = 132.8 Hz) and an unsymmetrical species characterized by two ABX resonances at δ = + 40.9 ppm ($^1J_{Rh\text{-}P}$ = 137.3 Hz, $^2J_{P\text{-}P}$ = 16.7 Hz) and δ = + 24.5 ppm ($^1J_{Rh\text{-}P}$ = 122.7 Hz, $^2J_{P\text{-}P}$ = 16.7 Hz). The presence of [Rh(η^3-TMPP-*O*)$_2$][BF_4] implies that certain reactions must participate in the overall reaction pathway. The formation of [Rh(η^3-TMPP-*O*)$_2$]$^+$ necessitates an initial oxidation of **12** to **13** By analogy to the CO chemistry of [Rh(η^3-TMPP)$_2$][BF_4]$_2$ (**3**), oxidation of **12** to **13** could, presumably, arise from reaction between **12** and a CO adduct of **12** Such an event is not unreasonable considering the accessible nature of the Rh(II)/Rh(III) redox couple for **12** ($E_{1/2(ox)}$ = - 0.02 V). The presence of [Rh(η^3-TMPP-*O*)$_2$]$^{1+}$ also implies that, during the course of the reaction, TMPP dissociates from one of the products and acts as a nucleophile in the dealkylation of [Rh^{III}(η^3-TMPP)(η^3-TMPP-*O*)]$^{2+}$. This conclusion is supported by the presence of a significant amount of [TMPP-CH_3]$^+$ in the NMR spectrum of the reaction.

4. Discussion

The results presented in this chapter demonstrate the susceptibility of $Rh^{II,III}$-TMPP complexes to dealkylation of a coordinated methoxy group. The thermodynamic driving force behind this reaction is undoubtedly the high positive charge on the metal center coupled with activated methyl groups. Although TMPP has been shown to be a highly basic 2 e$^-$ donor phosphine ligand with the lone pair, when the ligand is participating in an η^3 bonding mode it is a relatively poor 6 e$^-$ donor due to the weak donating ability of the pendent ether groups. Consequently, the neutral phosphine is unable to effectively counterbalance the high positive charge on the metal center, and as a result, the coordinated methoxy groups become activated

towards dealkylation. As the metal oxidation state increases, and hence the overall charge on the complex, dealkylation becomes increasingly more thermodynamically favorable. This point is nicely demonstrated by a comparison of the relatively stability of the $[Rh^{II}(\eta^3\text{-TMPP})_2]^{2+}$ (**3**) and $[Rh^{III}(\eta^3\text{-TMPP})_2]^{3+}$ (**4**) complexes towards dealkylation; compound **4** readily demethylates in the presence of very weak nucleophiles such as $[BF_4]^-$, while **3** generally requires strong nucleophiles. The Rh(III) oxidation state appears to be highly susceptible, as evidenced by the observation that *ax*-$[Rh^{III}(\eta^3\text{-TMPP})(\eta^3\text{-TMPP-}O)][BF_4]_2$ will undergo a second dealkylation in the presence of free iodide.

The introduction of a phenoxide donor into the metal coordination sphere sets up the possibility of preparing structural isomers based on the relative positions of the phosphine and phenoxide groups. As a result, there are two primary structural conformations, assuming a *cis*-phosphorus donor atom geometry is maintained; the phenoxide group may either be equatoiral or axial position with respect to the equatorial plane containing the phosphorus atoms. The favored structural conformation is highly dependent on the metal oxidation state. The relationship between the various isomers of the dealkylated and non-dealkylated complexes **3**, **4**, **5**, **12** and **13**is depicted in Figure 34. An important underlying principle that is pervasive in the chemistry of these phosphine complexes is the difference in substitutional lability between the +2 and +3 oxidation states of rhodium. The Rh(III) oxidation state, being a d^6 metal ion, is relatively substitutionally inert and therefore any structural rearrangements that may occur will be very slow or kinetically inhibited. In contrast, paramagnetic Rh(II) complexes are substitutionally labile and as a result, the distorted Rh^{II}-TMPP complexes are less structurally rigid. This lack of structural rigidity is demonstrated by

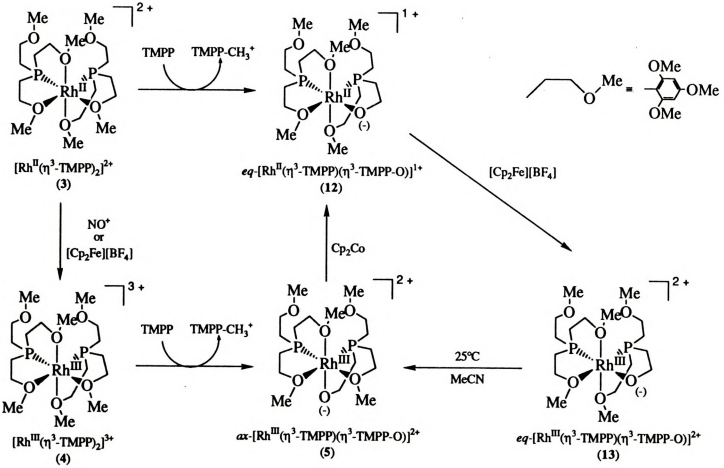

Figure 34. Reaction scheme depicting the relationship between the various isomers of dealkylated and non-dealkylated complexes **3**, **4**, **5**, **12** and **13**.

the facile axial to equatorial isomerization of $[Rh^{II}(TMPP)(TMPP\text{-}O)][BF_4]$ (**12**), while the analogous rearrangement for the Rh(III) d^6 complex is exceedingly slow.

Curiously, in each of the complexes described in this chapter, the phosphine lie *cis* to each other rather than in the sterically more logical *trans* orientation. Evidently, the preference for the *cis* geometry is electronic and not kinetic in origin. Presumably, the presence of the weak ether donors requires that the phosphine ligands remain *cis* in order to maximize electron donation to the relatively electron-poor metal center. Several observations support this conclusion. Previously, we noted that $[Rh(\eta^3\text{-}TMPP)_2][BF_4]_2$ (**3**) was present as a *cis*-phosphine conformation and that it could not be thermally converted to the *trans* orientation. One could conceivably argue that the steric bulk of the ligands prevents isomerization to the steric favored conformation and that the *cis* orientation of the phosphines resulted from the original attack of the phosphine on $[Rh_2(MeCN)_{10}][BF_4]_4$. This seems unlikely in light of the facile rearrangement of *ax*-$[Rh^{III}(\eta^3\text{-}TMPP)(\eta^3\text{-}TMPP\text{-}O)]^{2+}$ (**5**) upon reduction to the corresponding d^7 complex $[Rh^{II}(TMPP)(TMPP\text{-}O)]^{1+}$ (**12**). The substitutionally labile nature of the d^7 complexes allows the phenoxide group to readily change its relationship (axial/equatorial) to the neutral phosphine, yet in compound **3** the phosphorus atoms remain *cis* to each other. Moreover, introduction of strong donor ligands such as CO and CNR results in an immediate structural rearrangement to a *trans* phosphine geometry as exhibited by complexes **6** - **11**. This point is dramatically illustrated by the oxidation of $[Rh^{I}(TMPP)_2(CO)]^{1+}$ (**7**) to $[Rh^{II}(\eta^3\text{-}TMPP)_2]^{2+}$ (**3**). Although the phosphines are *trans* in the initial Rh(I)CO complex, oxidation followed by CO dissociation results in phosphine isomerization to the thermodynamically

favored *cis* orientation. These observations clearly support that the disposition of the phosphine ligands in these Rh(II) and Rh(III) complexes is not kinetic in origin but instead thermodynamic.

A final point regarding the dealkylation of TMPP to form the anionic phosphino-phenoxide needs to be addressed, namely, the effect that dealkylation has on the chemistry of these complexes. An important consequence of demethylation is that it limits the flexibility of the ligand by anchoring it at two positions rather than only one. Furthermore, the formation of a relatively non-labile metal-phenoxide bonds reduces the number of potential coordination sites for an incoming substrate. Nonetheless, these phenoxide groups do not occupy all of the coordination sites. The presence of two or three labile metal ether interactions still leaves open the possibility for further chemistry. Ironically, the formation of phenoxide donors may potentially induce higher lability in the remaining coordinated methoxy groups by providing more electron density at the metal. This in effect will reduce the electrophilic character of the metal and decrease the need for electron donation by the pendent ether groups and subsequently making them more labile. This will be particularly true for higher valent metal centers. Consequently, $[Rh^{III}(\eta^3\text{-TMPP})(\eta^3\text{-TMPP-}O)]^{2+}$ (**5**) and $[Rh^{III}(\eta^3\text{-TMPP-}O)_2]^{1+}$ (**14**, **15**) may prove to be more reactive towards addition of small substrates to the metal center. Comprehensive studies of these systems are needed to establish the use of phosphino-alkoxide groups as ancillary ligands for late transition metal complexes.

List of References

1. (a) Mehrotra, R. C.; Agarwal, S. K.; Singh, Y. P. *Coord. Chem. Rev.* **1985**, *68*, 101. (b) Bryndza, H. E.; Tam, W. *Chem. Rev.* **1988**, *88*, 1163.

2. (a) Bryndza, H. E.; Calabrese, J. C.; Marsi, M.; Roe, D. C.; Tam, W.; Bercaw, J. E. *J. Am. Chem. Soc.* **1986**, *108*, 4805. (b) Bryndza, H. E.; Fong, L. K.; Paciello, R. A.; Tam, W.; Bercaw, J. E. *J. Am. Chem. Soc.* **1987**, *109*, 1444. (c) Bryndza, H. E.; Domeille, P. J.; Tam. W.; Fong, L. K.; Paciello, R. A.; Bercaw, J. E. *Polyhedron* **1988**, *7*, 1441. (d) Hartwig, J. F.; Andersen, R. A.; Bergman, R. G. *Organometallics* **1991**, *10*, 1875.

3. For leading references see (a) Loren. S. D.; Campion, B. K.; Heyn, R. W.; Tilley, T. D.; Bursten, B. E.; Luth, K. W. *J. Am. Chem. Soc.* **1989**, *111*, 4712 and references therein. (b) Glueck, D. S.; Newman-Winslow, L. J.; Bergman, R. G. *Organometallics* **1991**, *10*, 1462. (c) Hartwig, J. F.; Andersen, R. A.; Bergman, R. G. *J. Organomet. Chem.* **1990**, *394*, 417. (d) Kegley, S. E.; Schaverian, C. J.; Freudenberger, J. H.; Bergman, R. G. *J. Am. Chem. Soc.* **1987**, *109*, 6563.

4. (a) Empsall, H. D.; Hyde, E. M.; Jones, C. E.; Shaw, B. L. *J. Chem. Soc., Dalton Trans.* 1974, 1980. (b) Mason, R.; Thomas, K. M.; Empsall, H. D.; Fletcher, S. R.; Heys, P. N.; Hyde, E. M. Jones, C. E; Shaw, B. L. *J. Chem. Soc., Chem. Comm.* 1974, 612. (c) Empsall, H. D.; Hyde, E. M.; Shaw, R. L. *J. Chem. Soc., Dalton Trans.* **1975**, 1690. (d) Empsall, H. D.; Heys, P. N.; McDonald, W. S.; Norton, M. C.; Shaw, B. L. *J. Chem. Soc., Dalton Trans.* **1978**, 1119.

5. (a) Dunbar, K. R.; Quillevéré, A. Inorg. Chem. submitted for publication. (b) Quillevéré, A. Ph. D. Dissertation, Michigan State University, 1992.

6. (a) Chen, S. J.; Dunbar, K. R. Inorg. Chem. 1991, 30, 2018. (b) Chen, S. J.; Dunbar, K. R. Inorg. Chem. 1990, 29, 588. (c) Dunbar, K. R.; Saharan, V.; Matonic, J. M. manuscript in preparation.

7. Gray, H. B.; Hendrickson, D. N.; Sohn, Y. S. *Inorg. Chem.* **1971**, *10*, 1559.

8. (a) Wayland, B. B.; Sherry, A. E. J. Am. Chem. Soc. 1989, 111, 5010. (b) Wayland, B. B.; Sherry, A. E.; Poszmik, G.; Bunn, A. G. J. Am. Chem. Soc. 1992, 114, 1673.

CHAPTER VIII

CHEMISTRY OF TRIS(2,4,6-TRIMETHOXYPHENYL)PHOSPHINE WITH RHODIUM (I) AND IRIDIUM (I) OLEFIN COMPLEXES

1. Introduction

In chapter III, we demonstrated that it was possible to prepare stable Rh(II) TMPP complexes from the solvated dinuclear precursor $[Rh_2(MeCN)_{10}][BF_4]_4$. In spite of this success, we were interested in synthesizing complexes of the general formula $[Rh(TMPP)_2]^{n+}$ (n= 1, 2, 3) from more conventional starting materials. The development of such synthetic strategies is particularly important for the isolation of homoleptic Ir/TMPP complexes, since the analogous solvated dinuclear Ir complex is unknown. Others have established that Rh(II) and Ir(II) phosphine complexes can be prepared by reaction of M(III) trihalides with excess phosphine in alcohol.[1] These conditions, however, are unsuitable for the preparation of $[M(TMPP)_2]^{n+}$ (n= 1, 2, 3), because of the susceptibility of these species to dealkylation. An alternative approach is to begin with partially solvated Rh(I) and Ir(I) olefin complexes which are prepared *in situ* by halide abstraction from the corresponding halide bridged dinuclear metal olefin complexes.[2a] Such systems have proven to be good precursors for a variety of group 8 metal phosphine complexes.[2] We set out to adapt this methodology to the preparation of Rh(I) and Ir(I) complexes of type $[M^I(TMPP)_2]^{1+}$. This chapter describes our efforts to prepare homoleptic TMPP complexes using Rh(I) and Ir(I) olefin complexes. In addition, the synthesis and characterization of the iridium dicarbonyl complex $[Ir(TMPP)_2(CO)_2][BF_4]$ is presented.

2. Experimental

A. Synthesis

All reactions were carried out under an argon atmosphere by the use of standard Schlenk-line techniques unless otherwise stated. TMPP (**1**) was

prepared as described in chapter II. The starting material, $[Ir(cod)Cl]_2$, was prepared from $IrCl_3 \cdot xH_2O$ using a standard literature procedure.[3] $[Rh(C_2H_4)_2Cl]_2$ was prepared according to a literature procedure.[4] $[Rh(cod)Cl]_2$ (Strem) and $NOBF_4$ (Strem) were obtained from commercial sources and used as received. The oxidizing agent, $[(p\text{-}BrC_6H_4)N][BF_4]$, was prepared by oxidation of the amine, $(p\text{-}BrC_6H_4)N$, with I_2 in the presence of Ag^+ following a modification of the procedure described by Bell *et al.*[5]

(1) Preparation of [Rh(cod)(η^2-TMPP)][BF_4] (16)

To a mixture of $[Rh(cod)Cl]_2$ (0.200 g, 0.406 mmol) and $AgBF_4$ (0.158 g, 0.812 mmol) was added 5 mL of THF. The resulting yellow suspension was stirred for 5 min before being filtered through a Celite plug into a 100 mL 3-necked flask equipped with an addition funnel containing a solution of TMPP (0.432 g, 0.811 mmol) in 15 mL of THF. The yellow solution was then cooled to approximately - 40°C with a dry ice / MeCN slush. The THF solution of TMPP was carefully added dropwise to the chilled solution over a period of 30 min. The reaction was stirred for an additional hour at -40°C, during which time a yellow solid separated from solution. Additional product was obtained from the solution by slow addition of diethyl ether (50 mL) while the solution was being stirred. The cold suspension was filtered in air and the yellow solid was washed with several portions of diethyl ether (4 x 10 mL) and dried under reduced pressure for 1-2 h; yield 0.574 g (85%). *Anal.* Calcd for $C_{35}H_{45}O_9F_4BPRh$: C, 50.62; H, 5.46. Found: C, 50.16; H, 5.58. ^1H NMR (CD_2Cl_2) δ, ppm: 3.68 (s, 36H, *o*-OCH_3), 3.84 (s, 18H, *p*-OCH_3), 6.14 (d, $^4J_{P\text{-}H}$ = 3.6 Hz, 12H, *m*-H), 1.80 (br, cod), 2.36 (br, cod). ^{31}P NMR (CD_2Cl_2) δ, ppm: + 1.4 (d, $^1J_{Rh\text{-}P}$ = 137.3 Hz). Cyclic voltammogram (0.2 M $TBABF_4$ / CH_2Cl_2, vs Ag/AgCl): $E_1(p,a)$ = + 0.60 V, $E_2(p,a)$ = + 1.16 V, $E_{p,c}$ = + 0.92 V. Mass spectrum (FAB, 3-nitrobenzyl alcohol) m/z: 742 (Rh(cod)(η^2-TMPP)$^+$).

(2) Preparation of Rh(cod)(η^2-TMPP-*O*) (17)

A solution of [Rh(cod)(η^2-TMPP)][BF_4] (**16**) (0.200 g, 0.240 mmol) and TMPP (0.128 g, 0.240 mmol) in 5 mL of MeCN was stirred at r. t. for 12 h. The solvent was removed under vacuum to yield a pale yellow residue. The yellow product was extracted by addition of 10 mL of Et_2O and a minimal amount of THF (an amount sufficient to dissolve the yellow solid completely). The solution was filtered to remove the [TMPP-CH_3][BF_4] by-product. The solvent was then removed under vacuum to produce a yellow powder; yield, 0.142 g (81%). ^{1}H NMR (CD_2Cl_2) δ, ppm: -OCH_3, 3.35 (s, 3H), 3.55 (s, 12H), 3.68 (s, 3H), 3.80 (s, 6H); *m*-H, 5.45 (t, 1H), 5.72 (dd, 1H), 6.04 (d, $^4J_{P\text{-}H}$ = 3.3 Hz, 4H); cod, 1.86 (br), 2.38 (br), 3.38 (br), 4.91 (br). ^{31}P NMR (CD_2Cl_2) δ, ppm: + 8.0 (d, $^1J_{Rh\text{-}P}$ = 157.2 Hz). Mass spectrum (FAB, ONPO) m/z: 728 (Rh(cod)(η^2-TMPP-*O*)$^+$).

(3) Reaction of [Rh(C_2H_4)$_2$Cl]$_2$ with TMPP

A solution of TMPP (0.548 g, 1.03 mmol) in 10 mL of MeCN was added dropwise to a cold suspension (0°C) of [Rh(C_2H_4)$_2$Cl]$_2$ (0.100 g, 0.257 mmol) and KBF_4 (0.064 g, 0.514 mmol). After the addition of the phosphine was complete, a slight vacuum was applied periodically to induce loss of ethylene. The reaction was allowed to warm slowly to r. t. After 2 h of stirring, the solvent was removed under reduced pressure. The resulting residue was dissolved in CH_2Cl_2 (10 mL) and filtered through a Celite plug to remove undissolved KCl. The filtrate was evaporated to a solid under reduced pressure which was washed with diethyl ether (2 x 10 mL) and dried *in vacuo*. ^{1}H and ^{31}P NMR spectroscopy showed that the solid was comprised of a mixture of [TMPP-CH_3]$^+$ and [TMPP-CH_2Cl]$^+$ together with a Rh species similar to the species observed upon reduction of [Rh(η^3-TMPP)$_2$][BF_4]$_2$ (**3**) with cobaltocene.

(4) Preparation of Ir(cod)(η^2-TMPP-*O*) (18)

To a solution of $[Ir(cod)Cl]_2$ (0.150 g, 0.223 mmol) and KBF_4 (0.056 g, 0.446 mmol) at 0°C was added dropwise to a solution of TMPP (0.475 g, 0.892 mmol) in 10 mL of MeCN. The solution color gradually converted from yellow to orange as the reaction was allowed to warm to r. t. After stirring for 2 h, the solvent was removed under vacuum to yield an orange residue. The solid was taken up with 10 mL of CH_2Cl_2 and filtered through a Celite plug to remove the KCl by-product. The Celite plug was further washed with 5 mL of CH_2Cl_2 to ensure complete transfer of the product. The volume of the solution was reduced to ~ 5 mL, and diethyl ether (20 mL) was slowly added while the solution was being stirred. The resulting yellow/white precipitate was removed by filtration and the orange filtrate was concentrated to approximately 5 mL. To the orange solution was added 20 mL of hexanes. The volume was again concentrated to 3-5 mL resulting in the formation an orange precipitate. The solid was filtered in air, washed with hexanes (2 x 10 mL), and dried under reduced pressure; yield, 0.302 g (83%). ^1H NMR (CD_3CN) δ, ppm: -OCH_3, 3.36 (s, 3H), 3.49 (s, 12H), 3.68 (s, 3H), 3.79 (s, 6H); *m*-H, 5.55 (t, 1H), 5.77 (dd, 1H), 6.09 (d, $^4J_{P\text{-}H}$ = 3.6 Hz, 4H).

(5) Preparation of $[Ir(TMPP)_2(CO)_2][BF_4]$ (19)

A 100 mL 3-necked flask, equipped with an addition funnel, gas inlet and a septum, was charged with $[Ir(cod)Cl]_2$ (0.200 g 0.30 mmol), $NaBF_4$ (0.065 g, 0.60 mmol) and MeCN (5 mL). The resulting solution was cooled to 0°C and gently purged with CO. A solution of TMPP (0.634 g, 1.20 mmol) in 10 mL of MeCN was added dropwise to the CO saturated solution over a period of ten minutes. After the addition was complete, the CO purge was discontinued, and the reaction was stirred under a CO atmosphere at 0°C. After 2 h, the solvent was removed under vacuum. The resulting residue was

dissolved in 5 mL of CH_2Cl_2 and filtered through a Celite plug. The Celite was further washed with 5 mL of CH_2Cl_2. The orange solution was concentrated to 4-6 mL and 35 mL of Et_2O was added slowly. The resulting bright orange precipitate was filtered in air; washed with 4 x 10 mL of diethyl ether and dried *in vacuo*; yield 0.666 g (80%). *Anal.* Calcd for $C_{57}H_{68}O_{20}F_4BCl_2P_2Rh$: C, 46.10; H, 4.62. Found: C, 46.75; H, 4.88. IR (CH_2Cl_2) cm^{-1}: ν(CO), 1993 (vs), 1946 (w). IR (Nujol, CsI) cm^{-1}: ν(CO), 1987 (s), 1942 (m). ^1H NMR (CD_3CN) δ, ppm: 3.38 (s, 36H, *o*-OCH_3), 3.77 (s, 18H, *p*-OCH_3), 6.06 (t, $^4J_{P-H}$ = 2.0 Hz, 12H, *m*-H). ^{31}P NMR ($CDCl_3$) δ, ppm: - 39.0 (s). Electronic absorption spectrum (CH_2Cl_2) λ_{max}, nm (ε): 547 (449), 490 (2300), 455 (sh) 386 (4510) 315 (sh). Cyclic voltammogram (0.1 M $TBABF_4$ / CH_2Cl_2, vs Ag/AgCl): $E_{p,a}$ = + 0.82 V, $E_1(p,c)$ = + 0.46 V, $E_2(p,c)$ = - 0.81 V.

(6) Reaction of TMPP with $[Ir(TMPP)_2(CO)_2][BF_4]$ (19)

A quantity of $[Ir(TMPP)_2(CO)_2][BF_4]$ (**19**) (0.100 g, 0.071 mmol) and TMPP (0.038 g, 0.071 mmol) was dissolved in 5 mL of MeCN. The orange solution was stirred at r. t. for 12 h. An infrared spectrum of the solution revealed that no reaction had occurred during this period. A condenser was connected to the flask and the solution was refluxed for 24 h during which time the solution color turned from orange to yellow. An IR spectrum of the solution was obtained after this period of time: IR (CH_3CN) cm^{-1}: ν(CO), 2051 (s), 1973 (s),1899 (w). The reaction was refluxed for an additional 24 h, after which time a small aliquot was removed and an IR spectrum was measured: IR (CH_3CN) cm^{-1}: ν(CO), 1998 (w, br) 2018 (w, br). The solvent was then removed under vacuum and the solid was redissolved in a 2:1 mixture of THF and diethyl ether. The yellow solution was filtered and pumped to dryness. The resulting solid was washed with diethyl ether (2 x 5 mL) and dried *in*

vacuo. The ^1H NMR spectrum of the solid in CD_3CN revealed the presence of $[TMPP\text{-}CH_3]^+$, but no other resonances were easily discernible.

(7) Oxidation of $[Ir(TMPP)_2(CO)_2][BF_4]$ (19)

(i) Chemical oxidation with $NOBF_4$. In a typical reaction, a solution of $[Ir(TMPP)_2(CO)_2][BF_4]$ (**19**) (0.100 g, 0.071 mmol) and $NOBF_4$ (0.009 g, 0.0.71 mmol) in 5 mL of MeCN was stirred at r. t. In the first minute a vacuum was applied to remove $NO_{(g)}$ or CO that may evolve from the reaction. Within several minutes, the solution color changed from orange to orange-red. An aliquot was removed after 30 min and its IR spectrum was recorded. IR (CH_3CN) cm^{-1}: ν(CO), 2079 (s), 2109 (w), 2148 (w), 2029 (vw). The reaction was stirred overnight, after which time the solution was pump to dryness, washed with 10 mL of Et_2O and dried *in vacuo*; yield, 0.053 g of crude product.

(ii) Chemical Oxidation with $[(p\text{-}BrC_6H_4)_3N][BF_4]$. In a typical reaction, a mixture of $[Ir(TMPP)_2(CO)_2][BF_4]$ (**19**) (0.100 g, 0.071 mmol) and $[(p\text{-}BrC_6H_4)_3N][BF_4]$ (0.041 g, 0.071 mmol) was dissolved in 5 mL of MeCN. The solution immediately became dark red/orange in color. The reaction was periodically subjected to a vacuum to help remove evolved CO from the solution. Within 30 min, the solution color began to lighten and an IR spectrum of the solution showed the presence of unreacted **19** together with several other ν(CO) bands indicative of a new compound or compounds; IR (CH_3CN) cm^{-1}: ν(CO), 2079 (s), 2110 (m), 2148 (m); **19**, 1991 (s), 1942 (w). The reaction was stirred overnight during which time the solution color became pale green and a pale precipitate had settled out. An aliquot of the green solution was removed and its IR spectrum was recorded; IR (CH_3CN) cm^{-1}: ν(CO), 2079 (vs), 2027 (w), 2148 (vw), 2110 (vw), 2046 (vw), 2009 (w). The solution was filtered and evaporated to a residue under reduced pressure

to yield a pale yellow/green solid. ^{1}H NMR (CD_3CN) δ, ppm: -OCH_3, 3.46 (s), 3.82 (s); *m*-H, 6.20 (t, $^4J_{P-H}$ = 2.2 Hz).

(iii) Bulk Electrolysis. Bulk electrolysis of $[Ir(TMPP)_2(CO)_2][BF_4]$ (**19**) was performed in a four-compartment electrolysis cell separated by coarse porosity sintered glass frits (Figure 35). A quantity of $[Ir(TMPP)_2(CO)_2][BF_4]$ (**19**) (0.050 g, 0.036 mmol) was added to a degassed CH_2Cl_2 solution of 0.05 M $[(Bu^n)_4N][BF_4]$ in the working compartment of the cell. The solution was electrolyzed at a potential of E = + 1.0 V using a Pt gauze working electrode. After 1 h, the solution color had changed from orange to yellow. A small aliquot of the solution was removed and its IR spectrum was recorded. IR (CH_2Cl_2) cm^{-1}: ν(CO), 2075 (m). The solution was then transferred via syringe into a Schlenk flask under Ar and was carefully layered with Et_2O (5 mL). After diffusion was complete, the remaining yellow solution was decanted away from the $[(Bu^n)_4N][BF_4]$ salt that had precipitated. The solvent was removed under vacuum to give a pale yellow solid. ^{1}H NMR (CD_3CN) δ, ppm: -OCH_3, 3.57 (s), 3.86 (s); *m*-H, 6.19 (t, $^4J_{P-H}$ = 1.8 Hz).

(8) Reaction of $[Ir(TMPP)_2(CO)_2][BF_4]$ (19) with Iodine

An amount of $[Ir(TMPP)_2(CO)_2][BF_4]$ (**19**) (0.050 g, 0.036 mmol) in 5 mL of MeCN was stirred with one equivalent of I_2 (0.009 g, 0.036 mmol). and $NaBF_4$ (0.004 g, 0.036). After stirring for 3 h, the solution color became yellow. A small aliquot was removed and its IR spectrum was recorded: IR (CH_3CN) cm^{-1}: ν(CO), 2148 (vw), 2073 (m), 2055 (s). The solution was pumped to dryness and dissolved in 5 mL of CH_2Cl_2. The yellow solution was then filtered through a Celite plug to remove the remaining undissolved sodium salt. The filtrate was evaporated under reduced pressure and dried under vacuum.

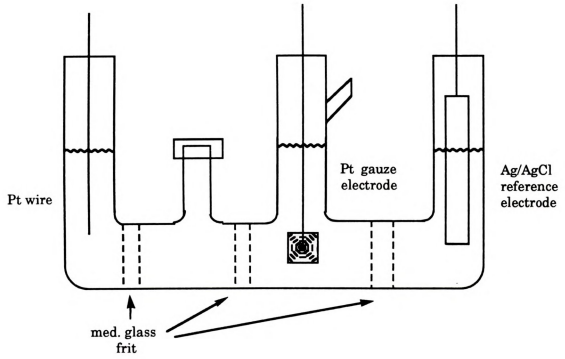

Figure 35. Schematic drawing of the electrolysis cell used in the electrochemical oxidation of $[Ir^{I}(TMPP)_2(CO)_2]^{1+}$ (**19**).

B. X-ray Crystallography

The structure of $[Ir(TMPP)_2(CO)_2][BF_4]$ (**19**) • CH_2Cl_2 was determined by application of general procedures that have been fully described elsewhere.[6] Geometric and intensity data were collected on a Rigaku AFC6S diffractometer with graphite-monochromated MoKα ($\lambda_{\bar{\alpha}}$ = 0.71069 Å) radiation and were corrected for Lorentz and polarization effects. Relevent crystallographic parameters for **19** are summarized in Table 15. All calculations were performed with the use of VAX computers on a cluster network within the Department of Chemistry at Michigan State University using the Texsan software package of the Molecular Structure Corporation.[7]

(1) $[Ir(TMPP)_2(CO)_2][BF_4]$ (19) • CH_2Cl_2

(i) Data Collection and Reduction. Single crystals of **19** suitable for X-ray analysis were obtained as a CH_2Cl_2 solvate from careful layering of Et_2O on a CH_2Cl_2 solution of **19**. A regular block shaped crystal with approximate dimensions, 0.23 x 0.34 x 0.15 mm^3, was selected and secured onto the tip of a glass fiber with epoxy cement. Least-squares refinement of 24 orientation reflections in the range $20 < 2\theta < 33°$ resulted in cell constants consistent with a triclinic cell. Intensity measurements were performed at 23 ± 3°C using the ω-2θ scan technique. Reflections with $I < 10\sigma(I)$ were re-scanned a maximum of two re-scans and the counts were accumulated to assure good counting statistics. Routine measurement of three check reflections at regular intervals throughout data collection revealed that the crystal had experienced 57% loss in diffraction intensity. A linear decay correction was applied to compensate for the observed loss. In addition, an empirical absorption correction was applied based on azimuthal scans of 3 reflections with Eulerian angle χ near 90° resulting in maximum and

Table 15. Summary of crystallographic data for $[Ir^{I}(TMPP)_2(CO)_2][BF_4] \cdot CH_2Cl_2$ (**19**)

Formula	$IrP_2O_{20}C_{57}H_{68}BF_4Cl_2$
Formula weight	1592.32
Space group	P-1
a, Å	13.512(2)
b, Å	18.348(3)
c, Å	13.358(2)
α, deg	97.26(1)
β, deg	90.55(1)
γ, deg	95.02(1)
V, Å^3	3272(2)
Z	2
d_{calc}, g/cm^3	1.616
μ (Mo Kα), cm^{-1}	41.73
Temperature, °C	23±2 °C
R^a	0.051
$R_w{}^b$	0.065
Quality-of-fit indicator^c	2.19

$^aR = \Sigma \; | \; |F_o| - |F_c| \; | / \Sigma |F_o|$

$^bR_w = [\Sigma w(|F_o| - |F_c|)^2 / \Sigma w |F_o|^2]^{1/2}$; $w = 1/\sigma^2(|F_o|)$

^{c}Quality-of-fit = $[\Sigma w(|F_o| - |F_c|)^2 / (N_{obs}\text{-Nparameters})]^{1/2}$

minimum transmission factors of 1.00 and 0.79. A total of 10,134 data were collected in the range of $4 \leq 2\theta \leq 47°$. After averaging equivalent reflections (R_{merge} = 3.4%), there remained 9652 unique data of which 6165 had $F_o^2 \geq 3\sigma(F_o)^2$.

(ii) Structure Solution and Refinement. The position of the Ir atom was located directly from a Patterson Fourier synthesis. The remaining non-hydrogen atoms were located by application of the program DIRDIF followed by several alternating least-squares cycles and Fourier maps.[8] Due to a disorder resulting from several random orientations, the $[BF_4]^-$ anion was modeled as an ideal tetrahedron with fixed bond distance and angles. With the exception of the $[BF_4]^-$ anion, all non-hydrogen atoms were refined with anisotropic thermal parameters. Hydrogen atoms were included in the structure factor calculation as fixed contributors at calculated positions and were not refined. In the end, final least-squares refinement of 731 parameters gave residuals of R = 0.051 and R_w = 0.065 and a quality-of-fit index of 2.19. Not unexpectedly, the highest remaining peak in the final Fourier difference map was 1.19 $e^-/Å^3$ and was associated with the disordered $[BF_4]^-$ anion.

3. Results

A. Synthesis and Characterization of [M(cod)(η^2-TMPP)]$^{1+}$ (M = Rh) and M(cod)(η^2-TMPP-*O*) (M = Rh, Ir)

One equivalent of TMPP readily reacts with the partially solvated Rh olefin complex $[Rh(cod)(solvent)_2]^+$, which is formed *in situ* by halide abstraction using Ag^+, to produce $[Rh(cod)(\eta^2\text{-TMPP})][BF_4]$ (**16**) (eq 20). The $[BF_4]^-$ salt of the cation is relatively insoluble in THF, and as a result, the

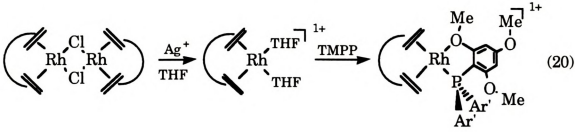

(20)

product is isolated as a fine yellow precipitate in high yield from THF. Although it is anticipated that the TMPP ligand participates in an η^2-bonding mode to the metal, thereby filling the vacant fourth coordination site, the ^1H NMR spectrum of **16** in CD_2Cl_2 exhibits a highly symmetrical pattern of resonances in which each phenyl ring is equivalent. Clearly, the phosphine is participating in a dynamic process that rapidly exchanges each of the non-coordinated phenyl rings with the coordinated ring. A similar fluxional process was also noted for (η^3-TMPP)$Mo(CO)_3$ and [Rh(η^2-TMPP)(TMPP)$_2$(CO)][BF_4] (**7**).[9] Furthermore, the coordinated diene is also apparently participating in a dynamic process as evidenced by the broad appearance of the ^1H NMR resonances for the cod ligand. The ^{31}P NMR spectrum exhibits the expected doublet at δ = + 1.4 ppm (d, $^1J_{Rh\text{-}P}$ = 137.3 Hz) as a result of one phosphorus nucleus experiencing ^{103}Rh-^{31}P coupling.

In an attempt to displace the coordinated olefin to form the homoleptic Rh(I) TMPP complex analogous to **3**, [Rh(cod)(η^2-TMPP)][BF_4] (**16**) was deliberately reacted with a second equivalent of TMPP. However, instead of substituting the diene, the phosphine behaved as a nucleophile resulting in the dealkylation of a coordinated methoxy group to give [TMPP-CH_3]$^+$ (eq 21) and the dealkylated complex, Rh(cod)(η^2-TMPP-*O*) (**17**), which was isolated from the phosphonium salt by extraction with a mixture of diethyl ether and a minimal amount of THF. Quite unexpectedly, **17** is relatively soluble in

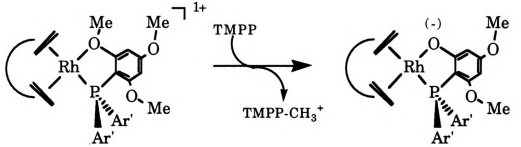

(21)

diethyl ether; this is presumably a consequence of its charge neutrality. Crystalline solids may be obtained by careful layering of hexanes onto CH_2Cl_2 solutions of **17**.

An infrared spectrum of Rh(cod)(η^2-TMPP-*O*) (**17**) shows the characteristic bands for coordinated TMPP and confirms the absence of the $[BF_4]^-$ anion consistent with the neutral formulation of **17**. A FAB mass spectrum of the compound exhibits a parent ion peak at 728 m/z in accord with the empirical formula $RhPC_{34}O_9H_{42}$. The ^1H NMR spectrum of Rh^I(cod)(η^2-TMPP-*O*) (**17**) in CD_2Cl_2 reveals a relatively symmetric resonance pattern. As was observed for the parent compound, the cyclooctadiene resonances are broad, indicating that a dynamic process is occurring in solution. The most striking feature of the spectrum is the appearance of the resonances corresponding to *meta*-protons on the phenyl rings of TMPP. The two multiplets that appear at δ = 5.45 and 5.72 ppm are assigned to the proximal and distal meta-protons of the chelating phenoxide ring. The observed coupling pattern arises from coupling of these magnetically distinct resonances to the phosphorus nucleus and to each other. The meta-protons of the two remaining phenyl rings are magnetically equivalent and appear as doublets at δ = 6.04 ppm ($^4J_{P\text{-}H}$ = 3.3 Hz). Evidently, there is still free rotation about the P-C bonds of the non-

coordinated phenyl rings, inspite of the fact that one phenyl ring is bonded to the metal. Of further interest is the ^{31}P NMR spectral properties of **17** in CD_2Cl_2; the ^{31}P NMR spectrum exhibits a doublet at δ = - 8.0 ppm ($^1J_{Rh\text{-}P}$ = 157.2 Hz), which is shifted upfield relative to **16**. Typically the formation of a five membered chelate ring involving phosphorus results in a significant downfield shift of the phosphorus resonance.[10] Apparently, however, in this case the chelation affect is more than compensated for by the formation ofa more strongly donating phenoxide interaction, which increases the electron density at the metal center, thereby further shielding the phosphorus nucleus. The net effect is an upfield shift of the phosphorus resonance.

The analogous iridium complex, Ir(cod)(η^2-TMPP-*O*) (**18**) was prepared by reaction of $[Ir(cod)Cl]_2$ with excess TMPP in the presence of KBF_4. Although it was not isolated, $[Ir(cod)(\eta^2\text{-TMPP})]^+$ is believed to be formed in the initial stages of the reaction. This species then undergoes dealkylation in the presence of additional phosphine to yield **18**. Compound **18** exhibits essentially the same solubility and stability properties as the rhodium complex Rh(cod)(η^2-TMPP-*O*) (**17**). The ^1H NMR spectrum of Ir(cod)(η^2-TMPP-*O*) (**18**) in CD_3CN exhibits three resonances at δ = 5.55 ppm (t), 5.77 ppm (dd), and 6.09 ppm (d, $^4J_{P\text{-}H}$ = 3.6 Hz) in a ratio of 1 : 1 : 4 corresponding to the meta-protons of the phenyl rings. Just as was observed for **17**, the spectrum indicates that one ring is tightly bonded to the metal leading to the observation of proximal and distal resonances for the two *meta*-protons on that ring. The remaining two phenyl rings, however, freely rotate about the P-C bond.

B. Synthesis and Spectroscopic Characterization of $[Ir(TMPP)_2(CO)_2][BF_4]$ (19)

$[Ir(TMPP)_2(CO)_2][BF_4]$ (**19**) was synthesized in manner similar to the method used for $[Rh(TMPP)_2(CO)]^+$ (eq 22). As in the rhodium chemistry, coordinated diene may be displaced from the iridium complex by CO in the presence of TMPP to give $[Ir(TMPP)_2(CO)_2]^+$ (**19**). A solution of 4 equivalents of TMPP in MeCN was added dropwise to a MeCN solution of $[Ir(cod)Cl]_2$ in the presence of MBF_4 (M = Ag^+, Na^+, or K^+). The addition was performed under an atmosphere of CO at 0°C with yields typically in the range 80-85%. A drastic reduction in yield was noted when THF was

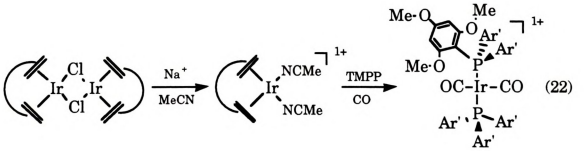

(22)

used as a solvent instead of MeCN, unlike the synthesis of $[Rh(TMPP)_2CO]^{1+}$ (**7**) which works very well with THF as a solvent. The choice of metathesis reagent apparently does not effect the yield, as Ag^+, Na^+, and K^+ have produced comparable yields fo **19**.

If the reaction is not purged with CO, the neutral complex Ir(cod)(TMPP-*O*) (**18**) is formed instead of **19**. As was observed in the analogous Rh system, CO is required to displace the cod. Otherwise, the second equivalent of TMPP acts as a nucleophile and dealkylates the coordinated phosphine instead of displacing the diene. However, unlike $[Rh(TMPP)_2(CO)_2]^{1+}$ (**6**), CO does not reversibly dissociate from **19** to form an

iridium monocarbonyl species. Only under more forcing thermal and photolytic conditions is the loss of CO apparent. Unfortunately, such conditions lead to a mixture of intractable products.

The infrared spectrum of $[Ir(TMPP)_2(CO)_2][BF_4]$ (**19**) in CH_2Cl_2 exhibits two carbonyl stretching vibrations at $\nu(CO) = 1993\ cm^{-1}$ vs and 1946 cm^{-1} (w). In the solid state these bands shift slightly and change intensity to $\nu(CO) = 1987\ cm^{-1}$ (s) and 1942 cm^{-1} (m). The ^1H NMR spectrum of **19** is consistent with a *trans* disposition of two magnetically equivalent phosphine ligands with resonances appearing at $\delta = 3.38$ (s, 36 H, *o*-OMe), 3.77 (s, 18 H, *p*-OMe), 6.06 (t, $^4J_{P-H}$=2.0 hz, 12H, *m*-H). The ^{31}P NMR spectrum of **19** ($CDCl_3$) exhibits a single resonance for both phosphines at $\delta = -39$ ppm. The cyclic voltammogram of $[Ir(TMPP)_2(CO)_2][BF_4]$ in 0.1 M $TBABF_4/CH_2Cl_2$ shows an irreversible oxidation at $E_{p,a}$= +0.82 V. Coupled with this oxidation are two chemical waves at E = +0.46 V and -0.81 V.

Of further interest is the observation that $[Ir(TMPP)_2(CO)_2][BF_4]$ (**19**) is emissive in the solid state at room temperature. Exposure of solid samples of **19** to long wave ultraviolet radiation produces a brilliant orange luminescence. Emission spectra have been previously found for other square planar Rh(I) and Ir(I) complexes.[11] Typically, the emissive state results from MLCT from the metal d_z^2 orbital to a low-lying ligand orbital of π symmetry. When the ligands are π-acceptors, such as CO or CN^-, the MLCT is interpreted as excitation from the metal d_z^2 orbital to the π^* orbital of the ligand.[11g] By analogy, we expect a similar charge transfer process to be responsible for the emissive properties of **19**. In contrast to the solid state behavior, solutions of $[Ir(TMPP)_2(CO)_2][BF_4]$ (**19**) do not appear to be luminescent at room temperature. This is in agreement with other square planar d^8 complexes.

C. Crystal Structure of $[Ir(TMPP)_2(CO)_2][BF_4]$ (19)

The identity of the product as $[Ir(TMPP)_2(CO)_2][BF_4]$ was confirmed by X-ray crystallography. An ORTEP diagram of the molecular cation is presented in Figure 36. A listing of pertinent bond distance and angles are found in Table 16. As expected, the complex is square planar with the phosphines situated *trans* to each other. Not surprisingly, the phosphine ligands are monodentate and there are no interacting methoxy groups along the axial direction (r(Ir-O) > 3.0 Å). Although the phosphines are magnetically equivalent in solution, they are not crystallographically identical, as the iridium atom does not lie on a crystallographic symmetry element. The Ir-P distances, 2.338(3) Å and 2.345(3) Å, are only slightly longer than those in the analogous Rh complex $[Rh(TMPP)_2(CO)_2][BF_4]$ (**6**) (2.327(1) Å and 2.332(1) Å). There are no distortions evident in the structure, as the angles between the ligands are nearly ideal. A packing diagram shows that the square planar Ir cations stack along the z-axis, but the closest distance between iridium centers is over 10 Å. So it appears that the observed emission properties are associated with the ligands and do not arise from association of cations in the solid state.

D. Oxidation of $[Ir(TMPP)_2(CO)_2][BF_4]$

Bulk electrolysis of $[Ir(TMPP)_2(CO)_2][BF_4]$ in 0.05 M $TBABF_4$ / CH_2Cl_2 at a potential of +1.1 V for 1 hour gave a yellow solution that exhibited a carbonyl stretch at $\nu(CO) = 2075\ cm^{-1}$(m). The ^1H NMR spectrum of the solid in CD_2Cl_2 showed resonances due to $[(^nBu)_4N]^+$ in addition to a new TMPP containing species: δ, ppm; 3.57 (s, broad), 3.86 (s), 6.19 (t). The triplet at 6.19 is indicative of a *trans* diphosphine complex and the breadth of the methoxy resonances suggest that some fluxionality is occurring.

Chemical oxidation of $[Ir(TMPP)_2(CO)_2][BF_4]$ with $NOBF_4$ in MeCN

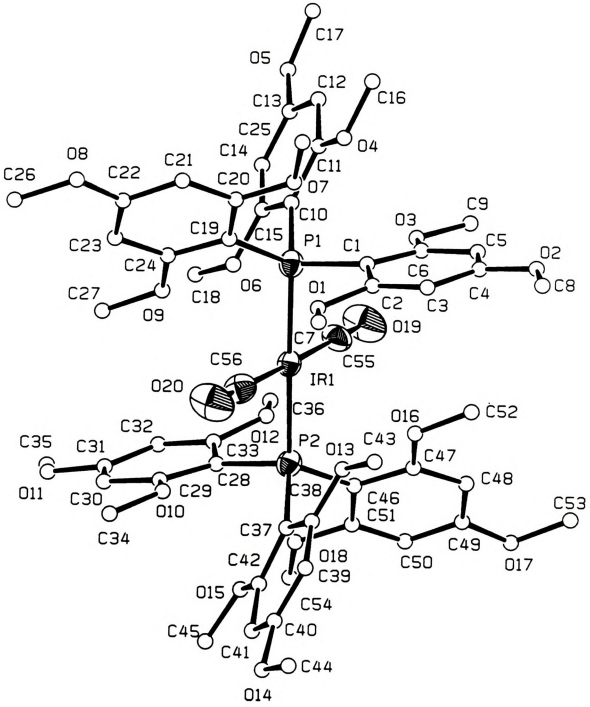

Figure 36. ORTEP representation of the molecular cation $[Ir^{I}(TMPP)_2(CO)_2]^{1+}$ (**19**).

Table 15. Selected bond distances (Å) and angles (deg) for $[Ir^{I}(TMPP)_2(CO)_2][BF_4] \cdot CH_2Cl_2$ (**19**).

Atom 1	Atom 2	bond distance
Ir(1)	P(1)	2.338(3)
Ir(1)	P(2)	2.345(3)
Ir(1)	C(55)	1.94(1)
Ir(1)	C(56)	1.89(1)
P(1)	C(1)	1.87(1)
P(1)	C(10)	1.84(1)
P(1)	C(19)	1.84(1)

Atom 1	Atom 2	Atom 3	bond angles
P(1)	Ir(1)	P(2)	178.4(1)
P(1)	Ir(1)	C(55)	90.0(4)
P(1)	Ir(1)	C(56)	90.4(4)
P(2)	Ir(1)	C(55)	88.4(4)
P(2)	Ir(1)	C(56)	91.2(4)
C(55)	Ir(1)	C(56)	177.8(6)
Ir(1)	P(1)	C(1)	100.5(4)
Ir(1)	P(1)	C(10)	115.8(4)
Ir(1)	P(1)	C(19)	118.8(4)

produced a red-orange solution. The infrared spectrum of the solution showed several bands at energies greater than 2000 cm^{-1}; these occur at 2079 cm^{-1} (s), 2148 cm^{-1} (w), 2109 cm^{-1} (w), 2029 cm^{-1} (vw). Presumably, the intense band at 2079 cm^{-1} corresponds to the same product formed in the bulk electrolysis experiment and is shifted due to solvent effects (MeCN versus CH_2Cl_2).

Oxidation of $[Ir(TMPP)_2(CO)_2][BF_4]$ (**19**) with the amminium salt $[(p\text{-}BrC_6H_4)_3N][BF_4]$ initially gave a deep blue solution that immediately became red-orange as the amminium salt was consumed. As in the other oxidation reactions of **19**, a vacuum was applied to help remove evolved CO from the solution. After a day of continual stirring the solution color changed from red-orange to green. An infrared spectrum of the green solution revealed the presence of a strong CO stretch at 2079 cm^{-1}. In addition to this stretch, several less intense bands were observed between 2009 cm^{-1} and 2148 cm^{-1}. An infrared spectrum of the solution taken during the orange stage shows not only the same bands, but also those corresponding to a significant amount of unreacted **19**, which implies that the reaction is not complete until the solution has become green. The ^1H NMR spectrum of the product (CD_3CN) shows three primary resonances at δ = 3.46 ppm (s), 3.82 ppm (s); *m*-H, 6.20 ppm (t, $^4J_{P\text{-}H}$ = 2.2 Hz). It is worth noting that the IR and NMR spectroscopic characteristics for the green product correspond to those observed for the compound prepared by bulk electrolysis and by chemical oxidation with NO^+.

Based on the aforementioned infrared and NMR spectral data, one can begin to draw several conclusions as to the identity of this oxidized product. The infrared spectrum of the oxidized product indicates that at least one CO ligand is still present. This is not surprising considering the large number of

Ir(III) carbonyl complexes that have been reported.[12] The shift of ν(CO) to higher energy is consistent with oxidation of the metal center which results in a decrease in the degree of π-back bonding present. Based on the sharp and unshifted natrure of the ^{1}H NMR spectrum, the product is diamagnetic, which is consistent an Ir(III) species. The triplet resonance observed for the meta protons indicates that the phosphines are situated *trans* to each other. The TMPP ligand resonances are magnetically equivalent and highly symmetric, consistent with either a monodentate bonding mode or a fluxional process that exchanges all potentially equivalent protons. A six coordinate complex, which one would expect if the compound is an Ir(III) species,

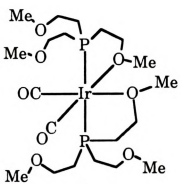

cis

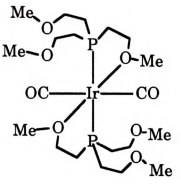

trans

requires that the phosphines are multidentate assuming no additional ligands have been added to the coordination sphere. If this is the case, the molecule must exhibit some fluxional behavior. Indeed, the slightly broadened appearance of the methoxy resonances indicates that an exchange process is operative. The infrared data combined with the NMR data suggest that the observed product is an Ir(III) dicarbonyl species containing either *cis* or *trans* carbonyl groups as shown below. Unfortunately, attempts to isolate pure crystalline samples have yielded only oily solids.

4. Discussion

The primary motivation for investigating the chemistry of TMPP with Rh(I) and Ir(I) olefin complexes was to develop efficient methods for preparing homoleptic TMPP complexes of rhodium and iridium. Others have found that compounds of the type $[M^{I}(diene)(solvent)_2]^{1+}$ are excellent precursors for a number of Rh(I) and Ir(I) phosphine complexes.[2] In the present study, TMPP easily displaces the coordinated solvent molecules to form $[Rh^{I}(cod)(\eta^2\text{-TMPP})]^{1+}$ (**1 6**). Addition of a second equivalent of phosphine, however, does not result in substitution of the olefin, but instead dealkylates the coordinated TMPP of **16** to produce Rh(cod)(η^2-TMPP-*O*) (**17**). The strong affinity of the metal for the olefin is further evident by the observation that **17** is inert with respect to substitution with additional TMPP. Reaction of **17** with excess TMPP under refluxing conditions produced only an intractable mixture of products. One possible solution to this problem would be to alter the nature of the coordinated olefin. Replacement of cod with an alkene may encourage dissociation in the absence of the chelate effect. Indeed, reaction of $[Rh(C_2H_5)_2Cl]_2$ with excess TMPP in the presence of KBF_4 led to the formation of the same product produced by cobaltocene reduction of $[Rh(\eta^3\text{-TMPP})_2][BF_4]_2$ (**3**). Although an analogous ethylene complex is not known for Ir, the corresponding cyclooctene complex $[Ir(C_8H_{14})_2Cl]_2$ could be used as a precursor to Ir-TMPP complexes.[13] Another approach to synthesizing compounds of the type M^{I}(TMPP)(TMPP-O) (M = Rh, Ir) is by hydrogenation the coordinated diene of **17** and **18** in a donating solvent followed by addition of TMPP. This method has proven effective in the formation of solvated metal phosphine complexes that are active hydrogenation catalysts.[14] A third possible route would be to use a non-olefin Rh(I) or Ir(I) precursor such as $M(acac)_2$.[15] Presumably, the

acetylacetonate ligand would be more susceptible to substitution than cyclooctadiene.

Although olefin-phosphine complexes are not novel, compounds **16 - 18** may be useful as synthetic building blocks for other Rh and Ir TMPP complexes. Removal of the diene by either simple substitution or through olefin hydrogenation could lead to the development of a new class of mixed ligand complexes that incorporate the advantages of TMPP with the added reactivity provided by other ligand sets. For example, it may be possible to prepare novel mixed phosphine/thiolate complexes with the general formula, $M^{III}(\eta^2\text{-TMPP})(\eta^2\text{-TMPP-}O)(SR)_2$ (M = Rh, Ir), by oxidative addition of alkyl disulfides to **17 - 18** in the presence of TMPP. As an additional point, many Rh and Ir olefin complexes serve as catalyst precursors.[14] The combination of a hard oxygen donor with a soft phosphorus donor may induce unusual catalytic properties. As a result, the potential application of these rhodium and iridium systems towards homogenous catalysis is currently under investigation.[16]

Previously, we found that $[Rh^I(TMPP)_2(CO)][BF_4]$ (**7**) may be chemically oxidized to yield the paramagnetic Rh(II) compound $[Rh(\eta^3\text{-}TMPP)_2][BF_4]_2$ (**3**). Oxidation of **7** yield an unstable Rh(II) carbonyl species that immediately undergoes dissociation. By analogy, we expected that oxidation of the iridium dicarbonyl complex **19** might yield an unstable Ir(II) dicarbonyl species that readily dissociates CO to form $[Ir^{II}(TMPP)_2]^{2+}$. Clearly, however, CO remains bonded to the metal as evidenced by IR spectroscopy. In any event, it is apparent that we may have reached a limitation of using a containing iridium carbonyl complex as a precursor to homoleptic Ir-TMPP species. Unlike the analogous chemistry of

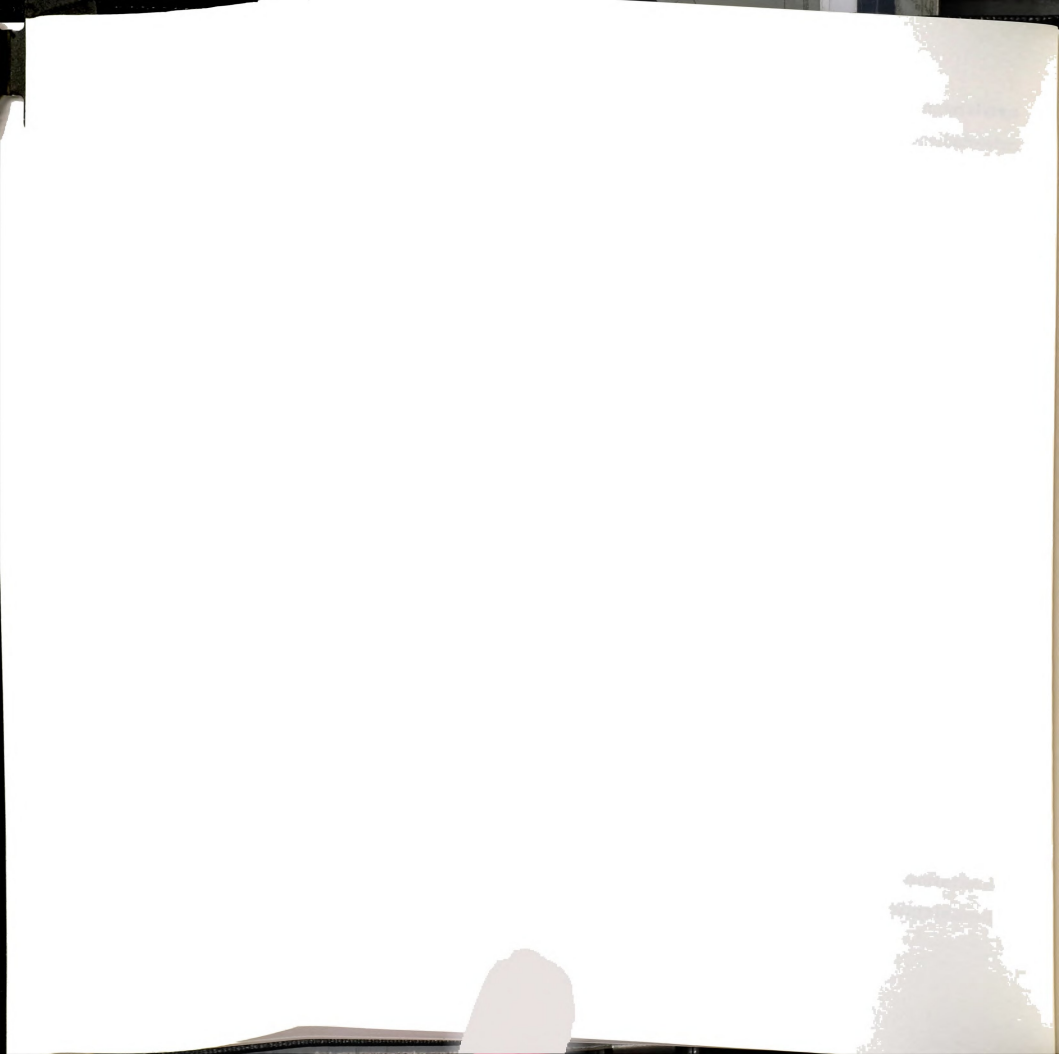

$[Rh(TMPP)_2(CO)_n]^{1+}$, CO is more tightly bound to iridium,[17] therefore the isolation of $[Ir^{II}(\eta^3\text{-}TMPP)_2]^{2+}$ may not be feasible using this approach.

List of References

1. (a) Bennett, M. A.; Lonstaff, P. A. *J. Am. Chem. Soc.*, **1969**,*91*, 6266. (b) Moers, F. G.; DeJong, J. A. M.; Beaumont, P. M. J. *J. Inorg. Nucl. Chem.* **1973**,*35*, 1915. (c) Masters, C.; Shaw, B. L. *J. Chem. Soc. (A)* **1971**, 3679. (d) Empsall, H. D.; Heys, P. N.; Shaw, B. L. *Transition Met. Chem.* **1978**, *3*, 165. (e) Empsall, H. D.; Hyde, E. M.; Pawson, D.; Shaw, B. L.; *J. Chem. Soc., Dalton Trans.* **1977**, 1292. (f) Mason, R.; Thomas, K. M.; Empasall, H. D.; Fletcher, S. R.; Heys, P. N.; Hyde, E. M. Jones, C. E; Shaw, B. L. *J. Chem. Soc., Chem. Comm.* **1974**, 612. (g) Empsall, H. D.; Hyde, E. M.; Shaw, R. L. *J. Chem. Soc., Dalton Trans.* **1975**, 1690. (h) Empsall, H. D.; Heys, P. N.; McDonald, W. S.; Norton, M. C.; Shaw, B. L. *J. Chem. Soc., Dalton Trans.* **1978**, 1119

2. (a) Schrock, R. R.; Osborn, J. A. *J. Am. Chem. Soc.* **1971**, *93*, 2397. (b) Shapley, J. R. Schrock, R. R. *J. Am. Chem. Soc.* **1969**,*91*, 2816. (c) Green, M.; Kuc, T. A.; Taylor, S. H. *J. Chem. Soc. (A)* **1971**, 2334. (d) Haines, L. M.; Singleton, E. *J. Chem. Soc., Dalton Trans.* **1972**, 1891. (e) Haines, L. M. *Inor. Nuc. Chem. Lett.* **1969**, *5*, 399. (f) Haines, L. M. *Inorg. Chem.* **1970**, 9, 1517.

3. Herde, J. L.; Lambert, J. C.; Senoff, S. V. *Inorg. Synth.* **1974**,*15*, 18.

4. Cramer, R. *Inorg. Synth.* **1974**,*15*, 14.

5. Bell, F. A.; Ledwith, A.; Sherrington, D. C. *J. Chem. Soc. (C)* **1969**, 2719.

6. (a) Bino, A.; Cotton, F. A.; Fanwick, P. E. *Inorg. Chem.* **1979**, *18*, 3558. (b) Cotton, F. A.; Frenz, B. A.; Deganello, G.; Shaver, A. *J. Organomet. Chem.* **1973**,*50*, 227.

7. TEXSAN - TEXRAY Structure Analysis Package, Molecular Structure Corporation, 1985.

8. DIRDIF: Direct Methods for Difference Structure, An Automatic Procedure for Phase Extension; Refinement of Difference Structure Factors. Beurskens, R. T. Technical Report 1984.

9. (a) Dunbar, K. R.; Haefner, S. C.; Burzynski, D. J. *Organometallics* **1990**,*9*, 1347. (b) Dunbar, K. R.; Haefner, S. C.; Bender, C. *J. Am. Chem. Soc.*, **1991**, *113*, 9540. (c) Dunbar, K. R.; Haefner, S. C.; Swepston, P. N. *J. Chem. Soc., Chem. Commun.* **1991**, 460.

10. (a) Garrou, P. E. *Inorg. Chem.* **1975**, *14*, 1435. (b) Garrou, P. E. *Chem. Rev.* **1981**, *81*, 229.

11. (a) Johnson, C. E.; Eisenberg, R.; Evans, T. R.; Burberry, M. S. *J. Am. Chem. Soc.* **1983**, *105*, 1795. (b) Fordyce, W. A.; Crosby, G. A. *Inorg. Chem.* **1982**, *21*, 1455. (c) Fordyce, W. A.; Crosby, G. A. *Inorg. Chem.* **1982**, *21*, 1023. (d) Fordyce, W. A.; Rau, H.; Stone, M. L.; Crosby, G. A. *Chem. Phys. Lett.* **1981**, *77*, 405. (e) Andrews, L. J. *Inorg. Chem.* **1978**, *17*, 3180. (f) Geoffroy, G. L.; Isci, H.; Litrenti, J. Mason, W. R. *Inorg. Chem.* **1977**, *16*, 1950. (g) Brady, R.; Flynn, B. R.; Geoffroy, G. L.; Gray, H. B.; Peone, J. Jr.; Vaska, L. *Inorg. Chem.* **1976**, *15*, 1485. (h) Geoffroy, G. L.; Wrighton, M. S.; Hammond, G. S.; Gray, H. B. *J. Am. Chem. Soc.* **1974**, *96*, 3105. (i) Brady, R.; Miller, W. V.; Vaska, L. *J. Chem. Soc., Chem. Commun.* **1974**, 393.

12. Leigh, G. J.; Richards, R. L. in *Comprehensive Organometallic Chemistry*; Wilkinson, G.; Stone, F. G. A.; Abel, E. W., eds.; Pergamon: New York, **1982**; vol. 5, p 553.

13. (a) Herde, J. L.; Lambert, J. C.; Senoff, S. V. *Inorg. Synth.* **1974**, *15*, 18. (b) Herde, J. L.; Senoff, *Inor. Nuc. Chem. Lett.* **1971**, 7, 1029.

14. (a) Crabtree, R. *Acc. Cham. Res.* **1979**, *12*, 331. (b) Schrock, R. R.; Osborn, J. A. *J. Am. Chem. Soc.* **1976**, *98*, 2134. (c) Schrock, R. R.; Osborn, J. A. *J. Am. Chem. Soc.* **1976**, *98*, 2143. Add halpern and catalyst precursor

15. Fackler, J. P. *Prog. Inorg. Chem.* **1966**, *7*, 361.

16. Horvath, I. work in progress.

17. Ibers, J. A.; Lilga, M. A. *Inorg. Chem.* **1984**, *23*, 3538.

CHAPTER IX

CONCLUSION

The results presented in this dissertation establish the use of tris(2,4,6-trimethoxyphenyl)phosphine as an excellent supporting ligand for the stabilization of divalent rhodium species. The mononuclear Rh(II) complex, $[Rh(\eta^3\text{-TMPP})_2][BF_4]_2$ (**3**) was isolated in high yield from a reaction of the solvated dinuclear Rh(II) species $[Rh_2(MeCN)_{10}][BF_4]_4$ with TMPP. $[Rh(\eta^3\text{-TMPP})_2][BF_4]_2$ (**3**) represents the first crystallographically characterized mononuclear Rh(II) complex. The remarkable stability of this metalloradical species provided us with an opportunity to study the chemistry of mononuclear rhodium in an unusual oxidation state. The combination of both hard and soft donor groups engenders the phosphine with the ability to stabilize a metal atom in a variety of coordination geometries and oxidation states. Although considered sterically encumbering, the ligand is nevertheless quite flexible as evidenced by the variety of fluxional and isomerization processes in which have been observed for metal complexes of TMPP. This flexibility has rendered it possible to access different oxidation states of the rhodium center while maintaining the same ligand set. Each of the complexes described in this study, exhibit one or more chemically accessible redox processes. The chemical relationship between the rhodium-TMPP complexes in this study is illustrated in Figure 37. The degree of methoxy interaction varies according to the rhodium oxidation states. Rather than serving to enforce a particular geometry on the metal center, the ligand adjusts to the available coordination sites and the electronic requirements of the metal center (Figure 38). This ability is readily apparent when one examines the structural changes in going from Rh(I) to Rh(III) species. As the metal center is oxidized, the hapticity of the phosphine ligand increases from η^1 to η^3 in response to the increased need for electron density at the metal center.

Figure 37. Synthetic routes to TMPP complexes of rhodium.[a]

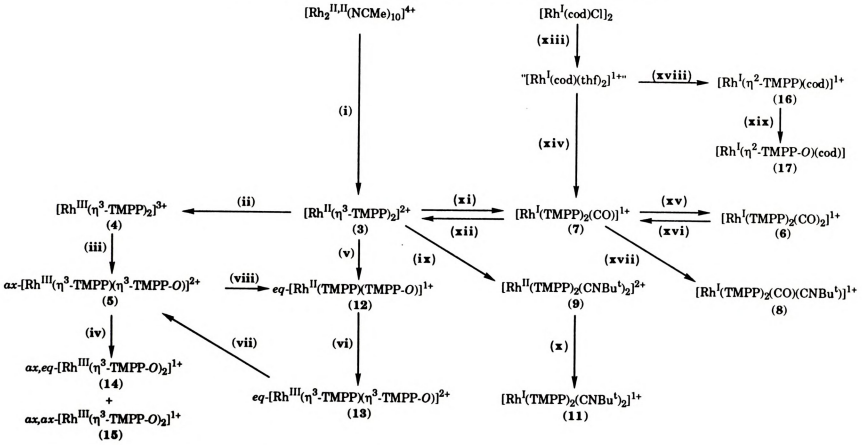

[a](i) TMPP (4 equiv), MeCN, 0°C. (ii) $NOBF_4$, MeCN, -40°C or $[Cp_2Fe][BF_4]$, CH_2Cl_2, -40°C. (iii) acetone, r. t., 24h. (iv) TMPP or $[(Bu^n)_4N][I]$. (v) TMPP, MeCN. (vi) $[Cp_2Fe][BF_4]$, MeCN, -15°C. (vii) MeCN, r.t. (viii) Cp_2Co, acetone. (ix) $CNBu^t$ (2 equiv), CH_2Cl_2. (x) Cp_2Co, CH_2Cl_2. (xi) Cp_2Co (excess), CO, CH_2Cl_2. (xii) $[Cp_2Fe][BF_4]$ (1 equiv), N_2, CH_2Cl_2, -15°C. (xiii) $AgBF_4$ (2 equiv), THF. (xiv) CO, TMPP (2 equiv), 0°C. (xv) CO, r. t. (xvi) Ar, r. t. (xvii) $CNBu^t$, CH_2Cl_2. (xviii) TMPP (1 equiv), THF, -40°C. (xix) TMPP, MeCN, r.t.

Bonding Modes of TMPP

TMPP (neutral)

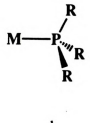

η^1

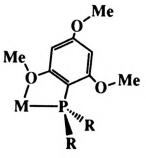

η^2

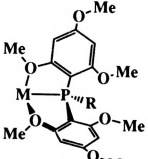

η^3

TMPP-O (anionic)

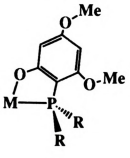

η^2

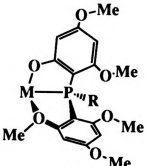

η^3

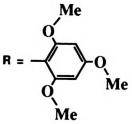

Figure 38. η^1 - η^3 bonding modes for TMPP and [TMPP-*O*]-

A critical point of the chemistry of TMPP was underscored in this research, *viz*, that although $[Rh(\eta^3\text{-TMPP})_2][BF_4]_2$ (**3**) is coordinatively saturated, the hemilabile nature of the ether groups allows for facile and often reversible substitution chemistry. It was found that the incoming ligand must possess certain electronic requirements as the Rh(II) phosphine complexes are resistant to attack by moisture or oxygen but are quite susceptible to π-acids such as CO, CNR and NO. The ability of the ether groups to participate in such "arm on, arm off" type of mechanism is critical for the future development of these complexes as viable systems for catalytic or stoichometric transformations of small substrates. The work described in chapter 5 demonstrates the possibility of exploiting the labile nature of the pendent methoxy substituents for the development of molecule-based chemical sensors. The future design of other selective chemical sensors based on complexes of TMPP appears to be very promising.

The complex chemistry of $[Rh(\eta^3\text{-TMPP})_2][BF_4]_2$ (**3**) with carbon monoxide provided valuable insight into the subtle electronic influences that govern the relative stabilities of the +1, +2 and +3 oxidation states. The reversible interaction of carbon monoxide with $[Rh(\eta^3\text{-TMPP})_2][BF_4]_2$ (**3**) was found to proceed through a series of redox reactions brought about by the initial disproportionation reaction between **3** and an intermediate Rh(II) carbonyl species. By reducing the π-acceptor strength of the incoming ligand through the use of alkyl isocyanide ligands, the redox pathway was shutdown and stable isocyanide adducts of **3** were isolated. At the time of their discovery, the complexes $[Rh^{II}(TMPP)_2(CNR)_2][BF_4]_2$ (R = Bu^t, Pr^i) represented the first mononuclear organometallic Rh(II) species sufficiently stable enough to be spectroscopically and crystallographically characterized.

The stability of these complexes provides for a rare opportunity to investigate the chemistry of an organometallic radical system.

For the purpose of future directions, it should be pointed out that a potential drawback to the use of TMPP as a supporting ligand is its documented susceptibility to nucleophilic attack at a coordinated methoxy substituent. This results in dealkylation of the coordinated ether group and formation of a metal-phenoxide bond. The tendency of these systems to dealkylate is highly dependent on the electrophilicity of the metal center. This point was illustrated by the relative stabilities of the molecular cations $[Rh^{II}(\eta^3\text{-TMPP})_2]^{2+}$ (**3**) and $[Rh^{III}(\eta^3\text{-TMPP})_2]^{3+}$ (**4**) towards dealkylation. As the electrophilicty of the metal center was increased, the ease of dealkylation also increased. It is expected that such behavior will be particularly troublesome for the more electrophilic early transition metals; as a result, this will necessarily limit the use of the free phophine form of TMPP to lower valent early and late transition metals.

One of our principlal goals prior to undertaking this chemistry was to the develop the coordination and organometallic chemistry of odd-electron systems. The work presented here has demonstrated that TMPP provides the proper combination of kinetic and thermodynamic stability for the isolation of mononuclear Rh(II) complexes. Clearly, based on the demonstrated ability of TMPP to stabilize Rh(II) metalloradicals, extension of this work to other d^7 metal systems is plausible. Indeed, recent work in our laboratories has led to the successful isolation of the Ni(III) complex, $[Ni(TMPP\text{-}O)_2]^{1+}$.[1] Unfortunately, initial efforts to synthesize analogous Ir(II) species have proven unsuccessful. This is attributed, in part, to the lack of a suitable precursor such as a solvated $[Ir_2]^{4+}$ species. Undoubtedly, further work in this area will ultimately result in the isolation of stable Ir(II)-TMPP systems.

As for complexes of Pd, Pt and Ru, nitrile complexes of these metals are known[2,3,4] and should provide excellent precursors for the synthesis of d^8 and d^6 metal TMPP complexes. These intermediates, in turn, may be either oxidized or reduced to the corresponding paramagnetic d^7 species. In related work, Gladfelter *et al.* have shown that paramagnetic Ru(I) carbonyl complexes are accessed by chemical oxidation of zero-valent $Ru(PR_3)_2(CO)_3$ species (R= phenyl, benzyl, *p*-tolyl, cyclohexyl).[5] Similar d^7 carbonyl species have also been isolated and crystallographically characterized for Re(0).[6] By analogy, the preparation of similar metalloradicals of the general formula $[M(TMPP)_2(CO)_x]^{n+}$ is feasible. These odd-electron carbonyl complexes will be especially intriguing in light of the rich chemistry already documented for TMPP complexes of Rh(I), Ir(I) and Mo(0) carbonyl compounds.

List of References

1. Dunbar, K. R.; Quillevéré, A submitted for publication.

2. Thomas, R. R.; Sen, A. *Inorg. Synth.* **1989**, 26, 128.

3. De Renzi, A.; Panunzi, A.; Vitagliano, A.; Paiaro, G. *J. Chem. Soc., Chem. Commun.* **1976**, 47.

4. (a) Rapaport, I.; Helm, L.; Merbach, A. E.; Bernhard, P.; Ludi, A. *Inorg. Chem.* **1988**, *27*, 873. (b) Bown, M.; Fontaine, X. L. R.; Greenwood, N. N.; Kennedy, J. D.; Thornton-Pett, M. *J. Chem. Soc., Dalton Trans.* **1987**, 1169. (c) Kölle, U.; Flunkert, G.; Görissen, R.; Schmidt, M. U.; Englert, U. *Angew. Chem. Int. Ed. Engl.* **1992**, *31*, 440.

5. Sherlock, S. J.; Boyd, D. C.; Moasser, Gladfelter, W. L. *Inorg. Chem.* **1991**, *30*, 3626.

6. (a) Walker, H. W.; Rattinger, G. B.; Belford, R. L.; Brown, T. L. *Organometallics* **1983**, *2*, 775. (b) Crocker, L. S.; Heinekey, D. M.; Schulte, G. K. *J. Am. Chem. Soc.* **1989**, *111*, 405.

APPENDICES

APPENDIX A

PHYSICAL MEASUREMENTS

APPENDIX A

PHYSICAL MEASUREMENTS

1. Infrared Spectroscopy Infrared spectra were recorded on a Perkin-Elmer 599 or a Nicolet 740 FT-IR spectrophotometer. Solid state spectra were measured as Nujol mulls between CsI plates. Solution spectra were recorded using CaF_2 solution cells.

2. NMR Spectroscopy ^1H NMR spectra were measured either on a WM 250-MHz Bruker spectrometer with an ASPECT 3000 computer, a Gemini 300-MHz, Varian 300-MHz or Varian 500-MHz spectrometer. Chemical shifts were referenced relative to the residual proton impurity of the deuterated solvent: d_2-methylene chloride, 5.32 ppm; d_3-acetonitrile, 1.93 ppm; d_6-acetone, 2.04 ppm; d_1-chloroform, 7.24. $^{13}C\{^1H\}$ NMR spectra were recorded on a Varian 300-MHz spectrometer operating at 73.1 MHz and were referenced relative to the ^{13}C solvent resonance. $^{31}P\{^1H\}$ NMR spectra were obtained on a Varian 300-MHz spectrometer operating at 121.4 MHz. Chemical shifts were referenced relative to an external standard of 85% H_3PO_4. Positive chemical shifts were reported downfield relative to H_3PO_4.

3. EPR Spectroscopy X-band EPR spectra were obtained using a Bruker ER200D spectrometer. To obtain an accurate measure of g values and line widths, a Bruker ER035M NMR Gaussmeter and a Hewlett-Packard 5245L frequency counter (with a 3-12 GHz adapter) were used to measure magnetic field strength and microwave frequency, respectively.

4. Electronic Absorption Spectroscopy Electronic absorption spectra were measured on a Hitachi U-2000 or a Cary 17 spectrophotometer.

5. Electrochemistry Electrochemical measurements were performed by using an EG&G Princeton Applied Research Model 362 scanning potentiostat in conjunction with a BAS Model RXY recorder. Cyclic voltammetry experiments were carried out at 22+2°C using 0.1 M tetra-*n*-butylammonium tetrafluoroborate ($TBABF_4$) as a supporting electrolyte, unless noted otherwise. Measurements were made at a scan rate of 200 mV/s using a platinum disk working electrode and a Ag/AgCl reference electrode. $E_{1/2}$ values, determined as $(E_{p,a}+E_{p,c})/2$, were referenced to a Ag/AgCl electrode and uncorrected for junction potentials. Under the same experimental conditions, the Cp_2Fe / Cp_2Fe^+ couple occurred at $E_{1/2}$ = +0.50 V.

6. Magnetic Susceptibility Variable temperature and field magnetic susceptibility measurements were carried out on a 10 KG BTI Superconducting Quantum Interference Device (SQUID) at Michigan State University. Additional solid state magnetic susceptibility measurements were determined at room temperature by using a Johnson-Matthey magnetic susceptibility balance. Solution magnetic susceptibility measurements were carried out by application of the Evans method on a Bruker 250-MHz or Varian 300-MHz spectrometer.

7. Mass Spectrometry Fast Atom Bombardment (FAB) mass spectrometry studies were performed on a JEOL HX double-focusing mass spectrometer housed at the National Institutes of Health / Michigan State University Mass Spectrometry Facility.

8. Elemental Analysis Elemental analyses were performed at Galbraith Laboratories, Inc.

APPENDIX B

CHEMISTRY OF TRIS(2,4,6-TRIMETHOXYPHENYL)PHOSPHINE WITH GROUP VI METALS

APPENDIX B

CHEMISTRY OF TRIS(2,4,6-TRIMETHOXYPHENYL)PHOSPHINE WITH GROUP VI METALS

1. Introduction

As our eventual goal in this research is to establish that TMPP, with its labile metal-ether interactions, is an excellent ligand for the design of reactive metal centers, we set out to prepare a complex that would allow us to probe the small molecule binding properties of a TMPP supported metal. Based on our newly acquired knowledge of the bonding capabilities of the ligand, we predicted that it would be possible to prepare compounds of general formula $(TMPP)ML_3$ for metals that ordinarily exhibit octahedral structures. A convenient backdrop for our work is the elegant research of Kubas and co-workers who demonstrated that highly donating, bulky phosphine ligands stabilize the five-coordinate complexes $M(CO)_3(PR_3)_2$ M(=Mo, W; R=C_6H_{11}, i-C_3H_7) which readily add molecular H_2 and N_2.[1] Since no examples of four-coordinate complexes of general formula $M(CO)_3(PR_3)$ have been reported, we set out to prepare such a monophosphine derivative with TMPP with the expectation that the product would exhibit unusual properties and reactivity. Herein, we report the synthesis of the novel fluxional molecule (η^3-TMPP)$Mo(CO)_3$ (TMPP = tris(2,4,6-trimethoxyphenyl)phosphine) from a reaction between (η^6-C_7H_8)$Mo(CO)_3$ and TMPP. In addition, the chemistry of TMPP with partially solvated mononuclear and dinuclear molybdenum halide complexes is also presented.

2. Experimental

A. Synthesis

All reactions were carried out under an argon atmosphere by the use of standard Schlenk-line techniques unless otherwise stated. The phosphine, tris(2,4,6-trimethoxyphenyl)phosphine (**1**), was prepared as described in Chapter II. The starting material, $(\eta^6\text{-}C_7H_8)Mo(CO)_3$, was purchased from Strem and used as received. $Mo_2Cl_4(MeCN)_4$ and $MoCl_3(THF)_3$ were prepared using standard literature procedures.[2,3] The tungsten starting material, $(\eta^6\text{-}C_7H_8)W(CO)_3$, was prepared following the literature procedure described by Kubas.[4]

(1) Preparation of $(\eta^3$-TMPP)$Mo(CO)_3$ (20)

In a typical synthesis, a quantity of $(\eta^6\text{-}C_7H_8)Mo(CO)_3$ (0.300 g, 1.10 mmol) and TMPP (0.587 g, 1.10 mmol) was dissolved in 10 mL of benzene that had been thoroughly purged with argon in order to remove dissolved N_2(g). The resulting suspension was stirred at r. t. for ca. 12 h. The orange supernatant was decanted and the yellow precipitate was washed with benzene (4 x 5 mL). The yellow product was recrystallized by dissolution in CH_2Cl_2 (10 mL), followed by slow addition of diethyl ether (10 mL). The solution was decanted and the yellow crystalline solid was washed with diethyl ether (3 x 5 mL) and dried *in vacuo*; yield, 0.624 g (80 %) IR (Nujol, CsI) cm^{-1}: v(CO), 1914.5 vs. 1775 vs. 1791 vs. IR (CH_2Cl_2) cm^{-1}: v(CO), 1921 vs, 1799 vs, 1782 vs. IR (C_6H_6) cm^{-1}: v(CO), 1930 vs. 1798 s. ^{1}H NMR (CD_2Cl_2, 20°C) δ ppm: -OCH_3, 3.55 (br), 3.81 (s); *m*-H, 6.15 (br). ^{1}H NMR ($C_6D_5CD_3$, -60°C) δ ppm: *o*-OCH_3, 2.80 (s, 6H), 3.19 (s, 6H), 3.81 (s, 6H); *p*-OCH_3, 3.33 (s, 6H), 3.44 (s, 3H); *m*-H, 5.77 (s, 2H), 5.86 (s, 2H), 6.01 (br, 2H). ^{1}H NMR (CD_2Cl_2, -40°C) δ ppm: *o*-OCH_3, 3.49 (s, 12H), 4.36 (s, 6H); *p*-OCH_3,

3.77 (s, 6H), 3.82 (s, 3H); *m*-H, 6.02 (s, 2H), 6.07 (d, $^4J_{P-H}$= 3.9 Hz, 2H), 6.15 (dd, 2H). ^{31}P NMR (CD_2Cl_2, 20°C) δ ppm: -1.9 (s).

(2) Reaction of TMPP with (η^6-C_7H_8)W(CO)$_3$

To a mixture of (η^6-C_7H_8)W(CO)$_3$ (0.215 g, 0.597 mmol) and TMPP (0.318 g, 0.597 mmol) was added 5 mL of diethyl ether. The resulting suspension was stirred for 12 h at r.t. During this time, a yellow solid precipitated from the solution. The yellow product was collected by filtration, washed with benzene (2 x 5 mL) and diethyl ether (4 x 10 mL), and dried under vacuum; yield of crude precipitate 0.333 g. IR (Nujol, CsI) cm^{-1}: ν(CO), 1910 vs. 1769 vs. IR (CH_2Cl_2) cm^{-1}: ν(CO), 1912 vs, 1789 vs, 1775 vs.

(3) Reaction of TMPP with MoCl$_3$(THF)$_3$

A solution of TMPP (0.382 g, 0.717 mmol) in 10 mL of THF was added dropwise to a solution of $MoCl_3(THF)_3$ (0.300 g, 0.717 mmol) in 5 mL of THF at 0°C. The reaction was stirred for ca. 12 h, during this time the solution was allowed to slowly warm to r. t. The resulting red solution was filtered through a Celite plug and then evaporated to yield a red solid. The solid was washed with diethyl ether (3 x 5 mL) and dried under reduced pressure; yield of red solid, 0.348 g. ^{1}H NMR (CD_3CN) δ ppm: -OCH_3, 3.51 (s), 3.82 (s); *m*-H, 6.14 (d, $^4J_{P-H}$ = 5.7 Hz).

(4) Reaction of TMPP with Mo$_2$Cl$_4$(MeCN)$_4$

(i) 4 equivalents. In a typical reaction, a mixture of $Mo_2Cl_4(MeCN)_4$ (0.250 g, 0.502 mmol) and TMPP (1.07 g, 2.01 mmol) was dissolved in 25 mL of MeCN at r.t. After 3 h, the solution had become green in color. The solvent was evaporated under reduced pressure to yield a green solid that was washed with 20 mL of benzene. The colorless benzene washing was evaporated to give a white powder (0.41 g) that was shown to be TMPP by ^{1}H NMR spectroscopy. The green residue was further washed with 10 mL of

diethyl ether and dried under vacuum; yield of crude solid, 0.48 g. A ^{1}H NMR spectrum of the crude product reveals the presence of only [TMPP-H]$^+$.

(ii) 6 equivalents. In a typical reaction, a solution of $Mo_2Cl_4(MeCN)_4$ (0.200 g, 0.402 mmol) and TMPP (1.28 g, 2.40 mmol) in 20 mL of MeCN was refluxed for 4 days. During this time, the solution color changed from green to dark brown with no further change throughout the reaction. The solution was then filtered through a Celite plug and evaporated to a residue. The brown solid was washed with benzene (2 x 10 mL) and diethyl ether (2 x 10 mL) and dried under vacuum; yield of brown solid, 0.766 g. ^{1}H NMR spectroscopy showed that the solid was primarily comprised of [TMPP-CH_3]$^+$.

B. X-ray Crystallography

The structure of (η^3-TMPP)Mo(CO)$_3$ (**20**) was determined by application of general procedures that have been fully described elsewhere.[5] Geometric and intensity data were collected on a Nicolet P3/F diffractometer with graphite monochromated MoKα ($\lambda_{\bar{\alpha}}$= 0.71073 Å) and were corrected for Lorentz and polarization effects. All calculations were performed on a VAXSTATION 2000 computer. Data reduction and refinement were performed using the programs from the Enraf-Nonius Structure Determination Package (SDP). Crystal parameters and basic information pertaining to data collection and structure refinement are summarized in Table 17

(1) (η^3-TMPP)Mo(CO)$_3$ (20) • CH_2Cl_2

(i) Data Collection and Reduction. Crystals of (η^3-TMPP)Mo(CO)$_3$ (**20**) • CH_2Cl_2 were obtained from slow diffusion of diethyl ether into a CH_2Cl_2 solution of **20**. A single crystal with approximate dimensions 0.60 x 0.40 x 0.15 mm^3 was selected and mounted onto the tip of a glass fiber with epoxy cement. Least-squares refinement of 25 carefully centered reflections in the

Table 17. Summary of crystallographic data for (η^3-TMPP)Mo(CO)$_3$ • CH_2Cl_2 (**20**).

Formula	$MoPCl_2O_{12}C_{31}H_{35}$
Formula weight	801.92
Space group	$P2_1/a$
a, Å	17.155(8)
b, Å	12.019(4)
c, Å	16.985(6)
α, deg	90
β, deg	95.69(3)
γ, deg	90
V, Å^3	3485(2)
Z	4
d_{calc}, g/cm^3	1.493
μ (Mo Kα), cm^{-1}	6.219
Temperature, °C	22±2 °C
R[a]	0.069
R_w[b]	0.084
Quality-of-fit indicator[c]	2.09

[a] $R = \Sigma \| |F_o| - |F_c| | / \Sigma |F_o|$

[b] $R_w = [\Sigma w(|F_o| - |F_c|)^2 / \Sigma w |F_o|^2]^{1/2}$; $w = 1/\sigma^2(|F_o|)$

[c] Quality-of-fit = $[\Sigma w(|F_o| - |F_c|)^2 / (N_{obs} - N_{parameters})]^{1/2}$

range $15 < 2\theta < 25°$ revealed that the compound $(\eta^3\text{-TMPP})Mo(CO)_3 \cdot CH_2Cl_2$ crystallized in a monoclinic space group $P2_1/a$ with a = 17.155(8) Å, b = 12.019(4) Å, c = 16.985(6) Å, β = 95.69(3) Å, V = 3485(2) Å^3. Axial photographs confirmed the monoclinic symmetry of the cell. Intensity measurement of three representative reflections at regular intervals throughout data collection revealed that a 41.7 % loss in diffraction intensity had occurred. A linear decay correction was applied to the data using the program CHORT in SDP. A Nicolet P3/F diffractometer was used to collect 3845 unique data in the range $4 \leq 2\theta \leq 43°$ at 22 ± 2°C; 2243 data with $Fo^2 > 3\sigma(Fo^2)$ were used in the refinement.

(ii) Structure Solution and Refinement. The position of the molybdenum atom was successfully located by application of the direct methods program in SHELXS-86. The remaining non-hydrogen atoms were located through successive least-squares refinements and difference Fourier maps. After the refinement had successfully converged with isotropic thermal parameters, an absorption correction based on the program DIFABS was applied to the data.[6] In the end, after anisotropic refinement of 424 parameters, residuals of R = 0.069 and R_w = 0.084 were obtained. The quality-of-fit index was 2.09 and the largest shift/esd was 0.08. A final difference Fourier map revealed that no peak remained over 0.86 e$^-$/Å^3 in height.

3. Results

A. Synthesis and Characterization of $(\eta^3\text{-TMPP})Mo(CO)_3$ (20)

One equivalent of TMPP reacts smoothly with $(\eta^3\text{-}C_7H_8)Mo(CO)_3$ at room temperature in benzene over the period of 6 hours to produce a yellow microcrystalline compound formulated as $(\eta^3\text{-TMPP})Mo(CO)_3$ (**20**) in 80%

yield. The product is insoluble in most common solvents except toluene and benzene in which it is sparingly soluble and dichloromethane in which it is very soluble but prone to decomposition over long periods of time. Yellow solutions of **20** are very air sensitive, turning brown immediately upon exposure to air. The solid and crystalline forms decompose slowly over the period of several hours.

The solution properties of (η^3-TMPP)Mo(CO)$_3$ attest to its high reactivity as it easily converts to Mo(CO)$_3$(NCCH$_3$)$_3$ in acetonitrile and is extremely air sensitive. The ^{1}H NMR spectrum of **20** revealed that an intramolecular exchange process involving the ortho-methoxy groups is occurring at room temperature. Variable temperature ^{1}H NMR data were obtained in d^8-toluene and CD_2Cl_2 over the range +20°C and -60°C and the results clearly indicate that all three rings are participating in a low energy fluxional process (Figure 39). The low temperature limiting spectrum at -60°C in d^8-toluene exhibits eight distinct resonances which integrate in accordance with the magnetically inequivalent meta, ortho and para groups observed in the solid state structure. At temperatures above -60°C the spectral features broaden and gradually collapse in a non-symmetrical manner due to a dynamic exchange of interacting and non-interacting ortho-methoxy groups. Concomitantly the para and meta regions broaden and eventually coalesce at ca -15°C. Similar behavior is observed in CD_2Cl_2, although in this solvent the low temperature limiting spectrum shows only one broad resonance for the non-interacting ortho-methoxy groups at δ = + 3.49 ppm (Figure 40). Attempts to obtain spectra at higher temperatures were thwarted by the thermal instability of the complex.

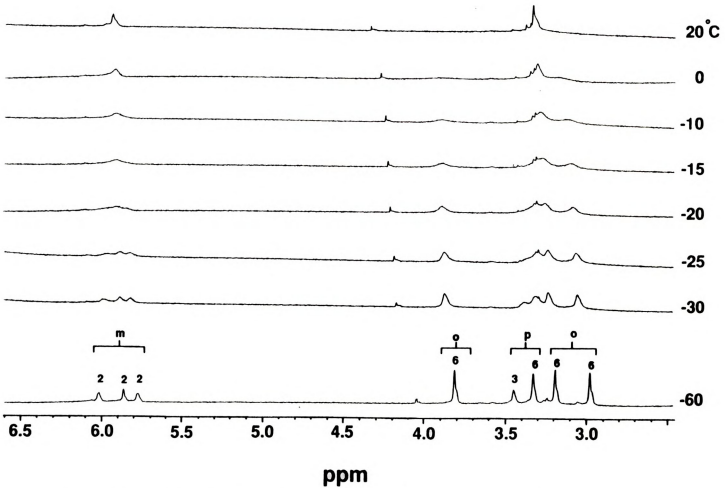

Figure 39. Variable temperature ^1H NMR spectra of (η^3-TMPP)Mo(CO)$_3$ (**20**) in d_8-toluene.

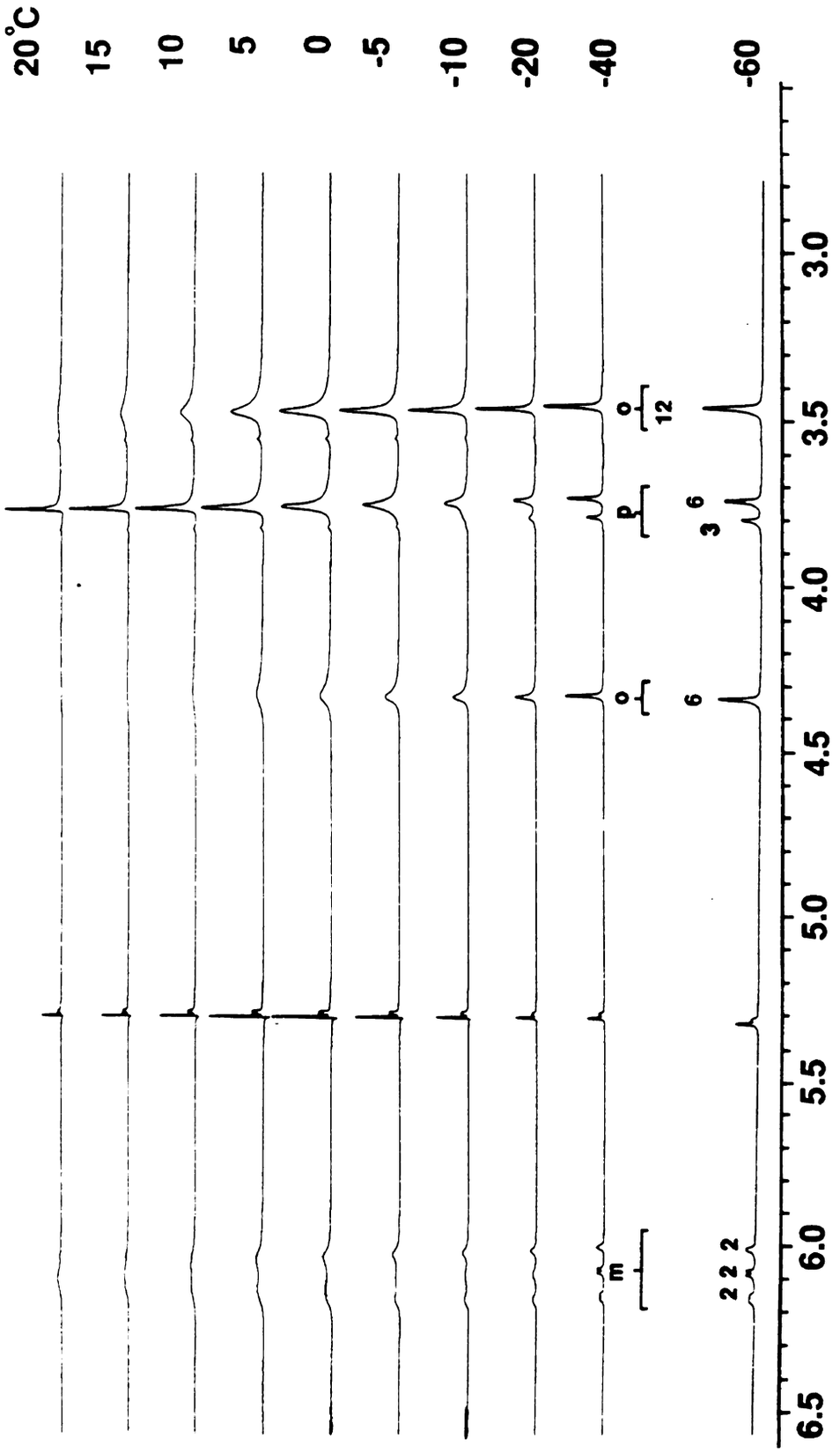

Figure 40. Variable temperature ^1H NMR spectra of (η^3-TMPP)Mo(CO)$_3$ (**20**) in CD_2Cl_2.

B. Molecular Structure of (η^3-TMPP)Mo(CO)$_3$ (20)

Single crystals of the title compound were grown by slow diffusion of diethyl ether into a CH_2Cl_2 solution of the compound at 0°C. An analysis of the X-ray data established the identity of the compound and revealed that the phosphine ligand occupies three positions in the coordination sphere of the molecule. As the ORTEP diagram in Figure 41 shows that (η^3-TMPP)Mo(CO)$_3$ (**20**) possesses a distorted octahedral geometry with two of the coordination sites being occupied by oxygens from ortho-methoxy substituents on two separate phenyl rings. This bonding mode has previously been noted in the structure of [Rh(η^3-TMPP)$_2$][BF$_4$]$_2$ (**3**).[7] The chelation effect provided by weakly interacting pendant methoxy groups accounts for the ease of isolation and moderate stability of **20**. The distortion of the coordination geometry about the Mo atom is evidenced most dramatically by the acute angles P(1)-Mo(1)-O of 71.6(2)° and 74.8(2)° for O(4) and O(9) respectively. These deviations from 90° are a consequence of the formation of the five-membered rings Mo-P-C-C-O. All other angles within the molecule are also non-ideal but to a lesser degree (Table 18). The high degree of flexibility of the TMPP ligand in achieving the observed bonding mode is apparent from an examination of the disparate Mo(1)-P(1)-C angles; these vary from 104.8(3)° for C(4) which is involved in a metallacycle, to 120.8(3)° for C(22) on the lone free ring. Other metric parameters within the molecule are typical for carbonyl-phosphine complexes. The Mo-O distances of 2.363(6) Å and 2.337(7) Å are long which is not unexpected for metal-ether interactions. The Mo-C distances are inequivalent (Table 18) with the Mo-C(2) distance trans to the phosphorus being the longest (1.97(1) Å).

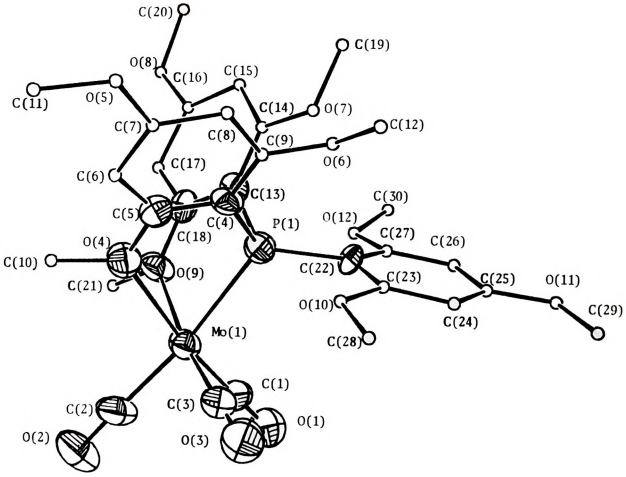

Figure 41. ORTEP representation of (η^3-TMPP)Mo(CO)$_3$ (**20**).

Table 18. Selected bond distances (Å) and angles (deg) for (η^3-TMPP)-$Mo(CO)_3$ (**20**).

Atom 1	Atom 2	bond distance
Mo(1)	P(1)	2.476(3)
Mo(1)	C(1)	1.85(1)
Mo(1)	C(2)	1.97(1)
Mo(1)	C(3)	1.92(1)
Mo(1)	O(4)	2.363(6)
Mo(1)	O(9)	2.337(7)

Atom 1	Atom 2	Atom 3	bond angles
P(1)	Mo(1)	C(1)	101.3(3)
P(1)	Mo(1)	C(2)	171.5(4)
P(1)	Mo(1)	C(3)	96.6(3)
P(1)	Mo(1)	O(4)	71.6(2)
P(1)	Mo(1)	O(9)	74.8(2)
C(1)	Mo(1)	C(2)	86.4(5)
C(1)	Mo(1)	C(3)	84.3(5)
Mo(1)	P(1)	C(4)	104.8(3)
Mo(1)	P(1)	C(22)	120.8(3)

C. Reaction of TMPP with $(\eta^6\text{-}C_7H_8)W(CO)_3$

The olefin complex $(\eta^6\text{-}C_7H_8)W(CO)_3$ reacts with one equivalent of TMPP in diethyl ether to yield a yellow precipitate similar to that observed for the analogous molybdenum reaction. Although the solubility of TMPP is only slight, it is sufficient to allow for complete reaction within several hours. The solid exhibits solubility properties similar to $(\eta^3\text{-TMPP})Mo(CO)_3$ (**20**) and appears to be just as air sensitive. An IR spectrum of the crude precipitate reveals that it is comprised of a mixture of carbonyl-containing products. By analogy to **20**, the bands at $\nu(CO)$ = 1910 and 1796 cm^{-1} are tentatively assigned to the monophosphine adduct $(\eta^3\text{-TMPP})W(CO)_3$. This product has been independently synthesized by reaction of the proprionitrile complex $W(CO)_3(NCEt)_3$ with TMPP in toluene.[8] A ^1H NMR spectrum of the precipitate in d^8-toluene also reveals a mixture of products, one of which exhibits broad features, indicative of a fluxional process occurring in solution. By analogy to the solution behavior of **20**, this species most likely corresponds to $(\eta^3\text{-TMPP})W(CO)_3$.

D. Reaction of TMPP with Solvated Molybdenum Chloride Complexes

Reaction of the $Mo_2^{II,II}$ dinuclear complex, $Mo_2Cl_4(MeCN)_4$, with excess TMPP invariably leads to the formation of quaternary phosphonium salts as evidenced by ^1H and ^{31}P NMR spectroscopy. The cations $[TMPP\text{-}H]^+$ and $[TMPP\text{-}CH_3]^+$ were the only detectable diamagnetic species in solution. The metal species are either paramagnetic and/or do not contain TMPP. Attempts to isolate metal containing species by repeated fractional crystallization yielded intractable mixtures of phosphonium salts. Similar results were observed in the chemistry of TMPP with first row metal halide compounds.[9] Through careful variation of the reaction conditions either

$[TMPP\text{-}H]^+$ or $[TMPP\text{-}CH_3]^+$ may be isolated as the sole phosphonium cation species. When the reaction is performed under mild conditions, $[TMPP\text{-}H]^+$ is the primary product observable by ^1H and ^{31}P NMR spectroscopy; under refluxing conditions formation of $[TMPP\text{-}CH_3]^+$ is favored. Formation of the alkyl phosphonium cation suggests that coordination of the phosphine to the metal occurs and that the coordinated ligand undergoes dealkylation to form a phosphino-phenoxide derivative of TMPP. This is not surprising considering the high oxophilicity of molybdenum which would promote dealkylation reactions. TMPP also reacts with $MoCl_3(THF)_3$ under mild conditions to give a red diamagnetic product that exhibits a symmetrical pattern of resonances in the ^1H NMR spectrum. The diamagnetism of the sample suggests the complex has dimerized, thereby facilitating communication between the unpaired electrons.

4. Discussion

The $(\eta^3\text{-TMPP})Mo(CO)_3$ (**2 0**) represents an unusual phosphine derivative of molybdenum tricarbonyl. A single crystal X-ray study revealed that the molecule is comprised of a Mo(0) center ligated by three carbonyl ligands and a TMPP ligand in a facial bonding mode. The metal-ether interactions from the pendant methoxy groups are quite labile. Variable temperature ^1H NMR spectra in d^8-toluene and CD_2Cl_2 revealed that a low-energy intramolecular exchange process is occurring. We envision that the exchange process occurs through the dissociation of one of the coordinated ether groups to form a five coordinate trigonal bipyramidal geometry. Rotation about the P-C bonds followed by association of a previously unbound methoxy substituent eventually equilibrates each of the phenyl rings. This process is depicted in Figure 42. The formation of similar five-coordinate,

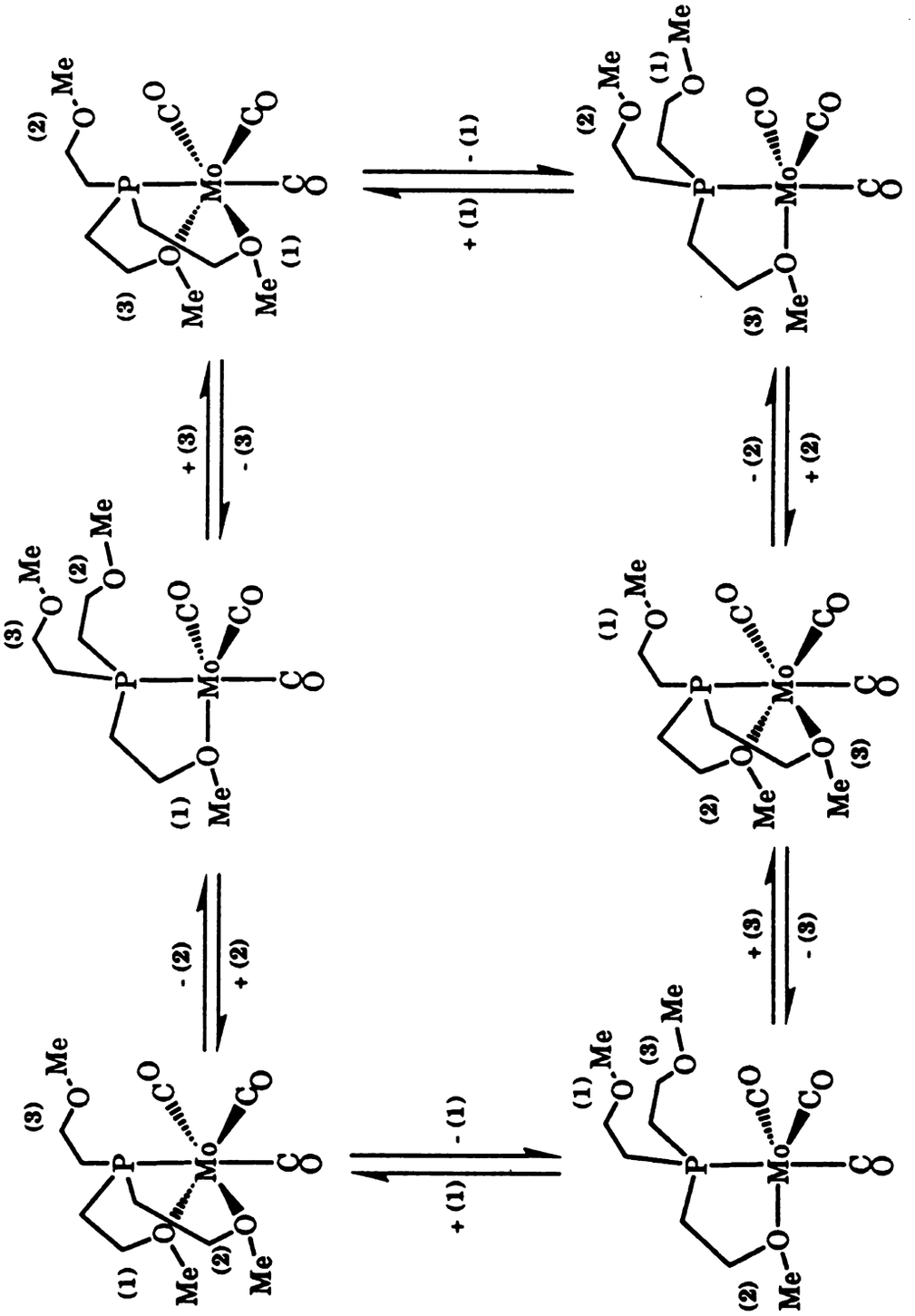

Figure 42. Proposed pathway for intramolecular exchange in (η^3-TMPP)Mo(CO)$_3$ (**20**).

trigonal bipyramidal intermediates has been proposed for isotopic scrambling in substitution reactions of octahedral metal carbonyl complexes.[10]

Our future interest in this molecule centers around its reactivity with small molecules. The solution lability of the metal-ether interactions is expected to provide the requisite open coordination sites for binding substrates. Indeed, work by others in our laboratory has shown that (η^3-TMPP)Mo(CO)$_3$ (**20**) readily adds an additional CO ligand to form the tetra carbonyl species (η^2-TMPP)Mo(CO)$_4$.[10] The addition of a fourth carbonyl ligand is irreversible, but the tetracarbonyl complex reversibley adds a second CO ligand to form the pentacarbonyl complex, (η^1-TMPP)Mo(CO)$_5$. These reactions further exemplify the lability of the metal-ether interactions in TMPP complexes.

List of References

1. (a) Kubas, G. J. *J. Chem. Soc. Chem. Commun.* **1990**, *29*, 0000. (b) Kubas, G. J.; Ryan, R. R.; Swanson, B. I.; Vergamini, P. J.; Wasserman, H. J. *J. Am. Chem. Soc.* **1984**, *106*, 451. (c) Kubas, G. J.; Ryan, R. R.; Wrobleski, D. A. *J. Am. Chem. Soc.* **1986**, *108* , 1339. (d) Wasserman, H. J.; Kubas, G. J.; Ryan, R. R. *J. Am. Chem. Soc.* **1986**, *108*, 2294. (e) Kubas, G. J.; Unkefer, C. J.; Swanson, B. I.; Fukushima, E. *J. Am. Chem. Soc.* **1986**, *108*, 7000. (f) Kubas, G. J.*Acc. Chem. Res.* **1988**,*21*, 120. (g) Kubas, G. J. *Comments Inorg. Chem.* **1988**,*7*, 17.

2. San Filippo, J.; Sniachoch, H. J.; Grayson, R. L. *Inorg. Chem.* **1974**, *13*, 2121.

3. Dilworth, J. R.; Richards, R. L.*Inorg. Synth.* **1980**, *20*, 119.

4. Kubas, G. J. *Inorg. Chem.* **1983**,*22*, 692.

5. Bino, A.; Cotton, F. A.; Fanwick, P. E. *Inorg. Chem.* **1979**, 18, 3558. (b) Cotton, F. A.; Frenz, B. A.; Deganello, G.; Shaver, A. *J. Organomet. Chem.* **1973**,*50*, 227.

6. Walker, N.; Stuart, D. *Acta. Cryst.* **1983**,*A39*, 158.

7. (a) Dunbar, K. R.; Haefner, S. C.; Pence, L. E. *J. Am. Chem. Soc.* **1989**, *111*, 5504. (b) Haefner, S. C.; Dunbar, K. R.; Bender, C. *J. Am. Chem. Soc.* **1991**, *113*, 9540.

8. Dunbar, K. R.; Sun, J.-S. unpublished results.

9. Quillevéré, A. Ph. D. dissertation, Michigan State University, **1992**.

10. Howell, J. A. S.; Burkinshaw, P. M. *Chem. Rev.* **1983**, *83*, 557.

11. Dunbar, K. R.; Sun, J.-S. manuscript in preparation.

APPENDIX C

COMPILATION OF ^{31}P NMR SPECTRAL DATA

APPENDIX C

Table 19. COMPILATION OF ^{31}P NMR SPECTRAL DATA

	Compound	Chemical[a] Shift	$J_{Rh\text{-}P}$ Hz	$J_{P_A\text{-}P_B}$ Hz
(1)	TMPP	– 66.3 (s)	–	–
(2)	TMPP=O	+ 10.8 (s)	–	–
(3)	$[Rh^{II}(\eta^3\text{-TMPP})_2][BF_4]_2$	not observed		
(4)	$[Rh^{III}(\eta^3\text{-TMPP})_2][BF_4]_3$	+ 37.4 (d)[b]	107	–
(5)	*ax*-$[Rh^{III}(\eta^3\text{TMPP})(\eta^3\text{-TMPP-}O)][BF_4]_2$	+ 37.9 (dd)[b]	139	13.7
		+ 31.5 (dd)[b]	140	13.7
(6)	$[Rh^{I}(TMPP)_2(CO)_2][BF_4]$	– 23.8 (d)[b]	116	–
(7)	$[Rh^{I}(TMPP)_2(CO)][BF_4]$	– 11.1 (d)[b]	128	–
(8)	$[Rh^{I}(TMPP)_2(CO)(CNBu^t)][BF_4]$	– 21.8 (d)[b]	128	–
(9)	$[Rh^{II}(TMPP)_2(CNBu^t)_2][BF_4]_2$	not observed		
(10)	$[Rh^{II}(TMPP)_2(CNPr^i)_2][BF_4]_2$	not observed		
(11)	$[Rh^{I}(TMPP)_2(CNBu^t)_2][BF_4]$	– 19.1 (d)[b]	129.7	–
		– 20.2 (d)[b]	129.7	–
(12)	*eq*-$[Rh^{II}(TMPP)(TMPP\text{-}O)][BF_4]$	not observed		
(13)	*eq*-$[Rh^{III}(\eta^3\text{-TMPP})(\eta^3\text{-TMPP-}O)][BF_4]_2$	+ 47.3 (dd)	108.8	13.8
		+ 22.5 (dd)	98.8	13.8
(14)	*ax,eq*-$[Rh^{III}(\eta^3\text{-TMPP-}O)_2][BF_4]$	+ 47.1 (dd)	137.3	16.7
		+ 19.9 (dd)	122.9	16.7
(15)	*ax,ax*-$[Rh^{III}(\eta^3\text{-TMPP-}O)_2][BF_4]$	+ 35.7 (d)	152.5	–

	Compound	Chemical[a] Shift	$J_{Rh\text{-}P}$ Hz	$J_{P_A\text{-}P_B}$ Hz
(16)	$[Rh^{I}(cod)(\eta^2\text{-TMPP})][BF_4]$	+ 1.4 (d)[b]	137.3	–
(17)	$Rh^{I}(cod)(\eta^2\text{-TMPP-}O)$	+ 8.0 (d)[b]	157.2	–
(18)	$Ir^{I}(cod)(\eta^2\text{-TMPP-}O)$	not measured		
(19)	$[Ir^{I}(TMPP)_2(CO)_2][BF_4]$	– 39.0 (s)[c]	–	–
(20)	$(\eta^3\text{-TMPP})Mo^{0}(CO)_3$	– 1.9 (s)[b]	–	–

[a] Chemical shift reported in CD_3CN relative to 85% H_3PO_4 unless noted otherwise.
[b] Chemical shift reported in CD_2Cl_2.
[c] Chemical shift reported in $CDCl_3$.